Charles University

Faculty of Medicine in Pilsen

Ph.D. Study program: Physiology and Pathological Physiology

Psychiatric-relevant impairments in mouse models of spinocerebellar ataxias

Dissertation

Supervisor: Jan Cendelín

Consultants: Pascal Hilber and Karel Ježek

Pilsen, *2022* **Filip Tichánek**

PREFACE

I declare that I prepared the Ph.D. thesis independently and that I stated all the information sources and literature. This work or a substantial portion thereof has not been submitted to obtain another academic degree or equivalent.

Pilsen,…….

…….

Filip Tichánek

ACKNOWLEDGEMENT

I thank mainly my supervisor, Jan Cendelín, for his effort, numerous advice, patience and for providing me with high level of freedom. I also thank my consultants, Pascal Hilber and Karel Ježek, for their inspiration and advice. I also thank my colleagues, Martina Šalomová and Jan Tůma among others, for their help and discussions. I thank the technicians of the Department of Pathological Physiology, namely Irena Pojerová, Helena Geciová, Eva Cendelínová, Filip Bezstarosta and Andrea Korandová, which contributed hugely to the work behind this thesis. Finally, I thank Jan Jedlička, Jitka Kuncová and Renata Šťastná as they performed mitochondrial experiments presented in this thesis.

Filip Tichánek

ABSTRAKT

Spinocerebelární ataxie (SCA) jsou heterogenní skupinou onemocnění charakteristických dysfunkcí mozečku a narušením pohybu. Mnoho pacientů s SCA ale trpí i narušením paměti a psychickými obtížemi, včetně apatie, deprese a úzkosti. Tyto problémy dále pacientům zhoršují kvalitu života a mohou i akcelerovat postup onemocnění. Jejich příčiny, včetně případného kauzálního vlivu narušené funkce mozečku, však nejsou jasné. Tato práce si klade se cíl přispět k pochopení povahy těchto potíží u SCA, a to prostřednictvím studia relevantních myších modelů.

Práce tedy zahrnovala výzkum abnormalit chování a funkcí mozku u myší s čistě olivocerebelární degenerací (lurcher) a u knock-in myšího modelu spinocerebelární ataxie 1 (myši SCA1). Metodika zahrnovala komplexní behaviorální testování, histologické techniky, biochemické analýzy, imunofluorescenční zobrazování a měření mitochondriálního oxidativního metabolismu. Získaná data byla následně analyzována moderními statistickými přístupy se statistickými simulacemi.

Experimenty potvrdily kognitivní deficity u myší lurcher i SCA1. U myší SCA1 experimenty odhalily řadu abnormalit v chování, které dosud nebyly u zvířecích modelů SCA nikdy popsány, včetně snížené prepulzní inhibice, poškození kognitivní flexibility a vyšší míry chování připomínající depresivní a úzkostné prožívání. Naproti tomu myši lurcher vykazovaly v některých ohledech opačné chování, konkrétně absenci „depresivního“ chování. Abnormality chování u SCA1 myší se začaly objevovat překvapivě dříve než znatelná ataxie a jejich mozky vykazovaly hipokampální atrofii, která byla doprovázená snížením markerů neuroplasticity a dramaticky narušenou hipokampální neurogenezí. Je zajímavé, že hipokampální atrofie započala dříve než mozečková degenerace a přímo odrážela míru některých behaviorálních deficitů, konkrétně „depresivního“ chování a snížení kognitivní flexibility. Výsledky tak naznačují, že psychické problémy u SCA1 jsou biologického původu a jsou částečně nezávislé na poškození mozečku a ataxii. Terapeutické cílení na tyto problémy se tak může míjet s léčbou cílenou na mozeček a ataxii.

ABSTRACT

Spinocerebellar ataxias (SCAs) constitute a heterogeneous group of diseases characterized by the dysfunction of the cerebellum and disturbed coordination of movements. Aside from these, many SCA patients suffer also from cognitive impairments and diverse mental issues, including apathy, depression and anxiety. Although often overlooked, growing evidence suggests their profound contribution to the reduced life quality and poor health outcomes. However, their nature remains largely unclear. This thesis aims to address this by studying the mouse models of hereditary ataxia.

To achieve this, psychiatric-relevant behavioural abnormalities and their underlying neuropathology were studied in mice with cerebellar-specific degeneration (lurcher) and the knock-in mouse model of spinocerebellar ataxia 1 (SCA1 mice). The methodology included complex behavioural testing, histological techniques, biochemical analyses, immunofluorescence imaging, and measuring the mitochondrial oxidative metabolism. Obtained data were then analysed using modern statistical approaches accompanied by computer-intensive methods such as bootstrapping simulations.

Experiments confirmed cognitive deficits in both lurcher and SCA1 mice. Interestingly, behavioural characterization identified numerous psychiatric-relevant behavioural impairments in SCA1 mice that have not been identified in any SCA animal model so far, including reduced prepulse inhibition, diminished cognitive flexibility, and increased anxiety- and depressive-like behaviour. This phenotype partially contrasts with the behaviour of cerebellar-specific lurcher mice, which showed a lack of depressive-like behaviour. In SCA1 mice, some psychiatric-relevant impairments preceded the onset of substantial ataxia. SCA1 mice also exhibited hippocampal atrophy with decreased neuroplasticity indicators, reduced mitochondrial bioenergetics and hugely impaired neurogenesis. Interestingly, the hippocampal atrophy commenced earlier than cerebellar degeneration and directly reflects some behavioural deficits, namely depressive-like behaviour and cognitive inflexibility. These results suggest that mental issues in SCA1 have biological roots partially independent of the cerebellum and suggest new avenues in the search for novel SCA1 therapies.

CONTENT

LIST OF ABBREVIATIONS

AD(H)D: Attention Deficit (Hyperactivity) Disorder
ADCA: Autosomal Dominant Cerebellar Ataxias
ARCA: Autosomal Recessive Cerebellar Ataxias
ASD: Autism Spectrum Disorder
BARS: Brief Ataxia Rating Scale
BDNF: Brain-Derived Neurotrophic Factor (brain protein)
BIC: Bayesian Information Criterion
CCAS: Cerebellar Cognitive-Affective Syndrome
CNS: Central Nervous System
CA(-SRLM): *Cornu ammonis* (*Strata radiatum* and *Strata Laconosum-Moleculare* layers)
DCX: Doublecortin (protein produced by young hippocampal neurons)
DG(-ML): Dentate Gyrus (molecular layer)
DMN: Default Mode Network
DLPC: Attention Deficit (Hyperactivity) Disorder
DRPLA: Dentatorubral-Pallidoluysian Atrophy
ELISA: Enzyme-linked immunosorbent assay
EPM: Elevated Plus Maze (rodent behavioural test)
FARS: Friedreich Ataxia Rating Scale
GAD: Glutamate Decarboxylase (enzyme)
GL: Granular Layer
HFA: High-Functioning Autism
IF: Impact Factor (indicator of citation rate of scientific publications)
IPL: Inferior Parietal Lobule
fMRi: Functional Magnetic Resonance Imaging
FST: Forced Swimming test
ICARS: International Cooperative Ataxia Rating Scale
KI: Knock-in (mice)
KO: Knock-out (mice)
LME: Linear Mixed-Effects Model (statistical procedure)
LTD: Long-Term Depression
LTP: Long-Term Potentiation
M1: Primary Motor Cortex
ML: Molecular Layer
MRI: Magnetic Resonance Imaging
MS: Multiple Sclerosis
MWM: Morris Water Maze (rodent behavioural test)
OF: Open Field (rodent behavioural test)
PC: Purkinje Cell

PCP: Purkinje Cell Protein
PSA-NCAM: Polysialylated-Neural Cell Adhesion Molecule (plasticity marker)
REM: Rapid Eyes Movement (phase of sleep)
ROC-AUC: Area under a receiver operating characteristic curve
SARA: Scale for the Assessment and Rating of Ataxia
SCA: Spinocerebellar Ataxia
tDCS: Transcranial Direct Current Stimulation
TG: Transgenic (mouse)
vlPAG: Ventrolateral Periaqueductal Grey (brain region)
VTA: Ventral Tegmental Area (brain region)
WT: Wild-type (mouse)
WTM: Water T-Maze (rodent behavioural test)

1 INTRODUCTION

Spinocerebellar ataxias (SCAs) constitute a heterogenous group of diseases that have in common the dysfunction of the cerebellum, a structure of the brain known for its role in the coordination of movements[1,2]. Unsurprisingly, SCAs are primarily characterized by motor deficits. However, they are also commonly coupled with additional non-motor symptoms, including diverse neuropsychiatric impairments[3]. Neuropsychiatric impairments are very common in some SCAs and growing evidence highlights their significant contribution to disease progression in SCA patients[4]. However, the mechanisms of the mental issues in SCAs are still not clear.

Nowadays, there is a consensus that the cerebellum has also diverse non-motor functions, including modulation of higher-order cognitive functions and emotions, potentially mediating the psychiatric issues in the hereditary ataxias[5–7]. In addition, having an untreatable disease, and expecting its gradual progress, poses huge emotional stress that may induce emotional dysregulation and, in turn, weaken the cognitive capacity[8,9]. Moreover, the neuropathology of many hereditary ataxias is complex as they usually reach multiple brain regions[10], and this complexity strongly varies across patients, reflecting gene dosage and congenital factors[10]. However, recognition of the relative contributions of these factors to the psychiatric impairments is extremely difficult via studying human patients only.

In contrast, mouse models may be studied in genetically uniform populations with pre-selected gene dosage or may even be engineered to express the implicated gene mutation in a narrowly specified cell type and spatially restricted brain region. Moreover, mice may be studied in immensely deep neuropathological details which are unachievable in human studies. This brings completely new possibilities to identify the relationship between specific pathology and abnormal behaviour. Although mouse behaviour and cognition are far less complex compared to humans, mouse studies may still help to resolve the questions which may be difficult to address otherwise.

This thesis works with *SCA-relevant models*. It includes not only the model of SCA1 *sensu-stricto* but also mice with selective cerebellar degeneration, as both may provide valuable information about the nature of the behavioural deficits in SCA.

The thesis starts with a ***Literature Review*** summarizing relevant knowledge. Three sections (2.1, 2.2, and 2.3) focus on the cerebellum and its functions. Section 2.1 is introductory and describes the basic structure, anatomy, and motor-related functions of the cerebellum; all of these are described to a minimalistic extent necessary to understand further sections. Two further sections (2.2 and 2.3) provide a detailed review of scientific understanding of the cerebellar role in higher-order cognition, emotional regulation, and contribution to psychiatric diseases. The next sections (2.4 and 2.5) focus on cerebellar diseases and their mouse models, with a special focus on hereditary cerebellar ataxias and especially spinocerebellar ataxias. Section 2.4 focuses on human patients whereas section 2.5 focuses on mouse models. Both sections review also psychiatric issues in SCAs and relevant behavioural impairments in their mouse models.

The next chapters describe individual ***Research***, each chapter describing one specific study. I decided to divide the original research into separate blocks because the research design of the second study partially depended on the results from the previous research. Description of the methods of the second research before presenting the results of the first research would thus undesirably reveal the story.

Each of the sections includes the following information:

(i) Conceptualization of the research
(ii) Listing the specific aims and hypotheses of a given research
(iii) Declaration of my contribution to the research
(iv) Methods and material used, including a description of statistical analysis
(v) Results and their brief interpretation

The last chapter, ***Articles***, lists scientific articles that I (co-)authored and which have been either directly used in this thesis (in terms of text, figures or tables; Articles 1-4) or cited in this thesis (Articles 5-8). The section shows full citations of the articles and declarations of my contributions to each of them.

2 LITERATURE REVIEW

2.1 Cerebellar basics

The cerebellum is a brain region with many unique features. Evolutionary, the cerebellum evolved as a part of the pons in the brainstem[1,11,12]. Although it constitutes only about 10% of the total brain volume, it makes up more than 60% of all neurons in the human brain[1]. Moreover, the cerebellum has a unique modular structure, consisting of repeating units creating many structurally homogenous microcircuits likely providing similar kinds of computations. With such a high number of neurons, the cerebellum evinces a huge computational power[13]. The cerebellum has been traditionally assumed to ensure motor functions, keeping posture, balance, motor learning and reflexes such as eyeblink conditioning[1]. However, newer pieces of evidence highlight its involvement also in pain processing[14], emotional regulation[15] and various aspects of the cognitive functions[16]. Because this thesis focuses specifically on the latter, the role of the cerebellum in these higher-order cognitive functions and emotions will be described in further sections in detail.

2.1.1 Gross cerebellar anatomy and connections

The surface of the cerebellum is constituted by the cerebellar cortex, which is highly folded into small folds called folia[1]. Interestingly, the cerebellum is highly folded even in other non-human mammals, including rodents[17] (which have the cerebral cortex unfolded). Many folia create bigger parts called lobules (there are 10 lobules in the human cerebellum). Lobules themselves are organized into three bigger organization units called lobes: *flocculonodular, anterior* and *posterior*, divided by *primary* and *posterior fissures*[1]. Moreover, the cerebellum also creates two hemispheres and midline zone called vermis.

Under the cerebellar cortex, there is white matter. Immersed in the white matter, there are three cerebellar nuclei: *fastigial nucleus*, *interposed nucleus* (divided into *emboliform* and *globose* in humans) and *dentate nucleus*[1]. The connections of the cerebellum, including the cerebellar nuclei, with the rest of the brain, are ensured via three types of paired cerebellar peduncles (*superior*, *middle* and *inferior*)[1].

From a more functional point of view, the cerebellum is conventionally divided into three parts, reflecting relatively distinct functions and connectivity with other parts of the central nervous system[1]. This division is hugely overlapping according to laterality and includes *vestibulocerebellum* (archicerebellum), *spinocerebellum* (paleocerebellum) and *cerebro-cerebellum* (neocerebellum)[12].

The vestibulocerebellum consists of the flocculonodular lobe and partially also the fastigial nucleus[18]. This part is evolutionary the oldest. It has rich connections to the vestibular nucleus and has a crucial role in the ability to keep balance, muscle tone and oculomotor control[1,12]. This part also integers the information from the vestibular system (from the semi-circular canals and vestibular nuclei) along with visual inputs (from the visual cortex throughout pontine nuclei and superior colliculi) to sustain spatial perception and balance[1,12].

The spinocerebellum is located in the middle of the cerebellum (vermis) and medial parts of the cerebellar hemispheres. It is mainly responsible for the control of limb movements[1,12], especially the proximal parts. It receives proprioceptive and somatosensory inputs from the spinal cord, but also visual and auditory systems[1,12]. The spinocerebellum sends information throughout the deep nuclei (particularly the fastigial nucleus) to the brainstem (pons, medulla oblongata and reticular formation), midbrain thalamus and ultimately (throughout the thalamus) into the cerebral cortex, contributing to descending motor system controlling limb and body movements[19]. The middle part of the spinocerebellum (the vermis) communicates with the fastigial nucleus and controls the movement of rather proximal body parts[1,12]. In contrast, more lateral parts of the spinocerebellum (paravermis) project to fastigial and (even more) interposed nuclei (creating further inputs to rubrospinal and corticospinal systems) and control rather proximal limb movements[1,12]. Vermis and paravermis also contribute to emotional processing and memory in mammals via their interconnections with the limbic system (see section 2.2 below)[20].

Cerebrocerebellum is evolutionary the youngest part of the cerebellum[1,12]. This part of the cerebellum is seemingly over-developed in primates compared to other mammals, even when compared to the cerebral cortex[21]. It consists of later parts of cerebellar hemispheres, communicating mainly with the dentate nucleus and further communicating with the ventromedial thalamus and cerebral cortex. It is responsible for the coordination

of distal limb movement, planning, organizing and timing the fine movements[1,22]. This part of the cerebellum also participates in diverse cognitive functions, especially executive functions and related working memory, complex planning and emotional control (see section 2.2 below)[6].

2.1.2 Cerebellar microcircuit

The cerebellar cortex consists of three layers – the molecular layer (the most superficial), Purkinje cells layer (middle) and granular layer[1,23]. The core component of the cerebellar microcircuits is the Purkinje cell (PC) with a body located in the Purkinje cell layer and dendritic arbours constituting the key component of the molecular layer[1]. The human brain contains approximately 30 million Purkinje cells. The dendritic arbours of the Purkinje cells are richly branched in two-dimensional space – the branches spread orthogonally to the direction of the cerebellar folia but are flat in the opposite direction (along with the folia), resembling the arms of a lawn rake[1]. The granular layer consists mainly of granular cells – one of the smallest and the most abundant neurons, reaching the numbers of 10-100 billion in the human brain[1].

The signal reaching the cerebellar nuclei comes from two possible sources: *climbing fibres* from the inferior olivary nucleus, or *mossy fibres* from pontine or spinal neurons[1,12]. The signal from both types of fibres reaches cerebellar nuclei and parallelly also granular cells and other cerebellar cortex interneurons (mossy fibres) or Purkinje cells (climbing fibres)[1,12]. The signal from these fibres is transmitted via excitatory synapses utilizing excitatory neurotransmitters aspartate (climbing fibres) or glutamate (mossy fibres)[12]. Whereas each climbing fibre stimulates dendritic arbours of only one Purkinje cell, each mossy fibre reaches many granular cells[1] and simultaneously also other interneurons (see below). Concerning the signal from mossy fibres (which is the prevailing cerebellar input), the excited granular cells send the excitatory signal to the dendritic arbours of the Purkinje cells via axons directing to the molecular layer called *parallel fibres*. The excited Purkinje cells then project the signal back to cerebellar nuclei via *simplex* spikes[1]. In contrast, PCs receiving the signal from climbing fibres produce slower *complex* spikes[1]. The action of the PCs is inhibitory.

Besides the above-mentioned neurons, the cerebellar computations and related learning are modulated by the activity of other cerebellar interneurons[24]. *Golgi cells* occur

in the granular layer and are stimulated by parallel and mossy fibres[1]. Their axons create inhibitory connections to granular cells, including their arbours, bodies and particularly axons (the parallel fibres), allowing feed-forward and feed-back inhibition of granular cells[1]. The granular layer contains also *unipolar brush cells* with an excitatory connection to the granular cells. The molecular layer contains two crucial interneurons: *stellate* and *basket* cells. They are stimulated by the parallel fibres of the granular cells and contribute to Purkinje cells inhibition[1]. Whereas *stellate* cells are co-activated together with close Purkinje cells (leading to inhibition of the proximal Purkinje cell), axons of *basket* cells are long and reach more distant Purkinje cells, leading to lateral inhibition and sharpening of the signal[1]. Another inhibitory type of interneuron, the *Lugaro cells*, occurs between granular and molecular layers and inhibits other cerebellar interneurons[25].

2.1.3 Basic mechanisms of cerebellar functions

Cerebellar signal processing differs from the processing of other parts of the brain in several ways. Firstly, the signal processing in the cerebellum is unidirectional – feedforward[1,23,26]. The signal reaching the cerebellum shows one direction with a strongly limited recurrent signal: the signal reaches the cerebellum, is processed by the cerebellum and leaves the cerebellum[23]. Together with high numbers of cerebellar neurons and a highly modular structure (allowing to provide high numbers of orthogonal computations at once), the unidirectional signal processing enables to eliminate reverberance of the signal and provides extremely fast responses to various independent inputs[27]. This situation differs from most of the other brain regions, including the cerebral cortex, where the signal could be processed bidirectionally with rich recurrent transmission and high signal reverberance, leading to sustaining patterns of neural activity[1].

What could be the advantages of these fast computational operations? Early theories from the sixties suggested that the role of the cerebellum is to create predictions (internal models) about intended actions and, subsequently, to compare the real outcome of the actions with the predictions[23,28–30]. According to this well-established concept, a simple motor command, such as taking a glass of water to the hand, could be well exemplified in the following sequence of actions and related neural activities[1,12,30]:

1. Generation of the idea “take the glass up” is driven by the activity of the frontal cerebral cortex.

2. The idea is further transmitted to the supplementary motor and pre-motor areas of the cerebral cortex.
3. Further, the idea comes to the basal ganglia which turn the motor programs on
4. The motor program enters the thalamus and goes further to other motor and sensory-motor brain regions, including the cerebellum
5. The information enters the corticospinal fibres and leads to muscle contraction
6. The initial position of the hand and its changes are monitored by the cerebellum, particularly throughout analyses of proprioceptive signals.
7. The cerebellum keeps the information about the initial and actual position, compares the actual position with the prediction and creates another prediction concerning the possible outcome of the movement if the actual motor program continued in the same way.
8. The cerebellum sends this information to other motor-related brain regions, including the motor cortex, to adjust the motor program accordingly.
9. The adjustment of the motor program results in smooth and timely precise movement of the hand

By this function, the cerebellum is expected to play the important role of the egocentric internal representation ("GPS" of the body), enabling us to create models of our body parts positions and to provide internally generated predictions about expected positions of our body in the future[29–34]. By this, the cerebellum supplies the rest of the motor-relevant brain regions with this information to fit appropriate motor programs. This concept, describing the cerebellum as a "neuronal prediction machine"[23] is nowadays well supported by both computational modelling and experimental research and has been further elaborated[27,28,30,35]. The cerebellum was specifically viewed as a machine for so-called *supervised learning*[27]. This term was implemented from the machine learning/artificial intelligence field and refers to machine learning algorithms utilizing labelling of the training data (e.g. predictive linear regression represents a form of supervised machine learning) and continual improvement of predictions of the outcome according to input data[36]. However, recent literature points out that cerebellar computations are far more complex[35]. Finally, growing evidence suggests that the predictive and anticipative power of the cerebellum plays an important role not only in motor movement and learning but even in higher-order cognitive functions and emotional regulation (see section 2.2 below)[13,28].

As the cerebellum mediates learning processes[1,37–39], neural plasticity is an essential component of related learning. In the case of the cerebellum, synaptic plasticity has been suggested to play a role in motor learning by David Marr[40] and James Albus[41] in 1969 and 1971 respectively. Both authors concluded that the cerebellum is a key brain region for motor learning. Moreover, both suggested the idea that synapses between parallel fibres and Purkinje cell dendrites are modified during motor learning and this long-term plasticity represents the neurobiological basis of motor learning. However, whereas David Marr proposed strengthening the synapse as the mechanism of the plasticity (*long-term potentiation*; LTP), James Albus suggested opposite, i.e., synaptic weakening (long-term depression; LTD). Further experimental works strongly supported the Albus's idea – concurrent stimulation of the parallel and/or climbing fibres causes decrease of the PCs response, supporting the LTD as an important mechanism of the motor learning[42]. Also, studies utilizing various behavioural paradigms suggested that the importance of the LTD goes beyond motor learning and constitutes the basis also for other types of cerebellar-dependent learning, for example, eyeblink conditioning[37] and spatial learning during darkness[43].

On the other hand, recent studies highlighted that synaptic potentiation between the parallel fibres and PCs dendrites contributes to motor learning as well[44]. Furthermore, the relative importance of the LTP vs. LTD was shown to vary considerably among different cerebellar subregions. The relative importance of the LTP/LTD differs according to the expression and immunoreactivity of zebrin[45]. The zebrin is expressed specifically in a subpopulation of the Purkinje cells and in the hippocampus and plays role in ATP synthesis[45]. Interestingly, the zebrin-positive PCs create stripes going across different lobes of the cerebellum in the sagittal direction although few lobes (e.g. lobes VI-VII and Crus I in rodents) have expanded zebrin-positive area or are almost completely zebrin-positive[45–47]. Recent studies showed that these stripes vary also functionally: zebrin-positive stripes seem to have different connectivity patterns with non-cerebellar brain regions and the zebrin-positive Purkinje cells show a lower firing rate[45,46]. Interestingly, the zebrin-positive PCs were documented to be more resistant to cell damage due to toxins, injury and possibly also diseases[47]. Typically, in zebrin-positive PCs, the LTP represents the main plasticity mechanism and vice versa[46]. Because zebrin-positive stripes tend to be more associated with non-motor cerebellar functions[30], the LTP may be more important for cognition and emotional regulation. Furthermore, long-term

modification of synaptic strength was reported to occur not only on synapses between parallel fibres and PCs but also between mossy fibres and cerebellar nuclei neurons[48], further underlining the fact that multiple plasticity mechanisms contribute to cerebellum-dependent learning[44,49].

2.1.4 Motor-related symptoms of cerebellar dysfunction

The diverse functions of the cerebellum could be well demonstrated in patients with cerebellar damage and/or dysfunction[1]. As the most noticeable are especially motor deficits, the description of the patients with cerebellar lesions led to the first hypothesis about the cerebellar role in motor coordination by Babinski in 1899[50].

The cerebellar damages and dysfunctions may be due to numerous causes, mainly cerebellar diseases (see section 2.4 for details). The aetiology of cerebellar diseases is, however, extremely heterogeneous. Individual diseases, but often also individual patients suffering from the same disease, differ in speed of progression, extent and location of cerebellar damage[51]. Thus, it is not surprising that the manifestation of cerebellar diseases could be quite variable. Nevertheless, some general features and basic symptoms of cerebellar dysfunctions can be defined (this categorization follows the publication of Kandel et al.[1]):

1. *Ataxia*: impaired coordination of movement, including (among others) problems with the accuracy of the movement, coordination of individual components of movements (asynergia), controlling the magnitude (*dysmetria*) and timing of the movements and problems with proper finishing of the movements[1,51]. The movements of the cerebellar patients could be described as uncoordinated and jerky[51]. As the movements are not finished properly, the patients often "overshoot" and the trajectories of the limb movements are not straight[51]. Repeated movements have impaired regularity (*adiadochokinesia*). The ataxia is not related only to discoordination of limbs, but also to impaired mouth coordination (leading to *dysarthria*), impaired saccade movement and eye allignment[51].
2. Impaired muscle tone: although *hypotonia* (decreased muscle tone) is more frequent in cerebellar patients, hypertonia may also occurs[1,51]. The hypotonia is associated with a decreased excitatory drive from the cerebellar nuclei to premotor

brain regions[52]. Therefore, it is more associated with damage to the cerebellar nuclei[52]. On the other hand, selective disturbances in the cerebellar cortex lead rather to reduced inhibition of the excitatory cerebellar output and thus its over-activity and hypertonia[52].

3. *Astasia-abasia*: Astasia implies an inability to keep a stable upright body posture whereas abasia refers to impaired walk[1]. Cerebellar patients often fall and their gait is unstable and irregular (in terms of timing as well as stride length). Moreover, to compensate for the unstable gait and impaired balance, the patients show a wider base between legs[51].
4. *Intention tremor*: patients evince tremor which is restricted to movement and is particularly strong at the end of the movement (when the person wants to stop the movement)[1]. This contrasts with tremors in other medical conditions related to striatal dysfunctions, such as Parkinson's syndrome, which evince resting tremor[1,51]. Moreover, intention tremor has a lower frequency and higher amplitude compared to parkinsonism-related tremor[51].

Besides the most typical symptoms, cerebellar patients often suffer from other symptoms, such as headache, dizziness, vertigo and oculomotor disturbances, including nystagmus[51]. Although dysphagia (swallowing problems) occurs in many neurological diseases, cerebellar impairments seem to contribute to this problem too[51]. Moreover, cerebellar patients also show a high rate of cognitive, emotional and other non-motor deficits[53]. As the research of these non-motor impairments is crucial for the conceptualization of my thesis, I dedicated them whole next section.

2.2 Cerebellar involvement in higher-order cognition and emotional processing

The first suggestion that the cerebellum plays a role in complex cognition and emotional regulation came in 1986 by Henrietta Leiner, her husband Alan Leiner and their team[16,54]. In their original proposal, based substantially on findings of evolutionary enlarged dentate nucleus in primates and particularly humans, they suggested that evolutionary more derived parts of dentate nucleus communicate with (pre)frontal associative cortex to modulate complex non-motor functions[55]. This hypothesis was further developed, especially via studies recruiting human cerebellar patients for neuroimaging[56,57]. This led to the identification of the so-called *Cerebellar cognitive-*

affective syndrome or *Schmahmann's syndrome*[58]. Currently, research has been further developed markedly: the cerebellar contribution to high-order cognitive and emotional control has been widely accepted and specific non-motor cerebellar subregions have been identified[58,59]. Moreover, current state-of-art neuroscience approaches, based on calcium imaging[60], conditioned modulation of specific neural activity via chemogenetic[61] and/or optogenetic[62] methods, opened new possibilities to understand the role of the cerebellum in various aspects of complex thinking and emotional regulation.

2.2.1 Cerebellar cognitive-affective syndrome

The Cerebellar cognitive-affective syndrome (hereinafter *CCAS*) has been proposed in 1998[57]. The original description mentioned three main clusters of symptoms of the cerebellar damage: (i) impaired executive functions (planning, set-shifting, verbal fluency, abstract reasoning and working memory); (ii) impaired spatial cognition (visuospatial memory disorganization); (iii) altered emotional regulation (blunted affect, disinhibited and inappropriate behaviour and impulsivity)[57]. These impairments were observed in patients with damage to posterior cerebellar lobes or vermis, but only minor disturbances were seen in cases with anterior lobes damage[57].

Following more than two decades of research and clinical observations[63], many other cognitive[64] or emotional disturbances[58,65] in the cerebellar patients were identified: language impairments including agrammatism[66] and cerebellar aphasia[67,68], premature behaviour and tendency to act without thinking about consequences (analogous to the above-mentioned impulsivity and inappropriate behaviour)[58]. The cerebellar patients were also described to exhibit impaired social cognition: they may be naive and overly trustful, without the capability to recognize the ulterior motives of other people, and present with a lack of empathy[7,69]. Their mood has been described to be unstable, with a tendency to low frustration tolerance and a higher propensity to stress, anxiety and depression[7]. The patients are distracted, have impaired attention control and sometimes show stereotypical and ritualistic habits[7]. A recent meta-analysis of available relevant studies of cognition in cerebellar patients (adult patients with isolated cerebellar lesions were compared to healthy controls) confirmed earlier findings partially[70]. The results of the analysis found several impairments in language processing and fluency (evaluated with variants of *verbal fluency tests*) impaired visuospatial abilities (evaluated with *Block*

design test and *Wechsler Memory Scale- Revisited visual memory test*) and damaged executive control (measured with several variants of *Stroop tests*)[70]. On the other hand, the analysis did not find a statistically significant difference in other tests of visual attention and task switching (*Trial making tests*), visuospatial abilities (*Rey complex figure tests*), attention (*Digit span tests*), aphasia (*Aphasia test*), figural fluency (*Five-point tests*) and inhibitory control (*Go/No-go test*)[70]. This meta-analysis was performed on adult patients only although children patients tend to show a more marked neuropsychological profile, compared to adults[58]. In general, damage to vermal areas usually resulted in impaired emotional processing whereas damage to the posterior hemispheres impacted cognitive functioning[7,58,63].

Some authors[30], however, argue that the studies of cerebellar patients may be problematic for several reasons: i) cerebellar patients are heterogeneous and some of them (especially those suffering from the degenerative disease) may have undetected yet functionally important impairments in non-cerebellar regions. ii) some tasks may be affected by ataxia and incoordination of movements. For example, even pressing the button during the test may be more difficult for a cerebellar patient, leading to higher attention to the motor aspects of the tests and thus biased results[30]. Studies of the cerebellar functions in humans with intact motor functions or employing much more homogenous mouse models with the known extent of pathophysiology thus may offer new perspectives on the non-motor cerebellar functions. On the other hand, the research on mouse models of cerebellar-specific degeneration strongly supports the above-mentioned findings[71] (see section 2.5).

2.2.2 Cerebellar contribution to cognition and emotional regulation

Neuroimaging studies of healthy participants suggested that various functions related to the cerebellum, and thus relevant for the CCAS, are associated with the functions of different cerebellar sub-regions. For example, Baumann et al. aimed to find cerebellar correlates of emotional processing (for 5 different emotions) using functional magnetic resonance (fMRi) on 30 subjects[72]. In general, emotions were mostly correlated with posterior vermal and paravermal regions (with exception of anger; Figure 1) and some of the emotions (anger and fear) tended to be distinctly more correlated to right hemisphere[72]. To be more specific, anger was strongly associated with vermal regions of

right lobules VI, VIIA and IX, right paravermal and hemispheric regions of lobules VI and Crus I[72]. Fear was associated with the activation of right paravermal lobules VI, Crus I and Crus II and right vermal lobes VI, VIIA and VIIB. Disgust correlated with left paravermal lobule VI and bilateral vermal lobules V, VI, VIIIA and IX. Sadness was related with vermal lobules VI, VIIA, VIIB and VIIIA (bilaterally) and with paravermal lobe VI (bilaterally) and Crus 1 (right), whereas happiness correlated with vermal and paravermal regions of lobe VIIIA[72]. Another study, meta-analysing brain activity during anger and aggression processing at more than 800 participants, also found particularly posterior vermis as a key region for anger processing whereas aggression was related to more anterior vermal regions[73].

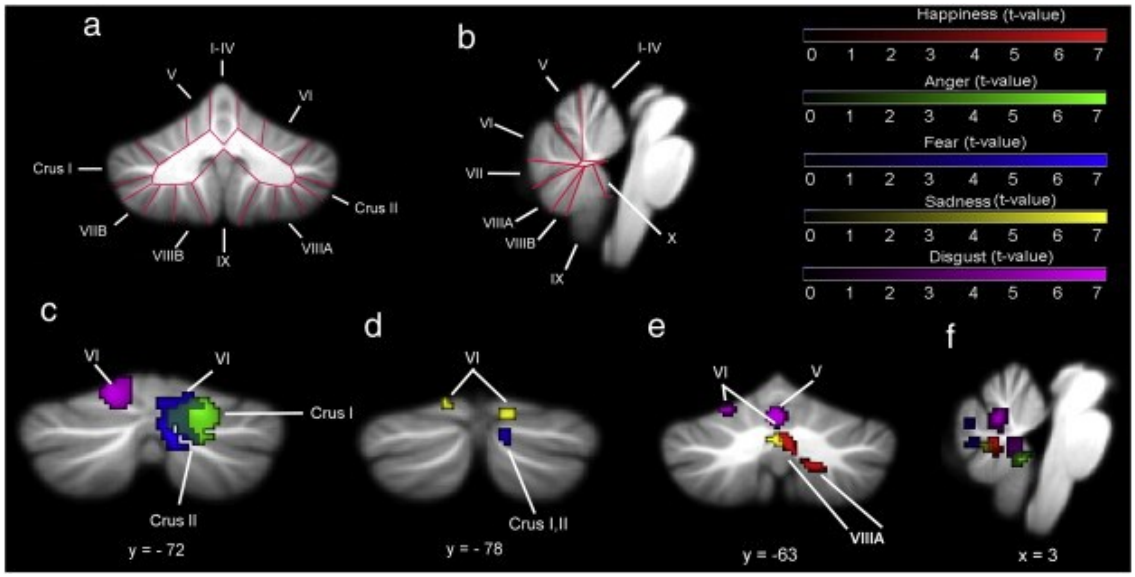

Figure 1. Visualised results of the study association between feeling of five different emotions and activation of cerebellar sub-regions. The figure was reprinted from NeuroImage, Vol. 61, Baumann and Mattingley: *Functional topography of primary emotion processing in the human cerebellum*, with permission of Elsevier (license number: 4962571356569; accessed by 2020-12-05).

Congruently, a complex meta-analysis of the functional imaging studies focused on cerebellar-modulated cognition and emotional processing came to similar conclusions[74]. Language processing activated right lobule VI and Crus I. Spatial processing activated left lobule VI. Executive functions and emotional processing were both associated with activation of lobules VI, Crus I and VII (VIIB specifically in case of executive control)[74]. In contrast, sensorimotor and motor tasks correlated with activation of anterior lobes V

and adjacent VI, and partially lobule VIII, altogether supporting at least partial spatial dissociation of the motor and non-motor cerebellar functions[74].

Interestingly, an emerging number of studies have highlighted that the cerebellum has important functions also for sleep and sleep-related memory consolidation[75,76]. Moreover, the cerebellum seems to be vulnerable to lack of sleep and simultaneously, cerebellar malfunctions may result in sleep disturbances[75,77].

Moreover, several studies suggested the role of the cerebellum in shaping individual personality traits[78]. For example, cerebellar volumes seem to be positively correlated with novelty seeking, reduced harm avoidance and with difficulty to understand own as well as others' emotions[78]. These results are congruent with the finding of a recent study on mice, showing that elevation of pro-neuroplastic *brain-derived neurotrophic factor* (BDNF) in the mouse cerebellum stimulates novelty seeking and exploration[79].

As all signals of the cerebellum are mediated throughout cerebellar nuclei, which could be specifically inactivated in rats and bigger animals by temporary inhibition of neural activity (with lidocaine, muscimol or similar compound) or by surgical disruption without the necessity to rely on state-of-art chemogenetic or optogenetic approaches[80–82]. Therefore, the effect of the inactivation of the specific cerebellar nucleus on cognition and behaviour has been studied since the nineties and the results have been mostly congruent with the known connectivity pattern of each nucleus. Temporary inactivation of the fastigial nucleus in rats was found to cause marked loss of social interest[83] and to induce stress-induced gastric damage[84], supporting the view that vermal-fastigial cerebellar output affects emotions, sociality and stress resilience. Similarly, inactivation or lesion of the dentate nucleus was found to impair spatial learning in the MWM[85] and disrupted egocentric spatial learning[86] in rats. Another study compared the effect of inactivation of the fastigial vs. dentate nucleus. Surprisingly, inactivation of any nucleus (fastigial or dentate) impaired spatial orientation although rats with fastigial nucleus inactivation were able to improve over time normally[87]. Moreover, dentate nucleus inactivation impaired effort-based decision making[81] and induced motivational deficit during exploration in the open field and operational appetitive task[88].

The cerebellar influence on emotional functions and related behaviour has also been evidenced in a recent study employing an optogenetic approach to modulate the activity of the vermal PCs to study aggression[89]. Although the aggression had been believed to be

primarily driven by the amygdala, optogenetic PCs stimulation in mice resulted in significantly reduced aggressive behaviour in a resident-intruder assay, as measured by decreased numbers of attacks towards the second mouse[89]. In contrast, vermal PCs inhibition stimulated aggressive behaviour in mice[89], supporting the view of the cerebellum as a significant contributor to emotional processing and related behaviour. Similarly, a very recent study found that dopamine D2 receptors on PCs play a crucial role in sociality and the reduction of their density disturbs sociability and social novelty-seeking in adult male mice without affecting motor skills[90].

Another study employed calcium imaging to study the activation of cerebellar granular cells in mice during delayed sugar-water reward[91]. Although some populations of granular cells responded mainly to sensorimotor aspects of the tasks, other granular cells were active specifically during reward anticipation or unexpected omission of the rewards. It suggests that the cerebellar granular cell may contribute to the neural coding of reward anticipation, analogously to cerebellar motor-related predictive and anticipatory processing[91].

Finally, another study showed that the cerebellum is required for the development of full mental capabilities[92]. In the experiment, chemogenetic disruption of interneurons in the molecular layer of several posterior cerebellar subregions in mice altered behaviour and cognition in juvenile mice, although the same chemogenetic disruption in adult age caused substantially weaker effects[92]. Specifically, the juvenile interneurons disruption led to impaired eyeblink conditioning (paravermal lobule VI and crus I), cognitive inflexibility (lobule VI), prolonged grooming in response to saline injection (indicative of persistent behaviour), reduced novelty seeking and exploration (both lobule VII), and reduced sociability (Crus I/II). On the other hand, acute disruption in adulthood sometimes led to the opposite outcome than the developmental disruption (e.g. increased vs. decreased exploratory behaviour after lobule VII disruption)[92]. These results thus suggest a cerebellar contribution to wide-brain maturation.

2.2.3 Cerebellar connectivity in emotions and higher-order cognition

The cerebellum has been proposed to modulate cognition via its connections to cortical associative areas, and emotional regulation through modulation of limbic regions[20]. The idea that the cerebellar function may have a general neuromodulatory effect on the forebrain has been published since the seventies[93,94]. 20 years of neuroimaging research have mostly supported this idea.

The cerebellar-cerebral loops were mapped extensively using viral tracing in mice[95] and non-human primates[19,22,96]. Retrograde tracing in apes showed that the primary motor cortex (M1) receives input from Purkinje cells located primarily in cerebellar lobules IV-VI, whereas the dorsolateral prefrontal cortex (DLPC; essential region for executive control[97]) received inputs from PCs of Crus II of the ansiform lobule. Congruently, the same pattern was observed with anterograde tracing: M1 area projects to the granular cerebellar cells in lobes IV-VI whereas DLPC projects dominantly to Crus II, both via pons, suggesting a closed cerebellar-cerebral loop. The prefrontal-cerebellar connections were shown to be mediated through the ventral dentate nucleus[98], sometimes referred to as the 'prefrontal' module of the nucleus, and thalamus[19]. Generally, the cerebellar connections with the motor cortex dominate over the prefrontal-cerebellar connections in non-human primates[19,99]. This asymmetry could, however, reflect the relative under-development of the macaque's prefrontal cortex, compared to the highly enlarged prefrontal cortex in humans. This is also supported by a study by Matano[21], who found that the ventral dentate nucleus (the 'prefrontal' module) is disproportionally enlarged in humans compared to the non-human primates.

The research performed directly on humans further extended our knowledge about cerebro-cerebellar connectivity[100,101]. The connections of the cerebellar hemispheres have been reported in diverse cortical regions, including various parts of the prefrontal cortex (including the ventromedial parts) and associative areas of parietal and temporal lobes[100–103], throughout different thalamic sub-regions[104]. Moreover, it was found that in humans (in contrast to apes), the dentate connections to associative cortical areas are comparably rich as the connections to the motor cortex[6].

During the past 15 years, neuroimaging studies focused more on whole neuronal networks, rather than activation of single areas individually, reflecting the finding that the brain activity patterns are usually strongly correlated during one state and anti-correlated

among different states[105]. This led to the identification of three main networks: *executive network, default mode network* (DMN) and *salience network*[106]. The executive network activates during a cognitively demanding task and includes activation at the lateral cortical region, particularly the dorsolateral prefrontal cortex (DLPC) and posterior parietal cortex (intraparietal sulcus)[107,108]. During resting states (daydreaming or autobiographical memory retrieval), the executive structures are inactivated whereas midline cortical structures of the DMN (ventromedial prefrontal cortex, precuneus) increase their activation dramatically[108]. The salience network includes particularly the anterior cingulate cortex and anterior insula and is responsible for the detection of salient stimuli, attentional shifting and switching between the networks[107]. The cerebellum has also been found to be part of these functional networks: one study found that particularly Crus I and II participate in the executive network, lobule VI in the salience network whereas lobule IX contributes to DMN[109]. In contrast, another study found evidence for a contribution of the mid-hemispheric Crus I and II in DMN[110]. This disagreement was discussed in the literature with a conclusion that different portions of Crus I were included in both studies and different Crus I subregions may be part of different networks[111]. Finally, cerebellar lobules VI and Crus I seem to be part of the salience network[109].

Interestingly, the communication between the cerebellum and cerebral cortex are richly sustained not only in an awake state, but also during sleeping, especially during the REM sleeping phase[75], and the cerebro-cerebellar communication during sleep is expected to play an important role in cortex-dependent memory consolidation[75].

Besides connections with the cerebral cortex, emerging evidence point out rich cerebellar connections to basal ganglia[102,112], and this interconnection may mediate some of the cognitive and emotional processes. Viral tracing in rodents revealed disynaptic cerebellar projections to the basal ganglia through various thalamic nuclei[113]. Bidirectional connections between these two structures in non-human primates (macaques) have also been evidenced with viral tracing[114]: the research suggested disynaptic projections of the dentate nucleus to the putamen, and disynaptic projections from the subthalamic nucleus to the cerebellar cortex, including specifically non-motor cerebellar sub-regions[114]. Moreover, the cerebellum is capable of rapid modulation of striatal functions and cortico-striatal plasticity in mice[115]. In humans, a fMRi study

revealed that the cerebello-thalamo-basal ganglionic network contributes to explicit learning[116].

Other functional studies point out interconnection between the cerebellum and nucleus accumbens, the structure of basal ganglia implicated in various emotions, reward system and addiction[117], and this connectivity is hypothesised to play a role in reward-based learning. Similarly, the ventral tegmental area (VTA) is also crucial for reward cognition[118,119] and, along with other structures (including nucleus accumbens), forms ‚limbic part' of basal ganglia. A recent study published in the *Science* journal identified strong cerebellar projections to the VTA, where the projections formed dense dopaminergic and noradrenergic synapses[120]. Interestingly, optogenetic stimulation of these projections resulted in a dramatic increase in VTA activity and affected place preference. In contrast, inhibition of the cerebellar-VTA projections dramatically reduced sociability in mice[120]. Altogether, these studies highlight the importance of the cerebellar connections to the basal ganglia in the modulation of reward behaviour and reward-related cognition.

The cerebellum creates rich connections also to other parts of the limbic system[20,94]. Particularly areas of the vermis and related fastigial nucleus create connections with the anterior cingulate cortex[121], which is essential for the perception of negative emotions, pain and saliency network[122]. A study utilizing tracers confirmed the existence of such connections and showed that the anterior cingulate cortex projects to ventral paraflocculus epsecially[123]. Moreover, the cerebellum creates connections between the hypothalamus and emotional-related areas of the brainstem to mediate somatic responses to the emotions[124]. For example, the fastigial nucleus has rich direct connections to ventrolateral periaqueductal grey (vlPAG), another key region in fear-related, defensive and maternal behaviour, essential also for "freezing" response to fearful stimuli and evaluation of potential danger[125–128]. A recent mouse study showed that stimulation of vlPAG by optogenetic approach robustly facilitated freezing[129]. Further, glutamatergic outputs from the fastigial nucleus were able to robustly activate approximately 20% of all GAD2- and Chx10-positive neurons and approximately 70% of dopaminergic TH-positive neurons in vlPAG slices[129]. Stimulation of the fastigial afferents in the vlPAG supported inhibition of the Chx10-positive neurons throughout D2 receptor activation. It

suggests that the vermal cerebellum may modulate the dopaminergic system of the vlPAG[129] and thus drive freezing response.

Finally, accumulating evidence highlight the potential importance of communication of the cerebellum with the hippocampus, another brain structure that plays a critical role in both emotional processing and higher-order cognition.

2.2.4 Interactions between cerebellum and hippocampus

The hippocampus is one of the most critical brain structures in both emotional processing and diverse cognitive functions. It is particularly known to be essential for spatial and episodic memory, spatial orientation, stress regulation, social discrimination and many others[130–132]. The idea of cerebello-hippocampal communication could arise by comparing their partially shared functions: both affect spatial processing and memory[13,71,130], learning for trace eyeblink conditioning[133–135], social behaviour and memory[69,136–140], stress resiliency[20,141], behavioural flexibility[139,142–144], and time perception[145–147]. Finally, hippocampal neurogenesis has been recently suggested to contribute to the preference for future reward[148], the traits inversely correlated with behavioural disinhibition and impulsivity seen in cerebellar patients[7] or mouse models of cerebellar degeneration[149–151]. Moreover, early physiological studies suggested, that the cerebellum and the hippocampus are functionally interconnected: stimulation of the cerebellar fastigial nucleus in cats resulted in an electrophysiological response in the hippocampus and the stimulation of the hippocampus led to a response in the lobule VI of the posterior cerebellar lobe[152].

Newer research has consistently shown that the cerebellum and the hippocampus collaborate to mediate successful trace eyeblink conditioning learning in rodents[134]. A study from 2009 even showed that the cerebellar activity during this task followed hippocampal theta oscillations and the absence of these hippocampal oscillations disturbs the cerebellar activity pattern needed for successful trace eyeblink conditioning[153]. Similarly, a recent preprint showed that the cerebellum modulates a coherence between hippocampal and medial prefrontal cortical gamma oscillations that are required for working spatial memory[154]. Disruption of the cerebellar lobule simplex activity impaired this hippocampal-prefrontal coherence and consequently the working spatial memory[154].

Another research utilized mice genetically engineered to lack long-term depression between parallel fibres-PCs cerebellar synapses to learn a spatial task in MWM[43]. Although these mice did not evince a deficit in navigation during the light period, their spatial learning was impaired when they had to rely on self-motion cues during darkness[43]. Moreover, electrophysiological recordings from the hippocampus revealed that their hippocampal spatial code (place cells activity) was disrupted during darkness, showing the cerebellar-hippocampal interaction as essential for spatial learning without visual cues[43,155,156]. In a recent study by the same laboratory, they used mouse PCs-specific knock-outs for calcineurin, with altered cerebellar functions and learning[157]. These mice evinced unstable hippocampal place cell representations and spatial orientation/memory deficits both under light and in the darkness[157]. Studies on humans partially support these findings. For example, functional connectivity of cerebellar lobules Crus I and VIIA to the hippocampus and parietal and prefrontal cortices were found to participate in several cognitive aspects of spatial orientations in humans[158]. Another study showed that the cerebellum may contribute to the retrieval of episodic events and the separation of overlapping memories into different representation[159] – the function which has been traditionally attributed to the hippocampus and its adult-born granular neurons[142]. These studies altogether suggest that the cerebellar output to the hippocampus may offer crucial information necessary for hippocampal positional processing and the hippocampal spatial representations[155,160].

Interestingly, recent studies employing optogenetic modulation suggest, that the cerebellum may not only acutely offer relevant information to the hippocampus but also may modulate the general level of hippocampal activity and excitability[161,162]. The first study aimed to use optogenetic stimulation or inhibition of the hippocampus or the cerebellum to regulate temporal lobe epileptic seizures in an intrahippocampal kainate mouse model (kainate is unilaterally injected into the hippocampus of adult mice). Direct manipulation with hippocampal activity was generally inefficient. On the other hand, excitation of parvalbumin interneurons and PCs in the vermis resulted in reduced both duration and frequency of the temporal lobe seizures[161]. Inhibition of the vermis and both excitation and inhibition of cerebellar hemispheres tended to reduce seizure duration but did not affect their frequecny[161]. In the following study, they focused on an optogenetic excitation or inhibition of fastigial output specifically. In line with previous research,

stimulation of the fastigial glutamatergic neurons was evidenced to robustly mitigate the temporal lobe epileptic seizures[162].

Although the cerebellum and the hippocampus seem to be interconnected functionally, an exact connectivity map has not been explored so far. A recent study by Bohne et al.[163] explored the connectivity pattern using both anterograde and retrograde viral traces. They identified rich connectivity from all the three cerebellar nuclei to the dentate gyrus of the hippocampus via a trisynaptic connection in the scheme: cerebellar nuclei > lateral thalamus > subiculum, retrosplenial and rhinal cortex > hippocampal dentate gyrus[163], confirming the existence of polysynaptic structural connectivity between the cerebellum and the hippocampus.

Finally, research on mouse models with specific degeneration of the cerebellar cortex shows that these mice evince an increased level of corticosterone both in basal and after stressful situation[164–166]. Given the fact that increased corticosterone concentration impairs specific sub-populations of hippocampal interneurons (parvalbumin-[167] and neuropeptide Y-positive[168]) and damages hippocampal neurogenesis[141,169,170], we can speculate that the cerebellar degeneration may indirectly cause a hippocampal cell loss and limit the hippocampal neurogenesis due to consistently increased corticosteroids levels. However, to my best knowledge, this hypothesis has never been explored so far.

2.3 Cerebellar contribution to psychiatric disorders

The above-mentioned findings have put more attention to potential role of the cerebellum in various psychiatric diseases. Growing pieces of evidence have shown that the cerebellar dysfunctions contribute to psychiatric diseases and that the modulation of the cerebellar functions may constitute their potential treatment[171]. In this section, I will focus mostly on the neurodevelopmental diseases for which there is robust evidence of cerebellar involvement, i.e.: autism spectrum disorder (ASD) and attention deficit and hyperactivity disorder (ADHD). Besides these, recent studies suggest cerebellar involvement in many other mental diseases, including schizophrenia[172–175], mood disorders[176–179], anxiety disorders[18,180], obsessive-compulsive disorder[181–183], post-traumatic stress disorder[184], dyslexia[185] or personality disorders[186,187]. Interestingly, multiple psychiatric diseases often run together in families and the genetic risk is shared across many different psychiatric diseases[188,189]. This led to the view that there are general

factors that influence liability to any psychiatric disorder, the 'p factor'[190]. A recent study used MRI and psychological testing in 1246 university students to find anatomical correlates of the disturbed mental state. Surprisingly, the study identified the grey matter volume of the left cerebellar lobule VIIb, along with visual cerebral cortex thickness, as the strongest volumetric predictors of general mental health[191]. From this point of view, the cerebellum may hypothetically constitute the neurobiological substrate for general mental resilience.

2.3.1 Cerebellar role in autism spectrum disorder

The cerebellar dysfunctions have been the most thoroughly studied in ASD and the cerebellum is nowadays considered to be one of the most consistent sites of neuroanatomical abnormalities in the ASD[192,193]. The ASD represent a broad spectrum of diseases, which are all characterized by impaired behavioural flexibility (i.e. stereotyped behaviour and preference for routine), impaired social cognition (e.g. lack of cognitive empathy and inability to read non-verbal communication correctly) and altered imagination[1]. The ASD is often related to mental retardation, but a substantial proportion of the ASD individuals show normal or high intelligence (*high-functioning autism* [HFA] and formerly also *Asperger syndrome*)[194]. A high rate of ASD (including HFA) individuals suffer also from other mental disorders, such as anxiety, mood disorder or obsessive-compulsive disorder[194]. Moreover, the majority of the patients have problems with fine motor control and show signs of *developmental coordination disorder*[195]. Conversely, children with cerebellar damage show apparent autistic traits[196].

The cerebellar implication in ASD has been suggested in early postmortem studies[197] which pointed out the abnormal size and reduced numbers of neurons in cerebellar nuclei of autistic patients[198,199]. Moreover, the postmortem studies documented reduced numbers of PCs, particularly in posterior subregions of the cerebella of autistic individuals[199]. In one of the studies, the visible loss of the PCs was very marked and was seen in all the 9 brains of autistic individuals[199]. Another recent study compared 8 postmortem brains of ASD patients and 8 age- and sex-matched controls and confirmed the reduced PCs density in autistic individuals[200]. Moreover, they identified Crus I and II as the sites of the most marked PCs loss[200]. Similarly, the PCs were repeatedly found to be significantly smaller in the ASD individuals, and some individuals had only half-sized PCs compared to

controls[201]. Correspondingly, expressions of numerous proteins related to neurotransmission and neuroplasticity were found to be distinctly abnormal in humans with ASD[202–205]. Moreover, cerebella of ASD patients were documented to evince neuroglial activation and other signs of neuroinflammation[206]. Finally, distinct cerebellar abnormalities have been repeatedly documented also in various mouse models of ASD, including *Shank*-deficient mice[207] and *Tsc* mutant mice[208]. Conversely, mouse models of cerebellar degeneration evince autistic-like behaviour[209].

The implication of the cerebellar dysfunctions in ASD is supported by imaging studies utilizing the MRI[210]. In the study of 52 autistic preschool children (aged 2-5 years), ASD individuals (including 12 HFA children) showed generally increased cerebellar volume, particularly in the grey matter of the anterior vermis and white cerebellar matter. Interestingly, the volume of the cerebellar white matter was increased by 36% in the ASD. Moreover, any of the 15 age-matched control children did not reach the average volume of the ASD group and all the 52 autistic children had higher cerebellar white matter volume than the average of the control group[210]. On the other hand, grey matter in some cerebellar subregions, particularly Crus I and II, was found reduced in the ASD children (8-13 years of age; N= 35 per group)[211], and the extent of the right Crus I and II grey matter volume predicted the severity of the behavioural symptoms[211]. Correspondingly, functional MRI (fMRI) showed abnormal functional cerebello-cerebral connectivity in individuals (both children and adults) with ASD[212]. In the ASD, the typical contralateral cerebellar-cerebral connectivity (particularly right cerebellar Crus I connection with contralateral prefrontal and parietal cerebral cortex) was weakened. In contrast, normally weak ipsilateral cerebellar-cerebral connections were strengthened in the ASD individuals[192,193,212,213]. Similarly, cerebellar connectivity within DMN was reduced in the ASD and negatively correlated with autistic traits in healthy individuals[214].

New insight into the role of the cerebellum, namely right Crus I, in ASD brought a recent study published in Nature Neuroscience[215]. In the first step, the authors confirmed that the activity of the right Crus I is coupled with activation of contralateral associative areas of the prefrontal cortex, temporal and parietal cortex (the structures implicated in the ASD patients) but is anticorrelated with the activation of the sensorimotor cortical regions[215]. Next, they used anodal transcranial direct-current stimulation (tDCS) in humans, and a chemogenetic approach in mice, to stimulate right Crus I and found that

the posterior cerebellar neuromodulation resulted in reduced right Crus I connectivity with the left inferior parietal lobule; this pattern was seen in both human participants and mice. Moreover, they confirmed that the right Crus I connectivity with the left inferior parietal lobule is reduced in autistic patients and mouse ASD model (PCs-specific *Tsc1*-mutant mouse). Further, they showed that right Crus I inhibition in healthy mice mimics the deficits of the ASD mouse models, including decreased social preference, reduced social novelty seeking and behavioural inflexibility in the water Y-maze test[208,215]. Correspondingly, the chemogenetic stimulation of the PCs in the right Crus I of the mouse ASD model reverse these deficits. These results thus provide robust evidence that the cerebellar Crus I may play important role in the ASD pathology and its modulation might be a promising tool for the management of the ASD symptoms[215].

2.3.2 Cerebellar contribution to attention deficit and hyperactivity disorder

Attention deficit (and hyperactivity) disorder (ADD/ADHD) is another neurodevelopmental disorder with relatively robust evidence of the cerebellar influence and with high overlap between its symptoms and the CCAS[216]. In children, ADHD manifests with problems with attentional control (problems with attentional shifting, inability to pay attention to "boring" yet objectively important stimuli), impulsivity (speaking and acting 'before thinking'), hyperactivity (in case of the ADHD *sensu stricto*, not in the ADD) and emotional lability[217,218]. In adults, hyperactivity is less prominent, but the individuals are unorganized, excessively procrastinating, overly daydreaming, risk-seeking and incapable to pay attention to details and 'boring' stimuli. The emotional instability usually persists into adulthood and commonly evolves into associated psychiatric comorbidities, most commonly anxiety and mood disorders and cluster B personality disorders[219–221].

Besides these core symptoms, approximately half of ADHD children also show poor fine and gross motor skills[216,222–225]. The motor deficits tend to improve over time[226] and with stimulant medication[227]. Interestingly, some studies suggested that the motor deficits predict substantially poorer outcomes in adult life (17 years later)[228] and predict better therapeutic response to methylphenidate medication[216], although evidence for this is incongruent[229,230]. Moreover, the severity of the motor symptoms correlates with ADHD symptoms[224,226]. The cerebellar-related impairments have been therefore suggested to

constitute a supplementary tool for identification of the children with ADHD and their distinction from paediatric bipolar disorder patients[216]. Moreover, some motor signs, such as swaying during a walk, partially persist into adulthood and correlate with reduced cerebellar grey matter volume[223].

Although ADHD is related to wide neuropathology, particularly in the prefrontal cortex, striatum, thalamus and related dopaminergic and noradrenergic circuits[231], cerebellar anatomical abnormalities are a common finding in the ADHD[216]. Moreover, the CCAS resembles the ADHD condition in many aspects, including behavioural disinhibition and impulsivity, attentional control deficit, social immaturity and emotional lability. Analogously, the disinhibited behaviour of the cerebellar mouse models also evokes a strong resemblance with ADHD-like behaviour. More importantly, the cerebellar implication in ADHD is nowadays well supported by structural imagining studies, showing that the cerebellum is one of the most affected brain structures[232]. The cerebellar volume is generally decreased approximately by 5% in ADHD children[231,233], with the most marked difference in posterior inferior vermis[234]. A more recent MRI study of 49 ADHD youths (8-18 years of age) and 59 age-matched controls also found a difference in the cerebellar volume, particularly in posterior cerebellar hemispheres, and found that the reduced vermal volume predicts higher ADHD severity[235]. Interestingly, long-term stimulant medication was related to a larger volume of the left cerebellar surface[235], suggesting its causal therapeutic effect. Correspondingly, an MRI study on 486 adults (214 ADHD patients, 96 unaffected siblings, and 176 healthy controls) identified the cerebellum, along with the prefrontal cortex, as the main affected brain regions[236]. Moreover, the study found that reduced volumes of cerebellar tonsils and culmen predict more severe inattention, whereas generally decreased cerebellar grey matter volume is associated with more severe impairments in executive functions[236]. Finally, another study pointed out increased serum antibodies against Purkinje cells (Yo-antibodies) in the population of children with ADHD[237]. Taken together, ADHD has been nowadays believed to have strong cerebellar involvement and to stem from dysfunction of frontal–striatal–cerebellar circuits[236,238].

2.4 Cerebellar diseases

The cerebellum may be damaged in many ways and the cerebellar diseases and damage are thus extremely variable. In general, the magnitude of the cerebellar ataxia is evaluated using several scales of ataxia[239], including the *International Cooperative Ataxia Rating Scale* (ICARS), the *Brief Ataxia Rating Scale* (BARS) and the *Scale for the Assessment and Rating of Ataxia* (SARA). Other scales constructed for specific cerebellar diseases are also available, for example, *Friedreich Ataxia Rating Scale* (FARS)[239].

2.4.1 Acquired and secondary cerebellar dysfunctions

The cerebellar impairments may be acquired by cerebellar injury as in the case of the first comprehensive description of cerebellar motor syndrome by Holmes in 1917[240]. Although the cerebellum is rarely injured by direct cerebellar-specific insult, research performed on both animal models and human patients after traumatic brain injury revealed that even indirect insult to the cerebrum often leads to secondary cerebellar damage[241]. This secondary cerebellar injury seems to contribute particularly to motor components of the traumatic brain injury[241]. The cerebellum could be also damaged by hypoxia and some evidence even show that the cerebellum (and particularly PCs) are among the brain structures the most sensitive to the hypoxia in adults[242] and is selectively damaged in prematurely born and/or hypoxic newborns[243,244]. The cerebellum is also highly sensitive to toxins, including alcohol: acute intoxication disturbs cerebellar function whereas chronic overuse causes substantial cerebellar damage[245]. Specific cerebellar damage may also occur after long-term use of high doses of lithium salts, chemotherapy, gadolinium and many other pharmacological compounds[246].

The cerebellum could be damaged by strokes (cerebellar strokes constitute 2% of all strokes)[247,248]. Various types of tumours may be located in the cerebellum, or close to it, and may damage the cerebellum[249]. Various infectious diseases (e.g., the virus responsible for varicella or Epstein–Barr virus causing mononucleosis) may cause acute cerebellar inflammation (acute cerebellitis) and permanent damage to the cerebellum[250]. The cerebellar ataxia could be also caused by bacterial infections, namely Lyme disease (*Borrelia burgdorferi sensu lato*) or infection by *Legionella* spp[251]. One of the most common cerebellar ataxia is caused by an autoimmune process triggered by gluten consumption[252]. This form is called *gluten ataxia* and constitutes 15% of all cerebellar

ataxias[253]. Fortunately, long-term avoidance the gluten often leads to nearly complete recovery within 2 years[252]. Similarly, the presence of antibodies against GAD may cause selective damage to the PCs and cerebellar damage[254]. In addition, paraneoplastic cerebellar degeneration is another cause of cerebellar damage due to autoimmunity. It is often triggered when tumour cells express proteins normally expressed by PCs[255–257]. Moreover, cerebellar dysfunction could be induced by vitamin B12 or succinic semialdehyde dehydrogenase deficiency[258–260]. The cerebellum could be also congenitally underdeveloped (e.g., pontocerebellar hypoplasia, Dandy-Walker malformation)[261]. Next, the cerebellum might be affected by many genetically-determined metabolic diseases, including various mitochondrial diseases[262,263], autoimmune thyroid diseases[264] or lysosomal Niemann–Pick disease[265]. Finally, substantial cerebellar dysfunction and related ataxia constitute one of the most often hallmarks of multiple system atrophy[266].

An increasing piece of evidence has pointed to cerebellar damage in relatively frequent neurological and neurodegenerative diseases which are characterized mainly by diffused or out-of-cerebellar neuropathology. The cerebellar damage is very common in multiple sclerosis (MS)[267], an autoimmune disease associated with inflammatory damage to myelin sheaths and unrelenting neurodegeneration[268–270]. The cerebellar dysfunctions in the MS include particularly lesions of the cerebellar peduncles, reduced cerebellar connectivity and cerebellar cortical atrophy[267,271,272]. A study performing an autopsy on MS patients revealed that on average 38% of the surface of the cerebellar cortex is atrophied in MS patients[272]. Moreover, the cerebellar dysfunctions correlated with both physical disability and cognitive dysfunctions of the MS patients[273]. Besides the MS, the increasing pieces of evidence point out cerebellar dysfunctions in the most common neurodegenerative diseases, such as Alzheimer's disease[274–276], Parkinson's diseases[277,278] or Frontotemporal dementia[279–281]. However, how much the cerebellar dysfunctions contribute to the impairments in these diseases is not clear.

Although the cerebellum could be affected in numerous neurodegenerative and neurological diseases, there is a group of hereditary diseases where the cerebellar dysfunctions and related cerebellar signs represent the main hallmarks of the diseases. They are collectively labelled as hereditary cerebellar ataxias[2].

2.4.2 Hereditary cerebellar ataxias

Hereditary cerebellar ataxias are an extremely heterogeneous group of cerebellar diseases, varying in terms of pathophysiological mechanisms as well as the relative importance of the non-cerebellar pathology[2]. This group of diseases is usually divided according to the mechanisms of inheritance into four clusters[2]: (1) autosomal recessive cerebellar ataxias (ARCA); (2) autosomal dominant cerebellar ataxias (ADCA); (3) X-linked; and (4) Ataxias with mitochondrial gene mutations[2]. The first category includes *Friedreich's ataxia*, *Ataxia–telangiectasia*, *Cerebrotendineous xanthomatosis* and other rare conditions[2]. The second category includes 7 types of *episodic ataxias*, *autosomal dominant spastic ataxia*, *dentatorubral-pallidoluysian atrophy* (DRPLA) and a large group of *spinocerebellar ataxias* (SCA)[2]. The X-linked hereditary ataxias include mainly X-linked sideroblastic anemia and ataxia and fragile X-associated ataxia[2]. The last group consists of ataxias with mitochondrial gene mutations. As the X-linked and mitochondrial mutation ataxias are rare with very diverse and complex symptomology (cerebellar dysfunction usually represents only a small portion of neuropathology)[2], I will focus more on the first two categories.

The autosomal-recessive hereditary ataxias are generally rare, with the maximal frequency of 3-4/100,000 in the case of *Friedreich's ataxia*[282–284]. Practically all these diseases have very complex pathology with damage to various inner organs and with the cerebellar pathology as one of many hallmarks[285]. Therefore, they may be viewed as multisystem diseases, rather than specific neurodegenerative diseases. As an example, the most common ARCA, *Friedreich's ataxia*, is caused by a mutation in the FXN gene, leading to a reduced level of mitochondrial protein *frataxin*[283]. It usually starts between the age of 5 to 20 years and affects multiple organs, including the heart, pancreas and spinal cords among others[282–284].

The autosomal-dominant hereditary ataxias constitute an extremely heterogeneous group of diseases too, but in contrast to the ARCA, their pathology is mostly restricted to the central nervous system[286]. Some of them evince very early onset (e.g., most of the episodic ataxias) whereas others tend to occur later in life (e.g., SCA6)[287]. Although some of these evince very complex neuropathology, extending beyond the cerebellum or even brain (e.g., retinal damage in SCA7)[288], others are purely cerebellar (e.g., SCA5)[10]. Although there are often slowly progressive, some progress fast and are fatal (SCA1-3

with the average duration of 5-20 years)[289]. One of the sub-groups, the episodic ataxias, is characterized by bouts of ataxia, frequently provoked by acute psychological or physical stress[290]. To date, 7 episodic ataxias have been identified[10]. Altogether, the episodic ataxias are very rare, with an incidence < 1:100,000[290]. The episodic ataxias usually commence in childhood or early adulthood and some types of the episodic ataxias tend to mitigate over time. Besides the bounds of ataxia, some of the episodic ataxias include migraine, epileptic seizures, or other symptoms[290].

The DRPLA is genetically caused by an expansion in the polyglutamine (CAG) repeats in the ATN-1 gene, coding Atrophin-1 protein[291,292]. Therefore, the DRPLA falls into the group of *polyglutamine diseases*, the diseases caused by CAG trinucleotide expansion, including several SCAs (types 1-3, 6-7, 12 and 17), *Huntington's disease* and *spinal and bulbar muscular atrophy*[293]. The CAG expansion in the ATN-1 gene leads to overall brain and spinal cord atrophy, and very complex symptomatology, sometimes resembling Huntington's disease rather than ataxia[287]. The DRPLA includes diverse symptoms, including ataxia, dementia, epileptic seizures and dystonia among other[294]. The onset may come in childhood but also in the elderly, depending on the number of the CAG repeats[291,292,294].

As SCAs are of the main interest of this thesis, representing a wide sub-group of the ADCA, I will focus on the SCA in more detail in the following section.

2.4.3 Spinocerebellar ataxias (SCAs)

The SCAs are diverse autosomal-dominant neurodegenerative diseases, associated particularly with cerebellar dysfunction and/or degeneration[295]. The first SCA (SCA 1) was identified in the early nineties and genetically characterized in 1994[296]. To date, at least 47 autosomal-dominant spinocerebellar ataxias have been identified[297]. Polyglutamine SCA types 1, 2, 3, 6 and 7 are the most common SCA types and include over 75% of all SCA cases[298]. Although features of the SCA types differ, the majority of the SCAs are primarily characterized by ataxia, incoordination of movements, loss of balance, dysarthria, and other cerebellar signs[293,299]. However, many SCAs have additional features, such as extrapyramidal signs (including dystonia, i.e., spasm and involuntary muscle movement, and parkinsonism symptoms), weakness or paralysis of the extraocular muscles, upper limb tremor, neuropathy and sensory impairments,

impaired cognition, and emotional disturbances (see sections 2.4.5 and 2.4.6 below) and many others[10]. Similarly, neuropathology in many SCAs often extends beyond the cerebellum and includes the brainstem, spinal cord, cerebral cortex, basal ganglia, thalamus, or retina[10,299,300]. According to the presence of the non-cerebellar symptoms, SCAs are commonly divided into the three clusters[10,297]:

1. ADCA I: The most serious sub-group with the most complex neuropathology extending beyond the cerebellum. This subgroup includes the majority of the SCAs. If DRPLA is included in this classification, it matches this category as well.
2. ADCA II: Cerebellar pathology + retinal degeneration (SCA 7).
3. ADCA III: Purely cerebellar SCAs, without marked neuropathology outside of the cerebellum (SCA 5, 6, 11, 23, 26, 30, 41 and 45) and with specific cerebellar-related symptoms[297].

Another classification divides the SCAs into two categories only: 1. with complex pathology (1st and 2nd category in the previous classification); 2. purely cerebellar[10]. Because of overlapping and unspecific symptoms, a reliable diagnosis requires genetic testing[301]. Most of the existing SCAs, their symptomatology and neuropathology are listed in Table 1. Next, I will focus more on the most prevalent SCA types, the SCA types 1, 2, 3, 6 and 7, altogether constituting the majority of all SCA cases.

SCA type (affected gene)	Type of mutation	SCA cluster	Specific features
SCA1 (ATXN1)[296,302]	Poly-CAG	Complex	Fast progression[303]
SCA2 (ATXN2)[304]	Poly-CAG	Complex	Marked spinal cord pathology
SCA3 (ATXN3)[305]	Poly-CAG	Complex	Marked striatal and cerebellar nuclei path.
SCA4 chrom. 16q22.1[306]	Point mutation	Complex	Areflexia, sensory neuropathy
SCA5 (SPTBN2)[307]	Point mutation	Purely cerebellar	Downbeat nystagmus
SCA6 (CACNA1A)[308]	Poly-CAG	Purely cerebellar	
SCA7 (ATXN7)[309]	Poly-CAG	ADCA II	Retinal degeneration, visual loss
SCA8 (ATXN8)[310,311]	Poly-CTG/CAG	Complex	Severe dysarthria
SCA10 (ATXN10)[312]	Poly-ATTCT	Complex	Epilepsy
SCA11 (TTBK2)[313]	Truncating mut.	Purely cerebellar	Tau deposits out of the cerebellum
SCA12 (PPP2R2B)[314]	Poly-CAG	Complex	Tremor (often the 1st sign)
SCA13 (Kcnc3)[315]	Missense mut.	Complex	Mental retardation
SCA14 (PKCγ)[316]	Missense mut.	Complex	Myoclonus
SCA15/16 (ITPR1)[317]	Partial deletion	Complex	Tremor
SCA17 (TBP)[318]	Poly-CAG/CAA	Complex	Dementia, psychosis and epilepsy
SCA18 (IFRD1)[319]	Missense mut.	Complex	Peripheral neuropathy
SCA19/22 (KCND3)[320]	Mutations	Complex	
SCA20 (DAGLA)[321]	12 gene duplication	Complex	Dentate nucleus calcifications; dysarthria without ataxia as the first symptom[322]
SCA21 (TMEM240)[323]	Missense mut.	Complex	Rest tremor
SCA23 (PDYN)[324]	Missense mut.	Purely cerebellar	
SCA25 (loc. 2p21-p13)[325]		Complex	Sensory neuropathy, intestinal symptoms
SCA26 (eEF2)[326]	Missense mut.	Purely cerebellar	
SCA27 (FGF14)[327]	Missense mut.	Complex	Cognitive impairments
SCA28 (AFGF3L2)[328,329]	Missense mut.	Complex	
SCA29 (ITPR1)[330,331]	Missense mut.	Complex	Congenital, non-progressive
SCA30 (loc. 4q34.3-q35.1)[332]		Purely cerebellar	
SCA31 (PLEKHG4)[333]	Poly-TGGAA	Complex	
SCA32 (chrom. 7q32-q33)[334]		Complex	Cognitive impairments; male infertility
SCA35 (TGM6)[335]	Missense mut.	Complex	Tremor. spasmodic torticollis
SCA36 (NOP56)[336]	Poly-GGCCTG	Complex	Motor neuron involvement
SCA37 (DAB1)[337]	Poly-ATTTC	Purely cerebellar	Altered vertical eye movement[338]
SCA38 (ELOVL5)[339]	Missense mut.	Complex	
SCA40 (CCDC88C)[340]	Missense mut.	Complex	
SCA41 (TRPC3)[341]	Mutation	Purely cerebellar	
SCA42 (CACNA1G)[342]	Missense mut.	Complex	
SCA43 (MME)[343]	Mutation	Complex	Axonal neuropathy
SCA44 (GRM1)[344]	Missense mut.	Complex	Intellectual disability
SCA45 (FAT2)[345]	Mutation	Purely cerebellar	
SCA46 (PLD3)[345]	Missense mut.	Complex	Sensory neuropathy
SCA47 (PUM1)[346]	Missense mut.	Complex	
SCA48 (STUB1)[347]	Mutation	Complex	Cognitive-psychiatric features

Table 1: Types of the autosomal-dominant spinocerebellar ataxias. 'Specific features' lists the symptoms and pathologies that are distinctly more common, severe or come earlier in the given SCA types compared to other SCA types. Abbreviations: 'mut'= mutation. 'path.'= pathology. 'loc.'= locus. 'chrom. = chromosome.

2.4.4 Most common SCA types

The **SCA1** has a global incidence of approximately 1-2/100,000, with strong variability among regions[10]. For example, the SCA1 constitutes the most common SCA type in Poland, Russia and South Africa[10,298]. The disease is caused by CAG expansion (over 38 CAG repeats) in the ATXN1 gene, coding ataxin-1 protein[296,302]. Ataxin-1 is widely expressed in the brain and its functions are not completely understood[348,349]. However, it seems to regulate the expression of other genes, including other gene regulators[348]. Interestingly, the variation in the ATXN1 gene was found to correlate with cognitive impairments in humans[350,351], and some research showed that variation in the ATXN1 gene may be associated with an increased risk of developing *amyotrophic lateral sclerosis* (ALS)[351–354] or *multiple sclerosis*[355,356]. The Ataxin-1 is also needed for normal cognitive functions and hippocampal neurogenesis according to the studies of Atxn1-deficient mice[357–360]. The SCA1 may start from infancy to late adulthood, depending also on the number of CAG repeats, but most commonly in middle age[10]. The disease is fatal, with an average survival of 10-20 years and 10-years survival estimated to 57%[289]. The survival is negatively correlated with the presence of dysphagia, higher SARA score and positively with Body Mass Index[289,361]. Of all the most common SCA types, the SCA1 evinces the most rapid ataxia and disability progression[303]. The beginning of the disease is usually characterized by loss of coordination and balance, impaired gait and dysarthria[10]. Over 50% of patients suffer also from muscle atrophy[10]. The terminal phases are characterized by bulbar problems, including attenuation of swallowing and coughing reflexes, possibly leading to aspiration pneumonia (the most common cause of death in SCA1 patients)[362]. Moreover, SCA1 patients often suffer from psychiatric symptoms, peripheral neuropathy, slow saccades, upper motor neuron signs, breathing difficulty and cardiac autonomic dysregulation[363,364]. The neuropathology in the SCA1 is characterized mainly by cerebellar cortex atrophy. In addition, cerebellar nuclei, brainstem, cerebral cortex, thalamus and other brain regions are significantly altered as well[349,365]. Widespread occurrence of nuclear inclusions of the expanded Ataxin-1 and neuroinflammation has also been noticed in the postmortem brains of SCA1 patients[365].

The **SCA2** is the most common SCA type in several countries, including Mexico, India, Argentina and Cuba (40-100/100,000 in some regions)[10,286,349] or the Czech Republic[366]. The disease is caused by CAG expansion (over 31-35 CAG repeats) in the

ATXN2 gene, coding the Ataxin-2 protein which plays a role in translational regulation and formation of stress granules[287]. Analogously to the ATXN1, the expanded CAG repeats (even in magnitude that does not cause the SCA2) may be related to a higher risk of Alzheimer's disease, cognitive impairments and ALS[350,367–370]. The course of the SCA2 resembles the course in the SCA1, with an average survival of 5-25 years from diagnosis and an estimated probability of 10-years survival of 73%[289]. Besides the cerebellar signs, SCA2 patients suffer from muscle pains, weakness and atrophy. In the later disease stages, patients suffer from bulbar dysfunctions[349]. Moreover, SCA2 patients often suffer from areflexia, retinal degeneration, Parkinsonism, fasciculation, neuropathy, cognitive deterioration, psychosis and other psychiatric issues[349]. In contrast to the SCA1, the SCA2 has minimal impact on cerebellar nuclei but involves cerebral cortex atrophy. Besides the cerebellar and brainstem degeneration, the SCA2 presents with complex neuropathology including degeneration of substantia nigra (which does not occur in the SCA1)[10,349], dysfunction of related nigrostriatal pathways and degeneration of the striatal brain structures[349]. The spinal cord pathology is marked in the SCA2 and includes degeneration of the posterior thoracic nucleus, anterior horn and atrophy in the spinocerebellar tracts and posterior columns[287,371,372].

The **SCA3**, or *Machado–Joseph disease*, is the most prevalent SCA type worldwide, with the highest incidence in China, Brazil and Portugal, constituting 20-50% of all SCAs[295]. The disease is caused by the CAG expansion (>44 repeats) in the ATXN3 gene, coding Ataxin-3 protein involved in ubiquitin-dependent protein quality control[287,373] and thus regulating the activity of many proteins in diverse pathways[374]. Similarly to the SCA1 and SCA2, the onset of the SCA3 strongly varies from patient to patient, most commonly around 40 years of age. 10-years survival in SCA3 patients was estimated to 73% although the life expectancy might be unaffected in mild disease form[289]. The disease sometimes starts with ataxia, dysarthria, unbalanced gait and other cerebellar signs[10]. However, symptoms in many other SCA3 patients are characterized mainly by extrapyramidal symptoms, signs of parkinsonism, dystonia, spasticity and areflexia, particularly in the patients with early-onset and more CAG repeats[10,349]. Other symptoms include neuropathy, amyotrophy, muscle fasciculations, cardiac denervation[364,375] and psychiatric impairments. Neuropathology differs from the previously described SCAs: the cerebellar neuropathology, including neuronal loss and atrophy, is much more severe in the cerebellar nuclei compared to the cerebellar cortex. Besides the cerebellar nuclei,

the SCA3 severally affects striatum and nigrostriatal pathways and brainstem (particularly pons)[349].

The **SCA6** constitutes approximately 15% of all SCA cases worldwide and is the second most frequent SCA in Japan[10]. It is caused by CAG expansion (>18 repeats) in the CACNA1A, a gene encoding a calcium channel α subunit which is richly expressed in the cerebellar Purkinje cells. The SCA6 has a relatively late onset (usually after 50 years of age), relatively slow progression and is not fatal. It manifests predominantly with purely cerebellar symptoms, such as motor incoordination, gait and balance disturbances, dysarthria, nystagmus, vertigo and suppression of the oculomotor reflex[10]. However, some patients in the late disease stages experience additional symptoms, such as hyperreflexia, sensory abnormalities or neuropathy[10]. SCA6 neuropathology is characterized mainly by atrophy of the cerebellar cortex, although less prominent (yet microscopically detectable) pathologies could be observed in the cerebral cortex, brainstem and cerebellar nuclei[376].

The **SCA7** constitutes approximately 5% of SCA cases and constitutes the most common subtype in Venezuela. It is caused by the CAG expansion (>36 repeats) in the ATXN7 gene encoding the Ataxin-7 protein[10]. The disease usually starts around 25 years of age and manifests with visual loss, due to pigmentary macular degeneration, and cerebellar signs, such as ataxia, imbalance and dysarthria[10]. Besides these typical symptoms, the patients sometimes experience muscle spasticity, increased tendon reflexes, pyramidal signs, parkinsonism, hearing loss or cognitive dysfunctions[10]. The SCA7 is characterized mainly by olivary-cerebellar atrophy, brainstem degeneration and macular and retinal degeneration[10].

2.4.5 Cognitive impairments in SCAs [A]

Cognitive impairments were reported repeatedly in many SCA types, including 1-3, 6, 7, 10, 12, 13, 14, 17, 19, 21, 27, 29, and 32[63,300,377–379]. The magnitude of neuropsychiatric impairments varies from patient to patient but also differs among different SCA types. In a few SCA types, these impairments may be extremely severe and may represent one of the main symptoms[380]. This may be particularly true for symptoms reaching the point of

[A] This (2.4.5) and following section (2.4.6) have been already published as a review[379] written exclusively by the author of this thesis (Article 1).

dementia, which are associated with a few SCA types. Specifically, dementia has been reported to occur frequently in SCA2 patients, especially those with higher CAG repeats and earlier onset[381,382]. Dementia is also one of the dominant features in SCA17[383]. In addition, a study of SCA7 patients from 4 African families revealed that dementia occurred in one-half of the 34 SCA7 patients, particularly in the later disease stage[384]. Similarly, dementia and other cognitive and behavioural impairments represent a core feature in SCA27[327,385]. Dementia may be coupled with psychosis, which was reported to occur particularly in SCA2[386] and SCA17[380], but also in SCA3 and SCA7[387]. All the SCA types associated with dementia include complex neuropathology[10,300,388].

However, the cognitive symptoms of SCAs do not reach the level of dementia in most cases. Instead, they often present as short-term and working memory impairments, loss of mental concentration, disturbances in executive functions, deficits in verbal fluency, visuospatial impairments and impaired cognitive flexibility[63,377,378,389,390]. The magnitude and frequency of the cognitive deficits in different SCA types seem to vary, possibly mirroring the distinct distribution of neuropathology.

Studies comparing the cognitive deficits in different SCA types have mostly focused on some of the most frequent types: 1, 2, 3 and 6. In most cases, these studies suggest that SCA6 (more cerebellar-specific) may have fewer cognitive impairments: one study found approximately one-half of the frequency of distinct memory problems compared to other SCA types[391] and another study identified impaired executive functions and attention span in SCA types 1-3, but not SCA6[3]. Studies comparing SCA types with widespread neuropathology (types 1-3) suggest that executive dysfunctions and verbal memory impairments may be more severe in SCA1 compared to other types and healthy controls[392,393], in correspondence with the common cerebral cortex atrophy in this type.

Studies of correlations between severity of regional-specific neuropathology and cognitive dysfunctions generally support a strong non-cerebellar contribution to cognitive dysfunction in SCAs. For example, cognitive functions were shown to correlate with cerebral association cortices pathology in SCA2, SCA6, SCA7 and SCA10 patients[377,394,395] although cerebellar pathology correlates with some cognitive deficits, at least in some SCA types, as well[377].

In SCAs, ataxia and physical disability progress over time[303,390,396,397]. Concerning cognitive functions, the decline over time may be less robust in the most common SCA

types. One study compared 20 SCA1 and 22 SCA2 patients with a matched 17 healthy controls in terms of complex neuropsychiatric functioning, with follow-up longitudinal monitoring of some of the participants[398]. Of multiple tests evaluated, only the Attentional Matrices Test (i.e. a test of selective attention and information processing speed) significantly worsened over 2 years. Other studies detected statistically significant cognitive decline over time[399,400] whereas others did not[390], although all these studies suffered from a small sample size. Interestingly, cognitive deficits were also observed in presymptomatic mutation carriers in SCA1[390].

To sum up, cognitive deficits are common and seem to be generally more severe in SCA types with more prominent out-of-cerebellar neuropathology. Therefore, although it is currently clear that the cerebellum modulates cognitive functions in a very complex manner[57], out-of-cerebellar contribution to the cognitive deficits in SCAs may still be very important. On the other hand, most studies suffer from a small sample size and may be confounded by unequal disease severity[401,402], the extent of pathology, additional emotional dysregulation[389] and other factors.

2.4.6 Emotional dysregulation in SCAs and its consequences

Besides the cognitive dysfunctions, affective dysregulation, such as depression, anxiety and apathy are common in many SCA types[403–405]. However, their nature is not understood and there is still controversy about whether they are of biological or rather emotionally-reactive origin.

One of the arguments supporting the causal biological origin is that the frequency of depression and associated symptoms differ among SCA types. In line with this, several studies suggested that the rate of depression[391], as well as suicidal ideation[4], is higher in SCA3 than in the other most common SCA types of comparable disability, suggesting a biological causative role of the SCA3 neuropathology. For example, one study found that the prevalence of depressive complaints was more than doubled in SCA3 compared to other SCA types[391].

On the other hand, other studies do not support that the rates of depression differ among types. One study reported a difference in some of the correlates of depression, such as suicidal ideation (65% in SCA3, 39-45% in other types) but not in the frequency of distinct clinical depression among SCA types (ranging between 22-31%)[4]. Further, the

biggest study of depression comorbidity in SCA, with over 100 participants in each of the 4 most common SCA types (1, 2, 3, 6), revealed a significantly higher prevalence of depression in all SCA types compared to healthy controls, but no significant difference among SCA types[406]. The study found that moderate to severe depression occurred in 20% of SCA patients and at least mild depression was present in over 50% of all SCA patients, except for the SCA6 group[406]. Moreover, over 20% of the SCA1 and SCA3 patients, and around 15% of SCA2 and SCA6 patients, answered that they would be "better off dead" or hurting herself/himself[406]. One study reported the most marked depression in SCA1 and SCA6, compared to SCA2 and SCA3, although patients with SCA1 and SCA6 were older and had more severe ataxia, and this bias was not statistically adjusted[3].

Depression seems to play a potentially important role in the quality of life and disease course in patients with SCAs. For example, the study by Lin et al.[407] showed that the relationship between ataxia and depression severity in SCA3 is bidirectional: more severe ataxia predicted more severe depressive symptoms, and *vice versa*, severe depression predicted more rapid physical deterioration and worsening of ataxia in the future[407]. Similarly, the above-mentioned longitudinal study[4] found that depression severity predicted ataxia progression, even after controlling for CAG repeats length, sex, age and time. Furthermore, depression significantly and consistently reduced the quality of life and led to a poorer functional status in SCA1, SCA3 and SCA6 patients, even after adjusting for ataxia severity[4]. Despite the consistent finding of a correlation between ataxia and depression, longitudinal studies did not show any statistically significant change in the level of depression over time, in contrast to their growing physical disability[4,398].

Taken together, although emotional dysregulation seems to be the real problem in SCAs, constituting a source of additional suffering for SCA patients, its nature is still not understood. To date, studies of SCA patients do not allow a reliable conclusion to be drawn as to whether the emotional dysregulation in SCAs is predominantly of reactive or biological origin, and whether any specific SCA-related neuropathology contributes causally and significantly to these problems. Moreover, most studies focused merely on depression although anxiety was reported to represent an even higher burden for patients with other motor neurological diseases, such as multiple sclerosis[408], and the cerebellar

dysfunction is expected to mediate anxiety[18]. As a different approach, studying the emotional-related behaviour in animal models of SCAs may accompany the research on human patients, bringing new and potentially valuable insights into this question.

2.5 Mouse models of hereditary cerebellar diseases[B]

Animal models are extremely useful tools to study the neurobiology of diseases, namely on the cellular or sub-cellular scale[409]. Compared to human patients, they have several advantages[409–411]:

1) *Homogeneity*: Whereas groups of patients are often highly heterogeneous in terms of the extent and specific distribution of neuropathology, age and genetics (e.g. number of CAG repeats in polyglutamine diseases), mice are inbred to high genetic homogeneity. They may be compared in exact age and at on-demand sample sizes. Furthermore, studies of human patients may be limited by a small number of patients in cases of rare diseases.

2) *Detailed neuropathology examination:* In mice, neural functions may be studied in extremely deep detail, compared to humans. For example, the formation of new synapses in alive mice in real-time is achievable with multi-photon imaging[412]. Similarly, it is possible to record the activity of a specific neuronal population in moving animals or isolate specific cells to study physiological or molecular processes on a sub-cellular scale[43]. These techniques are not currently available for human patients. Although immunohistochemistry techniques are useful to study the distribution of different proteins (and thus cell types) in the postmortem human brain, usually a long time between death and brain fixation might lead to degradation of some proteins and thus inaccurate imaging[413].

3) *Experimental treatment:* New therapeutic approaches pose a high risk of adverse effects and must be first studied using non-human models before their application in humans.

4) *Modelling specific aspects of the diseases*: Mice can be genetically engineered to show narrowly specified aspects of diseases without an effect of confounding

[B] This section was already published – partially as review written solely by the author of this thesis (Article 1)[379] and partially as a review written by numerous authors (Article 2)[409]. The text from the Article 2 used here was written solely by the author of this thesis.

pathological mechanisms. For example, mutation leading to the disease may be expressed in a narrowly defined neuronal population of restricted brain regions (e.g., Purkinje cell-specific expression[414]). It enables observing, for example, a specific impact of the disease-causing Purkinje cell degeneration on learning and memory, without the effect of widespread brain damage[415].

Mice are currently the most often used animal models and they are currently commercially available for the majority of the identified monogenetic diseases. The mice are phylogenetically and physiologically related to humans (in contrast to invertebrates) and their breeding maintenance is cheaper compared to rats[416]. On the other hand, their learning seems to be too simple to model higher-order cognition and behaviour compared to rats[417] and, even more, monkeys.

2.5.1 Development of mouse models of diseases

Spontaneous mutants were used traditionally before the era of genetic engineering. In the spontaneous mutants, the mutation leading to the neuropathology occurred spontaneously and mice were further bred to keep the mutation in the breed[418]. As an example, lurcher mutant mice[419] are spontaneous mutants that were used in the research of cerebellar degeneration before the identification of the homologous mutation in humans[420].

Transgenic mice (Tg) are used extensively in the research of the cerebellar ataxias, including the SCAs[421]. Transgenic mice are generated by the transmission of exogenous DNA into the nucleus of embryonal cells[422]. The expression of the transmitted gene is however random and there is no control over where the transgene ends up[409]. Intensity of expression of the transmitted gene is also partially unpredictable – too little expression leads to a non-pathogenic phenotype whereas too high expression often leads to developmental deficits[421]. Therefore, more lines of transgenic mice are usually generated and the breeds with optimal expression are further bred and used[421]. Also, spatial pattern of transgene expression in the mouse brain does not always reflect distribution of expression of the mutated gene in real human patients. Transgenic mice most often express the transgenes under specific promoters regulating their expression, for example, *pcp2* (expressed richly by cerebellar Purkinje cells) in the case of the SCA mice (pcp-Tg mice) [421]. Specific restriction of expression of pathological allele to one cell type might,

however, be useful for studies focused on the role of this specific cell type disturbance in the disease pathogenesis.

In contrast, *knock-in* (KI) mice are engineered to express the mutation under endogenous promotor[423]. This is provided by the insertion or substitution of the given sequence into the targeted locus. Therefore, knocking-in is more targeted and shows relatively stable expression[409]. Moreover, the expression pattern of the mutant gene follows the expression pattern of the original gene. For example, the KI mouse model of SCA1 (SCA1$^{154Q/2Q}$ mice) with 154 CAG (in one of the chromosomes) and 2 CAG (in the second chromosome) inserted repeats within exon 8 of the targeted endogenous mouse *Atxn1* locus. The mutant *Atxn1* is thus expressed by all the cells naturally expressing the ataxin-1.

In *knock-out* (KO) mice, the given gene is completely inactivated. KO mice are used also to study the functions of the genes which are mutated in the SCA[424]. KO mice are reliable mouse models for the hereditary ataxias that are caused by the deletion of specific genes. For example, mice with KO of the *Itpr1* gene represent the model of the SCA15/16, which is caused by the deletion of the *ITPR1* gene.

Furthermore, *conditional expression* of the mutated genes may be used in the context of both Tg as well as KI mice (conditional Tg, cond. KI)[409]. In such cases, tetracycline-inducible conditional mice are used[425]. In contrast to the previous methods, this approach enables keeping the developmental effects of the mutated gene under control and enables evaluation of the acute effect of the mutation before significant neurodegeneration occurs[426].

Current molecular techniques, such as CRISPER/Cas9 moved the generation of mouse models of diseases further, enabling the creation of any mouse model (with specified point mutation or expansion) on-demand very fast and cheaply[409].

2.5.2 Measuring functional impairments in mice

To efficiently use mouse models in translational research of brain diseases, we need reliable tests estimating the magnitude of given dysfunction *sensitively* and *specifically*. The test needs to be *sensitive* enough to detect even subtle changes/differences using reasonably small sample sizes. Simultaneously, the test should be *specific*, meaning that

it should reflect specific neurological or behavioural aspects of the disease without confounding by other dysfunctions and symptoms.

Motor skills and *motor learning* are the most commonly evaluated using the *rotarod test*[427,428]. In principle, a mouse is put to a small rotarod (approximately 5 cm in diameter) placed a few decimetres above ground (low enough not to injure the mouse, high enough to motivate the mouse not to fall). The rotarod moves usually between 0-60 rotations per minute (rpm). The time when the mouse falls is recorded and expressed as *rotarod latency* (to fall; s). The test is repeated over several days. The magnitude of improvement is considered to reflect *motor learning.* In the case of *accelerating rotarod*[429], the speed of the rotarod continuously increases, most often from 0 to 40 or 60 rpm, during 4-8 minutes. In contrast, *steady speed rotarod* has a constant speed, usually 30-40 rpm. A combination of both is also often used in practice when the speed is accelerating for a few minutes to 30 rpm and then kept stable after reaching this speed[430]. Studies comparing both versions of the rotarod suggested that constant speed rotarod shows higher sensitivity to pathological conditions in movement disorders models, but also lower specificity[431]. The rotarod is sensitive to cerebellar ataxia as well as other movement impairments caused by various brain damage.

Besides the rotarod test, other tests of motor coordination and balance exist. For example, the *elevated beam test* is another tool to evaluate balance and motor coordination[432]. In principle, the ability of the mouse to traverse the beam to get to shelter on the opposite side is evaluated. Although the rotarod test is generally considered to be more complex and objective, in some experiments, the beam test was shown to better detect the chemically-induced coordination deficits more sensitively than the rotarod test[433].

Gait analysis is another commonly used and useful tool to quantify ataxia and disrupted gait. Currently, two commercial systems are available: *DigiGait* and *CatWalk*[434]. Both systems measure a very high number of parameters, including stride length for each leg separately, variability in the gait measures and many others. In DigiGait, the mice are walking/running on a treadmill with a user-defined speed. In contrast, in CatWalk, the locomotion is spontaneous and is under the control of the animal tested. As many parameters depend on speed, the standardized speed may be advantageous. In general, ataxic rodents show higher variability in numerous gait

parameters and larger distances between left and right legs to compensate for lost balance. Models of other movement disorders may show side asymmetry, generally shorter strides (even when adjusting the speed in the case of the CatWalk) and other abnormalities[435].

Signs of limb *clasping* is another tool to evaluate the neurological function in the CNS disease mouse models This sign is widely used as sensitive, but it is not very specific as clasping is present in many different models of various neurological diseases[436].

Besides motor-related impairments, also studying the psychiatric-relevant deficits in mice has a long tradition in experimental psychiatry[437], and has also been done in various mouse models of cerebellar diseases[409,438]. Although there are plenty of tests developed to assess psychiatric-relevant behaviour, the following tests have been used in the context of SCA mouse models:

Cognitive functions are the most commonly tested in the *Morris Water Maze* (MWM) test[439,440], where rodents learn to locate a hidden platform using intra- and/or extra-maze distant cues in a circular pool for several days. Latency in reaching the platform, and total distance swam are recorded as the main parameters. Finally, the animals undergo a probe trial with an absent escape platform: an efficient learner should preferentially move in the quadrant where the hidden platform was previously placed. The MWM test performance is hippocampal-dependent and may be disrupted by hippocampal lesions and by chemically-induced changes in hippocampal plasticity[441–443]. The major disadvantage of the MWM is that it causes substantial stress and depends on unimpaired swimming and visual skills, which may all significantly confound the results[164]. Moreover, some mouse strains are not able to learn the task efficiently or lack the motivation to search for the platform[440].

The *Barnes Maze Test* evaluates complex hippocampal-dependent spatial memory as well but imposes lower stress[444,445]. In this test, the mouse walks on a circular surface, usually containing up to 20 holes, one of which provides an escape from the arena[446]. The mice learn to navigate efficiently to the “escape hole”, using similar visual cues as in the MWM.

The *Fear Conditioning* task is another very common behavioural paradigm. In principle, the mice learn to associate either neutral *conditional stimulus* (e.g. tone) and/or neutral *context* (location or interior) with an aversive stimulus (usually a weak electrical shock to the paws)[447]. If the mice learn to associate both stimuli, the originally neutral

stimuli (*cued conditioning*) and/or context (*contextual conditioning*) are sufficient to induce freezing (fearful) behaviour. The fear conditioning generally depends on the amygdala, particularly the basolateral amygdala[448], whereas contextual conditioning crucially also depends on proper hippocampal functions[449]. The device for *fear conditioning* can also be used for the evaluation of *prepulse inhibition* (PPI) which measures the ability to inhibit a startle response to a noisy tone when it is preceded by a weaker prepulse tone. The PPI deficit can be simply evaluated in humans and occurs in patients with schizophrenia, among others. It seems to be related to alteration in dopaminergic and glutamatergic neurotransmission[450] and dysfunction of the thalamus[451].

In the *Water T-maze* (WTM), mice learn to navigate to the hidden platform placed in one of the two arms of the T-shaped arena[452]. The test comprises two phases: the initial learning phase and the reversal learning phase. The initial learning is very fast (the mouse must remember the left/right side). Presumably, the parietal and retrosplenial cortex and striatal structures, which all play a role in egocentric navigation and/or left/right choices' memory[453], may be implicated in the initial learning. The reversal learning requires flexibility, which is assumed to depend mainly on proper functions of the frontal cerebral cortex[454,455] and hippocampal neurogenesis[144,456], although other structures may be implicated as well[457,458]. It is possible to use a Y-shaped[92], instead of a T-shaped arena.

The *Open Field* test (OF) is a simple and widely used test with many possible outcome measures, reflecting overall locomotor activity and anxiety-like behaviour[459]. The animal is put in an arena (usually 42-50 cm) and is left to explore the arena. Distance walked and relative time spent walking indicate the level of locomotor activity. Anxiety-like behaviour is typically reflected by thigmotaxis, i.e. % of the time spent, or % of distance walked, in proximity to the walls (5-10 cm)[459]. The potential of the OF to reflect anxiety-like behaviour was partially supported by early pharmacological studies that showed that acutely acting anxiolytics (e.g. benzodiazepines) decrease the thigmotaxis[460,461]. However, other drugs reducing anxiety after long-term use often do not show a similar effect in the OF, posing controversy about the reliability of this test to reflect human-like anxiety[460,462]. Furthermore, OF arena may be used also for other tests, such as two hippocampal-dependent tests of memory (the *Novel Object Recognition* test[463] and *Object-Location Memory* test[464]) and other tests indicating anxiety-like behaviour – *Novelty Suppressed Feeding*[465] for example.

The *Elevated Plus Maze* test (EPM) is another test used to indicate anxiety-like behaviour. The plus-shaped arena has two "open" and two "closed" arms[466] (with shading walls). The animals are usually motivated to explore the whole arena including the open arms, but may be simultaneously anxious, leading to more 'careful' behaviour and hiding in the 'safer' shaded arms[466]. An analogous test was also developed for humans in virtual reality[467]. The behaviour of mice in the EPM, as well as humans in the analogous test, is affected by GABA-modulating drugs (benzodiazepines)[467,468]. An analogous test is the *Dual Maze* test which allows familiarization with the arena, to reduce initial novel stress before exposure to the open arm[151].

The *Forced Swimming Test* (FST) is a test of depressive-like behaviour. The mice are placed in a container filled with water and left there for up to 10 minutes. The duration of immobility during FST reflects the motivational aspects of depressive-like emotionality[469]. In this test, rodent models of depression decrease their immobility in the FST even after acute application of antidepressants[470]. However, in depressed humans, antidepressants act after weeks of daily use, posing doubts about the validity of the FST to reflect emotions analogous to human depression[471,472].

The *Sucrose Test* is another test reflecting depressive-like behaviour[473]. Typically, separately housed mice are habituated to 2 bottles in the cage. Then, one bottle is filled with 1-5% sucrose, whereas the second contains clean water. Subsequently, fluid intake is measured daily for several (4-8) days and averaged[473]. In contrast to the FST, sucrose preference reflects anhedonia-like emotions, rather than a level of motivation[474]. Contrary to the FST and similar tests, depressive-like mice show significant improvement after long-term, but not acute, use of SSRI antidepressant[475,476], supporting the reliability of this test to indicate depressive-like emotions analogous to a human depressive state.

2.5.3 Functional impairments and neuropathology in SCA mice

Functional impairments and gross neuropathology in representative SCA mouse models are summarised in Table 2 and already published reviews[477–482]. The mouse models expressing the mutated gene specifically outside the brain (e.g. muscle-specific models of SCA17[483]) were not included in the table. Similarly, for the SCA types with expanded repeats (e.g. polyglutamine SCAs, CTG-repeats disorder SCA8 or ATTCT

expansion in SCA10), I did not include models without an analogous expansion in the affected gene (e.g. knock-out and other[484] mice).

Most of the listed mouse models display cerebellar dysfunctions and related motor impairments, corresponding with the fact that these impairments constitute the core hallmarks of the SCAs. As an exception, the mouse model of SCA11 (TTBK2-KI mice[485]) does not show any impairments in heterozygosity (in contrast to heterozygous human patients) and dies in the embryonal stage in case of homozygosity. Some models of SCA (e.g. FGF[486] and Kcn3.3[487] deficient mice) tend to display robust motor impairments on rotarod but no structural alteration of the cerebellum. In these mice, a detailed electrophysiological examination revealed abnormalities in Purkinje cells' firing frequency, or altered excitability of the excitatory synapses between parallel fibres and the Purkinje cells[488], suggesting that cerebellar synaptic deficits are sufficient to induce the motor deficits even in absence of gross neuroanatomical pathology. Similarly, the mouse model of SCA10 with artificially expanded ATTCT repeat within *LacZ* cells showed locomotor impairments and abnormal gait along with neuronal loss in several regions (pons, cerebral cortex and hippocampus) but no alterations in the cerebellum[489]. This also contrasts with the situation in human patients, which display severe cerebellar degeneration[312]. The authors of the original paper attributed this contrast to the different expression patterns of the mutant gene in the mouse model (driven by PrP promoter) vs. in human patients (driven by native ATXN10 promoter). I also speculate that the focus on neuronal loss may be incomplete as loss of cerebellar neurons often occurs in late disease stages after the onset of atrophy in Purkinje cells dendrites. In some SCA models[430], there are also incongruences between the documented onsets of motor dysfunction, possibly explainable by the different settings of the tests (accelerating vs. combined rotarod setting).

In humans, premature death accompanies many SCA types[295], most often due to brainstem pathology and related impairments in swallowing, breathing and coughing, altogether resulting in pulmonary infection and respiratory failure[289]. Premature death often occurs in SCA mouse models although the causes seem to be more complex than in human patients and include malnutrition and dehydration due to disability of self-care. The fact that mice with purely cerebellar phenotype usually do not die prematurely (Table 2) suggests that the premature death in SCA mice stems from complex neuropathology,

often including the brainstem (Table 2). However, specific brainstem-related impairments analogous to the human bulbar and respiratory symptoms have been rarely studied in mouse models. As exceptions, recent studies in mouse knock-in models of SCA1[490] and SCA7[491] reported respiratory dysfunction, correlating with pathology in hypoglossal neurons and nerves, in these mouse models.

Besides the SCA mouse models, many other mouse models, including many spontaneous mutants, were used as a model of hereditary cerebellar diseases. Due to current possibilities to generate the mouse models on-demands for a particular disease (or even a specific aspect of the disease), they are not used frequently nowadays. As an exception, we still work with *lurcher* mutant mice, as this mouse strain show very robust, fast and specific olivocerebellar degeneration. They are thus a good model to elucidate the effect of this specific degeneration on functional impairments, without confounding with widespread brain dysfunction/atrophy. They are still used in studies of how massively lost cerebellar functions can be restored/compensated[492,493]. The lurcher mice carry heterozygous lurcher grid2 mutation in the gene encoding δ2 subunit of the glutamate receptor[419]. These mice completely lose their cerebellar Purkinje cells within 2-3 months of life, together with incomplete but massive degeneration of inferior olive and cerebellar cortex interneurons (90% of the granule cells are lost as well)[419]. This leads to apparent ataxia, a tremendous deficit on the rotarod, irregular gait, and multiple behavioural abnormalities (described below in section 2.6.3).

Besides the described pathology, animal models are necessary to study (sub)cellular, molecular, and electrophysiological mechanisms of hereditary cerebellar diseases. Most of the mouse models with robust gross cerebellar pathology show also impaired cerebellar plasticity and disturbed electrophysiological properties of the PCs' synapses[478]. Similarly, abnormal distribution and density of multiple synaptic receptors of neurotransmitters often accompany other neuropathological features in the SCA mouse models. Moreover, diseased cerebella often evince ultrastructural damage, such as enlarged vacuoles in neurons (particularly PCs), abnormal numbers of primary dendrites of the PCs and shrinkage of the PCs' bodies. In the SCA1 mice, it was shown that the mutated Atxn1 affects cerebellar development, leading to abnormally high numbers of cerebellar interneurons[494,495].

Correspondingly, expressions of multiple genes and volumes of proteins related to neuroplasticity are also commonly reduced in mouse models of hereditary ataxias. For example, robust down-expression of the *vascular endothelial factor* (VEGF)[496], Homer-3 gene[497] and the gene encoding neuropeptide cholecystokinin[498] were identified in mouse models of SCA1. Interestingly, reversion of some of the genes was shown to have the potential to improve the neuropathology and functional impairments in the diseased mice[496,499]. In another example, SCA3 mice were shown to have decreased expression of the neuropeptide Y (NPY) in the cerebellar nuclei and striatum[500]. Interestingly, lentiviral overexpression, or intranasal delivery, of the NPY reduced neuroinflammation and increased BDNF levels in the affected brain regions and partially reversed functional impairments[500,501]. In some mouse models, the transcriptomic alterations are the only signs detected. For example, SCA2 mouse model Q42 KI show transcriptional changes in the gene neighbouring to the Atxn2 (Adam1a) in the cerebellum and brainstem along with motor impairments and reduced body weight but without any detectable gross neuropathology[502]. Other genes, for example, those related to neuroinflammation, were shown to be up-regulated in diverse SCA1 models[503,504], supporting the inflammatory contribution to the SCAs.

Furthermore, multiple SCA types show mitochondrial dysfunction, oxidative stress and related alteration in the expression of mitochondrial genes[409,505]. Mitochondrial dysfunction is considered to play a particularly important role in SCA12 and SCA28[329,409,506]. However, mitochondrial dysfunction and/or related oxidative stress was also found in SCA10 transgenic mice (LacZ[489]), two models of SCA1[507–509] and others. Interestingly, mitochondria-targeted treatment was further shown to improve neuropathology and functional impairments in some of the models[509].

Finally, although sparsely studied, mouse models of SCAs and other hereditary ataxias exhibit various cognitive and emotional-related abnormalities. Early studies in SCA1$^{154Q/2Q}$ mice reported impaired learning in the MWM task, impaired contextual conditioning and impaired plasticity in the hippocampus, the essential brain region in cognition and behaviour[412,430,510]. Another mouse model of SCA1, Pcp2-ATXN1[82Q] mice with cerebellar-specific pathology, was reported to evince abnormal behaviour such as lower cage activity and higher initial explorative behaviour[511]. Besides SCA1, cognitive dysfunction was also described in Fgf14-deficient mice[486], the mouse model of

SCA27, and other mouse models of ataxia, such as lurcher mice[164,512] and mouse models of episodic ataxia type 2[438].

Many SCA mouse models show hypoactivity[409]. However, reduced activity may be correlated with motor deficits and is thus usually interpreted as either the result of overall fatigue or/and ataxia. More interestingly, some models of SCA, namely Kv3.1/Kv3.3 double KO, a model of SCA13 with cerebellar neuropathology, as well as other mouse models with cerebellar-specific degeneration, showed hyperactivity and reduced signs of anxiety[487]. For example, one of the most traditionally used cerebellar-specific mutants, lurcher mice, also show numerous signs of seemingly reduced anxiety- and depressive-like behaviour in OF, EPM and/or FST, corresponding to reduced anxiety-like phenotype in cerebellar-specific SCA1 mice[149–151,165]. Congruently, both cerebellar granule- and Purkinje-cell-specific mouse models of episodic ataxia type 2 showed reduced signs of anxiety in OF although they showed avoidance of novelty feed during the Novelty Suppressed Feeding test[438]. These results thus do not mirror the situation in human patients with SCAs: whereas SCA patients often suffer from depressive moods and elevated anxiety, analogous impairments have not been described in animal models so far. This discrepancy thus represents an obstruction to studying the neuropathology of the emotional-related impairments in mouse models. This is thus a crucial gap that this thesis aims to address.

Disease (gene)	Mouse model (type)	CNS pathology	Functional deficits
SCA1 (ATXN1)	Pcp2-ATXN1[82Q][513]	Cb gliosis[504], PCs path.[414]	MD and ataxia[414], Increased exploration, mild Cog. dys.[414,415]
	Atxn1-78Q/78Q KI[511]		Mild MD
	Atxn1-154Q/2Q KI[430]	Cb gliosis.[504], PCs path., Brain shrin., Brainstem and spinal path.[490], Hp NL[360]	MD, ataxia and clasping[496], Cog. dys.[415,510], HypA, M.Wast, RBW, Resp. dys.[490], PreD
SCA2 (ATXN2)	BAC-Q72[514]	PCs path.	MD, RBW
	Pcp2-ATXN2-127Q[515]	PCs path.	MD.
	Pcp2-ATXN2-58Q[516]	PCs path.	MD, ataxia and clasping[516,517]
	ATXN2-75Q[518]	PCs path.	MD[518]
	Q42 KI[502]		MD, RBW
SCA3 (ATXN3)	YAC ATXN3-84Q[519]	Cb gliosis, NL (Cb, brainstem, SN)[520]	MD, ataxia, clasping, HypA, RBW, PreD
	Q71C[521]	NL in SN	MD, ataxia, HypA, RBW and PreD
	70.61[522]	PCs path.	MD, ataxia, clasping, HypA, RBW, PreD
	Q79HA[523]	PCs path.	MD, ataxia, clasping, HypA, RBW
	PrP/MJD77[524] (cond.)	PCs path.	MD, ataxia, clasping, hyperactivity
	HDProm-MJD148[525]	PCs path.	MD and abnormal activity
	hemi-CMVMJD94[526]	CN, Brainstem and thalamic path.	MD
	Ki91KI[527]	PCs path. and Cb and SN gliosis	MD
	Atxn-304Q KI[528]	PCs path.	MD and ataxia, RBW
SCA5 (SPTBN2)	ß-NISI KO[529]	PCs path.	MD and ataxia
	SCA5 184-2, 645[530]	PCs path.	MD and ataxia
SCA6 (CACNA1A)	SCA6-84Q KI[531]	PCs path.[532]	MD and impaired balance
	MPI-118Q KI[533]	PCs path.	MD and ataxia
SCA7 (ATXN7)	PrP-SCA7-c92Q[534,535]	PCs path., Retinal degeneration	MD, ataxia, clasping, Reduced exploration, Visual Dys., tremor, RBW, PreD
	Sca7-266Q/5Q KI[536]	PCs path., Retinal degeneration, Brain shrin., Brainstem path.[491]	MD and ataxia, HypA, Tremor and myoclonus, Visual Dys., RBW, M.Wast, Resp. dys., PreD[491]
	Ataxin-7-Q52[537]	PCs shrinkage and arbour atrophy	MD, ataxia, clasping, hypoactivity
SCA8 (ATXN8)	BAC-Exp[311]		MD and ataxia, HypA, M.Wast, kyphosis, RBW, PreD
SCA10 (ATXN10)	pcp2-LacZ[489]	Hp NL, path. in cortex and pons	Ataxia, clasping, HypA, epileptic seizures
SCA13 (Kcnc3)	Kv3.1 KO[538]		MD, RBW
	Kv3.3 KO[487]		Ataxia[539]
	Kv3.1/Kv3.3 double KO[487]		MD and ataxia, Hyperactivity and lower thigmotaxis, RBW, Tremor, myoclonus
SCA14 (PKCγ)	PKCγ H101Y[540]	PCs path.	Clasping
	S361G-PKCγ [541]	PCs path.	MD
SCA15/16 (ITPR1)	ITPR1-null mice[542]	General Brain shrin.	Ataxia, RBW, seizures and PreD
	Opt mice[543]		Impaired locomotion, RBW, seizures
	Itpr1-δ18/δ18[544]		MD
SCA17 (TBP)	TBP-71Q[545]	Cb gliosis, PCs path.	MD and clasping, RBW and kyphosis [546], tremor, seizures and PreD
	TBP-105Q[545]	Cb NL and gliosis, cerebral cortex path.	MDs and clasping, RBW and kyphosis, tremor, seizures and PreD
	L7-hTBP [547]	Cb gliosis, NL in Cb, brainstem, thalamus and striatum	MD, ataxia and clasping
	Nestin-TBP cond. KI[426]	PCs path.	MD, HypA, RBW, M.Wast. and kyphosis
	Inducible TBP KI[548]	PCs path.	MD, RBW. kyphosis, PreD
	Germline-TBP KI[483]	PCs path.	MD, M.Wast, RBW, PreD
SCA23 (PDYN)	$PDYN^{R212W}$ mice[549]	PCs path.	Ataxia
SCA27 (FGF14)	Fgf14-deficient mice[486]		MD, ataxia, clasping, hypoactivity, Cog. dys.[550], Hyperkinetic, tremor, seizures
SCA28 (AFGF3L2)	Afg3l2[551,552]	Cerebellar neuronal loss	MD, ataxia and clasping, Pelvic elevation
SCA42 (CACNA1G)	Cacna1g KI[553]	PCs loss and arbour atrophy	Ataxia

Table 2 (on the previous page): Representative mouse models of spinocerebellar ataxias, their neuropathology and functional impairments. Knock-in and Knock-out mice models include KI or KO at the end of the model's name. Otherwise, except for the Opt mice (spontaneous mutant), mice are transgenic. 'Cond.'= conditional expression of the mutated gene; 'PCs'= Purkinje cells; 'Cb'= cerebellar; 'Path.'= pathology; 'MD'= motor deficits; 'Cog.'= cognitive; 'Dys.'= dysfunction; 'Shrin.'= shrinkage; 'Hp'= hippocampal; 'NL'= neuronal loss; 'HypA'= hypoactivity; 'M.Wast'= muscle wasting; 'RBW'= reduced body weight; 'Resp.'= respiratory; 'PreD' = premature death; 'SN'= substantia nigra; 'CN'= cerebellar nuclei; 'PCs path.' indicates anything from measurably reduced volume of the cerebellar molecular layer, decreased complexity of the Purkinje cells dendritic arbours, decreased calbindin expression in the cerebellar layer or loss of the Purkinje cells. Hypoactivity and hyperactivity indicate altered distance walked in the open field, immobility time in the open field or changes in home cage activity. The table has already been published elsewhere[409] (Article 2).

3 AIMS

This thesis aims to contribute to the understanding of the mechanisms and nature of the psychiatric issues in SCAs via experiments on the mouse model of SCA1 and also the mouse model of selective olivo-cerebellar degeneration, the lurcher mice. Mainly, this thesis aims to:

1. Find out whether the mouse models of hereditary cerebellar ataxias suffer from robustly detectable psychiatric-relevant deficits, including cognitive impairments and altered emotional-related behaviour.
2. To evaluate independence between the ataxia and the behavioural psychiatric-relevant deficits in the mouse models
3. To estimate the importance of cerebellar and out-of-cerebellar neuropathology in psychiatric-relevant deficits in a mouse model of SCA1.
4. To identify behavioural tests whose results are not affected by ataxia of tested mice.

Although the research of this thesis is rather explorative, the following expectations can be established:

1. Given the occurrence of the cognitive and emotional-related mental issues in human patients with SCAs, analogous deficits may be expected also in mouse models of hereditary ataxia.
2. Although ataxia and related impairments are expected to confound the behavioural results, it is presumed that some of the behavioural impairments will be independent of the motor deficits.
3. Both cerebellar, as well as non-cerebellar contributions, are expected to play a role

Specific aims and hypotheses or expectations are further listed in separate research chapters.

4 RESEARCH #1 – BEHAVIOUR OF BLIND LURCHER MICE DURING SPATIAL TASK

Human patients with spinocerebellar ataxias often suffer from cognitive deficits and altered emotionality[4,398], possibly due to the causal effect of cerebellar dysfunction on cognitive functions and emotional regulation[63]. Similarly, to human patients, lurcher mice have also been repeatedly shown to have some analogous deficits. For example, they have been shown to have poor performance in spatial tasks although their spatial learning (improving over days) may be preserved to some extent[149,164]. However, the precise mechanism of how cerebellar degeneration impairs spatial performance in mice and humans is not clear. Theoretically, possible mechanisms may include: (i) its role in the integration of proprioceptive, vestibular, and motor signals during path integration[158,160]; (ii) disturbed integration of visual inputs with information of other senses[554,555]; (iii) impairment in motor skills which may result in an unstraight swim, and may disturb the ability to keep an intended swim direction.

Previous work, performed on mice with diminished LTD on the synapses connecting Purkinje cells with mossy fibers suggested that the cerebellum is especially crucial for the integration of proprioceptive, vestibular, and motor signals during path integration, whereas vision provides efficient correction when the cerebellar functions are impaired[43]. Moreover, cerebellar degeneration impacts emotional-related behaviour in mice: it induces stress over-reactivity and reduces anxiety-related behavioural indicators[149,150] which also may affect the apparent cognitive performance substantially.

To explore this, lurcher mutant mice and wild-type mice (WT) were examined in terms of performance and behaviour during a spatial orientation task. For this purpose, the C3H strain of lurcher and WT mice was used. In this strain, some of the animals (homozygotes for the *Pde6brd1* allele) evinced retinal degeneration and impaired vision[556], enabling the study of spatial performance and behaviour under the condition of disabled vision. The spatial performance was tested in the MWM task with stable spatial relation between the start position and the position of the hidden platform[557]. This design theoretically enables orientation using proprioceptive, vestibular, and motor signals during path integration without the necessity of vision.

4.1 Aims and hypotheses

1. To evaluate the relative importance of the potential mechanisms (described above) for the poor spatial cognition in mice with cerebellar degeneration
2. To test the hypothesis, that visual signals represent a necessary corrective factor for path integration in lurcher mice, enabling at least partial learning
3. To explore the potential effect of individual motor skills, swim speed and visual cues availability (all without confounding from the other factors) on the cognitive performance of WT and lurcher mice
4. To explore potential behavioural abnormalities in the lurcher mutant mice in response to the task which may be possibly overly difficult

Although the research is explorative, rather than explicit hypothesis-testing, it was predicted that disabled vision will lead to a total diminishing of residual spatial navigation and spatial learning in lurcher mice. For WT mice, it was predicted that loss of vision will lead to worsening the spatial skills although the spatial learning will be preserved to some extent. Moreover, it was also expected that blind lurcher mice may behave abnormally in response to the task that is expected to be overly difficult. Given the previously published papers, the influence of individual motor skills on performance in the MWM was not expected.

4.2 Declaration of author contributions

The study has been already published as an original article[512] with impact factor (IF_{2020}= 3.05; Article 1). Full citation of the publication:

Cendelin J, **Tichanek F**. Cerebellar degeneration averts blindness-induced despaired behavior during spatial task in mice. *Neuroscience Letters*. 2020;722:134854. doi:10.1016/j.neulet.2020.134854

The author of this thesis contributed significantly to the interpretation of results and manuscript writing. He had a dominant role in the statistical analysis of data. He did **not** participate in planning the study, original conceptualization (before the experiment) and experimental work.

4.3 Methods and material

4.3.1 Animals

Heterozygous lurcher mice and WT mice (both males and females) of the C3H strain, aged 4.5 to 7.5 months, were used for the experiment. The mice were kept in stable temperature and humidity with a 12/12 hour light/dark cycle. Food and water were available *ad libitum*. All experiments were conducted in full compliance with the European Union Guidelines for scientific experimentation on animals and with the permission of the Ethical Commission of the Faculty of Medicine in Pilsen. All efforts were made to minimize suffering. Blind animals (homozygotes for the *Pde6brd1* allele[556]) were recognised according to *post-mortem* histological examinations of eyeballs.

After completion of behavioural tests, the mice were euthanized with an overdose of Thiopental. Hematoxylin-eosin-stained frozen slices of the mouse eyeballs were subsequently used to histologically examine the presence of retinal degeneration determined according to the absence of the outer nuclear layer (retinal degeneration present: RD+, 'blind'; retinal degeneration absent: RD-, 'sighted'). Cerebellar degeneration was recognized according to apparently ataxic gait (absence of cerebellar degeneration: WT mice; cerebellar degeneration present: lurcher mice, 'Lc'). According to the presence of both retinal and cerebellar degeneration, mice were categorized into 4 experimental groups: sighted WT mice (RD- WT, n= 17); sighted lurcher mice (RD- Lc, n= 22); blind WT mice (RD+ WT, n= 13); and blind lurchers (RD+ Lc, n= 8).

4.3.2 Behavioural tests

All behavioural tests proceeded during the light period (6 am to 6 pm).

Motor skills were assessed via the rotarod test (TSE Systems GmbH, Moos, Germany). Mice were placed on a rod (4 cm in diameter). The rod was slowly accelerating from 0 to 60 rotations per minute (rpm) over 3 minutes. Motors skills were expressed as averaged latency to fall over four subsequent measurements with 12 min between trials.

The mice were also tested for spatial cognition in MWM (round pool, 100 cm in diameter) with a circular escape platform (7.5 cm in diameter) hidden 0.5 cm below the water surface. The MWM experiment lasted 17 days (D1-17). The position of the hidden escape platform and the starting position were stable to allow the use of both non-visual

idiothetic cues as well as visual information such as optic flow. Four trials were performed in 20-min intervals each day with the same starting point (Figure 2). If the mice did not reach the platform within 60 s, they were moved there manually. Mice were left on the platform for 30 s after each trial. Probe trials consisted of four 60-second trials. For the probe trials, the platform was removed from the maze and mice were let to move spontaneously for 60 seconds. The probe trial was performed on D18. The proportion of distance moved in the quadrant with the previously placed platform represents the parameter of interest. The mice were tracked using the EthoVision XT system (Noldus Inc., Wageningen, the Netherlands).

For each day of MWM, the following parameters were measured: 1) *latency* (s) to locate the hidden platform; 2) *successful trials* (%) indicating the proportion of trials in which the mouse reached the platform with latency < 60 s; 3) *swim speed* (cm/s; the mean speed of swimming); 4) *non-moving* (%) indicating the proportion of time spent in the non-moving state. 5) *distance moved* (cm) indicating total distance swam during the whole trial; 6) *approximation time* (s) indicating latency to get to platform proximity (< 3 cm from platform edge); 7) *direct swim* (%) indicating the proportion of trials with direct swimming to the hidden platform (i.e. successful trials with the distance moved < 1.3 × direct distance between the start and platform = 112 cm) per day; 8) *thigmotaxis* (%) measured as time spent at the periphery of the maze (< 10 cm from maze wall). To analyse the relationship between the performance of the mice in the MWM, swim speed and performance on the rotarod, final performance and final swim speed were expressed as a mean latency and swim speed respectively in the last two days (D16 and D17) of the water maze test. In the probe trial, relative time in quadrant (% of total time spent in the target quadrant, i.e. the quadrant where the platform was located in D1-17) was evaluated.

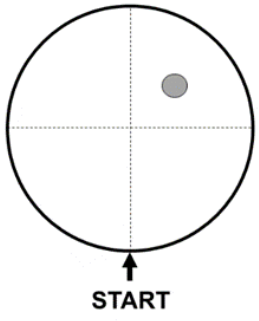

Figure 2. Schema of the spatial relation between the starting position and the escape platform position in the Morris water maze design that was used in the experiment.

4.3.3 Statistical analysis

Data were analysed via R statistical software[558]. The analyses were extended via the permutational (4999 randomizations) or bootstrapping (10000 simulations) techniques which do not rely on assumptions of parametric methods. Group comparisons were made via permutational ANOVA. The significance of the differences between the expected (25%) and actual duration of stay in the quadrant during the probe trials was evaluated using the BCa bootstrap[559] method with 'boot' R package[560]. For repeated measurements, effect of *day* (D1-D17), *genotype* (lurcher vs. WT), *vision* (sighted vs. blind) and their interactions on measured parameters were evaluated by permutational linear mixed effect model (lme) with an AR1 autocorrelation structure using the 'nlme'[561] and 'predictmeans'[562] R packages. Post-hoc comparisons were performed using the (paired) permutation t-test followed by false discovery rate correction[563]. To evaluate and separate the effects of *motor skills*, *vision*, and *final swim speed* on the *final performance* (separately for lurcher and WT mice), two general linear models (LM) supplemented by bootstrapping (10,000 simulations) of partial regression coefficients were performed. They enabled the evaluation of the effects of all predictors while adjusting the effects of the other factors. Since four lurcher mice (two RD- and two RD+) jumped from the rotarod immediately, they were removed from the analysis. Strongly unequal variances in residuals were stabilized by relevant transformation of response variable. Angular transformation was applied for percentage data (*successful trials*, *direct swim* and *non-moving*) whereas square-root transformation was used for *latency to fall* on rotarod. $P<0.05$ was considered statistically significant. Since the sex did not have any apparent effect on the evaluated outcome and did not improve predictive accuracy (assessed via Information Criteria; data not shown), the sex effect was ignored in the statistical analysis.

4.4 Results

4.4.1 Cerebellar degeneration, but not blindness, affects motor skills

Rotarod latency was strongly influenced by the *cerebellar degeneration* ($F_{(1,56)} = 418$; $P< 0.0002$). In contrast, *retinal degeneration* and interaction of both factors (*cerebellar degeneration* : *retinal degeneration*) did not have any statistically significant impact on

the rotarod latency. Lurcher mice reached approximately 10% of rotarod latencies in WT mice, independently of the blindness (Fig. 3).

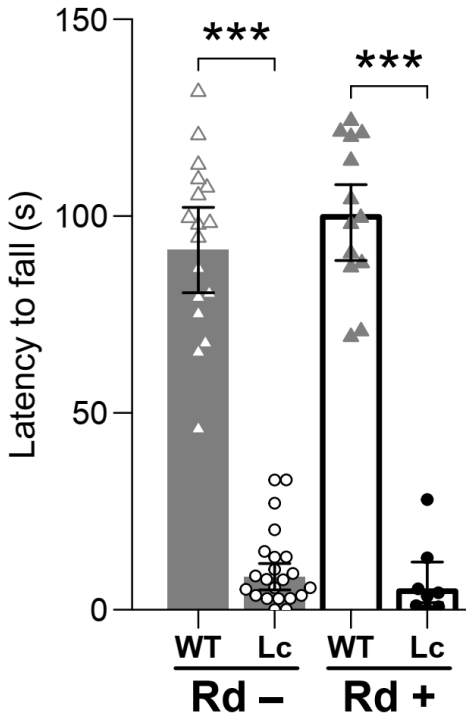

Figure 3. Rotarod latencies in WT and lurcher (Lc) mice, with preserved vision (RD-) or blind (RD+). Error bars= 95 % confidence intervals based on bootstrapping technique. *** $P < 0.001$.

4.4.2 Cerebellar degeneration impairs spatial skills

Effects of *cerebellar degeneration*, *retinal degeneration*, *day* of the MWM test and interaction of these factors on escape *latency*, *successful trials* % and *non-moving* %, based on permutational linear mixed-effects models, are summarized in Table 3 and visualized in Figure 4. Effects of the same predictors on *distance moved*, *swim speed*, *direct swim*, and *thigmotaxis* are seen in Table 4 and visualized in Figure 5.

Table 3. The effect of the *cerebellar degeneration* (CD), *retinal degeneration* (RD), *day* (D) of the MWM task and their interaction on *latency*, *successful trials* % and *non-moving* %. Degrees of freedom (df) show numerical df and denominal df.' n.s.= statistically non-significant (P≥0.05).

Factor	*df*	Latency		Successful trials		Non-moving	
		F	*P*	*F*	*P*	*F*	*P*
CD	1, 56	34.46	< 0.0002	25.1	< 0.0002	2.05	n.s.
RD	1, 56	57.47	< 0.0002	33.37	< 0.0002	5.75	0.0252
D	16, 896	9.91	< 0.0002	7.17	< 0.0002	4.51	< 0.0002
CD:RD	1, 56	29.47	< 0.0002	22.07	< 0.0002	12.33	0.0012
CD:D	16, 896	2.08	0.0224	2.13	0.0108	1.97	0.0382
RD:D	16, 896	3.97	< 0.0002	1.36	n.s.	2.39	0.0104
CD:RD:D	16, 896	2.03	0.0012	2.84	0.001	1.55	n.s.

Table 4. Role of *cerebellar degeneration* (CD), *retinal degeneration* (RD), *day* (D) of the MWM and their interaction on *distance moved*, swimming speed, *direct swim* % and *Thigmotaxis* %. Degrees of freedom (df) show numerical df and denominal df. n.s.= statistically non-significant (P≥0.05).

Factor	*df*	Distance moved		Swimming speed	
		F	*P*	*F*	*P*
CD	1, 56	45.54	< 0.0002	0.14	n.s.
RD	1, 56	28.58	< 0.0002	9.67	0.0044
D	16, 896	14.79	< 0.0002	5.06	< 0.0002
C4D:RD	1, 56	10.4	0.0022	3.56	n.s.
CD:D	16, 896	3.94	< 0.0002	2.29	0.0132
RD:D	16, 896	1.42	n.s.	2.76	0.0028
CD:RD:D	16, 896	0.81	n.s.	0.82	n.s.
Factor	*df*	Direct swim		Thigmotaxis	
		F	*P*	*F*	*P*
CD	1, 56	23.96	< 0.0002	0.09	n.s.
RD	1, 56	24.18	< 0.0002	22.05	< 0.0002
D	16, 896	4.4	< 0.0002	2.27	0.0046
CD:RD	1, 56	12.74	0.0006	16.9	< 0.0002
CD:D	16, 896	2.48	0.003	2.02	0.0238
RD:D	16, 896	2.26	0.0056	1.43	n.s.
CD:RD:D	16, 896	1.2	n.s.	2.6	0.0016

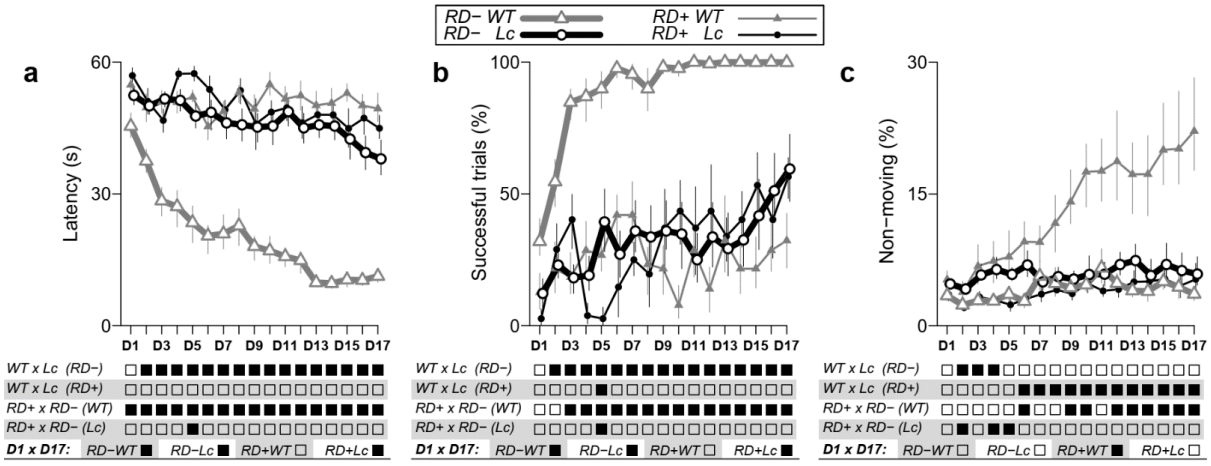

Figure 4. Mean escape *latency* (**a**), percentage of *successful trials* (**b**), and percentage of time spent *in the non-moving* state (**c**) on individual days (D1-D17) of the MWM in sighted WT mice (RD- WT); blind WT mice (RD+ WT); sighted lurcher (RD- Lc); and blind lurchers (RD+ Lc). Error bars= the standard error of the mean. Diagrams below the plots show statistical significance ($P< 0.05$: black squares; $P\geq 0.05$: empty squares) of planned comparisons between individual pairs of experimental groups and paired comparisons between D1 and D17 for experimental groups.

Sighted lurchers achieved, in comparison to sighted WT mice, substantially longer escape latencies (3-fold), lower frequency of successful trials and were not able to find the platform directly even on the latest experimental day (Fig. 4a,b, Fig 5c). However, both sighted and blind lurcher mice showed some improvements in the MWM performance between D1 and D17, as escape *latency* and *successful trials* % of both groups improved between the 1st and 17th day (Fig. 4a,b). There were no differences in *swim speed* between the sighted lurcher and sighted WT mice (Fig. 5b) and only minor differences in the non-moving behaviour (D2-D4; Fig. 4c); these parameters did not change during the experiment significantly (Fig. 4c, 5b).

4.4.3 Effect of retinal degeneration

In the WT mice, retinal degeneration was related to 5-fold longer escape *latencies*, half the percentage of *successful trials*, more than 5-fold higher percentage of the *non-moving* state (Fig. 4), gradual decrease of *swim speed* and lack of *directed swim* toward the platform (Fig. 5). Furthermore, the occurrence of the *non-moving* state increased significantly between D1 and D17 in the blind WT mice but not in other groups (Fig. 4c).

In contrast, in lurcher mice, the impact of retinal degeneration on performance and behaviour in the MWM was minimal (Fig. 4) as neither blind nor sighted lurcher mice showed signs of *non-moving* behaviour (Fig. 4). Surprisingly, both sighted and blind lurchers showed significant shortening of escape *latencies* and an increase of *successful trials* % (Fig. 4a,b) while their *swim speed* did not change significantly (Fig. 5b).

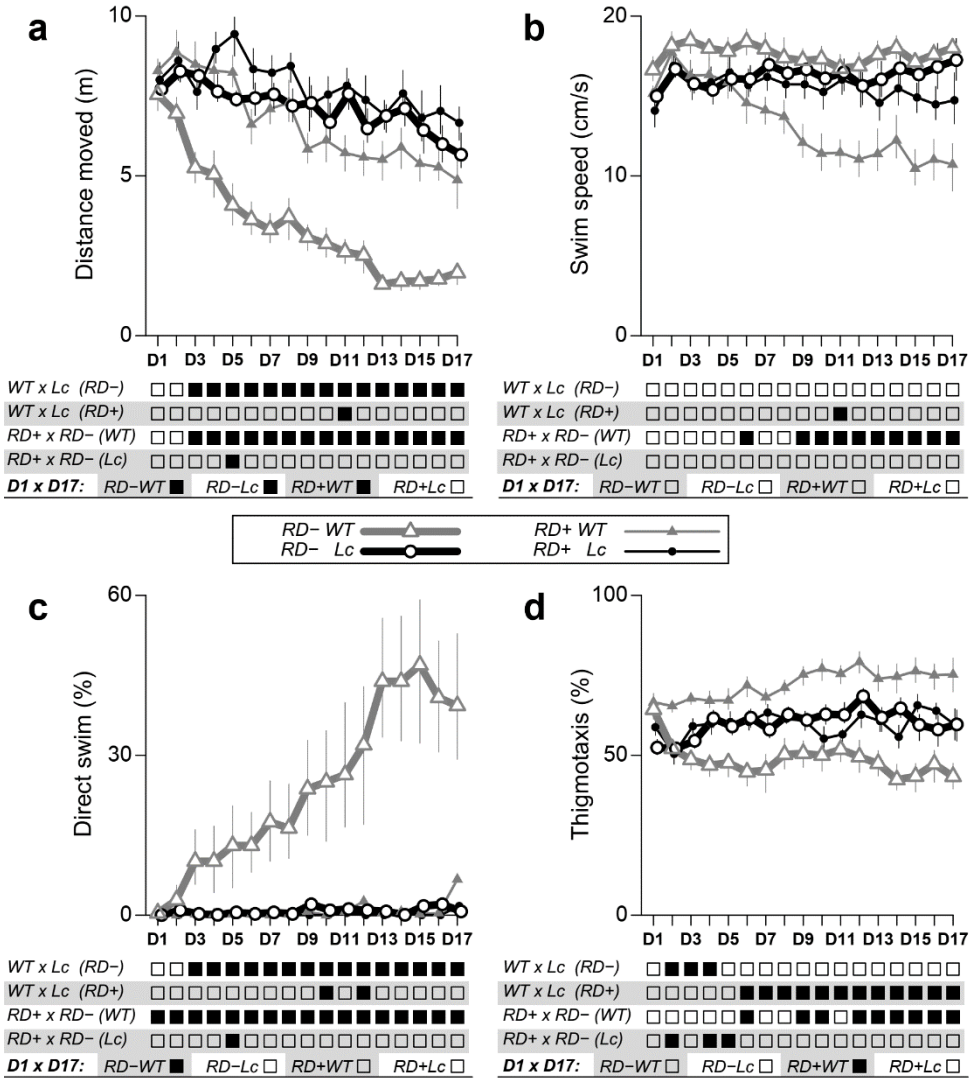

Figure 5. Mean *distance moved* (**a**), *swim speed* **(b)**, *direct swim* % (**c**) and *thigmotaxis* (**d**) on individual days (D1-D17) of the MWM in sighted WT mice (RD- WT); blind WT mice (RD+ WT); sighted lurchers (RD- Lc); and blind lurchers (RD+ Lc). Error bars= standard error of the mean. Diagrams below the plots show statistical significance (P< 0.05: black squares; P> 0.05: empty squares) of the difference between experimental groups and the difference in scores between D1 and D17 within experimental groups.

In the probe trials, only sighted WT mice preferred the target quadrant significantly (Fig. 6). However, both sighted and blind lurcher mice, despite their improvement in the MWM over days, spent approximately 25% of the time in the target quadrant, indicating random movement throughout the maze. Interestingly, blind WT mice remained close to the starting point and spent thus significantly less time in the target quadrant than could be expected given a random movement (Fig. 6).

Taken together, the blind WT mice were the only experimental group that showed a substantial non-moving behaviour compared with other experimental groups and that did not show any significant improvement in escape latencies and successful trials % during the MWM task.

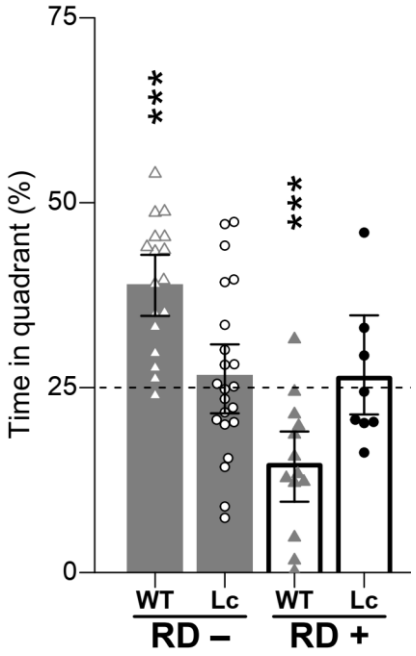

Figure 6. Mean percentage of time spent in the target quadrant during the probe trials in the Morris water maze according to cerebellar degeneration (WT vs. Lc) and blindness (RD- vs. RD+). Error bars represent 95% confidence intervals of the mean, based on BCa bootstrap simulations. *** P<0.001 (time spent in the target quadrant differs from 25%).

4.4.4 Partial effects

Linear models revealed that final latency in WT mice was primarily driven by the sight (P< 0.001), but was not affected by motor skills (P= 0.8) or swim speed (P= 0.1). In contrast, the performance of lurchers was driven by swim speed (P<0.001) and correlated with motor skills (P= 0.01) but not blindness (P= 0.8; Fig. 7; Table 5).

Table 5. Results of general linear models (LM) explaining final performance in WT (**a**) and lurcher (**b**) mice. SS= sum of squares. RSS= residual sum of squares. 95% confidence intervals (95% CI) and significance (P) are based on bootstrapping of the partial regression coefficients. n.s.= statistically non-significant (P≥0.05).

a) WT model	Variable	*df*	*SS*	*RSS*	*Coefficient*	*95% CI*	*P*
Residual *df:* 26	Swim Speed	1	332	2806	-0.9	-1.7 to 0.2	n.s.
	Latency on rotarod	1	5	2478	0.02	-0.2 to 0.1	n.s.
	Vision	1	4159	6632	-32	-43 to -20	<0.001
b) Lc model	Variable	*df*	*SS*	*RSS*	*Coefficient*	*95% CI*	*P*
Residual *df:* 22	Swim Speed	1	2098	5576	-1.8	-2.7 to -1	<0.001
	Latency on rotarod	1	1092	4571	-0.7	-1.3 to -0.2	0.012
	Vision	1	11	3490	-1.6	-11 to 9	n.s.

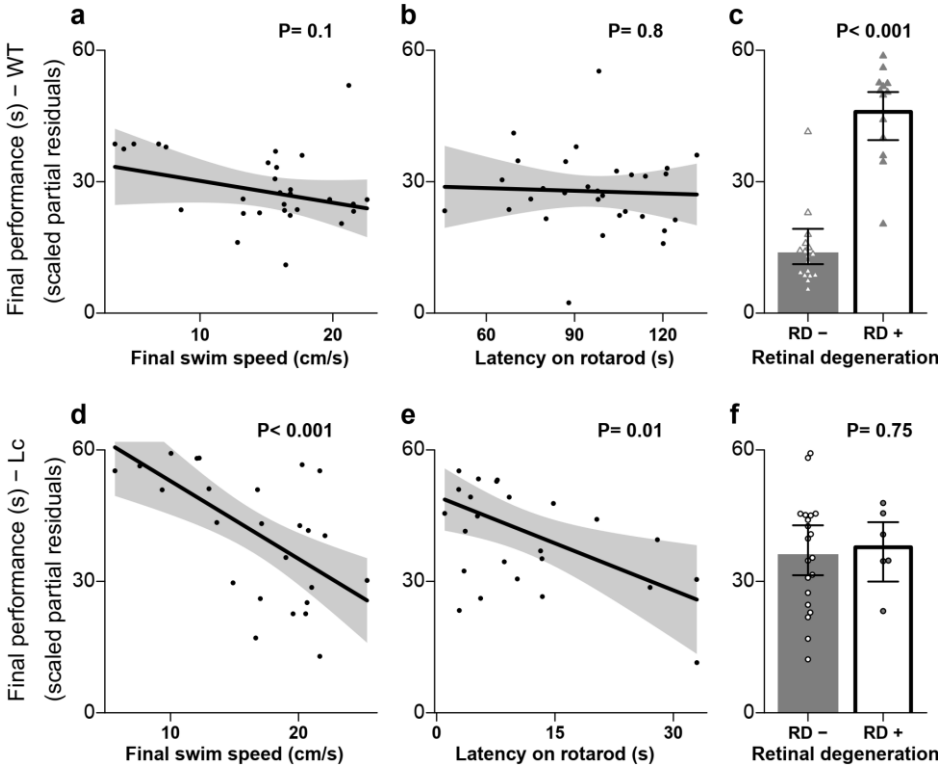

Figure 7. Partial effects of final swim speed (**a**, **d**), the latency on the rotarod (**b**, **e**), and retinal degeneration (**c**, **f**) on the final performance of wild type (**a**-**c**; WT) and lurcher (**d**-**f**; Lc) mice; predicted from linear models (Table 5). Grey areas and error bars= 95% confidence intervals. Points show partial residuals scaled to the measured means.

5 RESEARCH #2 – BEHAVIOURAL IMPAIRMENTS IN MOUSE MODEL OF SCA1

As seen in other SCAs, many SCA1 patients demonstrate neuropsychiatric issues[391–393,564] including cognitive impairments, anxiety, apathy and depression[4,392,398]. However, the question of whether these psychiatric impairments are causally linked to SCA neuropathology, or specifically the cerebellum, or whether they represent an emotional response to a diagnosis of the devastating incurable disease, remains controversial[4].

Surprisingly, results shown in the previous chapter and other studies showed that mice with cerebellar-specific degeneration display learning impairments but also unexpectedly reduced anxiety- and/or depressive-like behaviour. This contradicts the high occurrence of the depressive and anxious states in SCA patients. However, this discrepancy may be explained by the fact that most of SCAs show complex neuropathology[300] and the depressive and anxiety issues may thus stem from pathology in other brain regions than the cerebellum. To explore mechanisms of the psychiatric impairments in SCAs, research on mouse models may be extremely useful.

Research on the SCA1 mouse model with 154 CAG repeats within the endogenous ATXN1 locus (SCA1 $^{154Q/2Q}$; mice with brain-wide expression of the prolonged Atxn1) has shown that these mice exhibit learning impairments and an alteration to hippocampal plasticity-related functions such as synaptic dynamic disruption, synaptic loss and impaired neural progenitor cell proliferation[357,358,412,510]. However, behavioural deficits relevant to human states of depression, anxiety or apathy have not been reported to date with respect to any specific SCA animal models so far. Similarly, the relationship between the non-motor deficits and the specific neuropathology, including the hippocampal pathology, has never been explored as well. This research has aimed to fill this gap.

5.1 Aims and hypotheses

This study aims to explore potential psychiatric-relevant behavioural impairments in the SCA1 knock-in mouse model with the whole-brain expression of the diseased Atxn1. Furthermore, it aims to clarify what is the relationship between the non-motor deficits and ataxia in these mice and to identify the underlying neuropathology of the psychiatric-relevant impairments found. Explicitly, this research aims:

1. To find out whether the mouse model of SCA1 suffers from clearly detectable psychiatric-relevant deficits, including altered emotional-related behaviour
2. To evaluate whether the psychiatric-relevant deficits depend on ataxia in the SCA1 mice
3. To identify mouse behavioural tests that are robust toward confounding from ataxia, and which detect the non-motor impairments in mice sensitively
4. To estimate the importance of cerebellar and out-of-cerebellar neuropathology in psychiatric-relevant deficits in the mouse SCA1 model

5.2 Declaration of author contributions

The study has already been published as an original article[565] (Article 4) with impact factor (IF_{2020}= 4.38). Figures and some text passages of the article have been directly re-used here. All the figures and text passages re-used in this thesis have been written/constructed by the author of this thesis. Full citation of the article:

Tichanek F, Salomova M, Jedlicka J, Kuncova J, Pitule P, Macanova T, Petrankova Z, Zuma Z, Cendelin J. Hippocampal mitochondrial dysfunction and psychiatric-relevant behavioral deficits in spinocerebellar ataxia 1 mouse model. *Scientific Reports*. 2020;10:5418. doi:10.1038/s41598-020-62308-0

The author of this thesis was the first author. He conceptualized the study, performed most of the behavioural experiments (with big help of technicians and minor help of co-authors), performed the majority of work on histological and immunohistochemical staining and its analysis (with help of technicians and co-authors), performed all statistical analyses and visualizations and wrote the manuscript with comments of other co-authors. The author performed ELISA for corticosterone and creatinine but not for BDNF (this was performed by Martina Salomova). He had only a minor role in the evaluation of mitochondrial functions (this was performed mainly by Jan Jedlicka and Jitka Kuncova). He did not measure mitochondrial respiration, but only citrate-synthase activity (together with Jan Jedlicka and Zdenek Tuma and with help of Renata Stastna).

5.3 Methods and material

5.3.1 Animals

B6.129S-Atxn1^{tm1Hzo}/J *knock-in* mice (Jackson Laboratory)[430] were used. Heterozygous mice with 154 CAG repeats within exon 8 of the targeted endogenous mouse ATXN1 locus (SCA1 $^{154Q/2Q}$, hereinafter SCA1) were used along with homozygous control mice with normal CAG repeats in both ATXN1 loci (SCA1 $^{2Q/2Q}$, hereinafter WT). For practical reasons, only males were used in the experiments unless specified elsewhere (females were not available at the time in sufficient numbers for the experiments (they were allocated to maximize breeding). The mice were group-housed (≤ 5 animals per cage) unless specified otherwise. The animals were kept under controlled temperature (23 ± 1 °C) and humidity (30-70%) conditions with a 12 h light/dark cycle with food and water available *ad libitum*. All the experiments were conducted in full compliance with European Union Guidelines for Scientific Experimentation on Animals and with the permission of the Ethical Commission of the Faculty of Medicine in Pilsen. All the protocols followed in this study were approved by the Ethical Committee of the Ministry of Education, Youth and Sports of the Czech Republic (approval no. MSMT-10669/2016-4 and MSMT-27476/2016-2) according to the Guide for the Care and Use of Laboratory Animals (Protection of Animals from Cruelty Law - Act No. 246/92, Czech Republic). Maximal effort was made to minimize suffering.

5.3.2 Behavioural testing

Behavioural characterization involved the mice (SCA1 $^{154Q/2Q}$ and their healthy littermates [SCA1 $^{2Q/2Q}$]) undergoing a 4-week-long battery of behavioural tests (Fig. 8). 4 age cohorts were tested, starting the experiment at the following ages: I) 6 weeks (± 4 days), II) 10 weeks (± 6 days), III) 17-18 weeks and IV) 26-28 weeks. The numbers of animals per cohort (WT, SCA1) were following: I) 13 and 16, II) 12 and 14, III) 14 and 14 and IV) 18 and 12. The design of the behavioural and motor characterization experiment is shown in Fig. 8. Except for the 1st day, the mice were subjected to a maximum of 1 test per day.

Besides the basic behavioural characterization, other behavioural experiments (with new mice which had not undergone other behavioural tests) were done to validate the

findings from the basic characterization stage. One cohort of mice was subjected to the FST (11 WT and 11 SCA1) at the age of 6 weeks (± 4 days). The second cohort of mice underwent the sucrose preference test (21 WT and 7 SCA1) when aged between 10 and 12 weeks.

All the tests proceeded during the light period (6 am to 6 pm). All the mice were habituated to contact with the experimenters for at least 1 week prior to the commencement of the experiment. The following behavioural tests were used for behavioural characterization:

Elevated plus maze test (EPM): Mice were placed in the centre of the EPM arena (50 cm above the floor) consisting of 4 arms – 2 opposing open arms (30 x 5 cm) and 2 opposing closed arms (30 x 5 cm; 15 cm high walls). Mice were left to explore the platform for 6 minutes. The relative time spent in the open arms, expressed in % (*EPM open arms*) was evaluated.

Open field test (OF): Mice were placed in the centre of a plastic opaque arena (50 x 50 x 50 cm; 3 white walls and 1 partially dark wall) to freely explore the arena for 10 minutes. the total distance moved (*OF distance*; m), relative distance walked in < 5 cm from the arena edge from the 1st to the 10th minute per total distance (*OF thigmotaxis*; %) and relative time spent in the corners of 1 dm^2 of area, again from the 1st to the 10th minute (*OF corners*; %) were evaluated.

Object-location memory test (OLM): Mice were left to explore the OF arena with 4 objects that differed in colour, shape and surface (~6 cm of diameter, 6 to 12 cm of height; objects labelled A, B, C, D) for 6 minutes in each session (S). The test consisted of 4 sessions, with 2 sessions in 1 day with a 5-minute-long inter-session break. During the break, the arena was cleaned with ethanol. On the 1st day (S1 and S2) and S3 of the 2nd day, the object positions were stable. Before S4, the positions of 2 crosswise objects (B and D) were changed. Mouse entrances to objects' proximity (< 7 cm from the object; body centre) were counted and expressed as relative B-D pair exploration (compared to A-C pair exploration), separately for *pre-exchange* (S1-S3) and *post-exchange* (S4) *phases* of the OLM.

Acoustic startle response (ASR): The Startle and Fear Combined System (Panlab, Spain) device was used for the whole experiment. The device includes a sensor that detects the strength of the movements of the mouse (whole-body as well as partial-body

movement and utilizing a high-sensitivity weight transducer) in response to an acoustic stimulus (arbitrary unit; the device has been described elsewhere in details[566,567]). The mice were placed in a small plexiglass cylinder restrainer (5 x 10 x 3.5 cm) mounted on a grid floor in an acoustically-isolated box. Firstly, the mice were left to habituate to the chamber for 300 seconds with a white noise of 60 dB. Next, the mice were exposed to 72 strong stimuli (120 dB, 100 ms, pseudorandom inter-stimuli intervals between 4-10 seconds). Of the 72 stimuli, 24 were preceded by a prepulse sound stimulus (80 dB, 40 ms duration; 250 ms before the strong stimuli) and were labelled *predictable stimuli,* whereas 48 were not preceded by any sound (*unpredictable stimuli*). Following indices were measured: Maximum startle response amplitude (*startle amplitude*; arbitrary unit), the ratio between the startle response amplitudes after the *predictable* and relative to the *unpredictable* stimuli, thus reflecting the prepulse inhibition (*PPI*; %), and the average time between the *unpredictable* stimulus and the maximum startle amplitude (*startle latency*; ms). Since the mice were unable to walk during the procedure, the test was not affected by the abnormal mobility of the SCA1 mice. 3 individuals from the youngest cohort (1 WT and 2 SCA1) that showed persistent freezing with no movement were removed from the ASR analysis.

Gait: Gait characteristics were evaluated using the DigiGait device (Mouse Specifics, Inc., MA) with a continuously running belt, forcing the animals to walk at a speed set by the experimenter. Belt speeds of 12 and 18 cm/s were used. For all mice and both speeds, the aim was to get 5 records with > 10 steps. Animals that were not able to perform the experiment (no continuous walk with ≥ 10 steps for each of the speeds) were removed from the gait data analysis (6 weeks of age: 1 WT mouse; 10 weeks of age: 1 WT and 4 SCA1 mice; 17 weeks of age: 2 SCA1 mice; 26 weeks of age: 2 SCA1 mice). Gait parameters from multiple measurements and the left and right legs were averaged for each individual. See Suppl. Table S1 for a list of evaluated gait parameters.

Rotarod: The RotaRod Advanced (TSE Systems GmbH, Germany) device was used, with a rod diameter of 3.5 cm and slow acceleration from 0 to 60 RPM within 8 minutes. Mice underwent the rotarod test on 5 consecutive days with 5 measurements per day and an inter-trial interval of 20 minutes. Day-average values of latency to fall from the rotarod (*rotarod latency*, s) were used.

Morris water maze test (MWM): Mice learned to locate a hidden platform (the centre of the north-western quadrant) using intra-maze distant cues (pictures and symbols on the arena wall) for 7 consecutive days. Water was made opaque by white non-toxic (food) colouring and was at a temperature of 26(±1)°C. The pool had a diameter of 1 m, with a water depth of 21 cm and the platform 0.5 to 1 cm under the water surface. The mice underwent 4 trials per day, each with a different starting position and with 8-minute-long inter-trial intervals. Next, the animals underwent the probe trial (one session with starting position in the south: D8) with an absent escape platform. Thereafter, mice underwent a test of navigation to the visually marked platform (two days D8 and D9) to verify that the potential learning deficit is not caused by a visual deficit or lack of motivation. Each session lasted a maximum of 1 minute. Unsuccessful mice were slowly put onto the platform and forced to stay there for 30 seconds. . Latency to locate the platform (*MWM latency*, s) and the proportion of time when the animal was non-moving (swimming speed < 1.75 cm/s; *MWM non-moving*, %) averaged per day were assessed.

Water T-maze (WTM): The WTM test was performed as described elsewhere[452], with some modifications. The mice learned to navigate to the hidden platform (0.5 cm under the surface of the water) placed on one side of the T-shaped arena (arm width: 7 cm; arm lengths: 38 and 30 cm). The arena was filled with 15 cm of opaque water at 25(±1)°C. The test proceeded on 4 consecutive days (D1-D4) with 2 sessions (S1-S2) on D1 and 3 sessions on other days (D2-D4; 11 sessions in total). Each session consisted of 10 trials with at least 1 hour between sessions. Before the S1, the mice were left to spontaneously turn to one of the sides (repeated 5 times) to evaluate side preference. The platform was then placed on the non-preferred side for S1-S7 and reversed to the opposite side for S8-S11. After reaching the platform, the mice were left there for 15 seconds. The error rate was assessed manually (error= the mouse turned to the wrong arm first). S1-S2 and S8-S9 (2 sessions after the re-location) were considered *training* sessions, whereas the rest were considered *testing* sessions (S3-S7 and S10-S11). After turning to one of the arena arms, the mice were not allowed to return to the starting arm. If the mice demonstrated immobile behaviour, they were motivated to move via noise or the gentle touching of the tail, if necessary, until the mice reached the hidden platform. The overall error rate averaged across all the *testing* sessions (*T-maze errors*, %, S3-S8 and S10-S11), the error rate in the *testing* sessions specifically during the learning phase (*T-maze learning e.*, %, S3-S8) and the error rate in the S10-S11 (*T-maze inflexibility*, %, S10-S11) were assessed.

Forced swimming test (FST): The mice were placed in a cylindrical container (28 cm high, 18 cm diameter) filled with 15 cm of water (25±1 °C) and left there for 6 minutes. The duration of immobility across the whole of the test (*FST immobility*, %), but also specifically during the 1st half of the test (*FST initial immobility*, %) were assessed. Immobility was classified automatically according to a change in the pixels that reflected the area shape of the bodies of the mice (<5% pixel change averaged over 5 seconds).

Sucrose preference test: was performed as described elsewhere[473]. At first, separately housed mice were being habituated to 2 bottles in the cage (for 5 days). Then, one bottle was filled with 1% sucrose whereas the second contained water. Subsequently, fluid intake was measured daily for 4 days. Positions of the bottles were switched daily. The consumptions of both fluids were averaged over the 4 days and sucrose preference was expressed as relative sucrose consumption over the total fluid intake (%).

The behaviour in the EPM, OF, OLM, MWM and FST tests was automatically tracked and evaluated using EthoVision® XT 7.1 (Noldus Information Technology b.v., Netherlands). The pre-processed data obtained from the behavioural characterization are shown in Suppl. Data1, including those measured parameters that were not statistically evaluated.

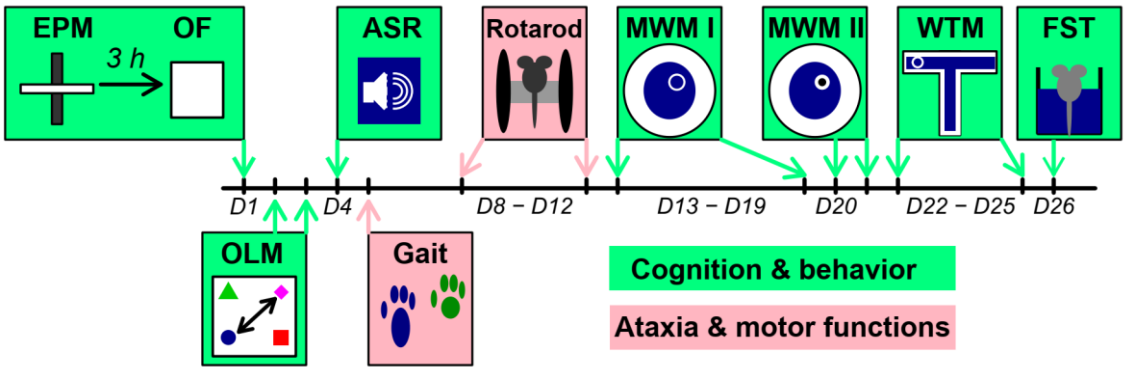

Figure 8. Design of the behavioural characterization experiments. D1 implies starting day of the experiment (i.e. 6, 10, 17 or 26 weeks of age). It includes the elevated plus maze test (EPM), the open field test (OF), object-location-memory test (OLM), the acoustic startle response and prepulse inhibition (ASR), the gait analysis, the rotarod test, the Morris water-maze test with the hidden (MWM I) and visually marked (MWM II) platform, the water T-maze test (WTM) and the forced swimming test (FST).

Out of all evaluated indicators from behavioural and motor characterization, the parameters which were highly sensitive toward the SCA1 genotype in at least two consecutive age cohorts were selected. The criteria were defined by the statistical significance of the difference between WT and SCA1 mice ($P < 0.01$) and by Cliff's delta effect size (> 0.6 or < -0.6). If there were several strongly correlating indicators from the same test, the one with the highest sensitivity and/or better interpretability was chosen. Following ***sensitive indicators*** were identified: *OF distance, OF thigmotaxis*, *rotarod latency* (averaged over days and trials), *MWM non-moving* (average from hidden platform phase; D1-D7); *T-maze errors* (average from S2-S7 and S10-S11) and *FST immobility*.

5.3.3 Histology

After completing the behavioural characterization, the mice were euthanized (aged 10, 15, 22 or 32 weeks) and transcardially perfused with Ringer's solution followed by 4% phosphate-buffered paraformaldehyde (PFA, pH 7.4). The brains were removed and left in PFA for 2 hours and then in sucrose of increasing concentration (15, 20, 30%) for 2 days. Finally, they were weighed and stored at -80°C. They were then cryo-sliced into 40 µm wide frontal slices and stained using Cresyl Violet (Nissl staining) or immunofluorescent methods.

The Nissl-stained slices were scanned using an *Olympus DP70* digital camera coupled to an *Olympus BX51* microscope (*Olympus, Japan*) with a *PlanApo N* 2x/0.08 objective. The volumes were assessed employing the point grid method and the Cavalieri principle using *Gimp* software. The assessed brain regions were selected according to previously published findings of the SCA1 pathology either in mice or human patients[300,365,430,490]. The selected regions are shown in figure 9. They include several cerebellar and hippocampal sub-regions, the hypoglossal nucleus and the thickness of the parietal cortex. Firstly, a preliminary analysis of the oldest age cohort (8 animals per group) was performed and, subsequently, those brain regions identified as the most genotype-sensitive were assessed across all the age cohorts ($N = 8$ WT and 10 SCA1 mice per cohort). The Allen Brain Atlas (http://atlas.brain-map.org) was used for orientation in the brain slices.

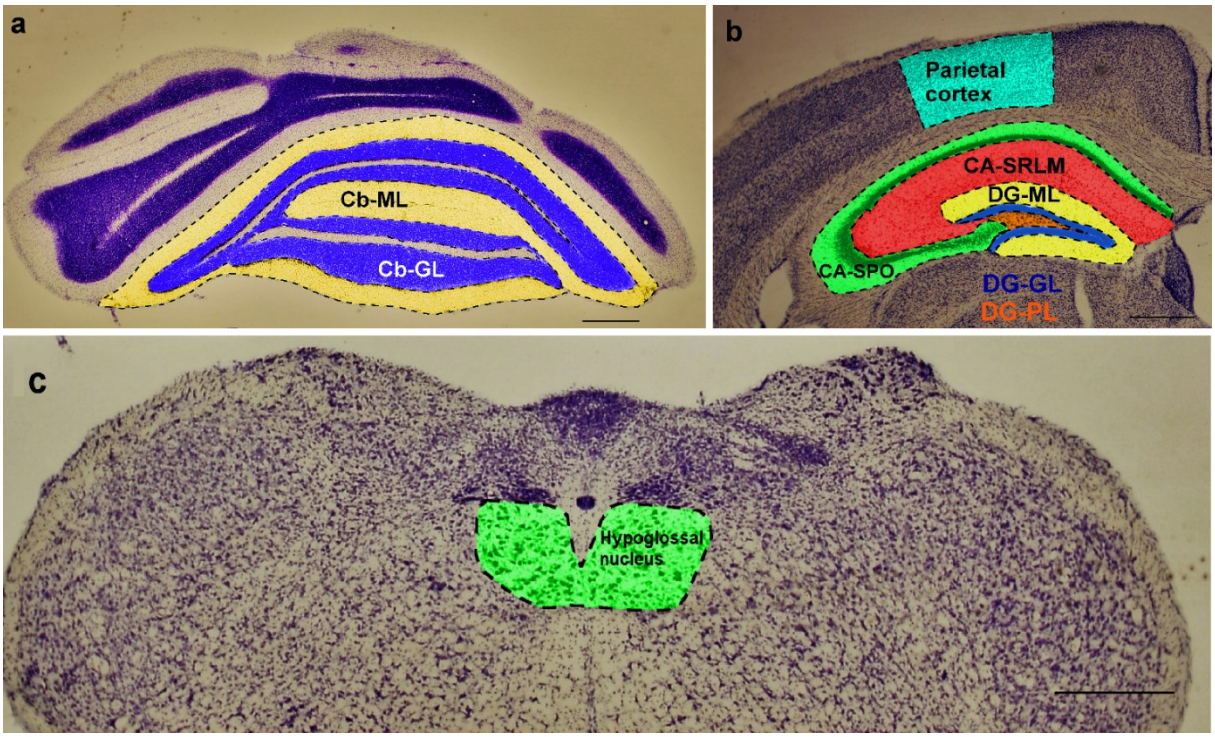

Figure 9. Representative images of the brain regions (Nissl-stained) that were histologically evaluated. (**a**) Representative image of the cerebellar VIII, IX and *Copula pyramidalis* lobules including molecular (Cb-ML) and granular (Cb-GL) layers. (**b**) Representative image of parietal cortex and various hippocampal subregions. CA= Cornu ammonis. DG= dentate gyrus. GL= granular layer. ML= molecular layer. SPO= *stratum pyramidale* and *oriens*. SRLM= *stratum radiatum* and *lacunosum-moleculare*. PL= polymorph layer (hilus). (**c**) Representative image of the hypoglossal nucleus in the mouse brainstem. Scale bars (**a-c**) = 500 µm.

To assess cerebellar volume, the volume of VIII, IX and *Copula pyramidalis* lobules, separately for molecular and granular layers, were measured. Every 4th slice and grid density of 200 µm was used. As the caudal edge of the cerebellum was often damaged, we started from the posterior part where both molecular and granular layers were present and without damage. For evaluation of hippocampal subregions' volumes, every 8th slice was used for *preliminary analysis* and every 4th slice for *final analysis*. Grid density was set at 200 µm in the case of *Cornu ammonis* (CA) subregions and molecular layer of dentate gyrus (DG) volume. A grid density of 66.7 µm was used for DG polymorph and DG granular layers' volume estimation. The sampling density that was used has already been shown to be sufficient to estimate the volume of different DG subregions in mice[568]. Parietal cortex thickness was directly measured from the 2nd to the 6th cortical layers. The 1st cortical layer was ignored as it was often damaged. The thickness was evaluated

by 5 evenly distributed measurements per side and slice. The measured region was defined as the cortex above the hippocampal DG where hippocampal CA extends under DG but does not reach the lower edge of the brain. For hypoglossal nucleus volume estimation, every 4th slice with a grid density of 200 µm was used. All histological data are shown in Suppl. Data1 along with data from behavioural characterization. See Suppl. Fig. S4 for representative images.

In the case of hippocampal volumes, absolute volumes were firstly evaluated. In the subsequent analysis, the brain weight was included as a covariate in the general linear model (supplemented by bootstrapping of partial regression coefficients) to obtain partial effect of the genotype on the hippocampal volume, adjusted for the confounding effect of the brain weight.

For evaluation of brain-behaviour correlations, only the most genotype-sensitive brain regions were included (Cb-ML, CA-SRLM and DG-ML), along with total brain weight (to investigate the association between the behaviour and non-specific brain atrophy) for the analysis. Then, the associations between volumes of these brain measures and *sensitive indicators* from the behavioural characterization were evaluated. Moreover, because cognitive flexibility was more impaired than initial learning during the water T-maze in young SCA1 mice and because the neurobiological substrate of the flexibility could substantially differ from the initial learning, the association of the brain measures with *T-maze inflexibility* was also explored.

5.3.4 Immunofluorescence staining

Immunofluorescent staining for the NeuN (a marker of mature neurons) and double staining for the DCX and PSA-NCAM (a marker of immature neurons and neuroplasticity processes respectively) were performed to assess a possible hippocampal neuronal loss and/or impaired neurogenesis/neuroplasticity in SCA1 mice (Fig. 10).

For the immunofluorescence, 5 animals (4 males and 1 female, aged 13-15 weeks) per group were used. None of the animals used for immunofluorescence had been previously exposed to behavioural tests.

The brains of the animals were perfused, processed, and cryo-sliced in the same way as the brains used for histology (see section 5.3.3). Slices were 40 µm thick.

Staining proceeded on three different staining occasions (staining *blocks*). For each staining *block*, 1 or 2 brains per group were sliced on a single day and stained at once using the same solutions of chemicals. As brains stained in a single *block* cannot be automatically considered independent samples (due to the effect of random inter-block variation), the numbers of brains stained in each *block* were the same for both groups (WT and SCA1). Every 6th slice was used for each animal and staining, commencing from the 12th slice containing the hippocampus (from the frontal part); 4 slices per animal in total.

NeuN staining was performed using mouse anti-NeuN primary antibodies (1/500, Millipore, MAB377) and Alexa Fluor® 488 anti-mouse secondary antibodies (Abcam, ab150117). For the DCX and PSA-NCAM double staining, rabbit anti-DCX (1/4000, Abcam, ab18723) was used along with mouse anti-PSA-NCAM (1/400, Bioscience, 14-9118-82) as the primary antibodies and Alexa Fluor® 594 goat anti-rabbit pre-adsorbed (Abcam, ab150084) and goat anti-mouse IgM cross-adsorbed (Thermofisher, A-21042) as the secondary antibodies. Finally, all slices were also co-stained with DAPI for visualizing cell nuclei.

Imaging was performed using a fluorescent *Olympus BX51* microscope and an *Olympus DP70* digital camera (Olympus, Japan). Detailed images were acquired using an Olympus IX83 spinning disk confocal microscope (Olympus, Germany). The images were acquired using a constant setting of the camera (e.g., in terms of exposition time). Images were analysed using *Fiji* software[569].

The NeuN staining was analysed by measuring the colour intensity while subtracting the immunofluorescent intensity in neighbouring sites without the presence of neuronal bodies (the CA strata oriens; Fig. 10) and via the manual estimation of the neuronal density in the pyramidal layers of two hippocampal sub-regions: CA1 and CA2/3. Concerning each of the assessed sub-regions, the NeuN fluorescent intensity was measured in 2 to 3 pairs of evenly distributed sampling circles, with diameters of approximately half the width of the given layer, in 1 of the hippocampi from each of the stained slices (Fig. 10). Estimation of densities of the pyramidal neurons proceeded in the same hippocampal regions as fluorescence intensity (in at least 1 depth of focus and on at least 2500 μm^2 of the CA pyramidal layer). Since the inclusion of the *block* as a covariate improved an estimated predictive accuracy in the case of NeuN

immunofluorescence in the CA2/3 (evaluated via Bayesian Information Criterium; see the description of the statistical methods below), the NeuN signal in the CA2/3 hippocampal subfield was adjusted for the effect of the *block* (the factor was included in the model as a fixed-effect covariate).

The PSA-NCAM$^+$DCX$^+$ neuronal densities in subgranular layer of DG were estimated at 4 slices per animal, using image sequences containing 3 to 8 depths of focus in at least 250 µm (390 µm on average) of the DG subgranular zone per slice. The DCX$^+$ neuronal dendrites were quantified using the number of crossing lines (at least 250 µm per evaluated DG; 425 µm on average) located in three positions: i) the border between the DG granular and molecular layers (*M/G*); ii) the inner half of the DG-ML (closer to the granular layer; *M-inr*); and iii) the outer half of the DG-ML (*M-out*). Finally, the PSA-NCAM immunofluorescent signal was measured in the DG hilus (DG-PL), DG-ML, CA4 pyramidal and CA1 lacunosum-moleculare (CA1-SLM) layers (Fig. 10).

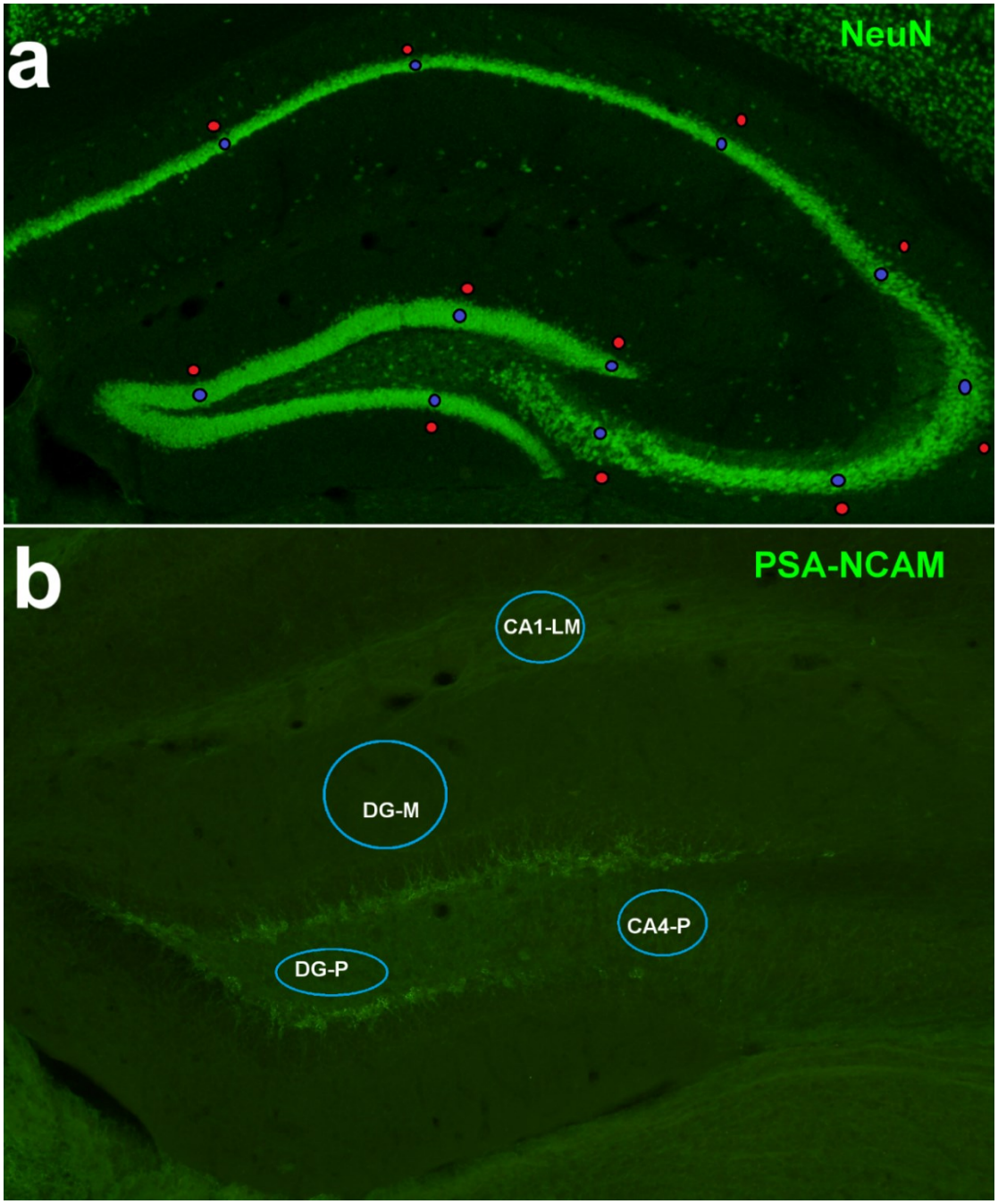

Figure 10. (**a**) Representative image of the hippocampus stained for NeuN. The circles show the area of the measurement of the fluorescence intensity (blue= measurements of interest; red= measurements of the background intensity for correction) and counting of $NeuN^+$ neurons. **(b)** Representative image of the hippocampus stained for PSA-NCAM. The circles represent the areas where the fluorescent intensity of the PSA-NCAM fluorescence signal was measured.

5.3.5 ELISA

To determine the hippocampal BDNF levels, the *BDNF SimpleStep* commercial enzyme-linked immunosorbent assay (ELISA) kit (ab212166, Abcam) was used according to the manufacturer's instructions. The data were normalized to the protein content measured via the use of a BCA1 kit (B9643; Sigma-Aldrich, Saint Louis, USA). The absorbance was measured using a *Tecan Infinite M200 Pro* microplate reader. The specimens were processed in duplicates and the values were averaged. The BDNF was originally measured in 8 animals per group (11-13 weeks of age). Since two of the animals (1 WT and 1 SCA1) evinced distinctly lower amounts of proteins than the other mice, and two other animals (1 WT and 1 SCA1) exhibited unexplainably high differences between the duplicates (tens of %), these cases were considered unreliable and were excluded.

Another independent cohort of mice (N = 9 *WT* and 9 *SCA1*; 10 weeks ± 4 days of age; housed individually for at least 2 weeks before the experiment) were restrained by hand (inducing substantial stress) for 40 seconds (between 07:30 and 08:00 am, i.e., 1.5 to 2 hours after the start of a light period) and their spontaneously released urine was sucked from a clean plastic container with a pipette. The procedure was repeated 65 (± 5) minutes later (1 hour is sufficient time for an increase of corticosterone after stress from the previous restrain). The urine was stored at -80°C until further processing. ELISA kits were used according to the manufacturer's instructions to measure the corticosterone (*Arbor Assays*; K014-H5) and creatinine (*Arbor Assays*; K002-H5) levels. The absorbance was measured using a *Tecan Infinite M200 Pro* microplate reader.

5.3.6 Mitochondrial high-resolution respirometry

The mitochondrial respiration was examined in the cerebellar and hippocampal tissue of another cohort of group-housed mice without previous exposition to any test (11-13 weeks of age; N = 5 WT and 6 SCA1 mice). All the mitochondrial experiments were performed in quadruplicate (4 measurements per mouse and brain structure).

Following cervical dislocation, the whole of the brain was extracted rapidly and the cerebellum and one hippocampus were dissected, dried and weighed and subsequently homogenized in MiR05[570] respiration medium using a PBI-Shredder O2k-Set

(OROBOROS INSTRUMENTS, Innsbruck, Austria). The entire procedure was performed on ice and all the buffer solutions were ice-cold.

The tissue homogenates were transferred into 4 calibrated Oxygraphs (O2k, OROBOROS INSTRUMENTS, Innsbruck, Austria), each equipped with 2 chambers (2 ml). The oxygen polarography was measured at 37°C in the O2k-chambers and the oxygen concentration (μM), as well as the oxygen flux per volume (pmol O2/s/ml), were recorded in real-time using DatLab software, version 7.3.0.3 (OROBOROS INSTRUMENTS, Innsbruck, Austria). The *substrate–uncoupler–inhibitor titration* (SUIT)[571] protocol was employed. The mitochondrial respiration was assessed in the following respiratory states: 1) complex I OXPHOS capacity in the ADP-activated state of oxidative phosphorylation (*P I*), 2) complex I + II OXPHOS capacity (*P I+II*), 3) maximum capacity for electron transport (*E I+II*), 4) complex II uncoupled capacity (*E II*) and 5) *complex IV* capacity. The oxygen concentration in the chambers was kept high enough to avoid oxygen limitation of respiration. The mitochondrial respiration was expressed in pmolO_2/s/mg of homogenized tissue. In subsequent analysis, the respiration was also adjusted for specific citrate synthase activity (log [mIU/mg]) by the inclusion of the factor as a covariate in mixed-effects model. When respiration of one sample distinctly differed from another three samples of the same animal across at least three parameters of respiration, it was removed as an outlier (a total of 4 samples for hippocampal and 2 for cerebellar data). See supplementary material of the published articles[565] for details.

5.3.7 Statistical analyses

All the statistical analyses and data visualizations were performed in *R* statistical software[572]. The parametric statistical analyses were extended by permutational or bootstrapping techniques (10 000 – 20 000 permutations/resampling; these extensions of parametric statistical methods are less sensitive to small sample size, do not rely on assumptions of parametric methods and are more robust toward outlier values[573]). Generally, the comparisons between the SCA1 and WT mice were conducted using the permutation t-test. The effect size was determined via *Cliff's d* and/or the standardized regression coefficient (*ß*), and their 95% confidence intervals (CI) were based on the *bias-corrected and accelerated* (BCa) *bootstrap* method[559] using the *effsize*[574] and *boot*[560]

R packages. The repeated/multiple measurements data were analysed via the permutation test of the *linear mixed-effects model* (LME), with the subject coded as a random factor (with random intercept) and with the *autoregressive 1* (AR1) variance-covariance structure in the case of the serial data, using the *nlme*[561] and *predictmeans*[562] R packages. The (paired) permutation t-test followed by the *False Discovery Rate* correction for multiple comparisons[563] was used as the posthoc test when required.

The multidimensional data were analysed via the *permutational multivariate analysis* of the variance (PERMANOVA) and visualized using *non-metric multidimensional scaling* (NMDS) using the *vegan*[575] R package in both cases. To identify those behavioural measures that might be affected by signs of ataxia in the young SCA1 mice, we examined whether the *sensitive indicators* correlated to abnormal gait. To reduce the dimensionality of the gait data, the *principal components* (PCs; using the *vegan* R package[575]) were extracted and subjected to *principal component regression*. The PCs were based on those gait parameters that differed between the genotypes significantly in at least 1 of the young cohorts and the direction of the genotype-related difference was stable across both cohorts. 4 parameters were chosen: 3 describing the stride lengths and 1 representing the coefficient of variance in the stride length (hind leg, 18 cm/s). The PC1 axis correlated principally with the stride length (thus explaining 48% of the variance), whereas the PC2 correlated with the variance coefficient of the stride length (hind leg, 18 cm/s; explaining 27% of the variance). Only the axis with a higher effect on the given parameter is presented.

The ROC curve, the area under the ROC curve (AUC), its 95% CI and the bootstrapping-based test of the difference between the AUCs were computed using *pROC*[576] R package. The ROC-AUC ranges from 0.5 (i.e., the parameter does not give bring any information about the genotype) to 1 (no overlap between WT and SCA1 mice). The *linear model* (LM) or the *generalized additive model*[577] (GAM), extended via the BCa bootstrapping of the (partial) regression coefficient(s) (ß), were used to evaluate (dissociate) the effect(s) of the numerical predictor(s) on a single response variable.

The Box-whisker plots indicate the inter-quartile (IQ) intervals (box), 1.5*IQ range (whiskers) and medians (middle lines). $P < 0.05$ was defined as significant.

5.4 Results

5.4.1 Emotional-related behavioural abnormalities in SCA1 mice

Results of a complex behavioural and motor characterization (performed across four age cohorts: aged 6, 10, 17 and 26 weeks) are shown in Suppl. Table S1.

The SCA1 mice exhibited abnormal behaviour in the open field test (OF; Fig. 11a-d). Specifically, the SCA1 mice were less active than the WT mice (Suppl. Table S1) and preferred moving along the walls (thigmotaxis; relative distance walked <5 cm from arena walls per total distance [0-1]) in all the age cohorts (Fig. 11a,d). Although the thigmotaxis partially correlated with the distance moved (Fig 11b), it remained significant even after adjustment for the distance moved (*OF adj. thigmotaxis*, Suppl. Table S1) and 25% of the most mobile SCA1 mice (from all cohorts together; distance moved: 40.2-68.71 m) were still more thigmotaxic than the comparably active WT mice (Fig. 11c). Similarly, the SCA1 mice exhibited higher avoidance of the open arms during the elevated plus maze test (EPM), although the effect was statistically significant only at the ages of 10 and 17 weeks (Suppl. Fig. S1). Overall, the results obtained from the OF and EPM indicate increased anxiety-like behaviour in the SCA1 mice.

The SCA1 mice had also reduced prepulse inhibition of the startle response in 3 of the 4 age cohorts (Fig. 11e). The older cohorts (17 and 26 weeks of age) also evinced a reduced startle amplitude and a prolonged latency of the startle response (Suppl. Fig. S1).

Finally, the SCA1 mice exhibited a significantly higher immobility time during the forced swimming test (FST) in the two youngest age cohorts (9 and 13 weeks of age; Fig. 11f). The increased duration of immobility was most pronounced in the first half (0-3 minutes) of the test when the genotype differences attained statistical significance across all the age cohorts (Suppl. Table S1). To investigate depressive-like behaviour without the effect of exposure to previous tests, a new cohort of mice (11 animals per group, 6 weeks of age) underwent the FST only. SCA1 mice were significantly more immobile than the WT mice only during the first half of the test (P-value: 0.2 [immobility averaged over 6 minutes] and 0.049 [the first 3 minutes of the FST]). To assess anhedonia-like emotionality, another cohort of mice underwent sucrose preference test. The SCA1 mice evinced a lower sucrose preference (Fig. 11g), supporting depressive-like behaviour in the SCA1 mice.

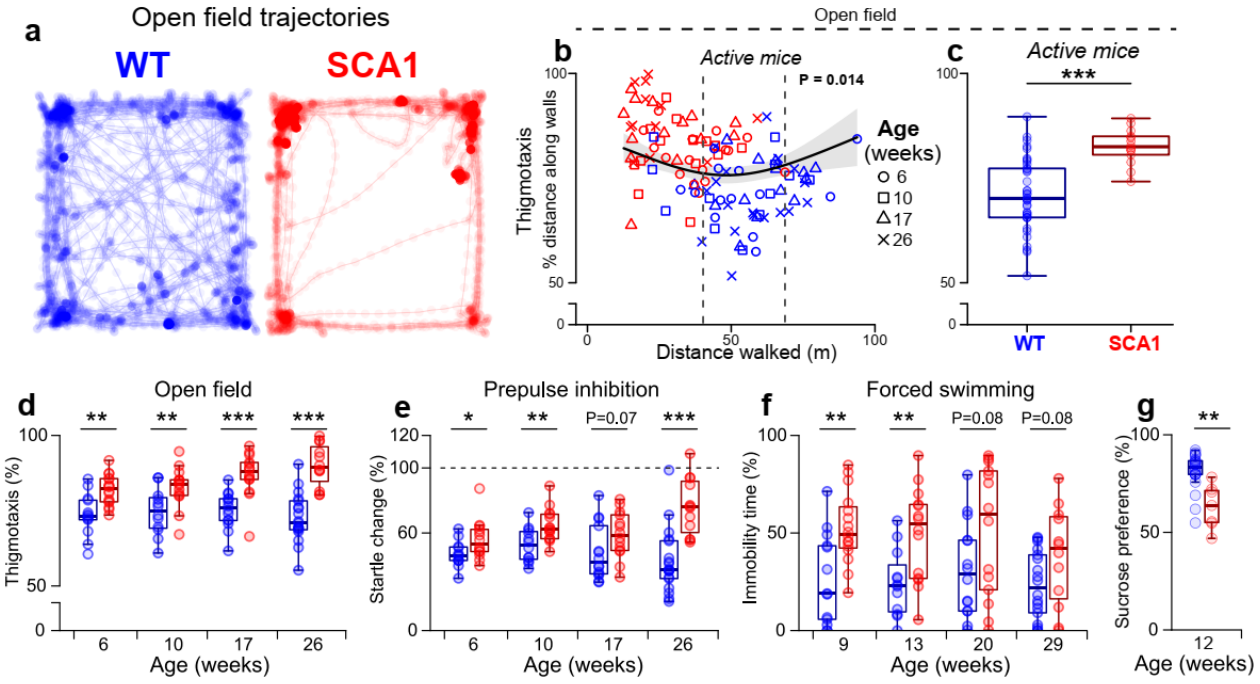

Figure 11. Psychiatric-relevant behavioural deficits in the SCA1 mice. (**a**) Representative OF trajectories for the WT and SCA1 mice (6 weeks of age). (**b**) Association between thigmotaxis and locomotion during the open field test. The P-value is based on the general additive model and reflects the significance of the partial effect of the *distance moved* adjusted for *genotype*. (**c**) Thigmotaxis in 25% of the most mobile SCA1 mice and comparably mobile WT controls (*distance moved* during OF*:* 40.2 – 68.71 m; all cohorts together; N = 14 SCA1 and 38 WT mice). (**d**) Thigmotaxis in the OF, indicating anxiety-like behaviour. (**e**) Relative change in the startle response amplitude following a prepulse stimulus, reflecting prepulse inhibition. (**f**) Relative immobility time during the FST, indicating depressive-like behaviour. (**g**) Relative 1% sucrose consumption in the sucrose preference test. * $P < 0.05$, ** $P < 0.01$, *** $P < 0.001$. The statistical significances are based on the permutation t-test. See Suppl. Table S1 for the detailed results.

5.4.2 Altered behaviour in cognitive tasks in the SCA1 mice

The object-location memory test did not reveal any genotype-related difference in terms of the exploration of newly replaced objects (Table 6).

Although SCA1 mice needed a longer time to reach both the hidden and visible platforms in the MWM (Suppl. Tables S2 and S3, Suppl. Fig. 1), they evinced a seemingly stronger tendency to non-moving behaviour during the MWM (Fig. 12a, Suppl. Tables S4 and S5). Whereas the genotype-related difference in the latency to find the hidden platform was minimal in the young mice (8 and 12 weeks of age) at the commencement of the MWM (Suppl. Table S3), the tendency to non-moving behaviour was profoundly

higher in the SCA1 mice from the 1st day of testing (Fig. 12a). This suggests that non-moving behaviour is not a secondary consequence of poor learning skills. Thus, the increased latency to find the platform in the MWM could not be interpreted as a cognitive deficit in the SCA1 mice. However, the SCA1 mice also learned more slowly to navigate toward the hidden platform in the water T-maze and demonstrated a profound inability to re-learn once the platform had been relocated to the opposite side (Fig. 12b, Suppl. Tables S6 and S7), suggesting substantially reduced memory and cognitive flexibility.

Table 6. Permutational linear mixed-effect models describing the relative exploration of object pairs during the object-location memory test in relation to *phase* (before the change of objects' position [*pre-exchange*] or after the change [*post-exchange*]), *genotype* (WT or SCA1) and their interaction. Individual subjects are included as a random factor.
W.A. = weeks of age. *d.f.* = degrees of freedom. *d.d.f.* = denominator degrees of freedom. P = significance derived from *linear mixed-effect model* (LME). Perm. P= significance from permutation test of LME model.

(a) 6 W.A.	**Variable**	***d.f.***	***d.d.f.***	**F**	**P**	**Perm. P**
	intercept	1	27	1364		
	Phase	1	27	6.7	0.0156	0.0134
	Genotype	1	27	1.1	0.2959	0.2969
	*Phase*Genotype*	1	27	3.3	0.0808	0.0722
(b) 10 W.A.	**Variable**	***d.f.***	***d.d.f.***	**F**	**P**	**Perm. P**
	intercept	1	24	854		
	Phase	1	24	23.5	<0.001	<0.001
	Genotype	1	24	1.9	0.1801	0.1642
	*Phase*Genotype*	1	24	3.4	0.0767	0.0686
(c) 17 W.A.	**Variable**	***d.f.***	***d.d.f.***	**F**	**P**	**Perm. P**
	intercept	1	26	757		
	Phase	1	26	0.6	0.4339	0.4342
	Genotype	1	26	0.06	0.805	0.8101
	*Phase*Genotype*	1	26	0.19	0.6671	0.6738
(d) 26 W.A.	**Variable**	***d.f.***	***d.d.f.***	**F**	**P**	**Perm. P**
	intercept	1	28	1078		
	Phase	1	28	13.5	0.001	<0.001
	Genotype	1	28	1.8	0.1858	0.1944
	*Phase*Genotype*	1	28	0.05	0.8195	0.8261

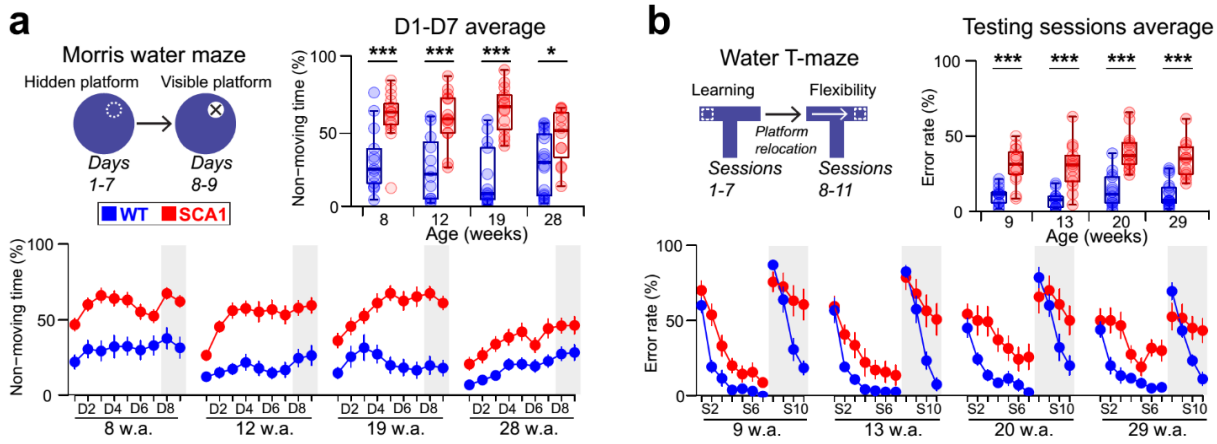

Figure 12. Altered behaviour and learning during the cognitive tasks in the SCA1 mice. (**a**) Relative non-moving time during the MWM, averaged over the first 7 days (D1-D7) of the experiment (top) and shown per each session specifically (below). (**b**) Error rate during the water T-maze test averaged over all the testing sessions (S3-S7 and S10-S11) of the experiment (top) and shown per each session specifically (below). The grey areas in the day/session-specific plots show the visible platform phase of the MWM (**a**) or the reversal phase of the water T-maze test (**b**). The day/session-specific plots (below) show the means ± SEMs. * $P < 0.05$, *** $P < 0.001$. The statistical significances are based on the permutation t-test. w.a.= age in weeks.

5.4.3 Non-motor deficits dominate over ataxia in young SCA1 mice

Although the older cohorts of SCA1 mice exhibited substantial motor impairments (tested at 18 and 27 weeks of age), the younger mice (tested at 7 and 11 weeks of age) performed only mildly or insignificantly worse on the accelerating rotarod than did the WT mice (Fig. 13a; Suppl. Tables S8 and S9). Similarly, the older SCA1 mice (tested at 17 and 26 weeks of age) had substantially abnormal gaits, whereas the younger SCA1 mice (tested at 6 and 10 weeks of age) evinced no significant gait dissimilarities from the controls (Fig. 13b, Suppl. Table S10).

Of all the indicators assessed in the characterization experiments (Suppl. Table S1), those with the highest sensitivity to the genotype (*sensitive indicators*) were selected. Following *sensitive indicators* were identified: distance moved in the OF, thigmotaxis in the OF, averaged rotarod latency, non-moving behaviour in the MWM (average from D1-D7), error rate in the water T-maze (average from S2-S7 and S10-S11) and immobility time in the FST.

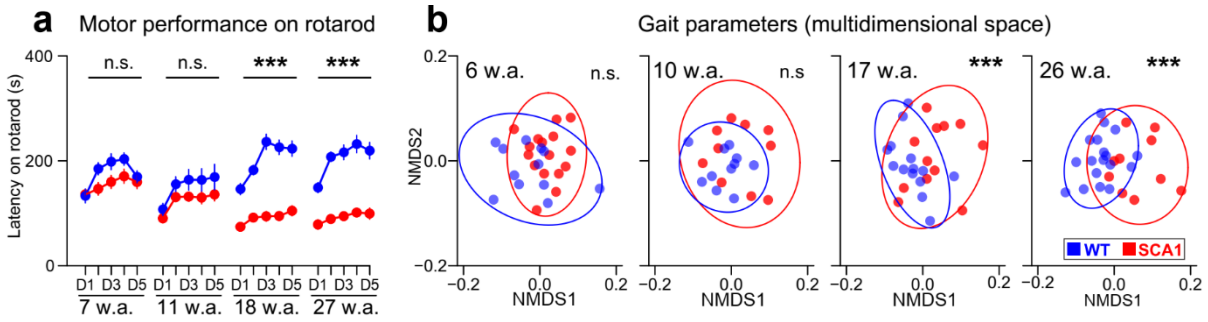

Figure 13. (**a**) Latency on the accelerating rotarod over 5 days (D) of the rotarod experiment. The points are means ± SEMs. The P-values are based on comparing the averaged values from the whole experiment via the permutation t-test. (**b**) Visualization of the dissimilarities in the gait parameters using non-metric multidimensional scaling (NMDS). The P-values are based on the permutational multivariate analysis of variance (PERMANOVA). The ellipses show the 90% confidence intervals for point occurrence (each point= 1 animal).

Generally, the *sensitive indicators* differed significantly between young (6-14 weeks) and old (17-31 weeks) SCA1 mice (Suppl. Table S11; Fig. 14). Since the functional impairment patterns did not differ significantly within these two groups, the data were merged into two datasets only (young and old mice) for further analysis. Since the young SCA1 mice did not exhibit profound ataxia (as a potential confounder of the behavioural results), greater attention was devoted to these age cohorts when analysing the behaviour and underlying neuropathology of the SCA1 mice.

To identify the behavioural measures which might be affected by signs of ataxia in the young SCA1 mice, it was examined whether the *sensitive indicators* correlated with decreased rotarod performance and/or abnormal gait (expressed via the *principal components* from the 4 most sensitive gait parameters; Suppl. Table S1). Gait and rotarod performance were inter-correlated and both revealed indications of their effect on the distance moved in the OF (Table 7), suggesting that the activity in the OF might be confounded even by subtle signs of ataxia in young SCA1 mice whereas other behavioural measures are not substantially affected by the subtle motor deficits.

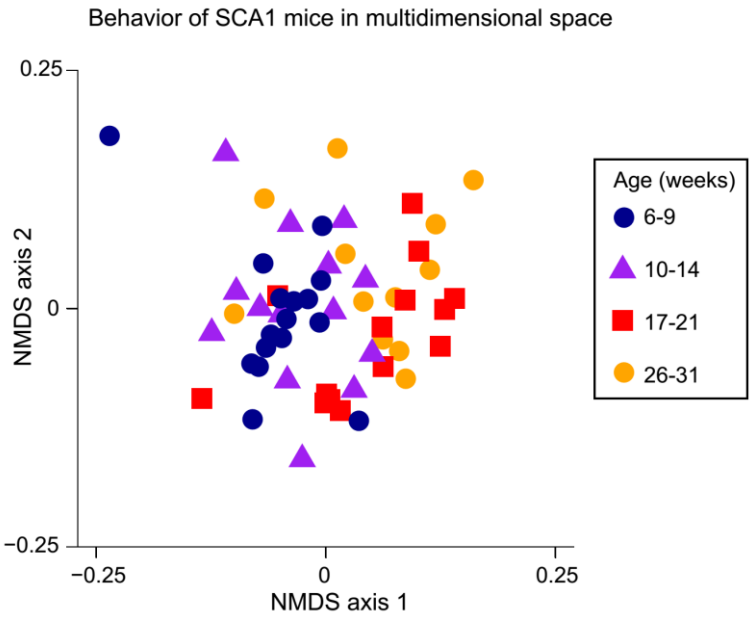

Figure 14. Non-metric multidimensional scaling (NMDS) showing the similarity of the functional impairments of SCA1 mice from differing age cohorts in multidimensional space. Each point represents one SCA1 mouse. The closer the points, the more similar were the mice in terms of their functional impairments. The significances of the effect of the age cohort on the *sensitive indicators* (based on the permutational analysis of variance, PERMANOVA) were as follows: $P < 0.001$ when all the data were used (age explains more than 17% of the variance in data), $P = 0.65$ for the dataset that included specifically mice ≤ 14 weeks of age (explained variance: 2.3%) and $P = 0.21$ (explained variance: 5.8%) for the dataset that included specifically mice ≥ 17 weeks of age.

To test whether the non-motor *sensitive indicators* characterize the early SCA1 mice significantly better than do their motor functions, a ROC curve visualising and quantifying the ability of the *sensitive indicators* to successfully classify the mice into genotypes (WT vs. SCA1) was constructed. All the non-motor *sensitive* indicators, except for distance walked in OF, distinguished the SCA1 mice from the WT mice more accurately than did rotarod latency at younger ages (Fig. 15a). In contrast, in older mice (>17 weeks of age), ataxia worsened rapidly and latency to rotarod thus differentiated older mice more accurately than most behavioural deficits (Fig. 15b). Taken together, the results suggest that the early SCA1 stage in the mouse model is characterized particularly by non-motor behavioural and cognitive deficits.

Table 7. Linear models describing an effect of indicators potentially sensitive to physical/motor deterioration (rotarod latency, activity in open field, gait and MWM non-moving) on the *sensitive indicators* in young (≤ 14 weeks of age) SCA1 mice. In the case of gait, the principal components (PrCs) were extracted and subjected to *principal component regression*. The PrCs were based on those gait parameters that differed between the genotypes significantly in at least 1 of the young cohorts and the direction of the genotype-related difference was stable across both cohorts. 4 parameters were chosen: 3 describing the stride lengths and 1 representing the coefficient of variance in the stride length (hind leg, belt speed 18 cm/s). The PrC1 axis correlated principally with the stride length (explaining 48% of the variance), whereas the PrC2 correlated with the variance coefficient of the stride length (hind leg, belt speed 18 cm/s; explaining 27% of the variance). Only the axis with a higher effect on the given parameter is presented. *d.f.*= degrees of freedom. β= standardized regression coefficient. CI= limits for 95% confidence intervals (CI-L: lower limit, CI-U: upper limit) based on bias-corrected and accelerated (BCa) bootstrap. P= significance based on parametric approach. boot. P= significance based on percentile bootstrap.

Model	$\mathbf{F}_{d.f.}$	β	**CI-L**	**CI-U**	**P**	**boot. P**
OF distance ~ Rotarod latency	$4.1_{1,28}$	0.36	-0.06	0.72	0.052	0.20
OF thigmotaxis ~ Rotarod latency	$0.00_{1,28}$	0.01	-0.29	0.64	0.98	0.97
MWM non-moving ~ Rotarod latency	$2.6_{1,28}$	-0.29	-0.77	0.24	0.12	0.41
T-maze errors rate ~ Rotarod latency	$0.26_{1,28}$	-0.1	-0.37	0.27	0.61	0.47
FST immobility ~ Rotarod latency	$1_{1,28}$	-0.09	-0.46	0.40	0.63	0.71
Rotarod latency ~ Gait PrC2	$11_{1,24}$	-0.56	**-0.98**	**-0.25**	**0.003**	**0.003**
OF distance ~ Gait PrC2	$4.9_{1,24}$	-0.4	**-0.81**	**-0.04**	**0.045**	0.062
OF thigmotaxis ~ Gait PrC2	$0.02_{1,24}$	0.03	-0.39	0.47	0.9	0.86
MWM non-moving ~ Gait PrC2	$2.2_{1,24}$	0.29	-0.1	0.8	0.15	0.22
T-maze errors rate ~ Gait PrC1	$2_{1,24}$	-0.28	-0.67	0.22	0.17	0.19
FST immobility ~ Gait PrC2	$0.7_{1,24}$	0.24	-0.26	0.52	0.42	0.39
OF thigmotaxis ~ OF distance	$0.3_{1,28}$	-0.1	-0.39	0.24	0.58	0.46
MWM non-moving ~ OF distance	$12.6_{1,28}$	-0.56	**-0.93**	**-0.19**	**0.001**	**0.004**
T-maze errors rate ~ OF distance	$0.93_{1,28}$	0.17	-0.18	0.70	0.35	0.42
FST immobility ~ OF distance	$1.25_{1,28}$	-0.2	-0.57	0.20	0.27	0.33
T-maze errors rate ~ MWM non-mov.	$0.07_{1,28}$	0.05	-0.41	0.37	0.80	0.78

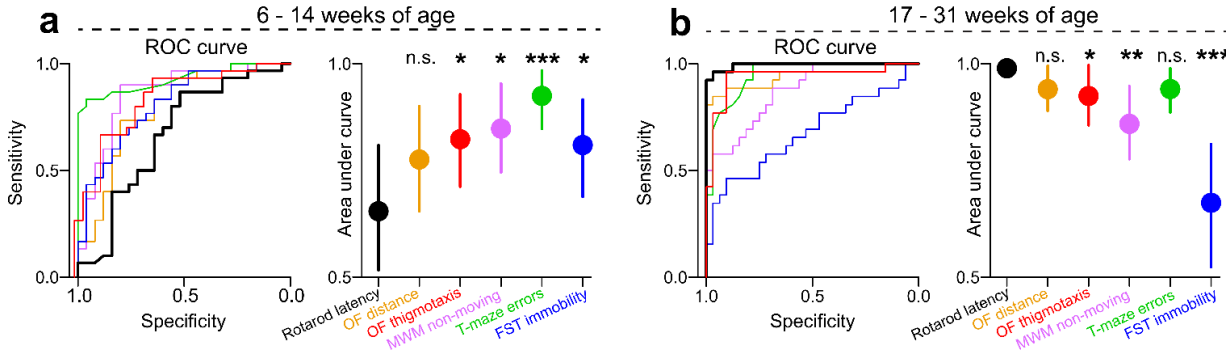

Figure 15. **(a-b)** ROC curve and area under the ROC curve showing the ability of the sensitive indicators to correctly classify the mice into genotypes. The vertical lines imply 95% confidence intervals. The significances are based on bootstrapping and indicate the difference between the AUC of a given indicator versus the AUC of rotarod latency. * P < 0.05, ** P < 0.01, *** P < 0.001. n.s. = not significant. w.a. = age in weeks. OF= open field. MWM= Morris water maze. FST= forced swimming test.

5.4.4 Hippocampal atrophy precedes cerebellar degeneration

To explore region-specific brain volumetric atrophy in the SCA1 mice, brain volumetry analyses were performed via the histological examination of the mouse brains from the behavioural characterization experiments. At first, a preliminary analysis (based on the oldest age cohorts, 8 animals per group) was performed. It identified the molecular layer of the cerebellum (its relative volume per granular layer volume [Cb-ML]) and two regions of the hippocampus (the dentate gyrus molecular layer [DG-ML] and the inner layers of the *Cornu ammonis* [stratum radiatum + lacunosum-moleculare; CA-SRLM]) as those regions of the brain most sensitive to volumetric atrophy in the SCA1 mice (Fig. 16a, Suppl. Table S12). Thus, these brain regions were assessed across all the age cohorts (N= 8 WT and 10 SCA1 mice per age cohort, 9 per group in the youngest cohort).

The relative Cb-ML volume gradually decreased as the disease progressed in the SCA1 mice. Whereas it was found to be only insignificantly or mildly reduced in the young (*pre-ataxic*) age cohorts, it was seen to have decreased dramatically in the older (*ataxic*) SCA1 mice (Fig. 16b).

In contrast, the hippocampal volumes (both CA-SRLM and DG-ML) were found to be significantly reduced in the SCA1 mice across all the age cohorts (Fig. 16c) and, thus, preceded the significant Cb-ML atrophy. However, the SCA1 mice also evinced reduced overall brain weight with respect to all the age cohorts (P< 0.05), and the hippocampal

volumes correlated with overall brain weight (Suppl. Tables S13 and S14). When the total brain weight was taken into account (included as a covariate in the general linear model along with the genotype effect), the significant genotype effect disappeared with concern to the CA-SRLM in 1 of the age cohorts (Suppl. Table S13). However, with respect to the DG-ML volume, the volumetric reduction in the SCA1 mice remained statistically significant for all the age cohorts (Suppl. Table S14), thus implying that the DG-ML atrophy in the SCA1 mice is not simply a consequence of overall brain tissue loss.

Subsequently, the association between the region-specific volumes and the individual severity of the functional impairments (the *sensitive parameters*) was investigated. For this, the focus was dedicated specifically to the *pre-ataxic* SCA1 mice without substantial ataxia and thus with a low risk of confounding by motor deficits. The Cb-ML and CA-SRLM volumes and total brain weight were not found to be associated with any of the functional impairments at the statistically significant level, although an apparent trend was evident toward a positive association between the error rate in the water T-maze test and the Cb-ML volume (Fig. 16d; Table 8). When the same analysis was repeated also for the absolute volume of the Cb-ML, a significant association with rotarod latency was found (Table 8). It supports that the cerebellar volume and cerebellar degeneration affect the motor-related measures but not the non-motor behavioural indicators in SCA1 mice.

On the other hand, DG-ML atrophy was associated with an increased tendency toward non-moving (unmotivated) behaviour in the MWM, more severe impairments in cognitive flexibility in the water T-maze test and increased depressive-like behaviour during the FST (Fig. 16d,e, Table 8).

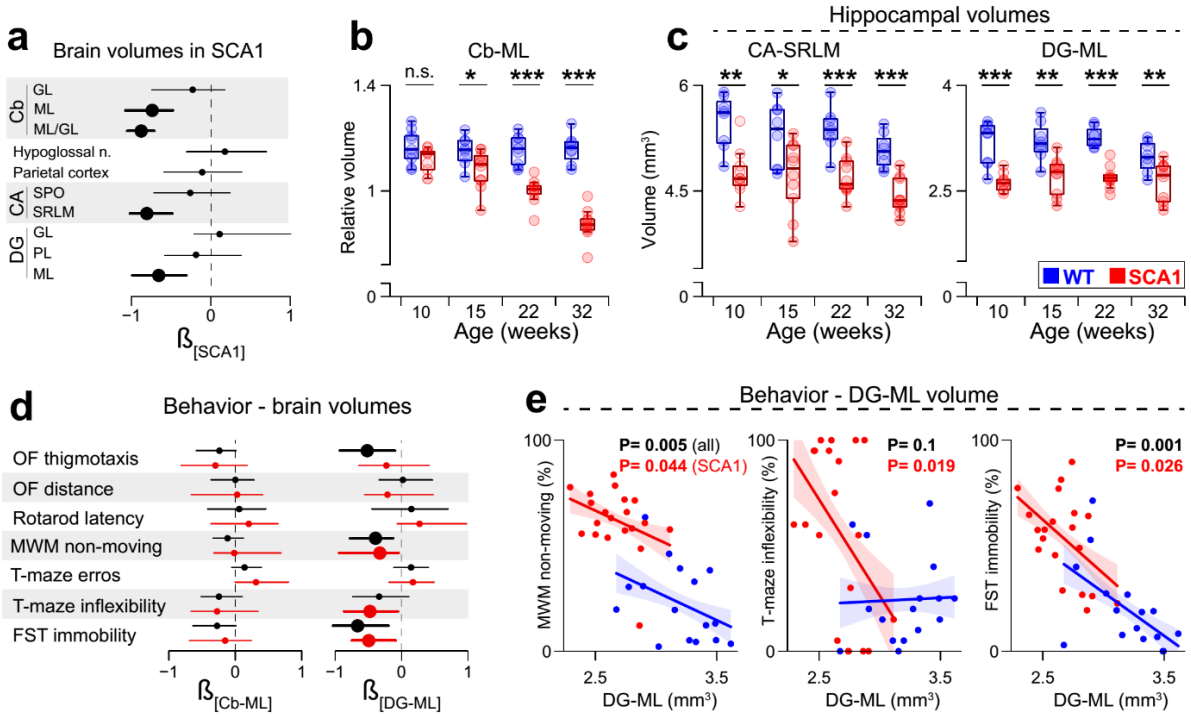

Figure 16. Hippocampal atrophy precedes cerebellar degeneration and reflects the severity of the behavioural deficits. (**a**) Standardized regression coefficients (ß) and 95% confidence intervals (95% CI) for the effect of the SCA1 genotype on brain volumes or thickness (for parietal cortex). The thickness of the line indicates that 95% CI did not cross zero. Cb= cerebellum. CA= *Cornu ammonis.* DG= dentate gyrus. GL= granular layer. ML= molecular layer. SPO= *stratum pyramidale* and *oriens*. SRLM= *stratum radiatum* and *lacunosum-moleculare*. PL= polymorph layer. **(b)** Cerebellar molecular per granular layer volumes ratio (Cb-ML). **(c)** CA-SRLM and DG-ML hippocampal volumes. * P < 0.05, ** P < 0.01, *** P < 0.001. n.s. = not significant. The P-values are based on the permutation t-test (**b-c**). **(d)** ß for the effect of the Cb-ML (left) and DG-ML (right) volumes on the *sensitive indicators*, with 95% CI. The thickness indicates that 95% CI did not cross zero. The black lines show the results of the models that included both the WT and SCA1 mice with the genotype as a covariate, whereas the red lines show the results obtained from the SCA1 mice-specific data (Suppl. Tables S15-S18). **(e)** Relationship between the DG-ML volumes and the *sensitive indicators* which were significantly associated with the DG-ML in the SCA1 mice: non-moving time in the MWM (D1-D7 average; left), error rate during the flexible phase of the water T-maze test (middle) and the immobility time during the FST (right). The lines indicate model fits and their standard errors. The P-values are based on percentile bootstrapping (**d-e**)

Table 8. Models describing the association between volume in a given brain region (cerebellar molecular layer volumes [**a**, **b**] *stratum radiatum* and *lacunosum-moleculare* of *Cornu ammonis* [**c**, CA-SRLM], overall brain weight [**d**], Dentate gyrus molecular layer [DG-ML, **e**]) and *sensitive indicators* in young SCA1 mice (N= 20 animals). *ß*= regression coefficient. CI= limits for 95% confidence intervals. P= parametric P-value. boot. P= percentile bootstrap-derived P-value.

a) **Cb-ML**	*ß*	CI-L	CI-U	P	boot. P
OF thigmotaxis	-0.22	-0.78	0.21	0.38	0.29
OF distance	0.03	-0.66	0.43	0.92	0.94
Rotarod latency	0.2	-0.37	0.61	0.42	0.57
MWM non-moving	-0.02	-0.3	0.64	0.95	0.93
T-maze errors rate	0.31	-0.002	0.89	0.19	0.054
T-maze inflexibility	-0.27	-0.65	0.35	0.29	0.24
FST immobility	-0.15	-0.7	0.2	0.51	0.41
b) **Absolute CB-ML**	*ß*	CI-L	CI-U	P	boot. P
OF thigmotaxis	-0.46	-0.97	0.05	0.047	0.059
OF distance	0.51	-0.12	0.81	0.014	0.15
Rotarod latency	**0.72**	**0.15**	**0.94**	**<0.001**	**0.044**
MWM non-moving	-0.62	-0.93	0.12	0.005	0.18
T-maze errors rate	0.18	-0.5	0.61	0.47	0.33
T-maze inflexibility	-0.33	-0.66	0.37	0.14	0.21
FST immobility	-0.28	-0.81	0.59	0.28	0.5
c) **CA-SRLM**	*ß*	CI-L	CI-U	P	boot. P
OF thigmotaxis	-0.10	-0.60	0.30	0.66	0.60
OF distance	-0.1	-0.66	0.31	0.68	0.58
Rotarod latency	0.12	-0.33	0.66	0.63	0.72
MWM non-moving	-0.2	-0.37	0.27	0.36	0.18
T-maze errors rate	0.1	-0.42	0.43	0.66	0.55
T-maze inflexibility	-0.15	-0.61	0.38	0.54	0.54
FST immobility	0	-0.41	0.54	1	0.96
d) **Brain weight**	*ß*	CI-L	CI-U	P	boot. P
OF thigmotaxis	-0.26	-0.57	0.16	0.62	0.13
OF distance	-0.24	-0.52	0.16	0.2	0.14
Rotarod latency	0.1	-0.2	0.59	0.61	0.60
MWM non-moving	-0.05	-0.45	0.42	0.79	0.80
T-maze errors rate	0.04	-0.34	0.34	0.84	0.80
T-maze inflexibility	-0.13	-0.49	0.22	0.50	0.47
FST immobility	-0.11	-0.47	0.42	0.57	0.63
e) **DG-ML**	*ß*	CI-L	CI-U	P	boot. P
OF thigmotaxis	-0.31	-0.70	0.31	0.29	0.23
OF distance	-0.31	-0.55	0.49	0.38	0.40
Rotarod latency	0.27	-0.04	1.01	0.25	0.16
MWM non-moving	**-0.33**	**-0.96**	**-0.06**	0.12	**0.044**
T-maze errors rate	0.17	-0.21	0.49	0.46	0.35
T-maze inflexibility	**-0.48**	**-0.86**	**-0.03**	**0.045**	**0.019**
FST immobility	**-0.49**	**-0.74**	**-0.08**	**0.024**	**0.026**

The association between non-motivated/despaired behaviour (concerning both MWM and FST) and the DG-ML volume was not found to be specific to the SCA1 mice, since including the WT mice in the analysis even strengthened the association (Suppl. Table S15). In contrast, the association of the DG-ML volume with cognitive flexibility in the water T-maze test was seen to be specific only to the SCA1 mice since it disappeared once the WT mice were included. In a similar way to the SCA1-specific brain behaviour association, the Cb-ML, CA-SRLM and brain weight were not significantly associated with any of the *sensitive indicators* when all the animals (WT and SCA1) were included (Suppl. Tables S16-S18).

In conclusion, the brain volumetry data indicate hippocampal, particularly DG-ML, volumetric atrophy that is directly linked to the individual severity of some of the behavioural deficits observed in the young SCA1 mice.

5.4.5 Impaired hippocampal neurogenesis in the SCA1 mice

To evaluate whether neuronal loss accompanies the hippocampal atrophy, the immunofluorescence staining of CA mature ($NeuN^+$) pyramidal neurons and immature (DCX^+PSA-$NCAM^+$) neurons in the DG (sub)granular layer (N= 5 per group; 13-15 weeks of age) were performed. The SCA1 mice exhibited a significant reduction in NeuN immunofluorescence in both the evaluated subregions (CA1 and CA2/3). However, the density of the $NeuN^+$ neurons evinced only an insignificant trend toward decreased neuronal densities in the SCA1 mice (Fig. 17a,c, Table 9), thus suggesting decreased NeuN expression/antigenicity without marked neuronal loss.

Interestingly, the SCA1 mice also evinced distinctly lower numbers of immature (DCX^+ PSA-$NCAM^+$) neurons in the DG subgranular layer (Fig. 17b,d, Table 10). In addition, the dendrites of the immature (DCX^+) neurons were dramatically impoverished and were practically absent in the outer parts of the DG-ML in the SCA1 mice (Fig. 17b,e). These results thus suggest that profoundly diminished neurogenesis accompanies hippocampal volumetric atrophy in the SCA1 mice.

Table 9. Results of linear mixed-effect models describing the (partial) effect of the SCA1 genotype on the density of NeuN+ neurons (**a**, **b**) and NeuN immunofluorescence intensity (**c**, **d**) in CA1 (**a**, **c**) and CA2/3 (**b**, **d**) hippocampal pyramidal layer. The fluorescence intensity was subtracted by the fluorescence of the background. Because adding a grouping factor (block) improved model fit (measured by BIC) in the case of NeuN signal in CA2/3, it was included in the model as a covariate. N= 5 mice per group with 4 evaluated sections per mouse. ß= standardized partial regression coefficient. CI= limits for 95% confidence intervals of ß based on percentile bootstrap. P= significance based on parametric approach. boot. P= significance based on percentile bootstrap.

(**a**) Neuronal density – CA1	*ß*	CI-L	CI-U	P	boot. P
Genotype	-0.28	-0.63	0.08	0.16	0.13
(**b**) Neuronal density – CA2/3	*ß*	CI-L	CI-U	P	boot. P
Genotype	-0.38	-0.75	0.01	0.09	0.054
(**c**) NeuN signal – CA1	*ß*	CI-L	CI-U	P	boot. P
Genotype	-0.53	-0.86	-0.21	0.013	<0.001
(**d**) NeuN signal – CA2/3	*ß*	CI-L	CI-U	P	boot. P
Block				0.014	
Genotype	-0.58	-0.81	-0.37	0.002	<0.001

Since the PSA-NCAM fluorescence of the non-neuronal morphology indicates the occurrence of neuroplasticity processes, such as neurite growth and formation of synapses[578–581], the PSA-NCAM immunofluorescence was measured in four hippocampal areas: the DG hilus, DG-ML, CA4 pyramidal and CA1 stratum lacunosum-moleculare (CA1-SLM) layers. The fluorescence was reduced in one (the CA1-SLM) but not in the other hippocampal areas (Fig. 17f. Table 10), suggesting that reduced neuroplasticity processes may also partially contribute to the hippocampal atrophy in the SCA1 mice.

Table 10. Results of linear mixed-effect models describing the effect of the genotype on immunofluorescent indicators of neurogenesis or neuroplasticity. The DCX+ neuronal dendrites were quantified by means of the number of crossing lines in three positions: i) molecular-granular layers border (M/G); ii) the inner half of the DG-ML (M-in) and iii) the outer half of the DG-ML (M-out). See Table 9 for abbreviations.

	ß	CI-L	CI-U	P	boot. P
$DCX^+PSA\text{-}NCAM^+$ neurons	-0.67	-0.99	-0.35	0.004	<0.001
DCX^+ dendrites (M/G)	-0.85	-1.08	-0.62	<0.001	<0.001
DCX^+ dendrites (M-in)	-0.84	-1.08	-0.60	<0.001	<0.001
DCX^+ dendrites (M-out)	-0.72	-1.02	-0.44	0.001	<0.001
PSA-NCAM signal (DG-PL)	-0.34	-0.88	0.21	0.26	0.23
PSA-NCAM signal (DG-ML)	-0.48	-0.92	0.05	0.12	0.074
PSA-NCAM signal (CA4-PL)	-0.36	-0.79	0.07	0.15	0.11
PSA-NCAM signal (CA1-SLM)	-0.49	-0.83	-0.15	0.022	0.005

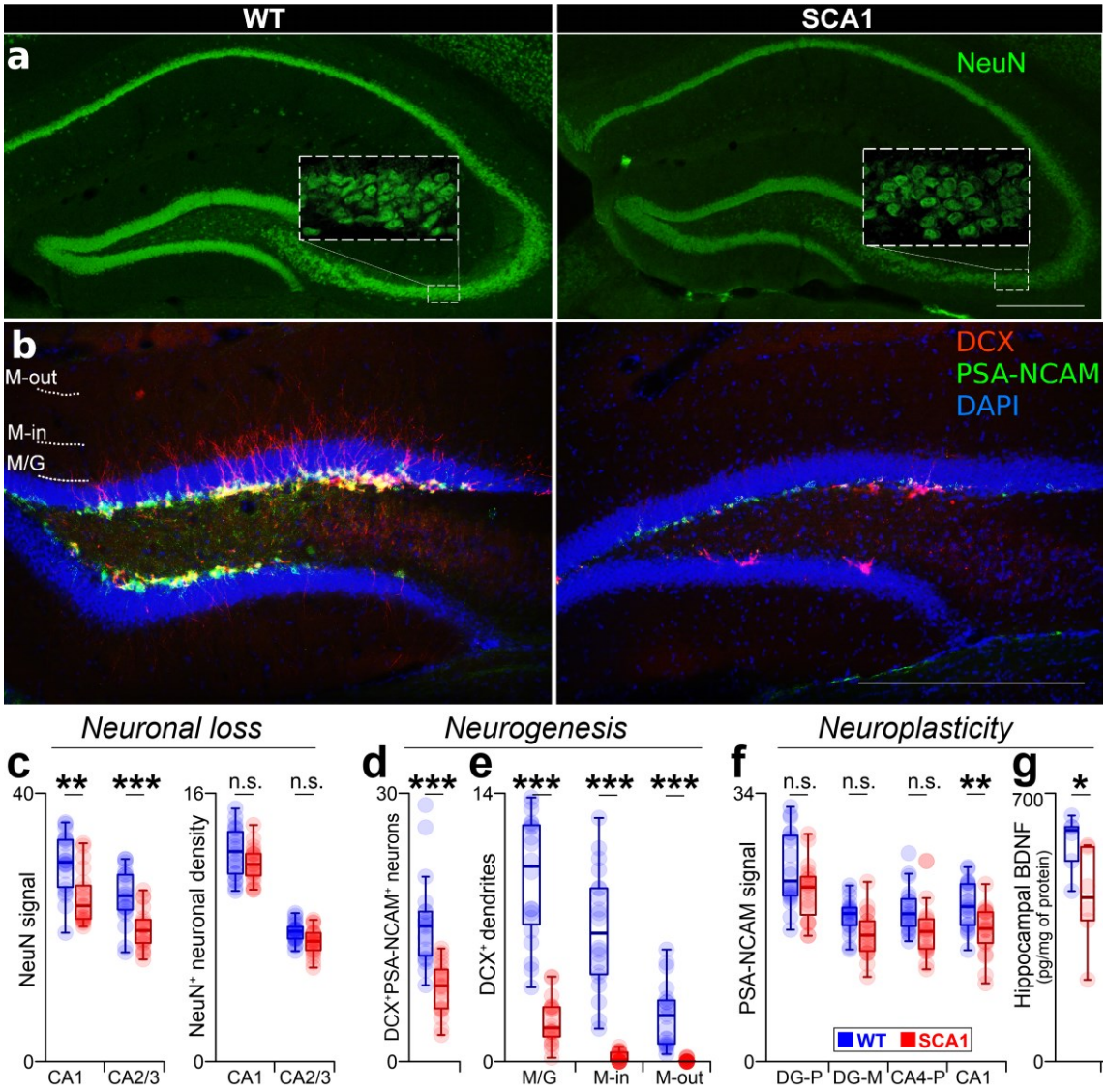

Figure 17. Impaired hippocampal neurogenesis in the SCA1 mice. (**a**) Representative images of hippocampal sections stained for NeuN. Scale bars (**a**-**b**) = 400 µm. (**b**) Representative images of the DG double-stained for DCX and PSA-NCAM (with DAPI). (**c**) NeuN immunofluorescence intensity in the CA1 (left) and CA2/3 (middle-left) pyramidal layers and the density of NeuN+ neurons (per 1,000 µm2) in the same hippocampal regions (right). (**d**) The density of DCX+PSA-NCAM+ neurons per 100 µm of the DG subgranular zone. (**e**) The density of DCX+ dendrites crossing the line on the border of the DG-G and DG-ML (M/G; left), inner part of the DG-ML (M-in; middle) and outer part of the DG-ML (M-out; right), per 100 µm. (**f**) PSA-NCAM immunofluorescence in the DG polymorph layer (left; DG-P), DG-ML (middle-left), CA4 pyramidal (middle-right; CA4-P) and CA1 stratum lacunosum-moleculare (right; CA1) hippocampal layers.

Since neuronal survival, neurogenesis and neurite growth depend on sufficient levels of neurotrophic factors, ELISA was subsequently employed to measure the hippocampal levels of *brain-derived neurotrophic factor* (BDNF) as a pivotal representative of the neurotrophic factor class. The hippocampal BDNF level was reduced in the SCA1 mice (Fig. 17g) which suggests the possible role of reduced BDNF levels in the aforementioned hippocampal impairments observed in these mice.

4.4.6 Normal urinary corticosterone level in the SCA1 mice

To test whether the increased stress response and the consequent increase in the corticosterone concentration contribute to the hippocampal impairments and abnormal behaviour or the correlation thereof, urinary corticosterone was measured at the basal state and 1 hour following the initiation of stress. While the corticosterone concentration (standardized per creatinine) was affected by the acute *stress* (within-subject factor; $F_{1,18}$= 79, P< 0.001), it was not significantly influenced by the *genotype* ($F_{1,18}$= 0.78, P= 0.4) nor the *stress*genotype* interaction ($F_{1,18}$= 0.48, P= 0.5; Fig. 18).

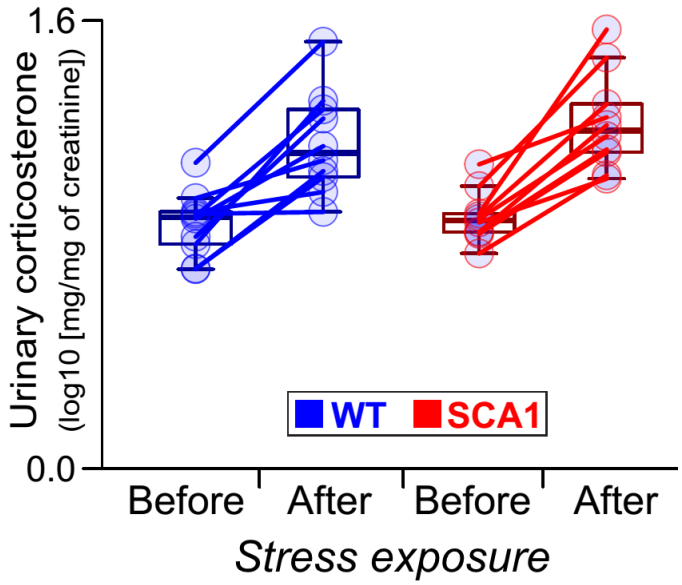

Figure 18. Urinary corticosterone (per creatinine) before and 1 hour after acute stress. The lines connect data points from the same animal.

5.4.6 Hippocampal mitochondrial dysfunction in the young SCA1 mice

To investigate whether the brain abnormalities and behavioural deficits identified might be related to mitochondrial dysfunction, high-resolution respirometry was employed to measure mitochondrial respiration and citrate synthase activity measurements in the cerebellar and the hippocampal tissue (Fig. 19a)

The SCA1 mice showed an apparent trend toward a decreased citrate synthase activity in the hippocampus of the SCA1 mice although this trend was not statistically significant (Fig. 19b, Table 11). However, the SCA1 mice did suffer from a reduction in mitochondrial respiration, which was surprisingly seen only in the hippocampus but was not detected in the cerebellum. Interestingly, the hippocampal tissue of the SCA1 mice exhibited compromised respiration in all the evaluated respiratory states, including reduced complex I OXPHOS capacity in the ADP-activated state of oxidative phosphorylation (*P I*), complex I + II OXPHOS capacity (*P I+II*), maximum capacity for electron transport (*E I+II*), complex II uncoupled capacity (*E II*) and *complex IV* capacity (Fig. 19c, Table 11). Moreover, when the citrate synthase activity was taken into account (included as a covariate in the mixed-effects model) the genotype effect on hippocampal respiration remained significant concerning all respiratory states except for P I (Suppl. Table S19). To validate the results of the previous study which pointed out the reduced complex I/maximal respiration ratio in the cerebellum of the SCA1 mice[509], the same analysis was performed. This analysis did not find evidence of a difference (P= 0.44).

These results suggest that a hippocampal mitochondrial deficit may provide an essential driver of hippocampal impairment and the related behavioural deficits in SCA1 mice.

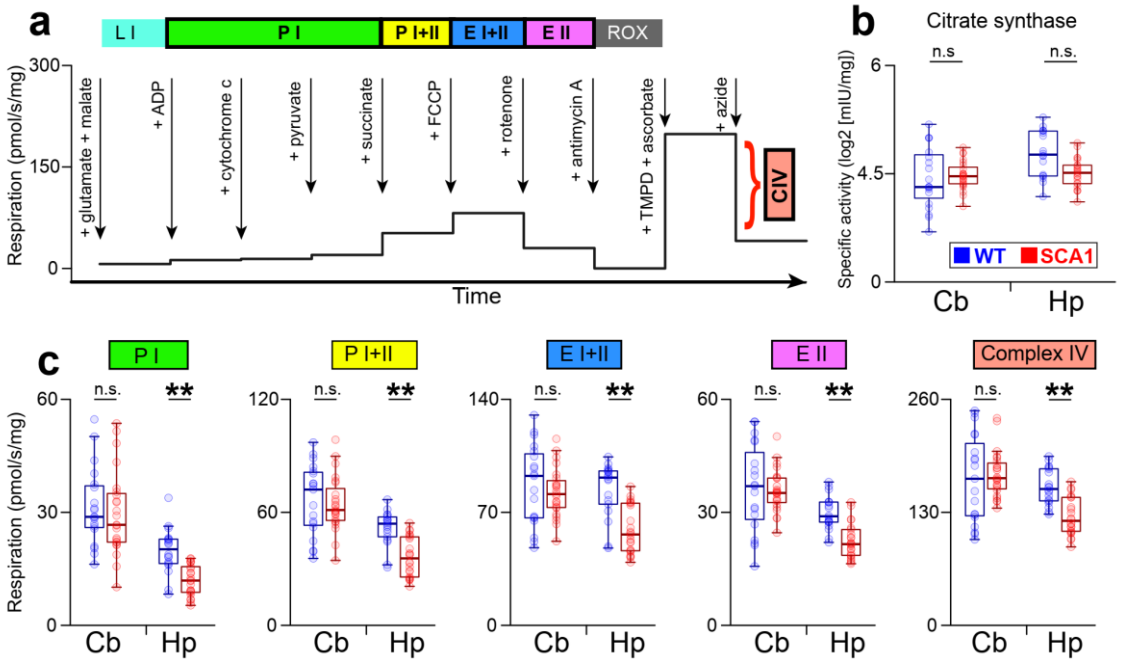

Figure 19: (**a**) Substrate-uncoupler-inhibitor titration protocol for measuring the mitochondrial respiratory capacity. (**b**) Enzymatic activity of citrate synthase in the cerebellar (Cb) and hippocampal (Hp) tissues (log [mIU/mg of tissue]). (**c**) Mitochondrial respiration (pmolO_2/s/mg of homogenized tissue) in different states of the substrate-uncoupler-inhibitor protocol, reflecting complex I OXPHOS capacity in the ADP-activated state of oxidative phosphorylation (*P I*), complex I + II OXPHOS capacity (*P I+II*), maximum capacity for electron transport (*E I+II*), complex II uncoupled capacity (*E II*) and *complex IV* capacity. * P< 0.05, ** P< 0.01, *** P< 0.001. n.s.= not significant.

Table 11. Results of linear mixed-effect models describing an effect of SCA1 genotype on the specific citrate synthase activity (log[mIU/mg of tissue]) and mitochondrial respiration (pmolO2/s/mg) in cerebellar (a) and hippocampal (b) tissue. See Table 9 for abbreviations.

(a) Cerebellum	*ß*	CI-L	CI-U	P	boot. P	perm. P
Citrate synthase activity	0.04	-0.54	0.59	0.90	0.90	0.91
P I	-0.09	-0.60	0.42	0.72	0.78	0.72
P I+II	-0.06	-0.58	0.45	0.82	0.81	0.83
E I+II	-0.12	-0.62	0.41	0.67	0.66	0.67
E II	-0.02	-0.55	0.54	0.93	0.92	0.93
Complex IV	0.06	-0.47	0.59	0.83	0.83	0.82
(b) Hippocampus	*ß*	CI-L	CI-U	P	boot. P	perm. P
Citrate synthase activity	-0.49	-1.00	0.00	0.08	0.05	0.058
P I	-0.62	-1.03	-0.20	0.018	0.004	0.007
P I+II	-0.63	-1.05	-0.21	0.016	0.003	0.005
E I+II	-0.65	-1.06	-0.25	0.011	0.002	0.003
E II	-0.67	-1.10	-0.23	0.014	0.002	0.006
Complex IV	-0.64	-1.09	-0.24	0.013	0.001	0.004

6 DISCUSSION

6.1 Combined effect of vision and cerebellar degeneration on motor skills

In lurcher mice, the result from rotarod latency was not affected by vision, suggesting that lurcher mice are not able to utilize the visual inputs for the motor command and that the vision is not capable to provide efficient compensation for the loss of motor coordination. This corresponds to a previous study where lurcher rotarod performance was also not affected by the vision[582]. Similarly, in WT mice, rotarod performance was also not dependent on retinal degeneration. However, the finding in WT mice was more surprising because previous experiments, including the study in the same mouse model, suggested the opposite[582] and studies in human subjects also suggested an obligatory role of the vision for equilibrium[583,584]. It is therefore difficult to draw a conclusion about the role of vision for motor skills and equilibrium in subjects with normal cerebellum.

6.2 Combination of retinal and cerebellar degeneration in spatial navigation

Concerning the MWM experiment with mice presenting with retinal and/or cerebellar degeneration, it revealed that blind mice are not capable to navigate to the hidden platform in the MWM even though the position between the start and the target is stable, allowing the usage of idiothetic navigational cues. This was also supported by the results from the probe trial, where the sighted WT mice represented the only group that preferred the target quadrant during the probe trial. This partially contrasts with previous studies on rats and mice, where a similar design was used and the animals were able to navigate in darkness efficiently after training[43,557]. On the other hand, rats are generally better learners compared to mice[585] and the mice in the study of Rochefort et al.[43] had been firstly learnt under the light and only then did the test proceeds during darkness. This may represent a substantial advantage compared to blind mice in the experiment of this thesis. Moreover, various mouse strains differ in terms of cognition substantially – the strain used for the experiment of this thesis (C3H) has already been shown to have poorer learning capability compared to some other mouse strains[586]. On the other hand, in both the above-cited experiments, the animals still evinced better navigation under a light[43,557], confirming that the visual cues provide extremely useful information not only for the allocentric navigation but also for path integration, where information about optic flow (without the use of specific spatial landmarks) can be utilised to visual-vestibular integration[587–589].

Although lurcher mice also preserved mild learning over testing days, they did not show a preference for the target quadrant during the probe trial, implying procedural rather than explicit spatial learning. Moreover, their performance was very poor compared to the sighted WT mice over almost all testing days and did not improve with vision. This suggests that lurcher mice struggle to efficiently utilize visual stimuli for navigation. This corresponds with the previous studies showing that lurcher mice have impaired navigation to both the hidden as well as a visually marked platform[87,149,164,586,590], supporting the crucial role of the cerebellum in the coordination of eyes movements, visuospatial and visual-vestibular integration and higher-order spatial cognition[155,156,589,591,592].

The performance of the lurcher mice in the MWM was not affected by vision but was influenced by swim speed and surprisingly also correlated with individual performance on the rotarod. The latency to locate the platform during the MWM was the most strongly affected by swim speed in lurchers. The swim speed may be coupled with exacerbated stress response as the acute stress commonly induces hyperlocomotion in rodents[471,593]. Although the found association may be expected given that swim speed increases the chance of finding the platform just due to stochastic reasons (i.e., even during a random non-directed swim), it partially supports a finding that the exacerbated stress response is not the main factor of poor performance in the MWM[164]. The finding of the correlation between the MWM and motor performance on the rotarod also contrasts with the study by Lolande et al.[594], which found no correlation between the motor performance and spatial performance in the MWM and assumed that the motor and spatial performance are independent deficits in mouse models of cerebellar degenerations. We can speculate that the found correlation may be associated with struggles to get on the platform or to keep a directed swim. However, the extremely strong magnitude of the ataxia in the lurcher mice does not allow any serious conclusions about the relationship. The contribution of the motor impairment to the reduced MWM performance will thus be better addressed using the mouse models with ‘softer’ motor dysfunction and wider inter-individual variability. Research focusing on behaviour and cognition in diverse mouse models of SCAs may therefore yield deeper insight into the relationship between ataxia and non-motor impairments. This topic is thus further discussed below.

6.3 Behavioural disinhibition in lurcher mice

WT mice with retinal degeneration did not learn in the MWM and developed behavioural despair, the passive floating on the water surface. Although this may be considered a possible cause of the poor performance, the linear model estimating the partial effects of swim speed and blindness, adjusting the effect of each other, pointed out the blindness as the primary driver of the poor performance. The behavioural despair thus seems to be a secondary consequence of the overly difficult task in the blind WT mice.

Most interestingly, there was a huge contrast in the response of the blind lurcher mice to the overly difficult task: blind lurchers did not develop any despair and continued to swim despite the difficulty of the task. This finding corresponds to the results of previous studies demonstrating reduced anxiety-like behaviour in EPM and OF and a dramatically mitigated behavioural despair during FST in the mouse models of cerebellar degeneration[149,150,595]. However, as some studies have shown, the apparently lower anxiety-like behaviour may have another cause than truly altered anxiety-like emotions: it has been shown that when the lurcher mice explore the open arms in EPM, their corticosterone level increases dramatically[165]. It was, therefore, suggested that this behaviour is not driven by the reduced anxiety-like emotions but rather behavioural disinhibition, the disability of behavioural control that is also present in diverse rodent models of ADHD[596,597]. From this perspective, cerebellar degeneration results in behavioural abnormality that resembles behavioural disinhibition and impulsivity seen in human patients with spinocerebellar ataxias and other cerebellar dysfunctions[7]. As an alternative explanation, the reduced anxiety-like and despaired behaviour may be due to higher perseveration (inability to stop the actions which have already begun), mirroring stereotyped and inflexible behaviour of the patients with cerebellar dysfunction[58,209,598].

6.4 Motor deficits and cerebellar atrophy in SCA1 mice

In contrast to the previous study[430], but correspondingly to the results of other studies[496,504], the results of this thesis revealed only minor and statistically insignificant deterioration in the rotarod performance of the young SCA1 mice (7 and 11 weeks of age). The discrepancy may stem from the different designs of the rotarod test: the rotarod used for experiments which did not find any difference in young mice employed a progressively accelerating rotarod (0-60 rpm). In contrast, the finding of the reduced

rotarod performance in young SCA1 mice was based on a combined rotarod setting with progressive acceleration till 30 rotations per minute (rpm) followed by a non-accelerating phase (constant speed of 30 rpm) till the end of testing. Congruently with the rotarod results, global analysis of gait using multivariate statistical techniques did not detect abnormal gait in young mice aged 6 and 10 weeks.

The conclusion from rotarod and gait analysis, that the noticeable motor deficits start after 11 weeks of age, is also supported by the histological results. The histological findings (see section 5.4.4) indicated that the noticeable cerebellar atrophy starts after 10 weeks of age and that the absolute volume of the cerebellar molecular layer correlates with the rotarod performance, suggesting that the motor deficit and the timing of its onset closely mirror the cerebellar atrophy and is congruent with the essential role of the cerebellum in motor functions[1].

There may be several reasons why other studies could find the genotype-related difference in the young SCA1 mice using the combined or constant-speed rotarod. Firstly, the rotarod test with constant speed is considered to be less specific[431] and more influenced by endurance[599]. Therefore, it may be expected that the results from constant-speed or combined rotarod settings are more prone to confounding by the level of motivation, which is apparently reduced in SCA1 mice (see result section 5.4.1). Secondly, given the presumably higher sensitivity of the stationary rotarod, we can also expect that the combined rotarod setting better detects unspecific brain impairments (see result section 5.4.1) or hypothetic brain developmental abnormality in SCA1 mice (so far found only in the cerebellum[600]).

6.4 Cognitive impairments in SCA-relevant mouse models

Besides the motor deficits, the behavioural experiments with a mouse model of SCA1 revealed also cognitive deficits. Some of these impairments have not been previously described in any mouse SCA model (reduced cognitive flexibility and prepulse inhibition) whereas reduced spatial performance in the MWM has been, along with fear conditioning deficit, repeatedly reported in the same mouse model[430,510].

However, the results of this thesis imply that MWM performance is confounded by increased immobility and thus cannot reliably reflect cognitive impairments in the SCA1

mice. This is further supported by the result of the probe trial, where the SCA1 mice remained in the proximity of the start position whereas WT mice moved randomly and did not prefer any quadrant. Interestingly, the result of another study of the same mouse model showed a similar pattern: persistence of SCA1 mice around the 'starting' point and random movement of WT mice with a preference of the target quadrant below 25%[510], incorrectly interpreted by authors as a learning deficit of SCA1 mice. However, the absence of the preference of the target quadrant in WT mice suggests that the MWM may be too difficult for the given mouse strain. This is in line with information that visual abilities and spatial learning differ across mouse strains and that these abilities are poor in 129S-related mouse strains, which has been used for the experiment in this thesis[440,601].

Similarly to the MWM, the object-location memory task was shown to be too difficult even for WT mice as they did not robustly discriminate between the relocated and stable objects. Given the fact that this test is generally more difficult than other similar tests, such as the novel object recognition test, using a simpler test should be preferred when working with the 129S-related mouse strains[602].

On the other hand, the T-test was very simple for WT mice but SCA1 strongly struggled in the test. The magnitude of the difficulties seemed to be age-dependent: whereas young SCA1 mice evinced a minimal dysfunction during the learning phase of the test, they strongly struggled to flexibly re-learn when the position of the hidden platform was changed, implying robustly reduced cognitive flexibility. In older cohorts, SCA1 mice evinced problems even with the initial learning. However, given the complex phenotype of the old SCA1 mice, including strong ataxia, the results from old cohorts are difficult to interpret. On the other hand, in young mice, impaired cognitive flexibility was present in mice without substantial ataxia and with a relatively preserved capability to learn the initial phase of the task. Moreover, the T-maze performance did correlate with neither motivation nor motor skills in young SCA1 mice (data not shown). It suggests that the cognitive flexibility deficit may be independent of other functional impairments in young SCA1 mice. Although the cognitive inflexibility was not previously reported in any SCA mouse model, it was reported in human patients with SCA10[377], in mice after the PCs loss[209] and in mice after chemogenetic inactivation of the posterior cerebellum[603].

The fact that knock-outs for Atxn1 have a profound cognitive deficit (despite lack of cerebellar degeneration and no motor impairments) corresponds well with the previous

findings of the role of the ATXN1/Atxn1 gene in cognition and cognitive-related disroders[350,359,360]. Moreover, it is congruent with the fact that loss of Atxn-1 function in mice induces impairments in hippocampal plasticity and neurogenesis, without causing a marked motor deficit or cerebellar degeneration[357,359,360]. This finding may thus have serious implications for the treatment of the SCA1 a possibly also other SCA types, as will be discussed below (section 6.5).

Very interesting is the finding of reduced prepulse inhibition in the SCA1 mice which may be considered neither purely cognitive nor emotional-related, but rather as an indicator of impaired sensorimotor gating[604]. The reduced prepulse inhibition is present in human patients with diverse neurodegenerative and psychiatric diseases, namely schizophrenia[450,605,606] and Alzheimer's disease[607,608], and their mouse models[609,610]. Although prepulse inhibition has not been demonstrated in the SCA mouse models so far, it has been reported in lurcher mice[37]. The finding also corresponds to the conclusion of several studies identifying the cerebellum as one of the structures partially contributing to prepulse inhibition[611,612].

The finding of learning-related impairments fits well with further studies of SCA1 and other cerebellar-relevant mouse models. Recently, a study by Asher et al. explored cognitive performance across different SCA1-relevant mouse models: the SCA1 mice with complex neuropathology ($SCA1^{154Q/2Q}$), a SCA1 mouse with cerebellar-specific pathology (Pcp2-ATXN1[82Q]), and either complete (Atxn1−|−) or partial (Atxn1−|+) knock-outs for Atxn1[415]. The study used two cognitive tasks – the Barnes Maze and Fear Conditioning. The study found that the complex model of SCA1, as well as Atxn1−|− mice, show robust deficits in spatial memory[415]. Although spatial deficit was present in cerebellar-specific SCA1 mice too, it was noticeably milder. Similarly, $SCA1^{154Q/2Q}$ and Atxn1−|− mice evinced profound impairment in recall 24 hours after Fear Conditioning and this deficit was, again, milder in cerebellar-specific SCA1 model[415]. Atxn1−|+ did not evince any cognitive deficit. These findings suggest that although cerebellar dysfunction contributes to the cognitive deficits, out-of-cerebellar neuropathology and loss of Atxn-1 function may play an additional and relatively important role in the cognitive deficits of mouse SCA models. This is also congruent with human studies, revealing that the cognitive deficit has a larger magnitude in the SCA types with complex neuropathology (SCA types 1-3), compared to the SCAs which are primarily cerebellar

(SCA6)[391]. The contribution of the cerebellum could be expected given the learning disabilities of other mice with cerebellar-specific dysfunction[149,438,486] and the well-known role of the cerebellum in the visuospatial integration and cognitive functions[13,53,155,555].

Results of this thesis and other studies collectively suggest that mouse models of SCAs and mouse models of selective cerebellar degeneration suffer from a complex cognitive deficit, possibly mirroring analogous deficit in human SCA patients. The mouse studies thus support the findings from human patients, reporting substantial cognitive impairments in many SCA types[392,395,399,400,564]. Most probably, the cerebellar dysfunction causally contributes to the cognitive deficits although complex out-of-cerebellar neuropathology plays a crucial role.

6.5 Emotional-related abnormalities in SCA1 mice

Besides the cognitive and motor deficits, SCA1 mice evinced also other non-motor impairments, such as depressive- and anxiety-like behaviour, which have not been previously demonstrated in any SCA model. These impairments had different time development in SCA1 mice than motor deficits: they occurred from the youngest age of testing and did not show signs of deterioration compared to ataxia. This is in agreement with studies on human SCA patients that have demonstrated that human SCA patients often suffer from emotional-related psychiatric issues, such as anxiety, depression and apathy[4,391,398]. The similarity between the emotional-related impairments in human SCA patients and the SCA1 mouse model is also supported by the observation that some psychiatric issues commonly emerge at or shortly after the disease's onset and their severity remains relatively stable over time in contrast to physical disability[4,391].

The results of this thesis partially agree with a recent study by Asher et al.[613]. The study explored emotional-related behaviour using EPM, FST and the Sucrose Test, across different SCA1-relevant mouse models[613]. In line with the results of this thesis, they detected signs of increased anxiety in complex SCA1$^{154Q/2Q}$ mice, but not depressive-like tendencies. This discrepancy may stem from several methodological differences: mouse strain background (B6.129S vs. C57/Bl6), sex (male vs. mixed), different sucrose concentration (1% vs. 4%), or previous exposure of mice to water (in case of FST results). Moreover, the age also slightly differed (10-29 vs. 8 weeks of age) and data from the

additional cohort of mice (6 weeks of age) also did not reveal robust genotype-related differences, suggesting that the robust depressive-like behaviour may start shortly before 10 weeks of age. Increased anxiety was also surprisingly detected in partial Atxn1 KO mice[613]. In contrast, cerebellar-specific SCA1 mice showed the opposite tendency, i.e. a higher exploration of the open arms in the EPM, suggesting a reduced anxiety-like phenotype[613]. These results thus support the indication of the contrasting effect of cerebellar vs. out-of-cerebellar pathology within SCA1, the former leading to behavioural disinhibition and apparently reduced anxiety-like behaviour (as discussed in the 6.3 section), whereas the latter induces the anxiety-like phenotype congruent with increased anxiety in SCA1 patients[614].

The contrast between the apparent anxiety in the SCA1 mice with complex vs. cerebellar-specific neuropathology collaborates with studies in mice with other SCAs or cerebellar-related diseases. For example, Kv3.1/Kv3.3 double KO, a model of SCA13 with cerebellar neuropathology, showed hyperactivity and reduced signs of anxiety[487]. Similarly, other mouse models with cerebellar-specific degeneration, e.g. lurcher mutant mice, also show numerous signs of seemingly reduced anxiety- and depressive-like behaviour in OF, EPM and/or FST, corresponding to reduced anxiety-like phenotype in cerebellar-specific SCA1 mice[149–151,165,512], as discussed above (6.3). Congruently, both cerebellar granule- and Purkinje-cell-specific mouse models of episodic ataxia type 2 evinced reduced signs of anxiety in OF[438]. Recently, reduced anxiety was also documented in a purely cerebellar mouse model of SCA6, interpreted aptly as 'impaired defensive escape responses'[615]. These findings thus support the previously suggested interpretation (see section 6.3) that cerebellar-specific damage causes behavioural disinhibition, or impaired defensive response[615], which may be analogous to disinhibition and impulsivity in patients with cerebellar dysfunction[616]. The cerebellar degeneration thus seems to not induce, but rather hide an anxiety-like phenotype presenting in SCA1 models with complex neuropathology. As partial Atxn1 knocked-out (Atxn1−|+) mice also present with an anxiety-like phenotype (despite the absence of other impairments), it suggests that the SCA1-related anxiety constitutes a separate component of the disease, independent of other functional impairments and cerebellar degeneration. Finally, all these results collectively suggest that the anxiolytic effect of the selective cerebellar dysfunction could be generalized beyond SCA1 mice.

The finding that partial or complete loss of Atxn1 function may be associated with a cognitive deficit or anxiety-like behaviour may have important consequences for the treatment of the psychiatric aspects of SCA1. Currently, a reduction of Ataxin-1 by molecular approaches has been proposed as a promising treatment of cerebellar and brainstem degeneration and related symptoms in SCA1[617]. If complete or even partial loss of ATXN1 function causes neuropsychiatric impairments, Ataxin-1 reduction via modern molecular approaches may not necessarily resolve this psychiatric aspect of SCAs.

6.6 Brain abnormalities in SCA1 mice

In line with the behavioural findings, this thesis identified atrophy and impaired plasticity in the hippocampus (the key brain structure in terms of cognition and emotions[130]) of the SCA1 mice. The reduced numbers of immature neurons, coupled with a complete impoverishment of their dendrites, imply hugely impaired neurogenesis in the SCA1 mice. This finding is congruent with the previously reported inhibition of the proliferation of hippocampal progenitor cells[358]. Moreover, the reduced intensity of the PSA-NCAM immunofluorescent signal in one of the hippocampal sub-regions suggests that reduced neurite growth and synapses formation may also contribute to the hippocampal atrophy of the SCA1 mice[578–580]. This corresponds to the reported dendrite pathology in hippocampal CA3 pyramidal neurons and altered the synaptic dynamics in the cerebral cortex of the same mouse model[412,510]. Finally, the results of this thesis showed the reduced NeuN immunofluorescence in the CA pyramidal layer without a significant reduction in the $NeuN^+$ neuronal density. It suggests that NeuN expression or antigenicity are reduced in SCA1 mice, possibly mirroring a diseased neuronal phenotype in the hippocampus of the SCA1 mice[618–621]. On the other hand, there was an insignificant trend toward decreased neuronal density in the SCA1 mice, which may indicate the commencement of neuronal loss, which has already been reported from the CA2 hippocampal region in SCA1 mice of old age[360]. On the other hand, this trend may be also caused by the confounding effect of significantly decreased NeuN expression which has been already demonstrated to lead to underestimation of the cell densities[619]. Finally, ELISA revealed a decrease in the hippocampal BDNF level. Although it has been demonstrated that BDNF level is reduced in the cerebellum of SCA1 mice[622], its reduction in the hippocampus has not been described in any other SCA animal model so far. Given

the crucial role of BDNF in neurite growth, neuronal survival and neurogenesis[623–625], one can speculate that BDNF deficiency may partially contribute to the hippocampal neuropathology described above and may represent a hopeful target for hippocampal-focused SCA1 therapy. In conclusion, the SCA1 mice suffer from hippocampal atrophy from a young age, which may be caused by a combination of impaired neuroplasticity processes, dendrite atrophy, suppressed proliferation of neuronal progenitors and markedly impaired neurogenesis; all of these mechanisms may be fastened by the reduction in neuroprotective proteins such as BDNF.

Furthermore, results also indicate a direct correlation between the DG-ML volume and the individual severity of some behavioural deficits, i.e. depressive-like behaviour and cognitive inflexibility. Although such a direct correlation has not previously been described in any SCA model, these results may be expectable given the reported DG atrophy in mouse models of mood disorders[626,627] and the correlation between DG volumetric atrophy and depression severity/duration in depressed humans[628–630]. Similarly, the revealed correlation between DG-ML atrophy and inflexibility in the SCA1 mice fit well with the known role of hippocampal neurogenesis, which is also related to the DG volume[626], for cognitive flexibility[144].

Moreover, stress is another factor that may, hypothetically, cause the hippocampal impairment as well as its correlation with abnormal behaviour. Stress leads to the release of corticosteroids (particularly corticosterone in mice) whose chronically elevated levels decrease the expression of pro-neuroplastic proteins, damage hippocampal neuronal bodies as well as dendrites, limit neurogenesis and consequently cause hippocampal atrophy[169,170,626,631]. The increased corticosterone release, either at baseline or after a stress event, thus could explain the behavioural and hippocampal observation in SCA1 mice. However, the young SCA1 mice evinced normal corticosterone levels and the CA-SRLM volume was not associated with behavioural deficits, despite the high sensitivity of CA to increased levels of corticosterone[626,631], thus suggesting that the elevated stress and subsequent increases of corticosterone do not mediate hippocampal atrophy and its direct link to the abnormal behaviour of the SCA1 mice. This finding may seem to contradict the behavioural findings of the increased anxiety- and depressive-like behaviour, which is usually associated with the increased humoral response to stress event[632–634]. On the other hand, a subtype of depressive disorder, the atypical depression

(representing approximately 15-30% of depressive disorders[635,636]) is known to be associated with a normal or even decreased level of corticosteroids in response to stress[637,638]. Therefore, the lack of a humoral over-reactivity to stress does not automatically contradict the depressive(-like) state in humans or animals. Interestingly, the finding of the normal corticosterone in SCA1 mice differs from findings from lurcher mutant mice, which evince an increased corticosterone level both at baseline and after stress event[164]. The mechanism of this increase in lurcher mice is however unclear. It may be hypothetically caused by very strong ataxia, disturbing day-to-day functioning and thus posing potentially huge stress. In contrast to lurcher mice, the SCA1 mice (at least at a young age, when the corticosterone was measured) evince only weak or no ataxia and their daily functioning in a cage is thus not substantially disturbed at a young age.

Although the results of this thesis suggest that the cerebellum is not hugely impacted at a young age, and the individual volume of cerebellar ML does not correlate with behaviour, there are several reasons why these findings must be interpreted with caution. One of the reasons is that even young SCA1 mice may suffer from alterations of the cerebellum without noticeable atrophy, potentially affecting the behaviour. For example, the SCA1 mice were shown to suffer from cerebellar inflammation even before the onset of cerebellar degeneration[504]. As cerebellar inflammation can induce depressive-like behaviour in mice[639], there is a possibility that cerebellar inflammation may contribute to the non-motor deficits in the SCA1 mice. Further, both SCA1 mice[622] and lurcher mice[640] were reported to evince reduced cerebellar BDNF levels which, in turn, was shown to affect explorative behaviour[79]. Moreover, specific abnormalities in systems of neurotransmitters in PCs may also affect diverse aspects of non-motor behaviour even without apparent alteration of motor functions[90,641]. Moreover, the cerebellum is part of the wide brain networks and exerts many functional connections to many brain regions, including the diverse regions of the cerebral cortex, limbic system, hippocampus, basal ganglia and many others[157,160,161,642]. Therefore, even subtle and easily undetected changes in cerebellar activity may result in wide alteration of wide brain networks and modify complex behaviour[172,178,643]. For all these reasons, it could be expected that a 'soft' and undetected cerebellar dysfunction may be present in SCA1 mice and can contribute to behavioural and cognitive deficits.

In conclusion, this thesis points to hippocampal impairments as the neuropathology that underlay some of the behavioural deficits seen in the SCA1 mice. These impairments do not seem to be caused by elevated stress hormone levels. This finding offers a potential biological explanation for the occurrence of psychiatric issues in human SCA1 patients. Although the finding must be validated directly via trials involving human patients, it corresponds to the essential role of the hippocampus in human emotion, cognition and psychiatric disorders[130].

6.7 Contribution of mitochondrial dysfunction to SCA1 neuropathology

The results of this thesis revealed mitochondrial dysfunction in the hippocampus, but not in the cerebellum, of the young SCA1 mice. Although mitochondrial dysfunction represents one of the common pathological mechanisms shared by various neurodegenerative diseases[644], it has been studied sparsely in spinocerebellar ataxias and most of the relevant studies focused exclusively on cerebellar tissue/cells[508,509,645]. The data did not support the previous studies which documented cerebellar mitochondrial dysfunction in SCA1 mice[509,645]. This could stem from the use of different methods (e.g. mass spectroscopy[645]) or differences in the SCA1 mouse models (Purkinje cell-specific SCA1 model[509]). However, considering the high ATXN1 gene expression in the hippocampus and the suggested role of ataxin-1 in mitochondrial bioenergetics[507], hippocampal mitochondrial dysfunction was not unexpected. Moreover, it is important to note that the plasticity-related functions in the hippocampus, such as neurogenesis and neurite growth, are energetically extremely demanding and crucially depend on proper mitochondrial functioning[646–650] whereas the mitochondrial dysfunction inhibits the hippocampal plasticity and leads to hippocampal atrophy and impaired behavior[651], i.e. the condition observed in the SCA1 mice. It may be therefore suggested that the mitochondrial dysfunction in SCA1 extends beyond the cerebellum and might be even more severe in the hippocampus, at least during the early (pre-ataxic) stages of SCA1. In this respect, mitochondrial dysfunctions may constitute an essential driver of plasticity-related hippocampal impairment, subsequent tissue atrophy and abnormal behaviour in SCA1.

Given this perspective, one may hypothesise that targeting the mitochondrial function represents a promising approach to enhancing hippocampal-related functions in SCA1.

Substances stimulating some mitochondrial functions have already been shown to improve cerebellar neuropathology in SCA1 mice[509,645]. Moreover, lithium, a drug that stimulates mitochondrial functions in various brain and mitochondrial diseases[652–655], has been shown to improve learning and hippocampal neuropathology in SCA1 mice[510]. On the other hand, the mitochondrial function depends on physical activity[656], which is reduced in SCA1 mice from an early age as shown by behavioural tests, and this lack of activity may lead to a secondary reduction in the mitochondrial function. In this case, forced physical activity would alleviate some of the deficits. Finally, it would be advisable to validate the role of hippocampal bioenergetics disruption directly on human SCA1 patients and/or a human-induced pluripotent stem cell neuronal culture derived from patients[657,658].

6.8 Relationship between behavioural impairments and cerebellar symptoms

The finding of a correlation between rotarod performance and spatial performance in MWM demonstrates the intuitive fact that the clear distinction between motor impairments and non-motor behavioural deficits is often hardly achievable. For example, the performance of lurcher mice in MWM has been considered to be affected by multiple factors, including the motor deficit, visuospatial integration and stress level[164,512]. Therefore, careful interpretation of the results of cognitive or emotional-related tests is thus necessary and the combination of multiple tests is strongly warranted.

Although it could not be completely excluded that some subtle signs of physical deterioration (e.g. subtle motor deficits or fatigue) remained undetected even in young SCA1 mice and contribute to the observed behavioural abnormalities, there are reasons to assume that at least some of the psychiatric-relevant impairments of the mouse model of SCA1 are independent of ataxia and related cerebellar dysfunction. At first, the experiments showed that the psychiatric-relevant impairments preceded the apparent ataxia in the SCA1 mice and results from the non-motor tests had significantly better performance in terms of ability to predict genotype. Secondly, the risk of confounding was eliminated as possible using statistical models adjusting for the effects of confounders. For example, analysis of thigmotaxis data from the open field included statistical adjustment for the effect of activity. Moreover, additional analysis was performed only with animals of comparable activity in both groups. All these analyses

led to the same conclusion that the SCA1 mice preferred to move along the walls of the arena. Moreover, this was further supported by a correlational analysis that revealed that some of the non-motor impairments are associated with hippocampal but not cerebellar atrophy. Moreover, scores in FST, T-maze and relative thigmotaxis in the open field were neither correlated with the results of motor-related tests (gait, rotarod performance) nor with overall activation (distance walked) in the open field. Interestingly, the fact that the mice with cerebellar-specific neuropathology exhibit several opposite abnormalities (lack of immobility in the FST and MWM, reduced thigmotaxis in the OF and higher relative times in the open arms in the EPM)[149,165,512,586,659] provides further support that the psychiatric-relevant impairments in the SCA1 constitute a separate aspect of the disease, independent on the cerebellar degeneration and motor dysfunction.

Still, data from this thesis should be interpreted carefully. As the relationship between behaviour and neuropathology is complex, the found correlation between behavioural impairments and hippocampal dysfunction is suggestive only. Deeper insight and more certainty may be achieved by inducing the expression of the implicated genes (e.g. prolonged Atxn1) in narrowly specified regions, e.g., the hippocampus or cerebral cortex. This will enable to study of the specific contribution of the out-of-cerebellar brain regions to neuropsychiatric-like deficits in SCAs without confounding by even subtle motor deficits and complex neuropathology.

Taken together, experiments of this thesis identified highly-sensitive and easily-measurable behavioural deficits in the SCA1 mice, analogous to psychiatric issues in humans, that seem partially independent of the ataxia and cerebellar degeneration: FST immobility, T-maze scores and thigmotaxis in OF. These tests thus will be useful for further rodent studies of psychiatric-relevant impairments in SCAs and the relevant therapeutic strategies.

7 CONCLUSION

1. This thesis identified several psychiatric-relevant abnormalities in the mouse model of SCA1 that have not been described so far in any SCA model. These include reduced prepulse inhibition, markedly impaired cognitive flexibility and anxiety- and depressive-like behaviour, which mirror issues in human patients.

2. Results of this thesis as well as further research by other authors[149,415,438] collectively suggest that mouse models of SCAs and mice with cerebellar-specific degeneration (lurcher mice) evince robust cognitive deficits, analogously to the patients with SCAs and cerebellar dysfunctions. The results imply that both cerebellar dysfunction and out-of-cerebellar neuropathology jointly contribute to the cognitive deficits in these mice and possibly also in human SCAs patients.

3. Results of this thesis and other relevant research[150,613,615] collectively imply the presence of emotional-related abnormalities in SCA-relevant mouse models. However, they seem to be less robust and more affected by the specific distribution and character of the neuropathology compared to the cognitive deficits. For example, whereas cerebellar-specific pathology seems to reduce signs of anxiety and depressive-like behaviour, possibly throughout inducing behavioural disinhibition, complex SCA1 phenotype induces the opposite behavioural pattern, i.e. anxiety- and depressive-like behaviour. It indicates that also emotional-related behavioural abnormalities have a significant out-of-cerebellar contribution which may be qualitatively different from the impact of cerebellar degeneration.

4. Research of this thesis revealed marked hippocampal neuropathology in the mouse model of SCA1, including reduced hippocampal neuroplasticity and neurogenesis, hippocampal atrophy and impaired hippocampal mitochondrial bioenergetics. Results also identified the hippocampal atrophy as a correlate of some psychiatric-relevant deficits, namely depressive-like behaviour and cognitive inflexibility. Although this association is suggestive, the possible role of the hippocampal impairments in SCA1 (and possibly also other SCA types) deserves further scientific efforts and validation in human patients.

5. At least in SCA1 mice, the psychiatric-relevant impairments seem to be relatively independent of motor deficits and cerebellar degeneration. Some of these deficits occur before the onset of marked ataxia and cerebellar degeneration. Moreover, most of the deficits do not correlate with the magnitude of the ataxia and cerebellar degeneration. Finally, the behavioural and hippocampal impairments occur also in partial or complete Atxn1 KO mice which do not suffer from cerebellar degeneration and ataxia[359]. These findings thus suggest that the psychiatric impairments in SCA1 may stem from out-of-cerebellar dysfunctions. From this perspective, the presence of psychiatric impairments in SCA1 patients should not be automatically interpreted as a result of the cerebellar cognitive-affective syndrome.

6. As psychiatric issues impose a huge burden on SCA patients, affecting overall health outcomes and disease progression, they deserve increased scientific attention aimed at identifying an effective treatment, which might potentially be not the same for disturbances of the cerebellar and out-of-cerebellar origin. Detailed research of mouse models relevant to SCAs may be indispensable for understanding the nature of the psychiatric impairments in SCAs.

ARTICLES

For all the articles used, I declare that I obtained the publishers' agreement that the published articles can be used in this thesis. Article 1[379] and Article 2[409] are reviews and some passages from these reviews have been used in the *Introduction*, *Literature Review* and *Discussion*. I declare that all the text used in this thesis was written solely by me. One review was written without co-authors (Article 1)[379]. The second review was written by numerous authors (Article 2)[409] but only the chapter written by me (with only minor corrections from co-authors and reviewers) has been used in this thesis[409]. The *Original Research* chapters consist of two published papers, Article 3[512] and Article 4[565]. As the text of Article 3 was primarily written by the first author (Jan Cendelin), the text from this article was not directly used in this thesis but I attempted to use my own words. As I had a dominant role in data visualization for Article 3, the figures are used in this thesis without changes. Article 4 was written by me as the first author with my dominant contribution[565]. Next, four other articles (with me as co-author) are relevant to the topic of this thesis and are cited in the text, but not directly used for this thesis (Articles 5 – 8)[150,492,493,640].

8.1 Article 1

> **Tichanek F**. Psychiatric-Like Impairments in Mouse Models of Spinocerebellar Ataxias. *Cerebellum*. Published online 2022. doi:10.1007/s12311-022-01367-7

Contribution: I was a single author.

Publisher agreement for use of the article in this thesis: The publisher agrees with the use of the article for this thesis and provided a 1-year license for its use (the license number: 5290171448132).

8.2 Article 2

Cendelin J, Cvetanovic M, Gandelman M, Hirai H, Orr HT, Pulst SM, Strupp M, **Tichanek F**, Tuma J, Manto M. Consensus Paper: Strengths and Weaknesses of Animal Models of Spinocerebellar Ataxias and Their Clinical Implications. *Cerebellum*. Published online 2021. doi:10.1007/s12311-021-01311-1

Contribution: I was the single author of the chapter *Functional Impairments and Their Neuropathological Correlates in SCA Mouse Models*. I also constructed *Table 2*.

Publisher agreement for use of the article in this thesis: The publisher agrees with the use of the article for this thesis and provided a 1-year license for its use (the license number: 5295481391046).

8.3 Article 3

Cendelin J, **Tichanek F**. Cerebellar degeneration averts blindness-induced despaired behavior during spatial task in mice. *Neuroscience Letters*. 2020;722:134854. doi:10.1016/j.neulet.2020.134854

Contribution: I had a dominant role in the statistical analysis and visualisation of data. I contributed to the interpretation of results and manuscript writing.

Publisher agreement for use of the article in this thesis: Publisher allows the use of articles of the author to his/her dissertation ("*Please note that, as the author of this Elsevier article, you retain the right to include it in a thesis or dissertation, provided it is not published commercially. Permission is not required, but please ensure that you reference the journal as the original source.*")

8.4 Article 4

Tichanek F, Salomova M, Jedlicka J, Kuncova J, Pitule P, Macanova T, Petrankova Z, Zuma Z, Cendelin J. Hippocampal mitochondrial dysfunction and psychiatric-relevant behavioral deficits in spinocerebellar ataxia 1 mouse model. *Scientific Reports*. 2020;10:5418. doi:10.1038/s41598-020-62308-0

Contribution: I conceptualized the study, performed most of the behavioural experiments (with help of technicians and minor help of co-authors), performed histological and immunohistochemical staining and its analysis (with big help of technicians and co-authors), performed all statistical analyses and data visualizations and wrote the manuscript with comments of other co-authors. I also performed ELISA for corticosterone/creatinine but not for BDNF (this was performed by Martina Salomova). I had a very minor role in the evaluation of mitochondrial functions (this was performed mainly by Jan Jedlicka and Jitka Kuncova).

Publisher agreement for use of the article in this thesis: The article has been published as an open access article distributed under the terms of the *Creative Commons CC BY* license permitting unrestricted use, distribution, and reproduction.

8.5 Article 5

Salomova M, **Tichanek F**, Jelinkova D, Cendelin J. Abnormalities in the cerebellar levels of trophic factors BDNF and GDNF in pcd and Lurcher cerebellar mutant mice. *Neuroscience Letters*. Published online February 25, 2020:134870. doi:10.1016/j.neulet.2020.134870

Contribution: Data analysis and visualization.

Publisher agreement: The article is only cited but not used in the thesis.

8.6 Article 6

Salomova M, **Tichanek F**, Jelinkova D, Cendelin J. Forced activity and environmental enrichment mildly improve manifestation of rapid cerebellar degeneration in mice. *Behavioural Brain Research*. 2021;401:113060. doi:10.1016/j.bbr.2020.113060

Contribution: Data analysis, writing an original draft for the results section. Minor contribution to conceptualization and interpretation.

Publisher agreement: The article is only cited but not used in the thesis.

8.7 Article 7

Cendelin J, Purkartova Z, Kubik J, Ulbricht E, **Tichanek F**, Kolinko Y. Long-Term Development of Embryonic Cerebellar Grafts in Two Strains of Lurcher Mice. *Cerebellum*. 2018;17(4):428-437. doi:10.1007/s12311-018-0928-3

Contribution: Data analysis.

Publisher agreement: The article is only cited but not used in the thesis

8.8 Article 8

Purkartova Z, **Tichanek F**, Kolinko Y, Cendelin J. Embryonic Cerebellar Graft Morphology Differs in Two Mouse Models of Cerebellar Degeneration. *The Cerebellum*. 2019;18(5):855-865. doi:10.1007/s12311-019-01067-9

Contribution: Data analysis.

Publisher agreement: The article is only cited but not used in the thesis

9 REFERENCES

1. Kandel E. *Principles of Neural Science*. 5th ed. (Kandel E, Schwartz JH, Jessell TM, Siegelbaum SA, Hudspeth AJ, eds.). McGraw-Hill; 2013.

2. Jayadev S, Bird TD. Hereditary ataxias: Overview. *Genetics in Medicine*. 2013;15(9):673-683. doi:10.1038/gim.2013.28

3. Klinke I, Minnerop M, Schmitz-Hübsch T, et al. Neuropsychological features of patients with spinocerebellar ataxia (SCA) types 1, 2, 3, and 6. *Cerebellum*. 2010;9(3):433-442. doi:10.1007/s12311-010-0183-8

4. Lo RY, Figueroa KP, Pulst SM, et al. Depression and clinical progression in spinocerebellar ataxias. *Parkinsonism and Related Disorders*. 2016;22:87-92. doi:10.1016/j.parkreldis.2015.11.021

5. Schmahmann JD. From movement to thought: Anatomic substrates of the cerebellar contribution to cognitive processing. *Human Brain Mapping*. 1996;4(3):174-198. doi:10.1002/(SICI)1097-0193(1996)4:3<174::AID-HBM3>3.0.CO;2-0

6. Strick PL, Dum RP, Fiez JA. Cerebellum and Nonmotor Function. *Annual Review of Neuroscience*. 2009;32(1):413-434. doi:10.1146/annurev.neuro.31.060407.125606

7. Schmahmann JD, Weilburg JB, Sherman JC. The neuropsychiatry of the cerebellum - insights from the clinic. *Cerebellum (London, England)*. 2007;6(3):254-267. doi:10.1080/14734220701490995

8. Trivedi MH, Greer TL. Cognitive dysfunction in unipolar depression: Implications for treatment. *Journal of Affective Disorders*. 2014;152-154(1):19-27. doi:10.1016/J.JAD.2013.09.012

9. Leavitt VM, Brandstadter R, Fabian M, et al. Dissociable cognitive patterns related to depression and anxiety in multiple sclerosis. *Multiple Sclerosis Journal*. 2020;26(10):1247-1255. doi:10.1177/1352458519860319

10. Taroni F, Chiapparini L, Mariotti C. Autosomal dominant spinocerebellar Ataxias and episodic Ataxias. In: *Handbook of the Cerebellum and Cerebellar Disorders*. Springer Netherlands; 2013:2193-2268. doi:10.1007/978-94-007-1333-8_101

11. Hodos W. Evolution of Cerebellum. In: *Encyclopedia of Neuroscience*. Springer Berlin Heidelberg; 2008:1240-1243. doi:10.1007/978-3-540-29678-2_3124

12. Nicholls JG, Martin AR, Fuchs PA, Brown DA, Diamond ME, Weisblat DA. *From Neuron to Brain, 5th Ed.* Sinauer Associates; 2012.

13. Koziol LF, Budding D, Andreasen N, et al. Consensus paper: The cerebellum's role in movement and cognition. *Cerebellum*. 2014;13(1):151-177. doi:10.1007/s12311-013-0511-x

14. Moulton EA, Schmahmann JD, Becerra L, Borsook D. The cerebellum and pain: Passive integrator or active participator? *Brain Research Reviews*. 2010;65(1):14-27. doi:10.1016/j.brainresrev.2010.05.005

15. Strata P, Sclefo B, Sacchetti B. Involvement of cerebellum in emotional behavior. *Physiol Res*. 2011;60(Strata 2009).

16. Buckner RL. The cerebellum and cognitive function: 25 years of insight from anatomy and neuroimaging. *Neuron*. 2013;80(3):807-815. doi:10.1016/j.neuron.2013.10.044

17. Sultan F, Glickstein M. The cerebellum: Comparative and animal studies. *Cerebellum*. 2007;6(3):168-176. doi:10.1080/14734220701332486

18. Hilber P, Cendelin J, Le Gall A, Machado M-L, Tuma J, Besnard S. Cooperation of the vestibular and cerebellar networks in anxiety disorders and depression. *Progress in neuro-psychopharmacology & biological psychiatry*. 2018;89(June 2018):310-321. doi:10.1016/j.pnpbp.2018.10.004

19. Ramnani N. The primate cortico-cerebellar system: anatomy and function. *Nature Reviews Neuroscience*. 2006;7(7):511-522. doi:10.1038/nrn1953

20. Blatt GJ, Oblak AL, Schmahmann JD. Cerebellar connections with limbic circuits: Anatomy and functional implications. In: *Handbook of the Cerebellum and Cerebellar Disorders*. Springer Netherlands; 2013:479-496. doi:10.1007/978-94-007-1333-8_22

21. Matano S. Proportions of the ventral half of the cerebellar dentate nucleus in humans and great apes. *American Journal of Physical Anthropology*. 2001;114(2):163-165. doi:10.1002/1096-8644(200102)114:2<163::AID-AJPA1016>3.0.CO;2-F

22. Kelly RM, Strick PL. Cerebellar loops with motor cortex and prefrontal cortex of a nonhuman primate. *Journal of Neuroscience*. 2003;23(23):8432-8444. doi:10.1523/jneurosci.23-23-08432.2003

23. Eccles JC, Ito M, Szentágothai J. *The Cerebellum as a Neuronal Machine*. Springer Berlin Heidelberg; 1967. doi:10.1007/978-3-662-13147-3

24. Jörntell H, Bengtsson F, Schonewille M, De Zeeuw CI. Cerebellar molecular layer interneurons - computational properties and roles in learning. *Trends in Neurosciences*. 2010;33(11):524-532. doi:10.1016/j.tins.2010.08.004

25. Dieudonné S, Dumoulin A. Serotonin-driven long-range inhibitory connections in the cerebellar cortex. *Journal of Neuroscience*. 2000;20(5):1837-1848. doi:10.1523/jneurosci.20-05-01837.2000

26. Raymond J, Lisberger S, Mauk M. The Cerebellum: A Neuronal Learning Machine? *ScienceNew Series*. 1996;272(5265):1126-1131. doi:10.1126/science.272.5265.1126

27. Dean P, Porrill J, Ekerot CF, Jörntell H. The cerebellar microcircuit as an adaptive filter: Experimental and computational evidence. *Nature Reviews Neuroscience*. 2010;11(1):30-43. doi:10.1038/nrn2756

28. Ito M. Control of mental activities by internal models in the cerebellum. *Nature Reviews Neuroscience*. 2008;9(4):304-313. doi:10.1038/nrn2332

29. Ebner TJ. Cerebellum and internal models. In: *Handbook of the Cerebellum and*

Cerebellar Disorders. Springer Netherlands; 2013:1281-1296. doi:10.1007/978-94-007-1333-8_56

30. Sokolov AA, Miall RC, Ivry RB. The Cerebellum : Adaptive Prediction for Movement and Cognition. *Trends in Cognitive Sciences*. 2017;xx(5):1-20. doi:10.1016/j.tics.2017.02.005

31. Rondi-Reig L, Paradis A-L, Lefort JM, Babayan BM, Tobin C. How the cerebellum may monitor sensory information for spatial representation. *Frontiers in systems neuroscience*. 2014;8(November):205. doi:10.3389/fnsys.2014.00205

32. Baumann O, Borra RJ, Bower JM, et al. Consensus Paper: The Role of the Cerebellum in Perceptual Processes. *Cerebellum*. 2015;14(2):197-220. doi:10.1007/s12311-014-0627-7

33. Heffley W, Hull C. Classical conditioning drives learned reward prediction signals in climbing fibers across the lateral cerebellum. *eLife*. 2019;8. doi:10.7554/eLife.46764

34. Streng ML, Popa LS, Ebner TJ. Cerebellar Representations of Errors and Internal Models. *Cerebellum*. Published online April 26, 2022:1-7. doi:10.1007/S12311-022-01406-3/FIGURES/3

35. Hull C. Prediction signals in the cerebellum: Beyond supervised motor learning. *eLife*. 2020;9. doi:10.7554/eLife.54073

36. Hastie T, Tibshirani R, Friedman J. *The Elements of Statistical Learning*. Springer New York; 2009. doi:10.1007/978-0-387-84858-7

37. Porras-García E, Cendelin J, Domínguez-Del-Toro E, Vožeh F, Delgado-García JM. Purkinje cell loss affects differentially the execution, acquisition and prepulse inhibition of skeletal and facial motor responses in Lurcher mice. *European Journal of Neuroscience*. 2005;21(4):979-988. doi:10.1111/j.1460-9568.2005.03940.x

38. López-Ramos JC, Houdek Z, Cendelín J, Vožeh F, Delgado-Garciá JM. Timing correlations between cerebellar interpositus neuronal firing and classically conditioned eyelid responses in wild-type and Lurcher mice. *Scientific Reports*. 2018;8(1):1-13. doi:10.1038/s41598-018-29000-w

39. Mccormick DA, Lavond DG, Clark GA, Kettner RE, Rising CE, Thompson RF. The engram found? Role of the cerebellum in classical conditioning of nictitating membrane and eyelid responses. *Bulletin of the Psychonomic Society*. 1981;18(3):103-105. doi:10.3758/BF03333573

40. Marr D. A theory of cerebellar cortex. *The Journal of Physiology*. 1969;202(2):437-470. doi:10.1113/jphysiol.1969.sp008820

41. Albus JS. A theory of cerebellar function. *Mathematical Biosciences*. 1971;10(1-2):25-61. doi:10.1016/0025-5564(71)90051-4

42. Galliano E, Potters J, Elgersma Y, et al. Synaptic Transmission and Plasticity at Inputs to Murine Cerebellar Purkinje Cells Are Largely Dispensable for Standard Nonmotor Tasks. 2013;33(31):12599-12618. doi:10.1523/JNEUROSCI.1642-13.2013

43. Rochefort C, Arabo A, André M, Poucet B, Save E, Rondi-reig L. Cerebellum Shapes Hippocampal Spatial Code. 2011;311:385-390.

44. Boyden ES, Katoh A, Raymond JL. CEREBELLUM-DEPENDENT LEARNING: The Role of Multiple Plasticity Mechanisms. *Annu Rev Neurosci*. 2004;27:581-609. doi:10.1146/annurev.neuro.27.070203.144238

45. Lin YC, Hsu CCH, Wang PN, Lin CP, Chang LH. The Relationship Between Zebrin Expression and Cerebellar Functions: Insights From Neuroimaging Studies. *Frontiers in Neurology*. 2020;11:315. doi:10.3389/fneur.2020.00315

46. Craciun I, Gutiérrez-Ibáñez C, Corfield JR, Hurd PL, Wylie DR. Topographic Organization of Inferior Olive Projections to the Zebrin II Stripes in the Pigeon Cerebellar Uvula. *Frontiers in Neuroanatomy*. 2018;12:18. doi:10.3389/fnana.2018.00018

47. Cerminara NL, Lang EJ, Sillitoe R V., Apps R. Redefining the cerebellar cortex as an assembly of non-uniform Purkinje cell microcircuits. *Nature Reviews Neuroscience*. 2015;16(2):79-93. doi:10.1038/nrn3886

48. Zheng N, Raman IM. Synaptic inhibition, excitation, and plasticity in neurons of the cerebellar nuclei. *Cerebellum*. 2010;9(1):56-66. doi:10.1007/s12311-009-0140-6

49. Jaeger D. Cerebellar nuclei and cerebellar learning. In: *Handbook of the Cerebellum and Cerebellar Disorders*. Springer Netherlands; 2013:1111-1130. doi:10.1007/978-94-007-1333-8_47

50. Babinski J. De l'asynergie cerebelleuse. *Rev Neurol*. 1899;7:806-816. Accessed January 25, 2022. https://ci.nii.ac.jp/naid/10008312274

51. Grimaldi G. Cerebellar motor disorders. In: *Handbook of the Cerebellum and Cerebellar Disorders*. Springer Netherlands; 2013:1597-1626. doi:10.1007/978-94-007-1333-8_71

52. Ruigrok TJH. Cerebellar Influences on Descending Spinal Motor Systems. In: *Handbook of the Cerebellum and Cerebellar Disorders*. Springer International Publishing; 2020:1-36. doi:10.1007/978-3-319-97911-3_23-2

53. Sherman JC, Schmahmann JD, Sherman JC. Cerebellar Cognitive Affective Syndrome. *International Review of Neurobiology*. 1997;41:433-440. doi:10.1016/S0074-7742(08)60363-3

54. Leiner HC, Leiner AL, Dow RS. Does the Cerebellum Contribute to Mental Skills? *Behavioral Neuroscience*. 1986;100(4):443-454. doi:10.1037/0735-7044.100.4.443

55. Leiner HC, Leiner AL, Dow RS. Cognitive and language functions of the human cerebellum. *Trends in Neurosciences*. 1993;16(11):444-447. doi:10.1016/0166-2236(93)90072-T

56. Schmahmann JD. An Emerging Concept: The Cerebellar Contribution to Higher Function. *Archives of Neurology*. 1991;48(11):1178-1187. doi:10.1001/archneur.1991.00530230086029

57. Schmahmann JD, Sherman JC. The cerebellar cognitive affective syndrome. *Brain*. 1998;121(4):561-579. doi:10.1093/brain/121.4.561

58. Tavano A, Grasso R, Gagliardi C, et al. Disorders of cognitive and affective development in cerebellar malformations. *Brain*. 2007;130(10):2646-2660. doi:10.1093/brain/awm201

59. Argyropoulos GPD, van Dun K, Adamaszek M, et al. The Cerebellar Cognitive Affective/Schmahmann Syndrome: a Task Force Paper. *Cerebellum*. 2020;19(1):102-125. doi:10.1007/s12311-019-01068-8

60. Göbel W, Helmchen F. In vivo calcium imaging of neural network function. *Physiology*. 2007;22(6):358-365. doi:10.1152/physiol.00032.2007

61. Campbell EJ, Marchant NJ. The use of chemogenetics in behavioural neuroscience: receptor variants, targeting approaches and caveats. *British Journal of Pharmacology*. 2018;175(7):994-1003. doi:10.1111/bph.14146

62. Fiala A, Suska A, Schlüter OM. Optogenetic approaches in neuroscience. *Current Biology*. 2010;20(20):R897-R903. doi:10.1016/j.cub.2010.08.053

63. Schmahmann JD. Cerebellar cognitive affective syndrome and the neuropsychiatry of the cerebellum. In: *Handbook of the Cerebellum and Cerebellar Disorders*. Springer Netherlands; 2013:1717-1752. doi:10.1007/978-94-007-1333-8_77

64. Steinlin M, Wingeier K. Cerebellum and cognition. In: *Handbook of the Cerebellum and Cerebellar Disorders*. Springer Netherlands; 2013:1687-1700. doi:10.1007/978-94-007-1333-8_75

65. Schutter DJLG. Human cerebellum in motivation and emotion. In: *Handbook of the Cerebellum and Cerebellar Disorders*. Springer Netherlands; 2013:1771-1782. doi:10.1007/978-94-007-1333-8_79

66. Silveri MC, Leggio MG, Molinari M. The cerebellum contributes to linguistic production: A case of agrammatic speech following a right cerebellar lesion. *Neurology*. 1994;44(11):2047-2050. doi:10.1212/wnl.44.11.2047

67. Fabbro F, Moretti R, Bava A. Language impairments in patients with cerebellar lesions. *Journal of Neurolinguistics*. 2000;13(2-3):173-188. doi:10.1016/S0911-6044(00)00010-5

68. De Smet HJ, Paquier P, Verhoeven J, Mariën P. The cerebellum: Its role in language and related cognitive and affective functions. *Brain and Language*. 2013;127(3):334-342. doi:10.1016/j.bandl.2012.11.001

69. Van Overwalle F, Manto M, Cattaneo Z, et al. *Consensus Paper: Cerebellum and Social Cognition*. The Cerebellum; 2020. doi:10.1007/s12311-020-01155-1

70. Ahmadian N, van Baarsen K, van Zandvoort M, Robe PA. The Cerebellar Cognitive Affective Syndrome—a Meta-analysis. *Cerebellum*. 2019;18(5):941-950. doi:10.1007/s12311-019-01060-2

71. Shipman ML, Green JT. Cerebellum and cognition: Does the rodent cerebellum participate in cognitive functions? *Neurobiology of Learning and Memory*.

2020;170:106996. doi:10.1016/j.nlm.2019.02.006

72. Baumann O, Mattingley JB. Functional topography of primary emotion processing in the human cerebellum. *NeuroImage*. 2012;61(4):805-811. doi:10.1016/j.neuroimage.2012.03.044

73. Klaus J, Schutter DJLG. Functional topography of anger and aggression in the human cerebellum. *NeuroImage*. 2021;226:117582. doi:10.1016/j.neuroimage.2020.117582

74. Stoodley CJ, Schmahmann JD. Functional topography in the human cerebellum: A meta-analysis of neuroimaging studies. *NeuroImage*. 2009;44(2):489-501. doi:10.1016/j.neuroimage.2008.08.039

75. Canto CB, Onuki Y, Bruinsma B, van der Werf YD, De Zeeuw CI. The Sleeping Cerebellum. *Trends in Neurosciences*. 2017;40(5):309-323. doi:10.1016/j.tins.2017.03.001

76. Silva-Marques B, Gianlorenço ACL, Mattioli R. Intracerebellar vermis histamine facilitates memory consolidation in the elevated T maze model. *Neuroscience Letters*. 2016;620:33-37. doi:10.1016/j.neulet.2016.03.010

77. DelRosso LM, Hoque R. The cerebellum and sleep. *Neurologic Clinics*. 2014;32(4):893-900. doi:10.1016/j.ncl.2014.07.003

78. Petrosini L, Cutuli D, Picerni E, Laricchiuta D. Viewing the Personality Traits Through a Cerebellar Lens: a Focus on the Constructs of Novelty Seeking, Harm Avoidance, and Alexithymia. *Cerebellum*. 2016;16(1):1-13. doi:10.1007/s12311-015-0754-9

79. Laricchiuta D, Andolina D, Angelucci F, et al. Cerebellar BDNF Promotes Exploration and Seeking for Novelty. *International Journal of Neuropsychopharmacology*. 2018;21(5):485-498. doi:10.1093/ijnp/pyy015

80. Martin JH, Cooper SE, Hacking A, Ghez C. Differential effects of deep cerebellar nuclei inactivation on reaching and adaptive control. *Journal of neurophysiology*. 2000;83(4):1886-1899.

81. Peterson TC, Villatoro L, Arneson T, Ahuja B, Voss S, Swain RA. Behavior modification after inactivation of cerebellar dentate nuclei. *Behavioral Neuroscience*. 2012;126(4):551-562. doi:10.1037/a0028701

82. Krupa DJ, Thompson RF. Reversible inactivation of the cerebellar interpositus nucleus completely prevents acquisition of the classically conditioned eye-blink response. *Learning & memory (Cold Spring Harbor, NY)*. 1997;3(6):545-556. doi:10.1101/lm.3.6.545

83. Behnke VK, Stevenson ME, Swain RA. Inactivation of the cerebellar fastigial nuclei alters social behavior in the rat. *Behavioral Neuroscience*. 2018;132(6):552-560. doi:10.1037/bne0000256

84. Zhu J-ZZ, Fei S-JJ, Zhang J-FF, et al. Muscimol microinjection into cerebellar fastigial nucleus exacerbates stress-induced gastric mucosal damage in rats. *Acta Pharmacologica Sinica*. 2013;34152(10):205-213. doi:10.1038/aps.2012.152

85. Joyal CC, Strazielle C, Lalonde R. Effects of dentate nucleus lesions on spatial and postural sensorimotor learning in rats. *Behavioural Brain Research*. 2001;122(2):131-137. doi:10.1016/S0166-4328(00)00390-9

86. Gaytán-Tocavén L, Olvera-Cortés ME. Bilateral lesion of the cerebellar-dentate nucleus impairs egocentric sequential learning but not egocentric navigation in the rat. *Neurobiology of Learning and Memory*. 2004;82(2):120-127. doi:10.1016/j.nlm.2004.05.006

87. Joyal CC, Meyer C, Jacquart G, Mahler P, Caston J, Lalonde R. Effects of midline and lateral cerebellar lesions on motor coordination and spatial orientation. *Brain Research*. 1996;739(1-2):1-11. doi:10.1016/S0006-8993(96)00333-2

88. Bauer DJ, Kerr AL, Swain RA. Cerebellar dentate nuclei lesions reduce motivation in appetitive operant conditioning and open field exploration. *Neurobiology of Learning and Memory*. 2011;95(2):166-175. doi:10.1016/j.nlm.2010.12.009

89. Jackman SL, Chen CH, Offermann HL, et al. Cerebellar purkinje cell activity modulates aggressive behavior. *eLife*. 2020;9. doi:10.7554/eLife.53229

90. Cutando L, Puighermanal E, Castell L, et al. Cerebellar dopamine D2 receptors regulate social behaviors. *Nature Neuroscience 2022*. Published online June 16, 2022:1-12. doi:10.1038/s41593-022-01092-8

91. Wagner MJ, Kim TH, Savall J, Schnitzer MJ, Luo L. Cerebellar granule cells encode the expectation of reward. *Nature*. 2017;544(7648):96-100. doi:10.1038/nature21726

92. Badura A, Verpeut JL, Metzger JW, et al. Normal cognitive and social development require posterior cerebellar activity. *eLife*. 2018;7(609):1-36. doi:10.7554/eLife.36401

93. Snider SR, Snider RS. Alterations in forebrain catecholamine metabolism produced by cerebellar lesions in the rat. *Journal of Neural Transmission*. 1977;40(2):115-128. doi:10.1007/BF01250563

94. Snider RS, Maiti A. Cerebellar contributions to the papez circuit. *Journal of Neuroscience Research*. 1976;2(2):133-146. doi:10.1002/jnr.490020204

95. Henschke JU, Pakan JMP. Disynaptic cerebrocerebellar pathways originating from multiple functionally distinct cortical areas. *eLife*. 2020;9:1-27. doi:10.7554/ELIFE.59148

96. Bostan AC, Strick PL. Cerebellar outputs in non-human primates: An anatomical perspective using transsynaptic tracers. In: *Handbook of the Cerebellum and Cerebellar Disorders*. Springer Netherlands; 2013:549-570. doi:10.1007/978-94-007-1333-8_25

97. Brunoni AR, Vanderhasselt MA. Working memory improvement with non-invasive brain stimulation of the dorsolateral prefrontal cortex: A systematic review and meta-analysis. *Brain and Cognition*. 2014;86(1):1-9. doi:10.1016/J.BANDC.2014.01.008

98. Middleton FA, Strick PL. Cerebellar projections to the prefrontal cortex of the primate. *Journal of Neuroscience*. 2001;21(2):700-712. doi:10.1523/jneurosci.21-02-00700.2001

99. Brodal P, Bjaalie JG. Salient anatomic features of the cortico-ponto-cerebellar pathway. *Progress in Brain Research*. 1997;114:227-250. doi:10.1016/s0079-6123(08)63367-1

100. Palesi F, Tournier JD, Calamante F, et al. Contralateral cerebello-thalamo-cortical pathways with prominent involvement of associative areas in humans in vivo. *Brain Structure and Function*. 2015;220(6):3369-3384. doi:10.1007/s00429-014-0861-2

101. Wagner MJ, Luo L. Neocortex–Cerebellum Circuits for Cognitive Processing. *Trends in Neurosciences*. 2020;43(1):42-54. doi:10.1016/j.tins.2019.11.002

102. Bostan AC, Dum RP, Strick PL. Cerebellar networks with the cerebral cortex and basal ganglia. *Trends in Cognitive Sciences*. 2013;17(5):241-254. doi:10.1016/j.tics.2013.03.003

103. Ramnani N. Frontal lobe and posterior parietal contributions to the cortico-cerebellar system. *Cerebellum*. 2012;11(2):366-383. doi:10.1007/s12311-011-0272-3

104. Percheron G, François C, Talbi B, Yelnik J, Fénelon G. The primate motor thalamus. *Brain Research Reviews*. 1996;22(2):93-181. doi:10.1016/0165-0173(96)00003-3

105. Greicius MD, Krasnow B, Reiss AL, Menon V. Functional connectivity in the resting brain: A network analysis of the default mode hypothesis. *Proceedings of the National Academy of Sciences of the United States of America*. 2003;100(1):253-258. doi:10.1073/pnas.0135058100

106. Raichle ME, MacLeod AM, Snyder AZ, Powers WJ, Gusnard DA, Shulman GL. A default mode of brain function. *Proceedings of the National Academy of Sciences of the United States of America*. 2001;98(2):676-682. doi:10.1073/pnas.98.2.676

107. Seeley WW, Menon V, Schatzberg AF, et al. Dissociable intrinsic connectivity networks for salience processing and executive control. *Journal of Neuroscience*. 2007;27(9):2349-2356. doi:10.1523/JNEUROSCI.5587-06.2007

108. Fox MD, Corbetta M, Snyder AZ, Vincent JL, Raichle ME. Spontaneous neuronal activity distinguishes human dorsal and ventral attention systems. *Proceedings of the National Academy of Sciences of the United States of America*. 2006;103(26):10046-10051. doi:10.1073/pnas.0604187103

109. Habas C, Kamdar N, Nguyen D, et al. Distinct Cerebellar Contributions to Intrinsic Connectivity Networks. *Journal of Neuroscience*. 2009;29(26):8586-8594. doi:10.1523/JNEUROSCI.1868-09.2009

110. King M, Hernandez-Castillo CR, Poldrack RA, Ivry RB, Diedrichsen J. Functional boundaries in the human cerebellum revealed by a multi-domain task battery. *Nature Neuroscience*. 2019;22(8):1371-1378. doi:10.1038/s41593-019-

0436-x

111. Buckner RL, Krienen FM, Castellanos A, Diaz JC, Thomas Yeo BT. The organization of the human cerebellum estimated by intrinsic functional connectivity. *Journal of Neurophysiology*. 2011;106(5):2322-2345. doi:10.1152/jn.00339.2011

112. Bostan AC, Dum RP, Strick PL. The basal ganglia communicate with the cerebellum. *Proceedings of the National Academy of Sciences of the United States of America*. 2010;107(18):8452-8456. doi:10.1073/pnas.1000496107

113. Ichinohe N, Mori F, Shoumura K. A di-synaptic projection from the lateral cerebellar nucleus to the laterodorsal part of the striatum via the central lateral nucleus of the thalamus in the rat. *Brain Research*. 2000;880(1-2):191-197. doi:10.1016/S0006-8993(00)02744-X

114. Hoshi E, Tremblay L, Féger J, Carras PL, Strick PL. The cerebellum communicates with the basal ganglia. *Nature Neuroscience*. 2005;8(11):1491-1493. doi:10.1038/nn1544

115. Chen CH, Fremont R, Arteaga-Bracho EE, Khodakhah K. Short latency cerebellar modulation of the basal ganglia. *Nature Neuroscience*. 2014;17(12):1767-1775. doi:10.1038/nn.3868

116. Sami S, Robertson EM, Chris Miall R. The time course of task-specific memory consolidation effects in resting state networks. *Journal of Neuroscience*. 2014;34(11):3982-3992. doi:10.1523/JNEUROSCI.4341-13.2014

117. Cauda F, Cavanna AE, D'agata F, Sacco K, Duca S, Geminiani GC. Functional connectivity and coactivation of the nucleus accumbens: A combined functional connectivity and structure-based meta-analysis. *Journal of Cognitive Neuroscience*. 2011;23(10):2864-2877. doi:10.1162/jocn.2011.21624

118. Nasser HM, Calu DJ, Schoenbaum G, Sharpe MJ. The dopamine prediction error: Contributions to associative models of reward learning. *Frontiers in Psychology*. 2017;8(FEB):244. doi:10.3389/fpsyg.2017.00244

119. Watabe-Uchida M, Eshel N, Uchida N. Neural Circuitry of Reward Prediction Error. *Annual Review of Neuroscience*. 2017;40(1):373-394. doi:10.1146/annurev-neuro-072116-031109

120. Carta I, Chen CH, Schott AL, Dorizan S, Khodakhah K. Cerebellar modulation of the reward circuitry and social behavior. *Science*. 2019;363(6424). doi:10.1126/science.aav0581

121. Vilensky JA, Van Hoesen GW. Corticopontine projections from the cingulate cortex in the rhesus monkey. *Brain Research*. 1981;205(2):391-395. doi:10.1016/0006-8993(81)90348-6

122. Etkin A, Egner T, Kalisch R. Emotional processing in anterior cingulate and medial prefrontal cortex. *Trends in Cognitive Sciences*. 2011;15(2):85-93. doi:10.1016/J.TICS.2010.11.004

123. Brodal P, Bjaalie JG, Aas JE. Organization of cingulo-ponto-cerebellar connections in the cat. *Anatomy and Embryology*. 1991;184(3):245-254.

doi:10.1007/BF01673259

124. Zhu JN, Yung WH, Kwok-Chong Chow B, Chan YS, Wang JJ. The cerebellar-hypothalamic circuits: Potential pathways underlying cerebellar involvement in somatic-visceral integration. *Brain Research Reviews*. 2006;52(1):93-106. doi:10.1016/j.brainresrev.2006.01.003

125. Watson TC, Cerminara NL, Lumb BM, Apps R. Neural correlates of fear in the periaqueductal gray. *Journal of Neuroscience*. 2016;36(50):12707-12719. doi:10.1523/JNEUROSCI.1100-16.2016

126. Assareh N, Sarrami M, Carrive P, McNally GP. The organization of defensive behavior elicited by optogenetic excitation of rat lateral or ventrolateral periaqueductal gray. *Behavioral Neuroscience*. 2016;130(4):406-414. doi:10.1037/BNE0000151

127. Lonstein JS, Stern JM. Site and behavioral specificity of periaqueductal gray lesions on postpartum sexual, maternal, and aggressive behaviors in rats. *Brain Research*. 1998;804(1):21-35. doi:10.1016/S0006-8993(98)00642-8

128. Wright KM, McDannald MA. Ventrolateral periaqueductal gray neurons prioritize threat probability over fear output. *eLife*. 2019;8. doi:10.7554/eLife.45013

129. Vaaga CE, Brown ST, Raman IM. Cerebellar modulation of synaptic input to freezing-related neurons in the periaqueductal gray. *eLife*. 2020;9:1-28. doi:10.7554/eLife.54302

130. Andersen P, Morris R, Amaral D, Bliss T, Keefe JO. *The Hippocampus Book*. (Andersen P, Morris R, Amaral D, Bliss T, O'Keefe J, eds.). Oxford University Press; 2006. doi:10.1093/acprof:oso/9780195100273.001.0001

131. Tzakis N, Holahan MR. Social Memory and the Role of the Hippocampal CA2 Region. *Frontiers in Behavioral Neuroscience*. 2019;13:233. doi:10.3389/FNBEH.2019.00233/BIBTEX

132. Cope EC, Waters RC, Diethorn EJ, et al. Adult-Born Neurons in the Hippocampus Are Essential for Social Memory Maintenance. *eNeuro*. 2020;7(6). doi:10.1523/ENEURO.0182-20.2020

133. Weiss C, Disterhoft JF. The impact of hippocampal lesions on trace-eyeblink conditioning and forebrain-cerebellar interactions. *Behavioral Neuroscience*. 2015;129(4):512-522. doi:10.1037/bne0000061

134. Woodruff-Pak DS, Disterhoft JF. Where is the trace in trace conditioning? *Trends in Neurosciences*. 2008;31(2):105-112. doi:10.1016/j.tins.2007.11.006

135. Lindquist DH, Steinmetz JE, Thompson RF. Cerebellum and eyeblink conditioning. In: *Handbook of the Cerebellum and Cerebellar Disorders*. Springer Netherlands; 2013:1175-1190. doi:10.1007/978-94-007-1333-8_50

136. Stevenson EL, Caldwell HK. Lesions to the CA2 region of the hippocampus impair social memory in mice. *European Journal of Neuroscience*. 2014;40(9):3294-3301. doi:10.1111/ejn.12689

137. Montagrin A, Saiote C, Schiller D. The social hippocampus. *Hippocampus*. 2018;28(9):672-679. doi:10.1002/hipo.22797

138. Sun Q, Li X, Li A, et al. Ventral Hippocampal-Prefrontal Interaction Affects Social Behavior via Parvalbumin Positive Neurons in the Medial Prefrontal Cortex. *iScience*. 2020;23(3):100894. doi:10.1016/j.isci.2020.100894

139. Rubin RD, Watson PD, Duff MC, Cohen NJ. The role of the hippocampus in flexible cognition and social behavior. *Frontiers in Human Neuroscience*. 2014;8(SEP):742. doi:10.3389/fnhum.2014.00742

140. Van Overwalle F, Baetens K, Mariën P, Vandekerckhove M. Social cognition and the cerebellum: A meta-analysis of over 350 fMRI studies. *NeuroImage*. 2014;86:554-572. doi:10.1016/j.neuroimage.2013.09.033

141. Anacker C, Luna VM, Stevens GS, et al. Hippocampal neurogenesis confers stress resilience by inhibiting the ventral dentate gyrus. *Nature*. Published online 2018:1. doi:10.1038/s41586-018-0262-4

142. Nakashiba T, Cushman JD, Pelkey KA, et al. Young dentate granule cells mediate pattern separation, whereas old granule cells facilitate pattern completion. *Cell*. 2012;149(1):188-201. doi:10.1016/j.cell.2012.01.046

143. Dickson PE, Cairns J, Goldowitz D, Mittleman G. Cerebellar contribution to higher and lower order rule learning and cognitive flexibility in mice. *Neuroscience*. 2016;345:1-11. doi:10.1016/j.neuroscience.2016.03.040

144. Anacker C, Hen R. Adult hippocampal neurogenesis and cognitive flexibility — linking memory and mood. *Nature Reviews Neuroscience*. Published online 2017. doi:10.1038/nrn.2017.45

145. Eichenbaum H. Time cells in the hippocampus: A new dimension for mapping memories. *Nature Reviews Neuroscience*. 2014;15(11):732-744. doi:10.1038/nrn3827

146. Lusk NA, Petter EA, MacDonald CJ, Meck WH. Cerebellar, hippocampal, and striatal time cells. *Current Opinion in Behavioral Sciences*. 2016;8:186-192. doi:10.1016/j.cobeha.2016.02.020

147. Spencer RMC, Ivry RB. Cerebellum and timing. In: *Handbook of the Cerebellum and Cerebellar Disorders*. Springer Netherlands; 2013:1201-1220. doi:10.1007/978-94-007-1333-8_52

148. Seib DR, Espinueva D, Princz-Lebel O, Chahley E, Floresco SB, Snyder JS. Hippocampal neurogenesis promotes preference for future rewards. *bioRxiv*. Published online August 23, 2018:399261. doi:10.1101/399261

149. Tuma J, Kolinko Y, Vozeh F, Cendelin J. Mutation-related differences in exploratory, spatial, and depressive-like behavior in pcd and Lurcher cerebellar mutant mice. *Frontiers in behavioral neuroscience*. 2015;9(May):116. doi:10.3389/fnbeh.2015.00116

150. Salomova M, Tichanek F, Jelinkova D, Cendelin J. Forced activity and environmental enrichment mildly improve manifestation of rapid cerebellar degeneration in mice. *Behavioural Brain Research*. 2021;401:113060.

doi:10.1016/j.bbr.2020.113060

151. Lorivel T, Cendelin J, Hilber P. Familiarization effects on the behavioral disinhibition of the cerebellar Lurcher mutant mice: use of the innovative Dual Maze. *Behavioural Brain Research*. 2021;398(September 2020):112972. doi:10.1016/j.bbr.2020.112972

152. Newman PP, Reza H. Functional relationships between the hippocampus and the cerebellum: an electrophysiological study of the cat. *The Journal of physiology*. 1979;287:405-426. doi:10.1113/jphysiol.1979.sp012667

153. Hoffmann LC, Berry SD. Cerebellar theta oscillations are synchronized during hippocampal theta-contingent trace conditioning. *Proceedings of the National Academy of Sciences*. 2009;106(50):21371-21376. doi:10.1073/pnas.0908403106

154. Liu Y, McAfee SS, Sillitoe R V, Heck DH. Cerebellar modulation of prefrontal-hippocampal gamma coherence during spatial working memory decisions. *bioRxiv*. Published online January 1, 2020:2020.03.16.994541. doi:10.1101/2020.03.16.994541

155. Lefort JM, Rochefort C, Rondi-Reig L. Cerebellar Contribution to Spatial Navigation: New Insights into Potential Mechanisms. *Cerebellum*. 2015;14(1):59-62. doi:10.1007/s12311-015-0653-0

156. Rochefort C, Lefort JM, Rondi-reig L, Timmann D. The cerebellum : a new key structure in the navigation system. *frontiers in neural circuits*. 2013;7(March):1-12. doi:10.3389/fncir.2013.00035

157. Lefort JM, Vincent J, Tallot L, et al. Impaired cerebellar Purkinje cell potentiation generates unstable spatial map orientation and inaccurate navigation. *Nature Communications*. 2019;10(1):2251. doi:10.1038/s41467-019-09958-5

158. Iglói K, Doeller CF, Paradis A, Benchenane K, Berthoz A, Burgess N. Interaction Between Hippocampus and Cerebellum Crus I in Sequence-Based but not Place-Based Navigation. *Cerebral Cortex*. Published online 2014. doi:10.1093/cercor/bhu132

159. Shiroma A, Nishimura M, Nagamine H, et al. Cerebellar Contribution to Pattern Separation of Human Hippocampal Memory Circuits. *Cerebellum*. Published online 2015:645-662. doi:10.1007/s12311-015-0726-0

160. Yu W, Krook-Magnuson E. Cognitive Collaborations: Bidirectional Functional Connectivity Between the Cerebellum and the Hippocampus. *Frontiers in Systems Neuroscience*. 2015;9(December):1-10. doi:10.3389/fnsys.2015.00177

161. Krook-Magnuson E, Szabo GG, Armstrong C, Oijala M, Soltesz I. Cerebellar Directed Optogenetic Intervention Inhibits Spontaneous Hippocampal Seizures in a Mouse Model of Temporal Lobe Epilepsy. *eNeuro*. 2014;1(1):1-27. doi:10.1523/ENEURO.0005-14.2014

162. Streng ML, Krook-Magnuson E. Excitation, but not inhibition, of the fastigial nucleus provides powerful control over temporal lobe seizures. *The Journal of Physiology*. 2020;598(1):171-187. doi:10.1113/JP278747

163. Bohne P, Schwarz MK, Herlitze S, Mark MD. A New Projection From the Deep

Cerebellar Nuclei to the Hippocampus via the Ventrolateral and Laterodorsal Thalamus in Mice. *Frontiers in Neural Circuits*. 2019;13:51. doi:10.3389/FNCIR.2019.00051/BIBTEX

164. Tuma J, Kolinko Y, Jelinkova D, Hilber P, Cendelin J. Impaired spatial performance in cerebellar-deficient Lurcher mice is not associated with their abnormal stress response. *Neurobiology of Learning and Memory*. 2017;140:62-70. doi:10.1016/j.nlm.2017.02.009

165. Hilber P, Lorivel T, Delarue C, Caston J. Stress and anxious-related behaviors in Lurcher mutant mice. *Brain Research*. 2004;1003(1-2):108-112. doi:10.1016/j.brainres.2004.01.008

166. Frederic F, Chautard T, Brochard R, et al. Enhanced Endocrine Response to Novel Environment Stress and Endotoxin in Lurcher Mutant Mice. *Neuroendocrinology*. 1997;66(5):341-347. doi:10.1159/000127257

167. Ruden JB, Dugan LL, Konradi C. Parvalbumin interneuron vulnerability and brain disorders. *Neuropsychopharmacology*. 2021;46(2):279-287. doi:10.1038/s41386-020-0778-9

168. Alviña K, Jodeiri Farshbaf M, Mondal AK. Long term effects of stress on hippocampal function: Emphasis on early life stress paradigms and potential involvement of neuropeptide Y. *Journal of Neuroscience Research*. 2021;99(1):57-66. doi:10.1002/jnr.24614

169. Gould E, Tanapat P. Stress and hippocampal neurogenesis. In: *Biological Psychiatry*. Vol 46. Elsevier; 1999:1472-1479. doi:10.1016/S0006-3223(99)00247-4

170. Saaltink DJ, Vreugdenhil E. Stress, glucocorticoid receptors, and adult neurogenesis: A balance between excitation and inhibition? *Cellular and Molecular Life Sciences*. 2014;71(13):2499-2515. doi:10.1007/s00018-014-1568-5

171. Garg S, Sinha VK, Tikka SK, Mishra P, Goyal N. The efficacy of cerebellar vermal deep high frequency (theta range) repetitive transcranial magnetic stimulation (rTMS) in schizophrenia: A randomized rater blind-sham controlled study. *Psychiatry Research*. 2016;243:413-420. doi:10.1016/J.PSYCHRES.2016.07.023

172. Moberget T, Doan NT, Alnæs D, et al. Cerebellar volume and cerebellocerebral structural covariance in schizophrenia: a multisite mega-analysis of 983 patients and 1349 healthy controls. *Molecular Psychiatry*. 2018;23(6):1512-1520. doi:10.1038/mp.2017.106

173. Andreasen NC, Pierson R. The Role of the Cerebellum in Schizophrenia. *Biological Psychiatry*. 2008;64(2):81-88. doi:10.1016/j.biopsych.2008.01.003

174. He H, Luo C, Luo Y, et al. Reduction in gray matter of cerebellum in schizophrenia and its influence on static and dynamic connectivity. *Human Brain Mapping*. 2019;40(2):517-528. doi:10.1002/hbm.24391

175. Laidi C, Hajek T, Spaniel F, et al. Cerebellar parcellation in schizophrenia and

bipolar disorder. *Acta Psychiatrica Scandinavica*. 2019;140(5):468-476. doi:10.1111/acps.13087

176. Shinn AK, Roh YS, Ravichandran CT, Baker JT, Öngür D, Cohen BM. Aberrant Cerebellar Connectivity in Bipolar Disorder With Psychosis. *Biological Psychiatry: Cognitive Neuroscience and Neuroimaging*. 2017;2(5):438-448. doi:10.1016/j.bpsc.2016.07.002

177. Lupo M, Olivito G, Siciliano L, et al. Evidence of Cerebellar Involvement in the Onset of a Manic State. *Frontiers in Neurology*. 2018;9(SEP):774. doi:10.3389/fneur.2018.00774

178. Chen G, Zhao L, Jia Y, et al. Abnormal cerebellum-DMN regions connectivity in unmedicated bipolar II disorder. *Journal of Affective Disorders*. 2019;243:441-447. doi:10.1016/j.jad.2018.09.076

179. Kim J, Cho H, Kim J, et al. Changes in cortical thickness and volume of cerebellar subregions in patients with bipolar disorders. *Journal of Affective Disorders*. 2020;271:74-80. doi:10.1016/j.jad.2020.03.087

180. Lee YJ, Guell X, Hubbard NA, et al. Functional Alterations in Cerebellar Functional Connectivity in Anxiety Disorders. *Cerebellum*. Published online November 18, 2020:1-10. doi:10.1007/s12311-020-01213-8

181. Xu T, Zhao Q, Wang P, et al. Altered resting-state cerebellar-cerebral functional connectivity in obsessive-compulsive disorder. *Psychological Medicine*. 2019;49(7):1156-1165. doi:10.1017/S0033291718001915

182. Tobe RH, Bansal R, Xu D, et al. Cerebellar morphology in Tourette syndrome and obsessive-compulsive disorder. *Annals of Neurology*. 2010;67(4):479-487. doi:10.1002/ana.21918

183. Narayanaswamy JC, Jose D, Kalmady S V., Agarwal SM, Venkatasubramanian G, Janardhan Reddy YC. Cerebellar volume deficits in medication-naïve obsessive compulsive disorder. *Psychiatry Research - Neuroimaging*. 2016;254:164-168. doi:10.1016/j.pscychresns.2016.07.005

184. Rabellino D, Densmore M, Théberge J, McKinnon MC, Lanius RA. The cerebellum after trauma: Resting-state functional connectivity of the cerebellum in posttraumatic stress disorder and its dissociative subtype. *Human Brain Mapping*. 2018;39(8):3354-3374. doi:10.1002/hbm.24081

185. Nicolson RI, Fawcett AJ, Dean P. Developmental dyslexia: The cerebellar deficit hypothesis. *Trends in Neurosciences*. 2001;24(9):508-511. doi:10.1016/S0166-2236(00)01896-8

186. Piccoli T, Maniaci G, Collura G, et al. Increased functional connectivity in gambling disorder correlates with behavioural and emotional dysregulation: Evidence of a role for the cerebellum. *Behavioural Brain Research*. 2020;390:112668. doi:10.1016/j.bbr.2020.112668

187. De Vidovich GZ, Muffatti R, Monaco J, et al. Repetitive TMS on left cerebellum affects impulsivity in borderline personality disorder: A pilot study. *Frontiers in Human Neuroscience*. 2016;10(DEC2016):582. doi:10.3389/fnhum.2016.00582

188. Martin J, Taylor MJ, Lichtenstein P. Assessing the evidence for shared genetic risks across psychiatric disorders and traits. *Psychological Medicine*. 2018;48(11):1759-1774. doi:10.1017/S0033291717003440

189. Hammerschlag AR, De Leeuw CA, Middeldorp CM, Polderman TJC. Synaptic and brain-expressed gene sets relate to the shared genetic risk across five psychiatric disorders. *Psychological Medicine*. 2020;50(10):1695-1705. doi:10.1017/S0033291719001776

190. Selzam S, Coleman JRI, Caspi A, Moffitt TE, Plomin R. A polygenic p factor for major psychiatric disorders. *Translational Psychiatry*. 2018;8(1). doi:10.1038/s41398-018-0217-4

191. Romer AL, Knodt AR, Houts R, et al. Structural alterations within cerebellar circuitry are associated with general liability for common mental disorders. *Molecular Psychiatry*. 2018;23(4):1084-1090. doi:10.1038/mp.2017.57

192. D'Mello AM, Stoodley CJ. Cerebro-cerebellar circuits in autism spectrum disorder. *Frontiers in Neuroscience*. 2015;9(NOV):408. doi:10.3389/fnins.2015.00408

193. Allen G. The Cerebellum in Autism. *Clinical Neuropsychiatry: Journal of Treatment Evaluation*. 2005;2(6):321-337.

194. Lord C, Brugha TS, Charman T, et al. Autism spectrum disorder. *Nature Reviews Disease Primers*. 2020;6(1):5. doi:10.1038/s41572-019-0138-4

195. Paquet A, Olliac B, Golse B, Vaivre-Douret L. Nature of motor impairments in autism spectrum disorder: A comparison with developmental coordination disorder. *Journal of Clinical and Experimental Neuropsychology*. 2019;41(1):1-14. doi:10.1080/13803395.2018.1483486

196. Bolduc ME, Limperopoulos C. Neurodevelopmental outcomes in children with cerebellar malformations: A systematic review. *Developmental Medicine and Child Neurology*. 2009;51(4):256-267. doi:10.1111/j.1469-8749.2008.03224.x

197. DeLong GR. The Cerebellum in Autism. In: *The Neurology of Autism*. Oxford University Press; 2005. doi:10.1093/acprof:oso/9780195182224.003.0003

198. Bauman M, Kemper TL. Histoanatomic observations of the brain in early infantile autism. *Neurology*. 1985;35(6):866-874. doi:10.1212/wnl.35.6.866

199. Kemper TL, Bauman ML. Neuropathology of infantile autism. *Molecular Psychiatry*. 2002;7:12-13. doi:10.1038/sj.mp.4001165

200. Skefos J, Cummings C, Enzer K, et al. Regional Alterations in Purkinje Cell Density in Patients with Autism. Sugihara I, ed. *PLoS ONE*. 2014;9(2):e81255. doi:10.1371/journal.pone.0081255

201. Fatemi SH, Halt AR, Realmuto G, et al. Purkinje cell size is reduced in cerebellum of patients with autism. *Cellular and Molecular Neurobiology*. 2002;22(2):171-175. doi:10.1023/A:1019861721160

202. Araghi-Niknam M, Fatemi SH. Levels of Bcl-2 and P53 Are Altered in Superior Frontal and Cerebellar Cortices of Autistic Subjects. *Cellular and Molecular*

Neurobiology. 2003;23(6):945-952. doi:10.1023/B:CEMN.0000005322.27203.73

203. Fatemi SH, Halt AR, Stary JM, Kanodia R, Schulz SC, Realmuto GR. Glutamic acid decarboxylase 65 and 67 kDa proteins are reduced in autistic parietal and cerebellar cortices. *Biological Psychiatry*. 2002;52(8):805-810. doi:10.1016/S0006-3223(02)01430-0

204. Fatemi SH, Stary JM, Halt AR, Realmuto GR. Dysregulation of Reelin and Bcl-2 Proteins in Autistic Cerebellum. *Journal of Autism and Developmental Disorders*. 2001;31(6):529-535. doi:10.1023/A:1013234708757

205. Purcell AE, Jeon OH, Zimmerman AW, Blue ME, Pevsner J. Postmortem brain abnormalities of the glutamate neurotransmitter system in autism. *Neurology*. 2001;57(9):1618-1628. doi:10.1212/WNL.57.9.1618

206. Vargas DL, Nascimbene C, Krishnan C, Zimmerman AW, Pardo CA. Neuroglial activation and neuroinflammation in the brain of patients with autism. *Annals of Neurology*. 2005;57(1):67-81. doi:10.1002/ana.20315

207. Peter S, Ten Brinke MM, Stedehouder J, et al. Dysfunctional cerebellar Purkinje cells contribute to autism-like behaviour in Shank2-deficient mice. *Nature Communications*. 2016;7(1):1-14. doi:10.1038/ncomms12627

208. Tsai PT, Hull C, Chu Y, et al. Autistic-like behaviour and cerebellar dysfunction in Purkinje cell Tsc1 mutant mice. *Nature*. 2012;488(7413):647-651. doi:10.1038/nature11310

209. Martin LA, Goldowitz D, Mittleman G. Repetitive behavior and increased activity in mice with Purkinje cell loss: a model for understanding the role of cerebellar pathology in autism. *European Journal of Neuroscience*. 2010;31(3):544-555. doi:10.1111/j.1460-9568.2009.07073.x

210. Akshoomoff N, Lord C, Lincoln AJ, et al. Outcome classification of preschool children with autism spectrum disorders using MRI brain measures. *Journal of the American Academy of Child and Adolescent Psychiatry*. 2004;43(3):349-357. doi:10.1097/00004583-200403000-00018

211. D'Mello AM, Crocetti D, Mostofsky SH, Stoodley CJ. Cerebellar gray matter and lobular volumes correlate with core autism symptoms. *NeuroImage: Clinical*. 2015;7:631-639. doi:10.1016/j.nicl.2015.02.007

212. Khan AJ, Nair A, Keown CL, Datko MC, Lincoln AJ, Müller RA. Cerebro-cerebellar resting-state functional connectivity in children and adolescents with autism spectrum disorder. *Biological Psychiatry*. 2015;78(9):625-634. doi:10.1016/j.biopsych.2015.03.024

213. Verly M, Verhoeven J, Zink I, et al. Altered functional connectivity of the language network in ASD: Role of classical language areas and cerebellum. *NeuroImage: Clinical*. 2014;4:374-382. doi:10.1016/j.nicl.2014.01.008

214. Jung M, Kosaka H, Saito DN, et al. Default mode network in young male adults with autism spectrum disorder: Relationship with autism spectrum traits. *Molecular Autism*. 2014;5(1):35. doi:10.1186/2040-2392-5-35

215. Stoodley, C.J.; D'Mello, A.M.; Ellegood, J.; Jakkamsetti, V.; Liu, P.; Nebel,

M.B.; Gibson, J.M.; Kelly, E.; Meng, F.; Cano, C.A.; Pascual, J.M.' Mostofsky, J.P.; Lerch, J.P.; Tsai P. Altered cerebellar connectivity in autism and cerebellar-mediated rescue of autism-related behaviors in mice. *Nature Neuroscience*. 2017;20(December):1744-1751. doi:10.1038/s41593-017-0004-1

216. Goetz M, Vesela M, Ptacek R. Notes on the Role of the Cerebellum in ADHD. *Austin J Psychiatry Behav Sci*. 2014;1(1):1013-3. Accessed December 28, 2020. www.austinpublishinggroup.com

217. Faraone S V., Rostain AL, Blader J, et al. Practitioner Review: Emotional dysregulation in attention-deficit/hyperactivity disorder - implications for clinical recognition and intervention. *Journal of Child Psychology and Psychiatry*. 2019;60(2):133-150. doi:10.1111/jcpp.12899

218. Brown TE. *Attention Deficit Disorder: The Unfocused Mind in Children and Adults.* Yale University Press; 2005.

219. Brown TE. Attention-deficit disorders and comorbidities in children, adolescents, and adults. Brown TE, ed. *Attention-deficit disorders and comorbidities in children, adolescents, and adults*. Published online 2000:xxi, 671-xxi, 671.

220. Melegari MG, Bruni O, Sacco R, Barni D, Sette S, Donfrancesco R. Comorbidity of Attention Deficit Hyperactivity Disorder and Generalized Anxiety Disorder in children and adolescents. *Psychiatry Research*. 2018;270:780-785. doi:10.1016/j.psychres.2018.10.078

221. Kuja-Halkola R, Lind Juto K, Skoglund C, et al. Do borderline personality disorder and attention-deficit/hyperactivity disorder co-aggregate in families? A population-based study of 2 million Swedes. *Molecular Psychiatry*. Published online 2018. doi:10.1038/s41380-018-0248-5

222. Fenollar-Cortés J, Gallego-Martínez A, Fuentes LJ. The role of inattention and hyperactivity/impulsivity in the fine motor coordination in children with ADHD. *Research in Developmental Disabilities*. 2017;69:77-84. doi:10.1016/j.ridd.2017.08.003

223. Hove MJ, Zeffiro TA, Biederman J, Li Z, Schmahmann J, Valera EM. Postural sway and regional cerebellar volume in adults with attention-deficit/hyperactivity disorder. *NeuroImage: Clinical*. 2015;8:422-428. doi:10.1016/j.nicl.2015.05.005

224. Tseng MH, Henderson A, Chow SMK, Yao G. Relationship between motor proficiency, attention, impulse, and activity in children with ADHD. *Developmental Medicine & Child Neurology*. 2004;46(6):381-388. doi:10.1017/S0012162204000623

225. Watemberg N, Waiserberg N, Zuk L, Lerman-Sagie T. Developmental coordination disorder in children with attention-deficit-hyperactivity disorder and physical therapy intervention. *Developmental Medicine & Child Neurology*. 2007;49(12):920-925. doi:10.1111/j.1469-8749.2007.00920.x

226. Goetz M, Schwabova J, Hlavka Z, et al. Cerebellar Symptoms Are Associated With Omission Errors and Variability of Response Time in Children With ADHD. *Journal of Attention Disorders*. 2017;21(3):190-199. doi:10.1177/1087054713517745

227. Kaiser ML, Schoemaker MM, Albaret JM, Geuze RH. What is the evidence of impaired motor skills and motor control among children with attention deficit hyperactivity disorder (ADHD)? Systematic review of the literature. *Research in Developmental Disabilities*. 2015;36:338-357. doi:10.1016/j.ridd.2014.09.023

228. Rasmussen P, Gillberg C. Natural outcome of ADHD with developmental coordination disorder at age 22 years: A controlled, longitudinal, community-based study. *Journal of the American Academy of Child and Adolescent Psychiatry*. 2000;39(11):1424-1431. doi:10.1097/00004583-200011000-00017

229. Tervo RC, Azuma S, Fogas B, Fiechtner H. Children with ADHD and motor dysfunction compared with children with ADHD only. *Developmental Medicine & Child Neurology*. 2007;44(6):383-390. doi:10.1111/j.1469-8749.2002.tb00832.x

230. Stray LL, Ellertsen B, Stray T. Motor function and methylphenidate effect in children with attention deficit hyperactivity disorder. *Acta Paediatrica*. 2010;99(8):1199-1204. doi:10.1111/j.1651-2227.2010.01760.x

231. Castellanos FX, Proal E. Large-scale brain systems in ADHD: Beyond the prefrontal-striatal model. *Trends in Cognitive Sciences*. 2012;16(1):17-26. doi:10.1016/j.tics.2011.11.007

232. Valera EM, Faraone S V., Murray KE, Seidman LJ. Meta-Analysis of Structural Imaging Findings in Attention-Deficit/Hyperactivity Disorder. *Biological Psychiatry*. 2007;61(12):1361-1369. doi:10.1016/j.biopsych.2006.06.011

233. Castellanos FX, Giedd JN, Marsh WL, et al. Quantitative brain magnetic resonance imaging in attention-deficit hyperactivity disorder. *Archives of General Psychiatry*. 1996;53(7):607-616. doi:10.1001/archpsyc.1996.01830070053009

234. Berquin PC, Giedd JN, Jacobsen LK, et al. Cerebellum in attention-deficit hyperactivity disorder: A morphometric MRI study. *Neurology*. 1998;50(4):1087-1093. doi:10.1212/WNL.50.4.1087

235. Ivanov I, Murrough JW, Bansal R, Hao X, Peterson BS. Cerebellar morphology and the effects of stimulant medications in youths with attention deficit-hyperactivity disorder. *Neuropsychopharmacology*. 2014;39(3):718-726. doi:10.1038/npp.2013.257

236. Duan K, Chen J, Calhoun VD, et al. Neural correlates of cognitive function and symptoms in attention-deficit/hyperactivity disorder in adults. *NeuroImage: Clinical*. 2018;19:374-383. doi:10.1016/j.nicl.2018.04.035

237. Passarelli F, Donfrancesco R, Nativio P, et al. Anti-Purkinje cell antibody as a biological marker in attention deficit/hyperactivity disorder: A pilot study. *Journal of Neuroimmunology*. 2013;258(1-2):67-70. doi:10.1016/j.jneuroim.2013.02.018

238. Krain AL, Castellanos FX. Brain development and ADHD. *Clinical Psychology Review*. 2006;26(4):433-444. doi:10.1016/j.cpr.2006.01.005

239. Bürk K. Clinical scales of cerebellar Ataxias. In: *Handbook of the Cerebellum*

and Cerebellar Disorders. Springer Netherlands; 2013:1785-1798. doi:10.1007/978-94-007-1333-8_80

240. Holmes G. The symptoms of acute cerebellar injuries due to gunshot injuries. *Brain*. 1917;40(4):461-535. doi:10.1093/BRAIN/40.4.461

241. Potts MB, Adwanikar H, Noble-Haeusslein LJ. Models of traumatic cerebellar injury. *Cerebellum*. 2009;8(3):211-221. doi:10.1007/s12311-009-0114-8

242. Cervos-Navarro J, Diemer NH. Selective vulnerability in brain hypoxia. *Critical Reviews in Neurobiology*. 1991;6(3):149-182. Accessed December 3, 2020. http://europepmc.org/article/med/1773451

243. Miller SP, Ferriero DM. From selective vulnerability to connectivity: insights from newborn brain imaging. *Trends in Neurosciences*. 2009;32(9):496-505. doi:10.1016/j.tins.2009.05.010

244. Srinivasan L, Allsop J, Counsell SJ, Boardman JP, Edwards AD, Rutherford M. *Smaller Cerebellar Volumes in Very Preterm Infants at Term-Equivalent Age Are Associated with the Presence of Supratentorial Lesions*. Accessed December 3, 2020. www.ajnr.org

245. Luo J. Effects of Ethanol on the Cerebellum: Advances and Prospects. *The Cerebellum 2015 14:4*. 2015;14(4):383-385. doi:10.1007/S12311-015-0674-8

246. Manto M, Perrotta G. Toxic-induced cerebellar syndrome: from the fetal period to the elderly. In: *Handbook of Clinical Neurology*. Vol 155. Elsevier B.V.; 2018:333-352. doi:10.1016/B978-0-444-64189-2.00022-6

247. Sarikaya H, Steinlin M. Cerebellar stroke in adults and children. *Handbook of Clinical Neurology*. 2018;155:301-312. doi:10.1016/B978-0-444-64189-2.00020-2

248. Stoodley CJ, MacMore JP, Makris N, Sherman JC, Schmahmann JD. Location of lesion determines motor vs. cognitive consequences in patients with cerebellar stroke. *NeuroImage: Clinical*. 2016;12:765-775. doi:10.1016/J.NICL.2016.10.013

249. Gudrunardottir T, Morgan AT, Lux AL, et al. Consensus paper on post-operative pediatric cerebellar mutism syndrome: the Iceland Delphi results. *Child's Nervous System*. 2016;32(7):1195-1203. doi:10.1007/S00381-016-3093-3/FIGURES/1

250. De Fraiture DMI, Sie TH, Boezeman EHJF, Haanen HCM. Cerebellitis as an uncommon complication of infectious mononucleosis. *The Netherlands Journal of Medicine*. 1997;51(2):79-82. doi:10.1016/S0300-2977(97)00035-1

251. Neophytides A, Khan S, Louie E. Subacute cerebellitis in Lyme disease. *International Journal of Clinical Practice*. 1997;51(8):523-524. Accessed January 25, 2022. https://europepmc.org/article/med/9536610

252. Hadjivassiliou M, Sanders DS, Woodroofe N, Williamson C, Grünewald RA. Gluten ataxia. *The Cerebellum 2008 7:3*. 2008;7(3):494-498. doi:10.1007/S12311-008-0052-X

253. Hadjivassiliou M, Sanders DD, Aeschlimann DP. Gluten-Related Disorders: Gluten Ataxia. *Digestive Diseases*. 2015;33(2):264-268. doi:10.1159/000369509

254. Kuchling J, Shababi-Klein J, Nümann A, Gerischer LM, Harms L, Prüss H. GAD Antibody-Associated Late-Onset Cerebellar Ataxia in Two Female Siblings. *Case Reports in Neurology*. 2014;6(3):264-270. doi:10.1159/000369784

255. Mitoma H, Manto M, Hampe CS. Immune-mediated cerebellar ataxias: from bench to bedside. *Cerebellum & Ataxias 2017 4:1*. 2017;4(1):1-14. doi:10.1186/S40673-017-0073-7

256. Jaeckle KA, Graus F, Houghton A, Cardon-Cardo C, Nielsen SL, Posner JB. Autoimmune response of patients with paraneoplastic cerebellar degeneration to a Purkinje cell cytoplasmic protein antigen. *Annals of Neurology*. 1985;18(5):592-600. doi:10.1002/ANA.410180513

257. Roberts WK, Darnell RB. Neuroimmunology of the paraneoplastic neurological degenerations. *Current Opinion in Immunology*. 2004;16(5):616-622. doi:10.1016/J.COI.2004.07.009

258. Pourié G, Martin N, Bossenmeyer-Pourié C, et al. Folate- and vitamin B12-deficient diet during gestation and lactation alters cerebellar synapsin expression via impaired influence of estrogen nuclear receptor α. *The FASEB Journal*. 2015;29(9):3713-3725. doi:10.1096/FJ.14-264267

259. Chakrabarty B, Dubey R, Gulati S, Yoganathan S, Kumar A, Kumar A. Isolated cerebellar involvement in vitamin B12 deficiency: A case report. *Journal of Child Neurology*. 2014;29(11):NP161-NP163. doi:10.1177/0883073813513498

260. Acosta MT, Munasinghe J, Pearl PL, et al. Cerebellar atrophy in human and murine succinic semialdehyde dehydrogenase deficiency. *Journal of Child Neurology*. 2010;25(12):1457-1461. doi:10.1177/0883073810368137

261. Poretti A, Boltshauser E, Doherty D. Cerebellar hypoplasia: Differential diagnosis and diagnostic approach. *American Journal of Medical Genetics Part C: Seminars in Medical Genetics*. 2014;166(2):211-226. doi:10.1002/AJMG.C.31398

262. Finsterer J, Zarrouk-Mahjoub S. Cerebellar atrophy is common among mitochondrial disorders. *Metabolic Brain Disease*. 2018;33(4):987-988. doi:10.1007/s11011-018-0238-y

263. Lax NZ, Hepplewhite PD, Reeve AK, et al. Cerebellar Ataxia in Patients With Mitochondrial DNA Disease. *Journal of Neuropathology & Experimental Neurology*. 2012;71(2):148-161. doi:10.1097/NEN.0b013e318244477d

264. Selim M, Drachman DA. Ataxia associated with Hashimoto's disease: Progressive non-familial adult onset cerebellar degeneration with autoimmune thyroiditis. *Journal of Neurology Neurosurgery and Psychiatry*. 2001;71(1):81-87. doi:10.1136/jnnp.71.1.81

265. Higashi Y, Murayama S, Pentchev PG, Suzuki K. Cerebellar degeneration in the Niemann-Pick type C mouse. *Acta Neuropathologica*. 1993;85(2):175-184. doi:10.1007/BF00227765

266. Yang HG, Wang N, Luo XG, et al. Cerebellar atrophy and its contribution to motor and cognitive performance in multiple system atrophy. *NeuroImage: Clinical*. 2019;23:101891. doi:10.1016/J.NICL.2019.101891

267. Weier K, Banwell B, Cerasa A, et al. The Role of the Cerebellum in Multiple Sclerosis. *Cerebellum*. 2015;14(3):364-374. doi:10.1007/s12311-014-0634-8

268. Kaufmann M, Schaupp A-L, Sun R, et al. Identification of early neurodegenerative pathways in progressive multiple sclerosis. *Nature Neuroscience 2022*. Published online June 20, 2022:1-12. doi:10.1038/s41593-022-01097-3

269. Filippi M, Bar-Or A, Piehl F, et al. Multiple sclerosis. *Nature Reviews Disease Primers 2018 4:1*. 2018;4(1):1-27. doi:10.1038/s41572-018-0041-4

270. Chaudhuri A. Multiple sclerosis is primarily a neurodegenerative disease. *Journal of Neural Transmission 2013 120:10*. 2013;120(10):1463-1466. doi:10.1007/S00702-013-1080-3

271. Dogonowski AM, Andersen KW, Madsen KH, et al. Multiple sclerosis impairs regional functional connectivity in the cerebellum. *NeuroImage: Clinical*. 2014;4:130-138. doi:10.1016/j.nicl.2013.11.005

272. Kutzelnigg A, Faber-Rod JC, Bauer J, et al. Widespread demyelination in the cerebellar cortex in multiple sclerosis. *Brain Pathology*. 2007;17(1):38-44. doi:10.1111/j.1750-3639.2006.00041.x

273. D'Ambrosio A, Pagani E, Riccitelli GC, et al. Cerebellar contribution to motor and cognitive performance in multiple sclerosis: An MRI sub-regional volumetric analysis. *Multiple Sclerosis*. 2017;23(9):1194-1203. doi:10.1177/1352458516674567

274. Tabatabaei-Jafari H, Walsh E, Shaw ME, Cherbuin N. The cerebellum shrinks faster than normal ageing in Alzheimer's disease but not in mild cognitive impairment. *Human Brain Mapping*. 2017;38(6):3141-3150. doi:10.1002/hbm.23580

275. Guo CC, Tan R, Hodges JR, Hu X, Sami S, Hornberger M. Network-selective vulnerability of the human cerebellum to Alzheimer's disease and frontotemporal dementia. *Brain*. 2016;139(5):1527-1538. doi:10.1093/brain/aww003

276. Jacobs HIL, Hopkins DA, Mayrhofer HC, et al. The cerebellum in Alzheimer's disease: Evaluating its role in cognitive decline. *Brain*. 2018;141(1):37-47. doi:10.1093/brain/awx194

277. Seidel K, Bouzrou M, Heidemann N, et al. Involvement of the cerebellum in Parkinson disease and dementia with Lewy bodies. *Annals of Neurology*. 2017;81(6):898-903. doi:10.1002/ana.24937

278. Fasano A, Laganiere SE, Lam S, Fox MD. Lesions causing freezing of gait localize to a cerebellar functional network. *Annals of Neurology*. 2017;81(1):129-141. doi:10.1002/ana.24845

279. Chen Y, Kumfor F, Landin-Romero R, Irish M, Hodges JR, Piguet O. Cerebellar atrophy and its contribution to cognition in frontotemporal dementias. *Annals of*

Neurology. Published online 2018. doi:10.1002/ana.25271

280. Chen Y, Kumfor F, Landin-Romero R, Irish M, Piguet O. The Cerebellum in Frontotemporal Dementia: a Meta-Analysis of Neuroimaging Studies. *Neuropsychology Review*. 2019;29(4):450-464. doi:10.1007/s11065-019-09414-7

281. Chen Y, Landin-Romero R, Kumfor F, et al. Cerebellar integrity and contributions to cognition in C9orf72-mediated frontotemporal dementia. *Cortex*. Published online January 31, 2022. doi:10.1016/J.CORTEX.2021.12.014

282. Schulz JB, Boesch S, Bürk K, et al. Diagnosis and treatment of Friedreich ataxia: a European perspective. *Nature Reviews Neurology 2009 5:4*. 2009;5(4):222-234. doi:10.1038/nrneurol.2009.26

283. Koeppen AH. The Hereditary Ataxias. *Journal of Neuropathology & Experimental Neurology*. 1998;57(6):531-543. doi:10.1097/00005072-199806000-00001

284. Koeppen AH. Friedreich's ataxia: Pathology, pathogenesis, and molecular genetics. *Journal of the Neurological Sciences*. 2011;303(1-2):1-12. doi:10.1016/J.JNS.2011.01.010

285. Fogel BL, Perlman S. Clinical features and molecular genetics of autosomal recessive cerebellar ataxias. *The Lancet Neurology*. 2007;6(3):245-257. doi:10.1016/S1474-4422(07)70054-6

286. Durr A. Autosomal dominant cerebellar ataxias: polyglutamine expansions and beyond. *The Lancet Neurology*. 2010;9(9):885-894. doi:10.1016/S1474-4422(10)70183-6

287. Paulson HL, Shakkottai VG, Clark HB, Orr HT. Polyglutamine spinocerebellar ataxias-from genes to potential treatments. *Nature Reviews Neuroscience*. 2017;18(10):613-626. doi:10.1038/nrn.2017.92

288. Michalik A, Martin JJ, Van Broeckhoven C. Spinocerebellar ataxia type 7 associated with pigmentary retinal dystrophy. *European Journal of Human Genetics 2004 12:1*. 2003;12(1):2-15. doi:10.1038/sj.ejhg.5201108

289. Diallo A, Jacobi H, Cook A, et al. Survival in patients with spinocerebellar ataxia types 1, 2, 3, and 6 (EUROSCA): a longitudinal cohort study. *The Lancet Neurology*. 2018;17(4):327-334. doi:10.1016/S1474-4422(18)30042-5

290. Jen JC, Graves TD, Hess EJ, Hanna MG, Griggs RC, Baloh RW. Primary episodic ataxias: diagnosis, pathogenesis and treatment. *Brain*. 2007;130(10):2484-2493. doi:10.1093/brain/awm126

291. Maruyama S, Saito Y, Nakagawa E, et al. Importance of CAG repeat length in childhood-onset dentatorubral- pallidoluysian atrophy. *Journal of Neurology*. 2012;259(11):2329-2334. doi:10.1007/S00415-012-6493-7/FIGURES/2

292. Koide R, Ikeuchi T, Onodera O, et al. Unstable expansion of CAG repeat in hereditary dentatorubral–pallidoluysian atrophy (DRPLA). *Nature Genetics 1994 6:1*. 1994;6(1):9-13. doi:10.1038/ng0194-9

293. Shao J, Diamond MI. Polyglutamine diseases: emerging concepts in pathogenesis

and therapy. *Human Molecular Genetics*. 2007;16(R2):R115-R123. doi:10.1093/HMG/DDM213

294. Schöls L, Bauer P, Schmidt T, Schulte T, Riess O. Autosomal dominant cerebellar ataxias: Clinical features, genetics, and pathogenesis. *Lancet Neurology*. 2004;3(5):291-304. doi:10.1016/S1474-4422(04)00737-9

295. Klockgether T, Mariotti C, Paulson HL. Spinocerebellar ataxia. *Nature Reviews Disease Primers*. 2019;5(1):1-21. doi:10.1038/s41572-019-0074-3

296. Banfi S, Servadio A, Chung M yi, et al. Identification and characterization of the gene causing type 1 spinocerebellar ataxia. *Nature Genetics*. 1994;7(4):513-520. doi:10.1038/ng0894-513

297. Sullivan R, Yau WY, O'Connor E, Houlden H. Spinocerebellar ataxia: an update. *Journal of Neurology*. 2019;266(2):533-544. doi:10.1007/s00415-018-9076-4

298. Krysa W, Sulek A, Rakowicz M, Szirkowiec W, Zaremba J. High relative frequency of SCA1 in Poland reflecting a potential founder effect. *Neurological Sciences*. 2016;37(8):1319-1325. doi:10.1007/s10072-016-2594-x

299. Manto MU. The wide spectrum of spinocerebellar ataxias (SCAs). *The Cerebellum 2005 4:1*. 2005;4(1):2-6. doi:10.1080/14734220510007914

300. Seidel K, Siswanto S, Brunt ERPP, Den Dunnen W, Korf H-WW, Rüb U. Brain pathology of spinocerebellar ataxias. *Acta Neuropathologica*. 2012;124(1):1-21. doi:10.1007/s00401-012-1000-x

301. Sequeiros J, Seneca S, Martindale J. Consensus and controversies in best practices for molecular genetic testing of spinocerebellar ataxias. In: *European Journal of Human Genetics*. Vol 18. Nature Publishing Group; 2010:1188-1195. doi:10.1038/ejhg.2010.10

302. Orr HT, Chung M yi, Banfi S, et al. Expansion of an unstable trinucleotide CAG repeat in spinocerebellar ataxia type 1. *Nature Genetics 1993 4:3*. 1993;4(3):221-226. doi:10.1038/ng0793-221

303. Diallo A, Jacobi H, Tezenas du Montcel S, Klockgether T. Natural history of most common spinocerebellar ataxia: a systematic review and meta-analysis. *Journal of Neurology*. 2020;(0123456789). doi:10.1007/s00415-020-09815-2

304. Sanpei K, Takano H, Igarashi S, et al. Identification of the spinocerebellar ataxia type 2 gene using a direct identification of repeat expansion and cloning technique, DIRECT. *Nature Genetics 1996 14:3*. 1996;14(3):277-284. doi:10.1038/ng1196-277

305. Kawaguchi Y, Okamoto T, Taniwaki M, et al. CAG expansions in a novel gene for Machado-Joseph disease at chromosome 14q32.1. *Nature Genetics 1994 8:3*. 1994;8(3):221-228. doi:10.1038/ng1194-221

306. Flanigan K, Gardner K, Alderson K, et al. Autosomal dominant spinocerebellar ataxia with sensory axonal neuropathy (SCA4): clinical description and genetic localization to chromosome 16q22.1. *American Journal of Human Genetics*. 1996;59(2):392. Accessed January 22, 2022. /pmc/articles/PMC1914712/?report=abstract

307. Ikeda Y, Dick KA, Weatherspoon MR, et al. Spectrin mutations cause spinocerebellar ataxia type 5. *Nature Genetics 2006 38:2*. 2006;38(2):184-190. doi:10.1038/ng1728

308. Zhuchenko O, Bailey J, Bonnen P, et al. Autosomal dominant cerebellar ataxia (SCA6) associated with small polyglutamine expansions in the α1A-voltage-dependent calcium channel. *Nature Genetics 1997 15:1*. 1997;15(1):62-69. doi:10.1038/ng0197-62

309. Gouw LG, Castañeda MA, McKenna CK, et al. Analysis of the Dynamic Mutation in the SCA7 Gene Shows Marked Parental Effects on CAG Repeat Transmission. *Human Molecular Genetics*. 1998;7(3):525-532. doi:10.1093/HMG/7.3.525

310. Koob MD, Moseley ML, Schut LJ, et al. An untranslated CTG expansion causes a novel form of spinocerebellar ataxia (SCA8). *Nature Genetics 1999 21:4*. 1999;21(4):379-384. doi:10.1038/7710

311. Moseley ML, Zu T, Ikeda Y, et al. Bidirectional expression of CUG and CAG expansion transcripts and intranuclear polyglutamine inclusions in spinocerebellar ataxia type 8. 2006;38(7):758-769. doi:10.1038/ng1827

312. Matsuura T, Yamagata T, Burgess DL, et al. Large expansion of the ATTCT pentanucleotide repeat in spinocerebellar ataxia type 10. 2000;26(2):191-194. doi:10.1038/79911

313. Houlden H, Johnson J, Gardner-Thorpe C, et al. Mutations in TTBK2, encoding a kinase implicated in tau phosphorylation, segregate with spinocerebellar ataxia type 11. *Nature Genetics 2007 39:12*. 2007;39(12):1434-1436. doi:10.1038/ng.2007.43

314. Holmes SE, O'Hearn EE, McInnis MG, et al. Expansion of a novel CAG trinucleotide repeat in the 5′ region of PPP2R2B is associated with SCA12. *Nature Genetics 1999 23:4*. 1999;23(4):391-392. doi:10.1038/70493

315. Herman-Bert A, Stevanin G, Netter JC, et al. Mapping of Spinocerebellar Ataxia 13 to Chromosome 19q13.3-q13.4 in a Family with Autosomal Dominant Cerebellar Ataxia and Mental Retardation. *The American Journal of Human Genetics*. 2000;67(1):229-235. doi:10.1086/302958

316. Klebe S, Durr A, Rentschler A, et al. New mutations in protein kinase Cγ associated with spinocerebellar ataxia type 14. *Annals of Neurology*. 2005;58(5):720-729. doi:10.1002/ANA.20628

317. Novak MJU, Sweeney MG, Li A, et al. An ITPR1 gene deletion causes spinocerebellar ataxia 15/16: A genetic, clinical and radiological description. *Movement Disorders*. 2010;25(13):2176-2182. doi:10.1002/MDS.23223

318. Zühlke CH, Spranger M, Spranger S, et al. SCA17 caused by homozygous repeat expansion in TBP due to partial isodisomy 6. *European Journal of Human Genetics 2003 11:8*. 2003;11(8):629-632. doi:10.1038/sj.ejhg.5201018

319. Lin P, Zhang D, Xu G, Yan C. Identification of IFRD1 variant in a Han Chinese family with autosomal dominant hereditary spastic paraplegia associated with

peripheral neuropathy and ataxia. *Journal of Human Genetics*. 2018;63(4):521-524. doi:10.1038/s10038-017-0394-7

320. Duarri A, Jezierska J, Fokkens M, et al. Mutations in potassium channel kcnd3 cause spinocerebellar ataxia type 19. *Annals of Neurology*. 2012;72(6):870-880. doi:10.1002/ANA.23700

321. Knight MA, Hernandez D, Diede SJ, et al. A duplication at chromosome 11q12.2-11q12.3 is associated with spinocerebellar ataxia type 20. *Human Molecular Genetics*. 2008;17(24):3847-3853. doi:10.1093/hmg/ddn283

322. Storey E, Knight MA, Forest SM, Gardner RJM. Spinocerebellar ataxia type 20. *Cerebellum*. 2005;4(1):55-57. doi:10.1080/14734220410019048

323. Delplanque J, Devos D, Huin V, et al. TMEM240 mutations cause spinocerebellar ataxia 21 with mental retardation and severe cognitive impairment. *Brain*. 2014;137(10):2657-2663. doi:10.1093/BRAIN/AWU202

324. Bakalkin G, Watanabe H, Jezierska J, et al. Prodynorphin mutations cause the neurodegenerative disorder spinocerebellar ataxia type 23. *American Journal of Human Genetics*. 2010;87(5):593-603. doi:10.1016/J.AJHG.2010.10.001/ATTACHMENT/C842B4A3-0007-49C0-AF79-B8DE84241E2C/MMC1.PDF

325. Stevanin G, Bouslam N, Thobois S, et al. Spinocerebellar ataxia with sensory neuropathy (SCA25) maps to chromosome 2p. *Annals of Neurology*. 2004;55(1):97-104. doi:10.1002/ANA.10798

326. Hekman KE, Yu GY, Brown CD, et al. A conserved eEF2 coding variant in SCA26 leads to loss of translational fidelity and increased susceptibility to proteostatic insult. *Human Molecular Genetics*. 2012;21(26):5472-5483. doi:10.1093/hmg/dds392

327. Brusse E, de Koning I, Maat-Kievit A, Oostra BA, Heutink P, van Swieten JC. Spinocerebellar ataxia associated with a mutation in the fibroblast growth factor 14 gene (SCA27): A new phenotype. *Movement Disorders*. 2006;21(3):396-401. Accessed January 27, 2021. http://doi.wiley.com/10.1002/mds.20708

328. Cagnoli C, Stevanin G, Brussino A, et al. Missense mutations in the AFG3L2 proteolytic domain account for ~1.5% of European autosomal dominant cerebellar ataxias. *Human Mutation*. 2010;31(10):1117-1124. doi:10.1002/HUMU.21342

329. Di Bella D, Lazzaro F, Brusco A, et al. Mutations in the mitochondrial protease gene AFG3L2 cause dominant hereditary ataxia SCA28. *Nature Genetics 2010 42:4*. 2010;42(4):313-321. doi:10.1038/ng.544

330. Zambonin JL, Bellomo A, Ben-Pazi H, et al. Spinocerebellar ataxia type 29 due to mutations in ITPR1: A case series and review of this emerging congenital ataxia. *Orphanet Journal of Rare Diseases*. 2017;12(1):1-8. doi:10.1186/s13023-017-0672-7

331. Huang L, Chardon JW, Carter MT, et al. Missense mutations in ITPR1 cause autosomal dominant congenital nonprogressive spinocerebellar ataxia. *Orphanet*

Journal of Rare Diseases. 2012;7(1):67. doi:10.1186/1750-1172-7-67

332. Storey E, Bahlo M, Fahey M, Sisson O, Lueck CJ, Gardner RJM. A new dominantly inherited pure cerebellar ataxia, SCA 30. *Journal of Neurology, Neurosurgery & Psychiatry*. 2009;80(4):408-411. doi:10.1136/JNNP.2008.159459

333. Sato N, Amino T, Kobayashi K, et al. Spinocerebellar Ataxia Type 31 Is Associated with "Inserted" Penta-Nucleotide Repeats Containing (TGGAA)n. *American Journal of Human Genetics*. 2009;85(5):544-557. doi:10.1016/J.AJHG.2009.09.019/ATTACHMENT/B5A0084E-294E-450D-BCFA-04D800C85EF4/MMC1.PDF

334. Jiang H, Zhu H-P, Gomez C. SCA32: An autosomal dominant cerebellar ataxia with azoospermia maps to chromosome 7q32-q33: 9. *Movement Disorders*. 2010;25.

335. Guo YC, Lin JJ, Liao YC, Tsai PC, Lee YC, Soong BW. Spinocerebellar ataxia 35. *Neurology*. 2014;83(17):1554-1561. doi:10.1212/WNL.0000000000000909

336. Kobayashi H, Abe K, Matsuura T, et al. Expansion of intronic GGCCTG hexanucleotide repeat in NOP56 causes SCA36, a type of spinocerebellar ataxia accompanied by motor neuron involvement. *American Journal of Human Genetics*. 2011;89(1):121-130. doi:10.1016/J.AJHG.2011.05.015/ATTACHMENT/D8CD0403-8DC4-4835-BC1B-08BEF09B65E7/MMC1.PDF

337. Corral-Juan M, Serrano-Munuera C, Rábano A, et al. Clinical, genetic and neuropathological characterization of spinocerebellar ataxia type 37. *Brain*. 2018;141(7):1981-1997. doi:10.1093/brain/awy137

338. Serrano-Munuera C, Corral-Juan M, Stevanin G, et al. New subtype of spinocerebellar ataxia with altered vertical eye movements mapping to chromosome 1p32. *JAMA Neurology*. 2013;70(6):764-771. doi:10.1001/jamaneurol.2013.2311

339. Di Gregorio E, Borroni B, Giorgio E, et al. ELOVL5 Mutations Cause Spinocerebellar Ataxia 38. *The American Journal of Human Genetics*. 2014;95(2):209-217. doi:10.1016/J.AJHG.2014.07.001

340. Tsoi H, Yu ACS, Chen ZS, et al. A novel missense mutation in CCDC88C activates the JNK pathway and causes a dominant form of spinocerebellar ataxia. *Journal of Medical Genetics*. 2014;51(9):590-595. doi:10.1136/JMEDGENET-2014-102333/-/DC1

341. Fogel B, Hanson S, Becker E. Mutation of the Murine Ataxia Gene TRPC3 Causes Cerebellar Ataxia in Humans (P1.009). *Neurology*. 2016;86(16 Supplement).

342. Li X, Zhou C, Cui L, et al. A case of a novel CACNA1G mutation from a Chinese family with SCA42. *Medicine*. 2018;97(36):e12148. doi:10.1097/MD.0000000000012148

343. Depondt C, Donatello S, Rai M, et al. MME mutation in dominant

spinocerebellar ataxia with neuropathy (SCA43). *Neurology Genetics*. 2016;2(5):94. doi:10.1212/NXG.0000000000000094

344. Watson LM, Bamber E, Schnekenberg RP, et al. Dominant Mutations in GRM1 Cause Spinocerebellar Ataxia Type 44. *The American Journal of Human Genetics*. 2017;101(3):451-458. doi:10.1016/J.AJHG.2017.08.005

345. Nibbeling EAR, Duarri A, Verschuuren-Bemelmans CC, et al. Exome sequencing and network analysis identifies shared mechanisms underlying spinocerebellar ataxia. *Brain*. 2017;140(11):2860-2878. doi:10.1093/BRAIN/AWX251

346. Gennarino VA, Palmer EE, McDonell LM, et al. A Mild PUM1 Mutation Is Associated with Adult-Onset Ataxia, whereas Haploinsufficiency Causes Developmental Delay and Seizures. *Cell*. 2018;172(5):924-936.e11. doi:10.1016/J.CELL.2018.02.006/ATTACHMENT/73FD4976-9FF3-4FF4-89C1-8F258C654BDE/MMC8.MP4

347. De Michele G, Galatolo D, Barghigiani M, et al. Spinocerebellar ataxia type 48: last but not least. *Neurological Sciences*. 2020;41(9):2423-2432. doi:10.1007/S10072-020-04408-3/FIGURES/2

348. Matilla-Dueñas A, Goold R, Giunti P. Clinical, genetic, molecular, and pathophysiological insights into spinocerebellar ataxia type 1. *Cerebellum (London, England)*. 2008;7(2):106-114. doi:10.1007/s12311-008-0009-0

349. Rüb U, Schöls L, Paulson H, et al. Clinical features, neurogenetics and neuropathology of the polyglutamine spinocerebellar ataxias type 1, 2, 3, 6 and 7. *Progress in Neurobiology*. 2013;104:38-66. doi:10.1016/J.PNEUROBIO.2013.01.001

350. Rosas I, Martínez C, Clarimón J, et al. Role for ATXN1, ATXN2, and HTT intermediate repeats in frontotemporal dementia and Alzheimer's disease. *Neurobiology of Aging*. 2020;87:139.e1-139.e7. doi:10.1016/j.neurobiolaging.2019.10.017

351. Gardiner SL, Harder AVE, Campman YJM, et al. Repeat length variations in ATXN1 and AR modify disease expression in Alzheimer's disease. *Neurobiology of Aging*. 2019;73:230.e9-230.e17. doi:10.1016/J.NEUROBIOLAGING.2018.09.007

352. Tazelaar GHP, Boeynaems S, De Decker M, et al. ATXN1 repeat expansions confer risk for amyotrophic lateral sclerosis and contribute to TDP-43 mislocalization. *Brain Communications*. 2020;2(2):14. doi:10.1093/BRAINCOMMS/FCAA064

353. Lattante S, Pomponi MG, Conte A, et al. ATXN1 intermediate-length polyglutamine expansions are associated with amyotrophic lateral sclerosis. *Neurobiology of Aging*. 2018;64:157.e1-157.e5. doi:10.1016/J.NEUROBIOLAGING.2017.11.011

354. Gonçalves JPN, de Andrade HMT, Cintra VP, et al. CAG repeats ≥ 34 in Ataxin-1 gene are associated with amyotrophic lateral sclerosis in a Brazilian cohort. *Journal of the Neurological Sciences*. 2020;414:116842.

doi:10.1016/j.jns.2020.116842

355. Ma Q, Didonna A. The novel multiple sclerosis susceptibility gene ATXN1 regulates B cell receptor signaling in B-1a cells. *Molecular Brain*. 2021;14(1):19. doi:10.1186/s13041-020-00715-0

356. Patsopoulos NA, Baranzini SE, Santaniello A, et al. Multiple sclerosis genomic map implicates peripheral immune cells and microglia in susceptibility. *Science*. 2019;365(6460). doi:10.1126/science.aav7188

357. Asher M, Johnson A, Zecevic B, Pease D, Cvetanovic M. ATAXIN-1 REGULATES PROLIFERATION OF HIPPOCAMPAL NEURAL PRECURSORS. *NEUROSCIENCE*. 2016;322:54-65. doi:10.1016/j.neuroscience.2016.02.011

358. Cvetanovic M, Hu YS, Opal P. Mutant Ataxin-1 Inhibits Neural Progenitor Cell Proliferation in SCA1. *Cerebellum*. 2017;16(2):340-347. doi:10.1007/s12311-016-0794-9

359. Matilla A, Roberson ED, Banfi S, et al. Mice lacking ataxin-1 display learning deficits and decreased hippocampal paired-pulse facilitation. *The Journal of neuroscience : the official journal of the Society for Neuroscience*. 1998;18(14):5508-5516. doi:10.1523/jneurosci.2978-04.2004

360. Suh J, Romano DM, Nitschke L, et al. Loss of Ataxin-1 Potentiates Alzheimer's Pathogenesis by Elevating Cerebral BACE1 Transcription. *Cell*. 2019;178(5):1159-1175.e17. doi:10.1016/j.cell.2019.07.043

361. Diallo A, Jacobi H, Schmitz-Hübsch T, et al. Body Mass Index Decline Is Related to Spinocerebellar Ataxia Disease Progression. *Movement Disorders Clinical Practice*. 2017;4(5):689-697. doi:10.1002/mdc3.12522

362. Yang CY, Lai RY, Amokrane N, et al. Dysphagia in spinocerebellar ataxias type 1, 2, 3 and 6. *Journal of the Neurological Sciences*. 2020;415:116878. doi:10.1016/J.JNS.2020.116878

363. Pradhan C, Yashavantha BS, Pal PK, Sathyaprabha TN. Spinocerebellar ataxias type 1, 2 and 3: a study of heart rate variability. *Acta Neurologica Scandinavica*. 2008;117(5):337-342. doi:10.1111/j.1600-0404.2007.00945.x

364. Netravathi M, Sathyaprabha TN, Jayalaxmi K, Datta P, Nirmala M, Pal PK. A comparative study of cardiac dysautonomia in autosomal dominant spinocerebellar ataxias and idiopathic sporadic ataxias. *Acta Neurologica Scandinavica*. 2009;120(3):204-209. doi:10.1111/j.1600-0404.2008.01144.x

365. Rub U, Burk K, Timmann D, et al. Spinocerebellar ataxia type 1 (SCA1): New pathoanatomical and clinico-pathological insights. *Neuropathology and Applied Neurobiology*. 2012;38(7):665-680. doi:10.1111/j.1365-2990.2012.01259.x

366. Bauer PO, Zumrova A, Matoska V, et al. Absence of spinocerebellar ataxia type 3/Machado–Joseph disease within ataxic patients in the Czech population. *European Journal of Neurology*. 2005;12(11):851-857. doi:10.1111/J.1468-1331.2005.01090.X

367. Ross OA, Rutherford NJ, Baker M, et al. Ataxin-2 repeat-length variation and

neurodegeneration. *Human Molecular Genetics*. 2011;20(16):3207-3212. doi:10.1093/HMG/DDR227

368. Farhan SMK, Gendron TF, Petrucelli L, Hegele RA, Strong MJ. OPTN p.Met468Arg and ATXN2 intermediate length polyQ extension in families with C9orf72 mediated amyotrophic lateral sclerosis and frontotemporal dementia. *American Journal of Medical Genetics Part B: Neuropsychiatric Genetics*. 2018;177(1):75-85. doi:10.1002/AJMG.B.32606

369. Ciura S, Sellier C, Campanari ML, Charlet-Berguerand N, Kabashi E. The most prevalent genetic cause of ALS-FTD, C9orf72 synergizes the toxicity of ATXN2 intermediate polyglutamine repeats through the autophagy pathway. *https://doi.org/101080/155486272016l189070*. 2016;12(8):1406-1408. doi:10.1080/15548627.2016.1189070

370. Laffita-Mesa JM, Paucar M, Svenningsson P. Ataxin-2 gene: a powerful modulator of neurological disorders. *Current opinion in neurology*. 2021;34(4):578-588. doi:10.1097/WCO.0000000000000959

371. Orozco G, Estrada R, Perry TL, et al. Dominantly inherited olivopontocerebellar atrophy from eastern Cuba. Clinical, neuropathological, and biochemical findings. *Journal of the Neurological Sciences*. 1989;93(1):37-50. doi:10.1016/0022-510X(89)90159-7

372. Estrada R, Galarraga J, Orozco G, Nodarse A, Auburger G. Spinocerebellar ataxia 2 (SCA2): Morphometric analyses in 11 autopsies. *Acta Neuropathologica*. 1999;97(3):306-310. doi:10.1007/s004010050989

373. Li X, Liu H, Fischhaber PL, Tang TS. Toward therapeutic targets for SCA3: Insight into the role of Machado-Joseph disease protein ataxin-3 in misfolded proteins clearance. *Progress in Neurobiology*. 2015;132:34-58. doi:10.1016/j.pneurobio.2015.06.004

374. Costa M do C, Paulson HL. Toward understanding Machado-Joseph disease. *Progress in Neurobiology*. 2012;97(2):239-257. doi:10.1016/j.pneurobio.2011.11.006

375. Kazuta T, Hayashi M, Shimizu T, Iwasaki A, Nakamura S, Hirai S. Autonomic dysfunction in Machado-Joseph disease assessed by iodine123-labeled metaiodobenzylguanidine myocardial scintigraphy. *Clinical Autonomic Research*. 2000;10(3):111-115. doi:10.1007/BF02278014

376. Gierga K, Schelhaas HJ, Brunt ER, et al. Spinocerebellar ataxia type 6 (SCA6): neurodegeneration goes beyond the known brain predilection sites. *Neuropathology and Applied Neurobiology*. 2009;35(5):515-527. doi:10.1111/j.1365-2990.2009.01015.x

377. Chirino-Pérez A, Vaca-Palomares I, Torres DL, et al. Cognitive Impairments in Spinocerebellar Ataxia Type 10 and Their Relation to Cortical Thickness. *Movement Disorders*. 2021;36(12):2910-2921. doi:10.1002/MDS.28728

378. Vališ M, Masopust J, Bažant J, et al. Cognitive changes in spinocerebellar ataxia type 2. *Neuroendocrinology Letters*. 2011;32(3):354-359. Accessed June 13, 2022. www.nel.edu

379. Tichanek F. Psychiatric-Like Impairments in Mouse Models of Spinocerebellar Ataxias. *Cerebellum*. Published online 2022. doi:10.1007/s12311-022-01367-7

380. De Michele G, Maltecca F, Carella M, et al. Dementia, ataxia, extrapyramidal features, and epilepsy: Phenotype spectrum in two Italian families with spinocerebellar ataxia type 17. *Neurological Sciences*. 2003;24(3):166-167. doi:10.1007/s10072-003-0112-4

381. Tang B, Liu C, Shen L, et al. Frequency of SCA1, SCA2, SCA3/MJD, SCA6, SCA7, and DRPLA CAG trinucleotide repeat expansion in patients with hereditary spinocerebellar ataxia from Chinese kindreds. *Archives of Neurology*. 2000;57(4):540-544. doi:10.1001/archneur.57.4.540

382. Dürr A, Smadja D, Cancel G, et al. Autosomal dominant cerebellar ataxia type I in Martinique (French West Indies). *Brain*. 1995;118(6):1573-1581. doi:10.1093/brain/118.6.1573

383. Nakamura K, Jeong S-Y, Uchihara T, et al. SCA17, a novel autosomal dominant cerebellar ataxia caused by an expanded polyglutamine in TATA-binding protein. *Human Molecular Genetics*. 2001;10(14):1441-1448. doi:10.1093/hmg/10.14.1441

384. Atadzhanov M, Smith DC, Mwaba MH, Siddiqi OK, Bryer A, Greenberg LJ. Clinical and genetic analysis of spinocerebellar ataxia type 7 (SCA7) in Zambian families. *Cerebellum and Ataxias*. 2017;4(1):17. doi:10.1186/s40673-017-0075-5

385. Paucar M, Lundin J, Alshammari T, et al. Broader phenotypic traits and widespread brain hypometabolism in spinocerebellar ataxia 27. *Journal of Internal Medicine*. 2020;288(February):103-115. doi:10.1111/joim.13052

386. Rottnek M, Riggio S, Byne W, Sano M, Margolis RL, Walker RH. Schizophrenia in a Patient With Spinocerebellar Ataxia 2: Coincidence of Two Disorders or a Neurodegenerative Disease Presenting With Psychosis? *American Journal of Psychiatry*. 2008;165(8):964-967. doi:10.1176/appi.ajp.2008.08020285

387. Turk KW, Flanagan ME, Josephson S, Keene CD, Jayadev S, Bird TD. Psychosis in Spinocerebellar Ataxias: a Case Series and Study of Tyrosine Hydroxylase in Substantia Nigra. *Cerebellum*. 2018;17(2):143-151. doi:10.1007/s12311-017-0882-5

388. Rolfs A, Koeppen AH, Bauer I, et al. Clinical features and neuropathology of autosomal dominant spinocerebellar ataxia (SCA17). *Annals of Neurology*. 2003;54(3):367-375. doi:10.1002/ANA.10676

389. Feng L, Chen DB, Hou L, et al. Cognitive Impairment in Native Chinese with Spinocerebellar Ataxia Type 3. *European Neurology*. 2014;71(5-6):262-270. doi:10.1159/000357404

390. Nigri A, Sarro L, Mongelli A, et al. Spinocerebellar Ataxia Type 1: One-Year Longitudinal Study to Identify Clinical and MRI Measures of Disease Progression in Patients and Presymptomatic Carriers. *Cerebellum*. Published online June 9, 2021:1-12. doi:10.1007/S12311-021-01285-0/FIGURES/3

391. McMurtray AM, Clark DG, Flood MK, Perlman S, Mendez MF. Depressive and

memory symptoms as presenting features of spinocerebellar ataxia. *The Journal of neuropsychiatry and clinical neurosciences*. 2006;18(3):420-422. doi:10.1176/appi.neuropsych.18.3.420

392. Bürk K, Globas C, Bösch S, et al. Cognitive deficits in spinocerebellar ataxia type 1, 2, and 3. *Journal of neurology*. 2003;250(2):207-211. doi:10.1007/s00415-003-0976-5

393. Ma J, Wu C, Lei J, Zhang X. Cognitive impairments in patients with spinocerebellar ataxia types 1, 2 and 3 are positively correlated to the clinical severity of ataxia symptoms. *International Journal of Clinical and Experimental Medicine*. 2014;7(12):5765-5771.

394. Chirino A, Hernandez-Castillo CR, Galvez V, et al. Motor and cognitive impairments in spinocerebellar ataxia type 7 and its correlations with cortical volumes. *European Journal of Neuroscience*. 2018;48(10):3199-3211. doi:10.1111/EJN.14148

395. Kawai Y, Suenaga M, Watanabe H, et al. Prefrontal hypoperfusion and cognitive dysfunction correlates in spinocerebellar ataxia type 6. *Journal of the Neurological Sciences*. 2008;271(1):68-74. doi:10.1016/J.JNS.2008.03.018

396. Jacobi H, du Montcel ST, Bauer P, et al. Long-term disease progression in spinocerebellar ataxia types 1, 2, 3, and 6: a longitudinal cohort study. *The Lancet Neurology*. 2015;14(11):1101-1108. doi:10.1016/S1474-4422(15)00202-1

397. Diallo A, Jacobi H, Cook A, et al. Prediction of Survival With Long-Term Disease Progression in Most Common Spinocerebellar Ataxia. *Movement Disorders*. 2019;34(8):1220-1227. doi:10.1002/mds.27739

398. Fancellu R, Paridi D, Tomasello C, Panzeri M, Castaldo A, Genitrini S. Longitudinal study of cognitive and psychiatric functions in spinocerebellar ataxia types 1 and 2. Published online 2013:3134-3143. doi:10.1007/s00415-013-7138-1

399. Roeske S, Filla I, Heim S, et al. Progressive cognitive dysfunction in spinocerebellar ataxia type 3. *Movement Disorders*. 2013;28(10):1435-1438. doi:10.1002/MDS.25512

400. Moriarty A, Cook A, Hunt H, Adams ME, Cipolotti L, Giunti P. A longitudinal investigation into cognition and disease progression in spinocerebellar ataxia types 1, 2, 3, 6, and 7. *Orphanet Journal of Rare Diseases*. 2016;11(1):1-9. doi:10.1186/s13023-016-0447-6

401. Rodríguez-Labrada R, Batista-Izquierdo A, González-Melix Z, et al. Cognitive Decline Is Closely Associated with Ataxia Severity in Spinocerebellar Ataxia Type 2: a Validation Study of the Schmahmann Syndrome Scale. *Cerebellum*. Published online July 27, 2021:1-13. doi:10.1007/S12311-021-01305-Z/FIGURES/3

402. Rodríguez-Labrada R, Velázquez-Pérez L, Ortega-Sánchez R, et al. Insights into cognitive decline in spinocerebellar Ataxia type 2: A P300 event-related brain potential study. *Cerebellum and Ataxias*. 2019;6(1):1-9. doi:10.1186/s40673-019-0097-2

403. Moro A, Moscovich M, Farah M, Camargo CHF, Teive HAG, Munhoz RP. Nonmotor symptoms in spinocerebellar ataxias (SCAs). *Cerebellum and Ataxias*. 2019;6(1):12. doi:10.1186/s40673-019-0106-5

404. Saute JAM, Da Silva ACF, Donis KC, Vedolin L, Saraiva-Pereira ML, Jardim LB. Depressive mood is associated with ataxic and non-ataxic neurological dysfunction in SCA3 patients. *Cerebellum*. 2010;9(4):603-605. doi:10.1007/s12311-010-0205-6

405. Cecchin CR, Pires AP, Rieder CR, et al. Depressive Symptoms in Machado-Joseph Disease (SCA3) Patients and Their Relatives. *Community Genetics*. 2007;10(1):19-26. doi:10.1159/000096276

406. Schmitz-Hübsch T, Coudert M, Tezenas du Montcel S, et al. Depression comorbidity in spinocerebellar ataxia. *Movement Disorders*. 2011;26(5):870-876. doi:10.1002/mds.23698

407. Lin M-T, Yang J-S, Chen P-P, et al. Bidirectional Connections between Depression and Ataxia Severity in Spinocerebellar Ataxia Type 3 Patients. *European Neurology*. 2018;79(5-6):266-271. doi:10.1159/000489398

408. Hanna M, Strober LB. Anxiety and depression in Multiple Sclerosis (MS): Antecedents, consequences, and differential impact on well-being and quality of life. *Multiple Sclerosis and Related Disorders*. 2020;44:102261. doi:10.1016/J.MSARD.2020.102261

409. Cendelin J, Cvetanovic M, Gandelman M, et al. Consensus Paper: Strengths and Weaknesses of Animal Models of Spinocerebellar Ataxias and Their Clinical Implications. *Cerebellum*. Published online 2021. doi:10.1007/s12311-021-01311-1

410. Jucker M. The benefits and limitations of animal models for translational research in neurodegenerative diseases. *Nature Medicine 2010 16:11*. 2010;16(11):1210-1214. doi:10.1038/nm.2224

411. Janus C, Welzl H. Mouse Models of Neurodegenerative Diseases: Criteria and General Methodology. *Methods in Molecular Biology*. 2010;602:323-345. doi:10.1007/978-1-60761-058-8_19

412. Hatanaka Y, Watase K, Wada K, Nagai Y. Abnormalities in synaptic dynamics during development in a mouse model of spinocerebellar ataxia type 1. *Scientific reports*. 2015;5(October):16102. doi:10.1038/srep16102

413. Moreno-Jiménez EP, Terreros-Roncal J, Flor-García M, Rábano A, Llorens-Martín M. Evidences for Adult Hippocampal Neurogenesis in Humans. *Journal of Neuroscience*. 2021;41(12):2541-2553. doi:10.1523/JNEUROSCI.0675-20.2020

414. Clark HB, Burright EN, Yunis WS, et al. Purkinje Cell Expression of a Mutant Allele of SCA1 in Transgenic Mice Leads to Disparate Effects on Motor Behaviors , Followed by a Progressive Cerebellar Dysfunction and Histological Alterations. 1997;17(19):7385-7395.

415. Asher M, Rosa JG, Rainwater O, et al. Cerebellar contribution to the cognitive

alterations in SCA1: Evidence from mouse models. *Human molecular genetics*. 2020;29(1):117-131. doi:10.1093/hmg/ddz265

416. Perlman RL. Mouse models of human diseaseAn evolutionary perspective. *Evolution, Medicine, and Public Health*. 2016;2016(1):170-176. doi:10.1093/EMPH/EOW014

417. Hok V, Poucet B, Duvelle É, Save É, Sargolini F. Spatial cognition in mice and rats: similarities and differences in brain and behavior. *Wiley Interdisciplinary Reviews: Cognitive Science*. 2016;7(6):406-421. doi:10.1002/WCS.1411

418. Davisson MT, Bergstrom DE, Reinholdt LG, Donahue LR. Discovery Genetics: The History and Future of Spontaneous Mutation Research. *Current Protocols in Mouse Biology*. 2012;2(2):103-118. doi:10.1002/9780470942390.MO110200

419. Zuo J, De Jager PL, Takahashi KA, Jiang W, Linden DJ, Heintz N. Neurodegeneration in Lurcher mice caused by mutation in δ2 glutamate receptor gene. *Nature*. 1997;388(6644):769-773. doi:10.1038/42009

420. Coutelier M, Burglen L, Mundwiller E, et al. GRID2 mutations span from congenital to mild adult-onset cerebellar ataxia. *Neurology*. 2015;84(17):1751-1759. doi:10.1212/WNL.0000000000001524

421. Clark HB, Orr HT. Spinocerebellar ataxia type 1--modeling the pathogenesis of a polyglutamine neurodegenerative disorder in transgenic mice. *Journal of neuropathology and experimental neurology*. 2000;59(4):265-270.

422. Kumar TR, Larson M, Wang H, McDermott J, Bronshteyn I. Transgenic Mouse Technology: Principles and Methods. *Methods in molecular biology (Clifton, NJ)*. 2009;590:335-362. doi:10.1007/978-1-60327-378-7_22

423. Ukai H, Kiyonari H, Ueda HR. Production of knock-in mice in a single generation from embryonic stem cells. *Nature Protocols 2017 12:12*. 2017;12(12):2513-2530. doi:10.1038/nprot.2017.110

424. Picciotto MR, Wickman K. Using knockout and transgenic mice to study neurophysiology and behavior. *Physiological Reviews*. 1998;78(4):1131-1163. doi:10.1152/PHYSREV.1998.78.4.1131/ASSET/IMAGES/LARGE/JNP.OC06F8.JPEG

425. Sun Y, Chen X, Xiao D. Tetracycline-inducible Expression Systems: New Strategies and Practices in the Transgenic Mouse Modeling. *Acta Biochimica et Biophysica Sinica*. 2007;39(4):235-246. doi:10.1111/J.1745-7270.2007.00258.X

426. Huang S, Ling JJ, Yang S, Li XJ, Li S. Neuronal expression of TATA box-binding protein containing expanded polyglutamine in knock-in mice reduces chaperone protein response by impairing the function of nuclear factor-Y transcription factor. *Brain*. 2011;134(7):1943-1958. doi:10.1093/brain/awr146

427. Shiotsuki H, Yoshimi K, Shimo Y, et al. A rotarod test for evaluation of motor skill learning. *Journal of Neuroscience Methods*. 2010;189(2):180-185. doi:10.1016/J.JNEUMETH.2010.03.026

428. Brooks SP, Dunnett SB. Tests to assess motor phenotype in mice: a user's guide. *Nature Reviews Neuroscience 2009 10:7*. 2009;10(7):519-529.

doi:10.1038/nrn2652

429. Jones BJ, Roberts DJ. The quantitative measurement of motor inco-ordination in naive mice using an accelerating rotarod. *Journal of Pharmacy and Pharmacology*. 1968;20(4):302-304. doi:10.1111/j.2042-7158.1968.tb09743.x

430. Watase K, Weeber EJ, Xu B, et al. A long CAG repeat in the mouse Sca1 locus replicates SCA1 features and reveals the impact of protein solubility on selective neurodegeneration. *Neuron*. 2002;34(6):905-919. doi:10.1016/S0896-6273(02)00733-X

431. Monville C, Torres EM, Dunnett SB. Comparison of incremental and accelerating protocols of the rotarod test for the assessment of motor deficits in the 6-OHDA model. *Journal of Neuroscience Methods*. 2006;158(2):219-223. doi:10.1016/j.jneumeth.2006.06.001

432. Brooks SP, Dunnett SB. Tests to assess motor phenotype in mice: A user's guide. *Nature Reviews Neuroscience*. 2009;10(7):519-529. doi:10.1038/nrn2652

433. Stanley JL, Lincoln RJ, Brown TA, McDonald LM, Dawson GR, Reynolds DS. The mouse beam walking assay offers improved sensitivity over the mouse rotarod in determining motor coordination deficits induced by benzodiazepines. *Journal of Psychopharmacology*. 2005;19(3):221-227. doi:10.1177/0269881105051524

434. Xu Y, Tian NX, Bai QY, Chen Q, Sun XH, Wang Y. Gait Assessment of Pain and Analgesics: Comparison of the DigiGait™ and CatWalk™ Gait Imaging Systems. *Neuroscience Bulletin*. 2019;35(3):401-418. doi:10.1007/S12264-018-00331-Y/TABLES/1

435. Babuska V, Houdek Z, Tuma J, et al. Transplantation of Embryonic Cerebellar Grafts Improves Gait Parameters in Ataxic Lurcher Mice. *The Cerebellum*. 2015;14(6):632-641. doi:10.1007/s12311-015-0656-x

436. Lalonde R, Strazielle C. Brain regions and genes affecting limb-clasping responses. *Brain Research Reviews*. 2011;67(1-2):252-259. doi:10.1016/J.BRAINRESREV.2011.02.005

437. Crawley JN. Behavioral Phenotyping Strategies for Mutant Mice. *Neuron*. 2008;57(6):809-818. doi:10.1016/J.NEURON.2008.03.001

438. Bohne P, Mourabit DB El, Josten M, Mark MD. Cognitive deficits in episodic ataxia type 2 mouse models. *Human Molecular Genetics*. 2021;30(19):1811-1832. doi:10.1093/HMG/DDAB149

439. Morris R. Developments of a water-maze procedure for studying spatial learning in the rat. *Journal of Neuroscience Methods*. 1984;11(1):47-60. doi:10.1016/0165-0270(84)90007-4

440. Vorhees C V., Williams MT. Morris water maze: Procedures for assessing spatial and related forms of learning and memory. *Nature Protocols*. 2006;1(2):848-858. doi:10.1038/nprot.2006.116

441. Logue SF, Paylor R, Wehner JM. Hippocampal lesions cause learning deficits in inbred mice in the Morris water maze and conditioned-fear task. *Behavioral*

Neuroscience. 1997;111(1):104-113. doi:10.1037/0735-7044.111.1.104

442. Garthe A, Kempermann G. An old test for new neurons: Refining the morris water maze to study the functional relevance of adult hippocampal neurogenesis. *Frontiers in Neuroscience*. 2013;0(7 MAY):63. doi:10.3389/FNINS.2013.00063/BIBTEX

443. Ma QL, Zuo X, Yang F, et al. Loss of MAP Function Leads to Hippocampal Synapse Loss and Deficits in the Morris Water Maze with Aging. *Journal of Neuroscience*. 2014;34(21):7124-7136. doi:10.1523/JNEUROSCI.3439-13.2014

444. Harrison FE, Hosseini AH, McDonald MP. Endogenous anxiety and stress responses in water maze and Barnes maze spatial memory tasks. *Behavioural Brain Research*. 2009;198(1):247-251. doi:10.1016/J.BBR.2008.10.015

445. Paul CM, Magda G, Abel S. Spatial memory: Theoretical basis and comparative review on experimental methods in rodents. *Behavioural Brain Research*. 2009;203(2):151-164. doi:10.1016/J.BBR.2009.05.022

446. Pitts M. Barnes Maze Procedure for Spatial Learning and Memory in Mice. *BIO-PROTOCOL*. 2018;8(5). doi:10.21769/bioprotoc.2744

447. Rustay N, Browman K, Curzon P. Cued and Contextual Fear Conditioning for Rodents. In: Buccafusco JJ, ed. *Methods of Behavior Analysis in Neuroscience. 2nd Edition.* CRC Press/Taylor & Francis; 2008:19-37. doi:10.1201/noe1420052343.ch2

448. Rogan MT, Stäubli U V., LeDoux JE. Fear conditioning induces associative long-term potentiation in the amygdala. *Nature 1997 390:6660*. 1997;390(6660):604-607. doi:10.1038/37601

449. Anagnostaras SG, Gale GD, Fanselow MS. Hippocampus and Contextual Fear Conditioning: Recent Controversies and Advances. Published online 2001. doi:10.1002/1098-1063

450. Mena A, Ruiz-Salas JC, Puentes A, Dorado I, Ruiz-Veguilla M, De la Casa LG. Reduced Prepulse Inhibition as a Biomarker of Schizophrenia. *Frontiers in Behavioral Neuroscience*. 2016;10:202. doi:10.3389/fnbeh.2016.00202

451. Wolf R, Matzke K, Paelchen K, Dobrowolny H, Bogerts B, Schwegler H. Reduction of prepulse inhibition (PPI) after neonatal excitotoxic lesion of the ventral thalamus in pubertal and adult rats. *Pharmacopsychiatry*. 2010;43(3):99-109. doi:10.1055/S-0029-1242823/ID/30

452. Guariglia SR, Chadman KK. Water T-maze: A useful assay for determination of repetitive behaviors in mice. *Journal of Neuroscience Methods*. 2013;220(1):24-29. doi:10.1016/j.jneumeth.2013.08.019

453. Krumin M, Lee JJ, Harris KD, Carandini M. Decision and navigation in mouse parietal cortex. *eLife*. 2018;7. doi:10.7554/eLife.42583

454. Birrell JM, Brown VJ. Medial Frontal Cortex Mediates Perceptual Attentional Set Shifting in the Rat. *Journal of Neuroscience*. 2000;20(11):4320-4324. doi:10.1523/JNEUROSCI.20-11-04320.2000

455. Brown VJ, Bowman EM. Rodent models of prefrontal cortical function. *Trends in Neurosciences*. 2002;25(7):340-343. doi:10.1016/S0166-2236(02)02164-1

456. Kempermann G. New neurons for "survival of the fittest." *Nature Reviews Neuroscience 2012 13:10*. 2012;13(10):727-736. doi:10.1038/nrn3319

457. Rikhye R V., Gilra A, Halassa MM. Thalamic regulation of switching between cortical representations enables cognitive flexibility. *Nature Neuroscience 2018 21:12*. 2018;21(12):1753-1763. doi:10.1038/s41593-018-0269-z

458. Darvas M, Palmiter RD. Contributions of Striatal Dopamine Signaling to the Modulation of Cognitive Flexibility. *Biological Psychiatry*. 2011;69(7):704-707. doi:10.1016/J.BIOPSYCH.2010.09.033

459. Gould TD, Dao DT, Kovacsics CE. The Open Field Test. In: Gould TD, ed. *Mood and Anxiety Related Phenotypes in Mice: Characterization Using Behavioral Tests*. Humana Press; 2009:1-20. doi:10.1007/978-1-60761-303-9_1

460. Prut L, Belzung C. The open field as a paradigm to measure the effects of drugs on anxiety-like behaviors: a review. *European Journal of Pharmacology*. 2003;463(1-3):3-33. doi:10.1016/S0014-2999(03)01272-X

461. Birkett MA, Shinday NM, Kessler EJ, Meyer JS, Ritchie S, Rowlett JK. Acute anxiogenic-like effects of selective serotonin reuptake inhibitors are attenuated by the benzodiazepine diazepam in BALB/c mice. *Pharmacology Biochemistry and Behavior*. 2011;98(4):544-551. doi:10.1016/J.PBB.2011.03.006

462. Gray VC, Hughes RN. Drug-, dose- and sex-dependent effects of chronic fluoxetine, reboxetine and venlafaxine on open-field behavior and spatial memory in rats. *Behavioural Brain Research*. 2015;281:43-54. doi:10.1016/J.BBR.2014.12.023

463. Leger M, Quiedeville A, Bouet V, et al. Object recognition test in mice. *Nature Protocols*. 2013;8(12):2531-2537. doi:10.1038/nprot.2013.155

464. Assini FL, Duzzioni M, Takahashi RN. Object location memory in mice: Pharmacological validation and further evidence of hippocampal CA1 participation. *Behavioural Brain Research*. 2009;204(1):206-211. doi:10.1016/J.BBR.2009.06.005

465. Samuels BA, Hen R. Novelty-Suppressed Feeding in the Mouse BT - Mood and Anxiety Related Phenotypes in Mice: Characterization Using Behavioral Tests, Volume II. In: Gould TD, ed. *Mood and Anxiety Related Phenotypes in Mice*. Humana Press; 2011:107-121. Accessed January 1, 2022. https://doi.org/10.1007/978-1-61779-313-4_7

466. Walf AA, Frye CA. The use of the elevated plus maze as an assay of anxiety-related behavior in rodents. *Nature Protocols 2007 2:2*. 2007;2(2):322-328. doi:10.1038/nprot.2007.44

467. Biedermann S V., Biedermann DG, Wenzlaff F, et al. An elevated plus-maze in mixed reality for studying human anxiety-related behavior. *BMC Biology 2017 15:1*. 2017;15(1):1-13. doi:10.1186/S12915-017-0463-6

468. Garcia AMB, Cardenas FP, Morato S. The effects of pentylenetetrazol,

chlordiazepoxide and caffeine in rats tested in the elevated plus-maze depend on the experimental illumination. *Behavioural Brain Research*. 2011;217(1):171-177. doi:10.1016/J.BBR.2010.09.032

469. Slattery DA, Cryan JF. Using the rat forced swim test to assess antidepressant-like activity in rodents. *Nature Protocols 2012 7:6*. 2012;7(6):1009-1014. doi:10.1038/nprot.2012.044

470. Kara NZ, Stukalin Y, Einat H. Revisiting the validity of the mouse forced swim test: Systematic review and meta-analysis of the effects of prototypic antidepressants. *Neuroscience & Biobehavioral Reviews*. 2018;84:1-11. doi:10.1016/J.NEUBIOREV.2017.11.003

471. Anyan J, Amir S. Too Depressed to Swim or Too Afraid to Stop? A Reinterpretation of the Forced Swim Test as a Measure of Anxiety-Like Behavior. *Neuropsychopharmacology*. 2018;43(5):931-933. doi:10.1038/npp.2017.260

472. Kasper S, Spadone C, Verpillat P, Angst J. Onset of action of escitalopram compared with other antidepressants: Results of a pooled analysis. *International Clinical Psychopharmacology*. 2006;21(2):105-110. doi:10.1097/01.YIC.0000194375.42589.C3

473. Serchov T, van Calker D, Biber K. Sucrose Preference Test to Measure Anhedonic Behaviour in Mice. *BIO-PROTOCOL*. 2016;6(19). doi:10.21769/bioprotoc.1958

474. Liu M-Y, Yin C-Y, Zhu L-J, et al. Sucrose preference test for measurement of stress-induced anhedonia in mice. *Nature Protocols 2018 13:7*. 2018;13(7):1686-1698. doi:10.1038/s41596-018-0011-z

475. Becker M, Pinhasov A, Ornoy A. Animal Models of Depression: What Can They Teach Us about the Human Disease? *Diagnostics 2021, Vol 11, Page 123*. 2021;11(1):123. doi:10.3390/DIAGNOSTICS11010123

476. Willner P. Validity, reliability and utility of the chronic mild stress model of depression: a 10-year review and evaluation. *Psychopharmacology 1997 134:4*. 1997;134(4):319-329. doi:10.1007/S002130050456

477. Cendelin J. From mice to men: lessons from mutant ataxic mice. *Cerebellum & Ataxias*. 2014;1(1):4. doi:10.1186/2053-8871-1-4

478. Cook AA, Fields E, Watt AJ. Losing the Beat: Contribution of Purkinje Cell Firing Dysfunction to Disease, and Its Reversal. *Neuroscience*. Published online June 14, 2020. doi:10.1016/j.neuroscience.2020.06.008

479. Lalonde R, Strazielle C. Motor Performances of Spontaneous and Genetically Modified Mutants with Cerebellar Atrophy. *Cerebellum*. 2019;18(3):615-634. doi:10.1007/s12311-019-01017-5

480. Cui Y, Yang S, Li X-J, Li S. Genetically modified rodent models of SCA17. *Journal of Neuroscience Research*. 2017;95(8):1540-1547. doi:10.1002/jnr.23984

481. Da Conceição Alves-Cruzeiro JM, Mendonça L, De Almeida LP, Nóbrega C.

Motor dysfunctions and neuropathology in mouse models of spinocerebellar ataxia type 2: A comprehensive review. *Frontiers in Neuroscience*. 2016;10(DEC):1-14. doi:10.3389/fnins.2016.00572

482. Colomer Gould VF. Mouse Models of Spinocerebellar Ataxia Type 3 (Machado-Joseph Disease). *Neurotherapeutics*. 2012;9(2):285-296. doi:10.1007/s13311-012-0117-x

483. Huang S, Yang S, Guo J, et al. Large Polyglutamine Repeats Cause Muscle Degeneration in SCA17 Mice. *Cell Reports*. 2015;13(1):196-208. doi:10.1016/j.celrep.2015.08.060

484. Duvick L, Barnes J, Ebner B, et al. SCA1-like disease in mice expressing wild-type Ataxin-1 with a serine to aspartic acid replacement at residue 776. *Neuron*. 2010;67(6):929-935. doi:10.1016/j.neuron.2010.08.022

485. Bouskila M, Esoof N, Gay L, et al. TTBK2 kinase substrate specificity and the impact of spinocerebellar- ataxia-causing mutations on expression, activity, localization and development. *Biochemical Journal*. 2011;437(1):157-167. doi:10.1042/BJ20110276

486. Wang Q, Bardgett ME, Wong M, et al. Ataxia and paroxysmal dyskinesia in mice lacking axonally transported FGF14. *Neuron*. 2002;35(1):25-38. doi:10.1016/S0896-6273(02)00744-4

487. Espinosa F, McMahon A, Chan E, et al. Alcohol hypersensitivity, increased locomotion, and spontaneous myoclonus in mice lacking the potassium channels Kv3.1 and Kv3.3. *Journal of Neuroscience*. 2001;21(17):6657-6665. doi:10.1523/jneurosci.21-17-06657.2001

488. Hurlock EC, McMahon A, Joho RH. Purkinje-cell-restricted restoration of Kv3.3 function restores complex spikes and rescues motor coordination in Kcnc3 mutants. *Journal of Neuroscience*. 2008;28(18):4640-4648. doi:10.1523/JNEUROSCI.5486-07.2008

489. White M, Xia G, Gao R, et al. Transgenic mice with SCA10 pentanucleotide repeats show motor phenotype and susceptibility to seizure: A toxic RNA gain-of-function model. *Journal of Neuroscience Research*. 2012;90(3):706-714. doi:10.1002/jnr.22786

490. Orengo JP, van der Heijden ME, Hao S, Tang J, Orr HT, Zoghbi HY. Motor neuron degeneration correlates with respiratory dysfunction in SCA1. *Disease Models & Mechanisms*. 2018;1(January):dmm.032623. doi:10.1242/dmm.032623

491. Fusco AF, Pucci L, McCall AL, et al. Respiratory Dysfunction in a Mouse Model of Spinocerebellar Ataxia 7. In: *The FASEB Journal*. Vol 34. Wiley; 2020:1-1. doi:10.1096/fasebj.2020.34.s1.05924

492. Cendelin J, Purkartova Z, Kubik J, Ulbricht E, Tichanek F, Kolinko Y. Long-Term Development of Embryonic Cerebellar Grafts in Two Strains of Lurcher Mice. *Cerebellum*. 2018;17(4):428-437. doi:10.1007/s12311-018-0928-3

493. Purkartova Z, Tichanek F, Kolinko Y, Cendelin J. Embryonic Cerebellar Graft Morphology Differs in Two Mouse Models of Cerebellar Degeneration. *The*

Cerebellum. 2019;18(5):855-865. doi:10.1007/s12311-019-01067-9

494. Edamakanti CR, Martina M, Opal P, et al. Mutant ataxin1 disrupts cerebellar development in spinocerebellar ataxia type 1 Graphical abstract Find the latest version : Mutant ataxin1 disrupts cerebellar development in spinocerebellar ataxia type 1. 2018;128(6):2252-2265. doi:10.1172/JCI96765

495. Edamakanti CR, Opal P. Developmental Alterations in Adult-Onset Neurodegenerative Disorders: Lessons from Polyglutamine Diseases. *Movement Disorders*. 2021;36(7):1548-1552. doi:10.1002/MDS.28657

496. Cvetanovic M, Patel JM, Marti HH, Kini AR, Opal P. Vascular endothelial growth factor ameliorates the ataxic phenotype in a mouse model of spinocerebellar ataxia type 1. *Nature Medicine*. 2011;17(11):1445-1447. doi:10.1038/nm.2494

497. Ruegsegger C, Stucki DM, Steiner S, et al. Impaired mTORC1-Dependent Expression of Homer-3 Influences SCA1 Pathophysiology. *Neuron*. 2016;89(1):129-146. doi:10.1016/j.neuron.2015.11.033

498. Ingram M, Wozniak EAL, Duvick L, et al. Cerebellar Transcriptome Profiles of ATXN1 Transgenic Mice Reveal SCA1 Disease Progression and Protection Pathways. *Neuron*. 2016;89(6):1194-1207. doi:10.1016/j.neuron.2016.02.011

499. Hu YS, Do J, Edamakanti CR, et al. Self-assembling vascular endothelial growth factor nanoparticles improve function in spinocerebellar ataxia type 1. *Brain*. 2019;142(2):312-321. doi:10.1093/brain/awy328

500. Duarte-neves J, Gonçalves N, Cunha-santos J, et al. Neuropeptide Y mitigates neuropathology and motor de fi cits in mouse models of Machado – Joseph disease. *Human Molecular Genetics*. 2015;24(19):5451-5463. doi:10.1093/hmg/ddv271

501. Duarte-Neves J, Cavadas C, Pereira de Almeida L. Neuropeptide Y (NPY) intranasal delivery alleviates Machado–Joseph disease. *Scientific Reports 2021 11:1*. 2021;11(1):1-9. doi:10.1038/s41598-021-82339-5

502. Damrath E, Heck M V., Gispert S, et al. ATXN2-CAG42 Sequesters PABPC1 into Insolubility and Induces FBXW8 in Cerebellum of Old Ataxic Knock-In Mice. Orr HT, ed. *PLoS Genetics*. 2012;8(8):e1002920. doi:10.1371/journal.pgen.1002920

503. Sheeler C, Rosa JG, Ferro A, McAdams B, Borgenheimer E, Cvetanovic M. Glia in Neurodegeneration: The Housekeeper, the Defender and the Perpetrator. *International Journal of Molecular Sciences 2020, Vol 21, Page 9188*. 2020;21(23):9188. doi:10.3390/IJMS21239188

504. Cvetanovic M, Ingram M, Orr H, Opal P. Early activation of microglia and astrocytes in mouse models of Spinocerebellar Ataxia Type 1. *Neuroscience*. 2015;48(19):289-299. doi:10.1097/MPG.0b013e3181a15ae8.Screening

505. Matilla-Dueñas A, Ashizawa T, Brice A, et al. Consensus paper: Pathological mechanisms underlying neurodegeneration in spinocerebellar ataxias. *Cerebellum*. 2014;13(2):269-302. doi:10.1007/S12311-013-0539-Y/FIGURES/2

506. Dagda RK, Merrill RA, Cribbs JT, et al. The spinocerebellar ataxia 12 gene product and protein phosphatase 2A regulatory subunit Bβ2 antagonizes neuronal survival by promoting mitochondrial fission. *Journal of Biological Chemistry*. 2008;283(52):36241-36248. doi:10.1074/JBC.M800989200/ATTACHMENT/4BDDF0A9-61F4-47B4-BA48-EB8F9AAFDEF2/MMC1.PDF

507. Sánchez I, Balagué E, Matilla-Dueñas A. Ataxin-1 regulates the cerebellar bioenergetics proteome through the GSK3β-mTOR pathway which is altered in Spinocerebellar ataxia type 1 (SCA1). *Human Molecular Genetics*. 2016;25(18):4021-4040. doi:10.1093/hmg/ddw242

508. Ripolone M, Lucchini V, Ronchi D, et al. Purkinje cell cox deficiency and mtdna depletion in an animal model of spinocerebellar ataxia type 1. *Journal of Neuroscience Research*. 2018;96(9):1576-1585. doi:10.1002/jnr.24263

509. Ferro A, Carbone E, Zhang J, et al. Short-term succinic acid treatment mitigates cerebellar mitochondrial OXPHOS dysfunction, neurodegeneration and ataxia in a Purkinje-specific spinocerebellar ataxia type 1 (SCA1) mouse model. *PLoS ONE*. 2017;12(12):1-20. doi:10.1371/journal.pone.0188425

510. Watase K, Gatchel JR, Sun Y, et al. Lithium therapy improves neurological function and hippocampal dendritic arborization in a spinocerebellar ataxia type 1 mouse model. *PLoS Medicine*. 2007;4(5):0836-0847. doi:10.1371/journal.pmed.0040182

511. Lorenzetti D, Watase K, Xu B, Matzuk MM, Orr HT, Zoghbi HY. Repeat instability and motor incoordination in mice with a targeted expanded CAG repeat in the Sca1 locus. *Human molecular genetics*. 2000;9(5):779-785. doi:ddd080 [pii]

512. Cendelin J, Tichanek F. Cerebellar degeneration averts blindness-induced despaired behavior during spatial task in mice. *Neuroscience Letters*. 2020;722:134854. doi:10.1016/j.neulet.2020.134854

513. Burright EN, Brent Clark H, Servadio A, et al. SCA1 transgenic mice: A model for neurodegeneration caused by an expanded CAG trinucleotide repeat. *Cell*. 1995;82(6):937-948. doi:10.1016/0092-8674(95)90273-2

514. Dansithong W, Paul S, Figueroa KP, et al. Ataxin-2 Regulates RGS8 Translation in a New BAC-SCA2 Transgenic Mouse Model. Orr HT, ed. *PLOS Genetics*. 2015;11(4):e1005182. doi:10.1371/journal.pgen.1005182

515. Hansen ST, Meera P, Otis TS, Pulst SM. Changes in Purkinje cell firing and gene expression precede behavioral pathology in a mouse model of SCA2. *Human Molecular Genetics*. 2013;22(2):271-283. doi:10.1093/hmg/dds427

516. Huynh DP, Figueroa K, Hoang N, Pulst SM. Nuclear localization or inclusion body formation of ataxin-2 are not necessary for SCA2 pathogenesis in mouse or human. *Nature Genetics*. 2000;26(1):44-50. doi:10.1038/79162

517. Liu J, Tang T-SS, Tu H, et al. Deranged calcium signaling and neurodegeneration in spinocerebellar ataxia type 2. *Journal of Neuroscience*. 2009;29(29):9148-9162. doi:10.1523/JNEUROSCI.0660-09.2009

518. Aguiar J, Fernández J, Aguilar A, et al. Ubiquitous expression of human SCA2 gene under the regulation of the SCA2 self promoter cause specific Purkinje cell degeneration in transgenic mice. *Neuroscience Letters*. 2006;392(3):202-206. doi:10.1016/j.neulet.2005.09.020

519. Cemal CK, Carroll CJ, Lawrence L, et al. YAC transgenic mice carrying pathological alleles of the MJD1 locus exhibit a mild and slowly progressive cerebellar deficit. *Human Molecular Genetics*. 2002;11(9):1075-1094. doi:10.1093/hmg/11.9.1075

520. Chen X, Tang TS, Tu H, et al. Deranged calcium signaling and neurodegeneration in spinocerebellar ataxia type 3. *Journal of Neuroscience*. 2008;28(48):12713-12724. doi:10.1523/JNEUROSCI.3909-08.2008

521. Goti D, Katzen SM, Mez J, et al. Neurobiology of Disease A Mutant Ataxin-3 Putative – Cleavage Fragment in Brains of Machado – Joseph Disease Patients and Transgenic Mice Is Cytotoxic above a Critical Concentration. 2004;24(45):10266-10279. doi:10.1523/JNEUROSCI.2734-04.2004

522. Bichelmeier U, Schmidt T, Hübener J, et al. Nuclear localization of ataxin-3 is required for the manifestation of symptoms in SCA3: In vivo evidence. *Journal of Neuroscience*. 2007;27(28):7418-7428. doi:10.1523/JNEUROSCI.4540-06.2007

523. Chou AH, Yeh TH, Ouyang P, Chen YL, Chen SY, Wang HL. Polyglutamine-expanded ataxin-3 causes cerebellar dysfunction of SCA3 transgenic mice by inducing transcriptional dysregulation. *Neurobiology of Disease*. 2008;31(1):89-101. doi:10.1016/j.nbd.2008.03.011

524. Boy J, Schmidt T, Wolburg H, et al. Reversibility of symptoms in a conditional mouse model of spinocerebellar ataxia type 3. *Human Molecular Genetics*. 2009;18(22):4282-4295. doi:10.1093/hmg/ddp381

525. Boy J, Schmidt T, Schumann U, et al. A transgenic mouse model of spinocerebellar ataxia type 3 resembling late disease onset and gender-specific instability of CAG repeats. *Neurobiology of Disease*. 2010;37(2):284-293. doi:10.1016/j.nbd.2009.08.002

526. Silva-Fernandes A, Costa M do C, Duarte-Silva S, et al. Motor uncoordination and neuropathology in a transgenic mouse model of Machado-Joseph disease lacking intranuclear inclusions and ataxin-3 cleavage products. *Neurobiology of Disease*. 2010;40(1):163-176. doi:10.1016/j.nbd.2010.05.021

527. Switonski PM, Szlachcic WJ, Krzyzosiak WJ, Figiel M. A new humanized ataxin-3 knock-in mouse model combines the genetic features, pathogenesis of neurons and glia and late disease onset of SCA3/MJD. *Neurobiology of Disease*. 2015;73:174-188. doi:10.1016/j.nbd.2014.09.020

528. Haas E, Incebacak RD, Hentrich T, et al. A Novel SCA3 Knock-in Mouse Model Mimics the Human SCA3 Disease Phenotype Including Neuropathological, Behavioral, and Transcriptional Abnormalities Especially in Oligodendrocytes. *Molecular Neurobiology*. 2021;1:1-28. doi:10.1007/s12035-021-02610-8

529. Perkins EM, Clarkson YL, Sabatier N, et al. Loss of β-III spectrin leads to

Purkinje cell dysfunction recapitulating the behavior and neuropathology of spinocerebellar ataxia type 5 in humans. *Journal of Neuroscience*. 2010;30(14):4857-4867. doi:10.1523/JNEUROSCI.6065-09.2010

530. Armbrust KR, Wang X, Hathorn TJ, et al. Mutant β-III spectrin causes mGluR1α mislocalization and functional deficits in a mouse model of spinocerebellar ataxia type 5. *Journal of Neuroscience*. 2014;34(30):9891-9904. doi:10.1523/JNEUROSCI.0876-14.2014

531. Watase K, Barrett CF, Miyazaki T, et al. Spinocerebellar ataxia type 6 knockin mice develop a progressive neuronal dysfunction with age-dependent accumulation of mutant CaV2.1 channels. *Proceedings of the National Academy of Sciences of the United States of America*. 2008;105(33):11987-11992. doi:10.1073/pnas.0804350105

532. Jayabal S, Ljungberg L, Erwes T, et al. Rapid Onset of Motor Deficits in a Mouse Model of Spinocerebellar Ataxia Type 6 Precedes Late Cerebellar Degeneration. *eNeuro*. 2015;2(6). doi:10.1523/ENEURO.0094-15.2015

533. Unno T, Wakamori M, Koike M, et al. Development of Purkinje cell degeneration in a knockin mouse model reveals lysosomal involvement in the pathogenesis of SCA6. *Proceedings of the National Academy of Sciences of the United States of America*. 2012;109(43):17693-17698. doi:10.1073/pnas.1212786109

534. Garden GA, Libby RT, Fu YH, et al. Polyglutamine-Expanded Ataxin-7 Promotes Non-Cell-Autonomous Purkinje Cell Degeneration and Displays Proteolytic Cleavage in Ataxic Transgenic Mice. *Journal of Neuroscience*. 2002;22(12):4897-4905. doi:10.1523/jneurosci.22-12-04897.2002

535. La Spada AR, Fu YH, Sopher BL, et al. Polyglutamine-expanded ataxin-7 antagonizes CRX function and induces cone-rod dystrophy in a mouse model of SCA7. *Neuron*. 2001;31(6):913-927. doi:10.1016/S0896-6273(01)00422-6

536. Yoo SY, Pennesi ME, Weeber EJ, et al. SCA7 knockin mice model human SCA7 and reveal gradual accumulation of mutant ataxin-7 in neurons and abnormalities in short-term plasticity. *Neuron*. 2003;37(3):383-401. doi:10.1016/S0896-6273(02)01190-X

537. Chou AH, Chen CY, Chen SY, et al. Polyglutamine-expanded ataxin-7 causes cerebellar dysfunction by inducing transcriptional dysregulation. *Neurochemistry International*. 2010;56(2):329-339. doi:10.1016/j.neuint.2009.11.003

538. Ho CS, Grange RW, Joho RH. Pleiotropic effects of a disrupted K+ channel gene: Reduced body weight, impaired motor skill and muscle contraction, but no seizures. *Proceedings of the National Academy of Sciences of the United States of America*. 1997;94(4):1533-1538. doi:10.1073/pnas.94.4.1533

539. Joho RH, Street C, Matsushita S, Knopfel T. Behavioral motor dysfunction in Kv3-type potassium channel-deficient mice. *Genes, Brain and Behavior*. 2006;5(6):472-482. doi:10.1111/j.1601-183X.2005.00184.x

540. Zhang Y, Snider A, Willard L, Takemoto DJ, Lin D. Loss of Purkinje cells in the PKCγ H101Y transgenic mouse. *Biochemical and Biophysical Research*

Communications. 2009;378(3):524-528. doi:10.1016/j.bbrc.2008.11.082

541. Ji J, Hassler ML, Shimobayashi E, Paka N, Streit R, Kapfhammer JP. Increased protein kinase C gamma activity induces Purkinje cell pathology in a mouse model of spinocerebellar ataxia 14. *Neurobiology of Disease*. 2014;70:1-11. doi:10.1016/j.nbd.2014.06.002

542. Matsumoto M, Nakagawa T, Inoue T, et al. Ataxia and epileptic seizures in mice lacking type 1 inositol 1,4,5-trisphosphate receptor. *Nature*. 1996;379(6561):168-171. doi:10.1038/379168a0

543. Street VA, Bosma MM, Demas VP, et al. The type 1 inositol 1,4,5-trisphosphate receptor gene is altered in the opisthotonos mouse. *Journal of Neuroscience*. 1997;17(2):635-645. doi:10.1523/jneurosci.17-02-00635.1997

544. van de Leemput J, Chandran J, Knight MA, et al. Deletion at ITPR1 Underlies Ataxia in Mice and Spinocerebellar Ataxia 15 in Humans. Orr H, ed. *PLoS Genetics*. 2007;3(6):e108. doi:10.1371/journal.pgen.0030108

545. Friedman MJ, Shah AG, Fang ZH, et al. Polyglutamine domain modulates the TBP-TFIIB interaction: Implications for its normal function and neurodegeneration. *Nature Neuroscience*. 2007;10(12):1519-1528. doi:10.1038/nn2011

546. Portal E, Riess O, Nguyen HP. Automated home cage assessment shows behavioral changes in a transgenic mouse model of spinocerebellar ataxia type 17. *Behavioural Brain Research*. 2013;250:157-165. doi:10.1016/j.bbr.2013.04.042

547. Chang Y-C, Lin C-Y, Hsu C-M, et al. Neuroprotective effects of granulocyte-colony stimulating factor in a novel transgenic mouse model of SCA17. *Journal of Neurochemistry*. 2011;118(2):288-303. doi:10.1111/j.1471-4159.2011.07304.x

548. Yang S, Huang S, Gaertig MA, Li XJ, Li S. Age-dependent decrease in chaperone activity impairs MANF expression, leading to Purkinje Cell degeneration in inducible SCA17 Mice. *Neuron*. 2014;81(2):349-365. doi:10.1016/j.neuron.2013.12.002

549. Smeets CJLM, Jezierska J, Watanabe H, et al. Elevated mutant dynorphin A causes Purkinje cell loss and motor dysfunction in spinocerebellar ataxia type 23. *Brain*. 2015;138(9):2537-2552. doi:10.1093/brain/awv195

550. Wozniak DF, Xiao M, Xu L, Yamada KA, Ornitz DM. Impaired spatial learning and defective theta burst induced LTP in mice lacking fibroblast growth factor 14. *Neurobiology of Disease*. 2007;26(1):14-26. doi:10.1016/j.nbd.2006.11.014

551. Maltecca F, Magnoni R, Cerri F, Cox GA, Quattrini A, Casari G. Haploinsufficiency of AFG3L2, the gene responsible for spinocerebellar ataxia type 28, causes mitochondria-mediated Purkinje cell dark degeneration. *Journal of Neuroscience*. 2009;29(29):9244-9254. doi:10.1523/JNEUROSCI.1532-09.2009

552. Maltecca F, Aghaie A, Schroeder DG, et al. The mitochondrial protease AFG3L2 is essential for axonal development. *Journal of Neuroscience*. 2008;28(11):2827-

2836. doi:10.1523/JNEUROSCI.4677-07.2008

553. Hashiguchi S, Doi H, Kunii M, et al. Ataxic phenotype with altered CaV3.1 channel property in a mouse model for spinocerebellar ataxia 42. *Neurobiology of Disease*. 2019;130:104516. doi:10.1016/j.nbd.2019.104516

554. Onuki Y, Van Someren EJW, De Zeeuw CI, Van Der Werf YD. Hippocampal-cerebellar interaction during spatio-temporal prediction. *Cerebral Cortex*. 2015;25(2):313-321. doi:10.1093/cercor/bht221

555. Passot JB, Sheynikhovich D, Duvelle É, Arleo A. Contribution of cerebellar sensorimotor adaptation to hippocampal spatial memory. *PLoS ONE*. 2012;7(4):42-46. doi:10.1371/journal.pone.0032560

556. Chang B, Hawes NL, Hurd RE, Davisson MT, Nusinowitz S, Heckenlively JR. Retinal degeneration mutants in the mouse. *Vision Research*. 2002;42(4):517-525. doi:10.1016/S0042-6989(01)00146-8

557. Moghaddam M, Bures J. Contribution of egocentric spatial memory to place navigation of rats in the Morris water maze. *Behavioural Brain Research*. 1996;78(2):121-129. doi:10.1016/0166-4328(95)00240-5

558. R Core Team. R: A Language and Environment for Statistical Computing. Published online 2022. https://www.r-project.org

559. Diciccio TJ, Efron B. *Bootstrap Confidence Intervals*. Vol 11.; 1996. Accessed September 24, 2018. https://www.jstor.org/stable/pdf/2246110.pdf?refreqid=excelsior%3A8cb1ab7bd8b406a7018006c64c8ef50c

560. Canty A, Ripley BD. boot: Bootstrap R (S-Plus) Functions. Published online 2017. Accessed September 24, 2018. https://cran.r-project.org/web/packages/boot/index.html

561. Pinheiro J, Bates D, DebRoy S, Sarkar D, R Core Team. nlme: Linear and Nonlinear Mixed Effects Models. Published online 2018. Accessed September 24, 2018. https://cran.r-project.org/web/packages/nlme/citation.html

562. Luo D, Ganesh S, Koolaard J. predictmeans: Calculate Predicted Means for Linear Models. Published online 2018. Accessed September 24, 2018. https://cran.r-project.org/web/packages/predictmeans/index.html

563. Benjamini Y, Hochberg Y. Controlling the false discovery rate: a practical and powerful approach to multiple testing. *Journal of the Royal Statistical Society Series B (Methodological)*. 1995;57:289-300.

564. Sokolovsky N, Cook A, Hunt H, Giunti P, Cipolotti L. A preliminary characterisation of cognition and social cognition in spinocerebellar ataxia types 2, 1, and 7. *Behavioural Neurology*. 2010;23(1-2):17-29. doi:10.3233/BEN-2010-0270

565. Tichanek F, Salomova M, Jedlicka J, et al. Hippocampal mitochondrial dysfunction and psychiatric-relevant behavioral deficits in spinocerebellar ataxia 1 mouse model. *Scientific Reports*. 2020;10:5418. doi:10.1038/s41598-020-62308-0

566. Chaussenot R, Edeline JM, Le Bec B, El Massioui N, Laroche S, Vaillend C. Cognitive dysfunction in the dystrophin-deficient mouse model of Duchenne muscular dystrophy: A reappraisal from sensory to executive processes. *Neurobiology of Learning and Memory*. 2015;124:111-122. doi:10.1016/j.nlm.2015.07.006

567. Darbra S, Pallarès M. Alterations in neonatal neurosteroids affect exploration during adolescence and prepulse inhibition in adulthood. *Psychoneuroendocrinology*. 2010;35(4):525-535. doi:10.1016/j.psyneuen.2009.08.020

568. Basler L, Gerdes S, Wolfer DP, Slomianka L, Murray KD. Sampling the Mouse Hippocampal Dentate Gyrus. 2017;11(December):1-10. doi:10.3389/fnana.2017.00123

569. Schindelin J, Arganda-Carreras I, Frise E, et al. Fiji: an open-source platform for biological-image analysis. *Nature Methods 2012 9:7*. 2012;9(7):676-682. doi:10.1038/nmeth.2019

570. Komlódi T, Sobotka O, Krumschnabel G, et al. Comparison of Mitochondrial Incubation Media for Measurement of Respiration and Hydrogen Peroxide Production. In: Humana Press, New York, NY; 2018:137-155. doi:10.1007/978-1-4939-7831-1_8

571. Doerrier C, Garcia-Souza LF, Krumschnabel G, Wohlfarter Y, Mészáros AT, Gnaiger E. High-Resolution FluoRespirometry and OXPHOS Protocols for Human Cells, Permeabilized Fibers from Small Biopsies of Muscle, and Isolated Mitochondria. In: Humana Press, New York, NY; 2018:31-70. doi:10.1007/978-1-4939-7831-1_3

572. R Development Core Team. R: A Language and Environment for Statistical Computing. Published online 2020. https://www.r-project.org/

573. Good PI. *Permutation, Parametric, and Bootstrap Tests of Hypotheses*. 3rd ed. Springer; 2005. doi:10.1007/b138696

574. Torchiano M. *Effsize - a Package for Efficient Effect Size Computation*.; 2016. doi:10.5281/ZENODO.1480624

575. Oksanen J, Blanchet FG, Friendly M, et al. *Package "vegan" Title Community Ecology Package*.; 2019. Accessed April 15, 2019. https://cran.r-project.org/web/packages/vegan/vegan.pdf

576. Robin X, Turck N, Hainard A, et al. pROC: an open-source package for R and S+ to analyze and compare ROC curves. *BMC Bioinformatics*. 2011;12(1):77. doi:10.1186/1471-2105-12-77

577. Wood SN. Fast stable restricted maximum likelihood and marginal likelihood estimation of semiparametric generalized linear models. *Journal of the Royal Statistical Society: Series B (Statistical Methodology)*. 2011;73(1):3-36. doi:10.1111/j.1467-9868.2010.00749.x

578. Varbanov H, Dityatev A. Regulation of extrasynaptic signaling by polysialylated NCAM: Impact for synaptic plasticity and cognitive functions. *Molecular and*

Cellular Neuroscience. 2017;81:12-21. doi:10.1016/j.mcn.2016.11.005

579. Dityatev A, Dityateva G, Sytnyk V, et al. Polysialylated neural cell adhesion molecule promotes remodeling and formation of hippocampal synapses. *Journal of Neuroscience*. 2004;24(42):9372-9382. doi:10.1523/JNEUROSCI.1702-04.2004

580. Kang K, Joo S, Choi JY, et al. Tissue-based metabolic labeling of polysialic acids in living primary hippocampal neurons. *Proceedings of the National Academy of Sciences of the United States of America*. 2015;112(3):E241-E248. doi:10.1073/pnas.1419683112

581. Boldrini M, Fulmore CA, Tartt AN, et al. Human Hippocampal Neurogenesis Persists throughout Aging. *Cell Stem Cell*. Published online 2018:589-599. doi:10.1016/j.stem.2018.03.015

582. Korelusová I, Cendelín J, Vozeh F. Motor and visuospatial abilities in a model of olivocerebellar and retinal degeneration – Lurcher mutant mice of C3H strain. *Prague medical report*. 2007;108(1):37-48.

583. Schmid M, Nardone A, De Nunzio AM, Schmid M, Schieppati M. Equilibrium during static and dynamic tasks in blind subjects: no evidence of cross-modal plasticity. *Brain*. 2007;130(8):2097-2107. doi:10.1093/BRAIN/AWM157

584. Toth AJ, Harris LR, Zettel J, Bent LR. Vision can recalibrate the vestibular reafference signal used to re-establish postural equilibrium following a platform perturbation. *Experimental Brain Research*. 2017;235(2):407-414. doi:10.1007/S00221-016-4801-7/TABLES/1

585. Cressant A, Besson M, Suarez S, Cormier A, Granon S. Spatial learning in Long-Evans Hooded rats and C57BL/6J mice: Different strategies for different performance. *Behavioural Brain Research*. 2007;177(1):22-29. doi:10.1016/J.BBR.2006.11.010

586. Cendelin J, Tuma J, Korelusova I, Vozeh F. The effect of genetic background on behavioral manifestation of Grid2Lc mutation. *Behavioural Brain Research*. 2014;271:218-227. doi:10.1016/j.bbr.2014.06.023

587. Cheung A, Ball D, Milford M, Wyeth G, Wiles J. Maintaining a Cognitive Map in Darkness: The Need to Fuse Boundary Knowledge with Path Integration. *PLoS Computational Biology*. 2012;8(8). doi:10.1371/journal.pcbi.1002651

588. Zaidel A, Turner AH, Angelaki DE. Multisensory Calibration Is Independent of Cue Reliability. *Journal of Neuroscience*. 2011;31(39):13949-13962. doi:10.1523/JNEUROSCI.2732-11.2011

589. Fetsch CR, Deangelis GC, Angelaki DE. Visual–vestibular cue integration for heading perception: applications of optimal cue integration theory. *European Journal of Neuroscience*. 2010;31(10):1721-1729. doi:10.1111/J.1460-9568.2010.07207.X

590. Lalonde R, Lamarre Y, Smith AM. Does the mutant mouse lurcher have deficits in spatially oriented behaviours? *Brain Research*. 1988;455(1):24-30. doi:10.1016/0006-8993(88)90109-6

591. Bodranghien F, Bastian A, Casali C, et al. Consensus Paper: Revisiting the Symptoms and Signs of Cerebellar Syndrome. *Cerebellum*. 2016;15(3):369-391. doi:10.1007/s12311-015-0687-3

592. Angelaki DE, Hess BJM. Self-motion-induced eye movements: Effects on visual acuity and navigation. *Nature Reviews Neuroscience*. 2005;6(12):966-976. doi:10.1038/nrn1804

593. Strekalova T, Spanagel R, Dolgov O, Bartsch D. Stress-induced hyperlocomotion as a confounding factor in anxiety and depression models in mice. *Behavioural pharmacology*. 2005;16(3):171-180. doi:10.1097/00008877-200505000-00006

594. Lalonde R, Thifault S. Absence of an association between motor coordination and spatial orientation in lurcher mutant mice. *Behavior Genetics*. 1994;24(6):497-501. doi:10.1007/BF01071563

595. Lalonde R. Immobility Responses in Lurcher Mutant Mice. *Behavior Genetics*. 1998;28(4):309-314. doi:10.1023/A:1021627631721

596. Leo D, Gainetdinov RR. Transgenic mouse models for ADHD. *Cell and Tissue Research 2013 354:1*. 2013;354(1):259-271. doi:10.1007/S00441-013-1639-1

597. Zhou M, Rebholz H, Brocia C, et al. Forebrain overexpression of CK1δ leads to down-regulation of dopamine receptors and altered locomotor activity reminiscent of ADHD. *Proceedings of the National Academy of Sciences of the United States of America*. 2010;107(9):4401-4406. doi:10.1073/PNAS.0915173107/SUPPL_FILE/PNAS.200915173SI.PDF

598. Pierce K, Courchesne E. Evidence for a cerebellar role in reduced exploration and stereotyped behavior in autism. *Biological Psychiatry*. 2001;49(8):655-664. doi:10.1016/S0006-3223(00)01008-8

599. Deacon RMJ. Measuring Motor Coordination in Mice. *Journal of Visualized Experiments : JoVE*. 2013;(75):2609. doi:10.3791/2609

600. Edamakanti CR, Do J, Didonna A, Martina M, Opal P. Mutant ataxin1 disrupts cerebellar development in spinocerebellar ataxia type 1. *The Journal of Clinical Investigation*. 2018;128(6):2252-2265. doi:10.1172/JCI96765

601. Brown RE, Wong AA. The influence of visual ability on learning and memory performance in 13 strains of mice. *Learning & Memory*. 2007;14(3):134-144. doi:10.1101/LM.473907

602. Dere E, Huston JP, De Souza Silva MA. Episodic-like memory in mice: Simultaneous assessment of object, place and temporal order memory. *Brain Research Protocols*. 2005;16(1-3):10-19. doi:10.1016/j.brainresprot.2005.08.001

603. Verpeut JL, Bergeler S, Kislin M, et al. Cerebellar contributions to a brainwide network for flexible behavior. *bioRxiv*. Published online December 8, 2021:2021.12.07.471685. doi:10.1101/2021.12.07.471685

604. Gómez-Nieto R, Hormigo S, López DE. Prepulse Inhibition of the Auditory Startle Reflex Assessment as a Hallmark of Brainstem Sensorimotor Gating Mechanisms. *Brain Sciences 2020, Vol 10, Page 639*. 2020;10(9):639. doi:10.3390/BRAINSCI10090639

605. Kohl S, Heekeren K, Klosterkötter J, Kuhn J. Prepulse inhibition in psychiatric disorders – Apart from schizophrenia. *Journal of Psychiatric Research*. 2013;47(4):445-452. doi:10.1016/J.JPSYCHIRES.2012.11.018

606. Swerdlow NR, Weber M, Qu Y, Light GA, Braff DL. Realistic expectations of prepulse inhibition in translational models for schizophrenia research. *Psychopharmacology*. 2008;199(3):331-388. doi:10.1007/S00213-008-1072-4/FIGURES/2

607. Ueki A, Goto K, Sato N, Iso H, Morita Y. Prepulse inhibition of acoustic startle response in mild cognitive impairment and mild dementia of Alzheimer type. *Psychiatry and Clinical Neurosciences*. 2006;60(1):55-62. doi:10.1111/J.1440-1819.2006.01460.X

608. Jafari Z, Kolb BE, Mohajerani MH. Prepulse inhibition of the acoustic startle reflex and P50 gating in aging and alzheimer's disease. *Ageing Research Reviews*. 2020;59:101028. doi:10.1016/J.ARR.2020.101028

609. Powell SB, Zhou X, Geyer MA. Prepulse inhibition and genetic mouse models of schizophrenia. *Behavioural Brain Research*. 2009;204(2):282-294. doi:10.1016/J.BBR.2009.04.021

610. McCool MF, Varty GB, Del Vecchio RA, et al. Increased auditory startle response and reduced prepulse inhibition of startle in transgenic mice expressing a double mutant form of amyloid precursor protein. *Brain Research*. 2003;994(1):99-106. doi:10.1016/J.BRAINRES.2003.09.025

611. Kumari V, Gray JA, Geyer MA, et al. Neural correlates of tactile prepulse inhibition: a functional MRI study in normal and schizophrenic subjects. *Psychiatry Research: Neuroimaging*. 2003;122(2):99-113. doi:10.1016/S0925-4927(02)00123-3

612. Chiou LC, Lee HJ, Ernst M, et al. Cerebellar α6-subunit-containing GABAA receptors: a novel therapeutic target for disrupted prepulse inhibition in neuropsychiatric disorders. *British Journal of Pharmacology*. 2018;175(12):2414-2427. doi:10.1111/BPH.14198

613. Asher M, Rosa JG, Cvetanovic M. Mood alterations in mouse models of Spinocerebellar Ataxia type 1. *Scientific Reports*. 2021;11(1):1-11. doi:10.1038/s41598-020-80664-9

614. Chrastil ER, Sherrill KR, Aselcioglu I, Hasselmo ME, Stern CE. Individual Differences in Human Path Integration Abilities Correlate with Gray Matter Volume in Retrosplenial Cortex, Hippocampus, and Medial Prefrontal Cortex. *Eneuro*. 2017;i(April):ENEURO.0346-16.2017. doi:10.1523/ENEURO.0346-16.2017

615. Bohne P, Rybarski M, Mourabit DB-E, Krause F, Mark MD. Cerebellar contribution to threat probability in a SCA6 mouse model. *Human Molecular Genetics*. 2022;ddac135. doi:10.1093/HMG/DDAC135

616. Schmahmann JD. Disorders of the cerebellum: Ataxia, dysmetria of thought, and the cerebellar cognitive affective syndrome. *Journal of Neuropsychiatry and Clinical Neurosciences*. 2004;16(3):367-378. doi:10.1176/jnp.16.3.367

617. Friedrich J, Kordasiewicz HB, O'Callaghan B, et al. Antisense oligonucleotide-mediated ataxin-1 reduction prolongs survival in SCA1 mice and reveals disease-associated transcriptome profiles. *JCI insight*. 2018;3(21). doi:10.1172/jci.insight.123193

618. Yousef A, Robinson JL, Irwin DJ, et al. Neuron loss and degeneration in the progression of TDP-43 in frontotemporal lobar degeneration. *Acta neuropathologica communications*. 2017;5(1):68. doi:10.1186/s40478-017-0471-3

619. Duan W, Zhang YP, Hou Z, et al. Novel Insights into NeuN: from Neuronal Marker to Splicing Regulator. *Molecular Neurobiology*. 2016;53(3):1637-1647. doi:10.1007/s12035-015-9122-5

620. Wu KL, Li YQ, Tabassum A, Lu WY, Aubert I, Wong CS. Loss of neuronal protein expression in mouse hippocampus after irradiation. *Journal of Neuropathology and Experimental Neurology*. 2010;69(3):272-280. doi:10.1097/NEN.0b013e3181d1afe4

621. Collombet JM, Masqueliez C, Four E, et al. Early reduction of NeuN antigenicity induced by soman poisoning in mice can be used to predict delayed neuronal degeneration in the hippocampus. *Neuroscience Letters*. 2006;398(3):337-342. doi:10.1016/j.neulet.2006.01.029

622. Mellesmoen A, Sheeler C, Ferro A, Rainwater O, Cvetanovic M. Brain derived neurotrophic factor (BDNF) delays onset of pathogenesis in transgenic mouse model of spinocerebellar ataxia type 1 (SCA1). *Frontiers in Cellular Neuroscience*. 2019;12(January):1-8. doi:10.3389/fncel.2018.00509

623. Liu PZ, Nusslock R. Exercise-mediated neurogenesis in the hippocampus via BDNF. *Frontiers in Neuroscience*. 2018;12(FEB):1-6. doi:10.3389/fnins.2018.00052

624. Ghosh A, Carnahan J, Greenberg ME. Requirement for BDNF in activity-dependent survival of cortical neurons. *Science*. 1994;263(5153):1618-1623. doi:10.1126/science.7907431

625. Lipsky RH, Marini AM. Brain-derived neurotrophic factor in neuronal survival and behavior-related plasticity. *Annals of the New York Academy of Sciences*. 2007;1122:130-143. doi:10.1196/annals.1403.009

626. Schoenfeld TJ, McCausland HC, Morris HD, Padmanaban V, Cameron HA. Stress and Loss of Adult Neurogenesis Differentially Reduce Hippocampal Volume. *Biological Psychiatry*. 2017;82(12):914-923. doi:10.1016/j.biopsych.2017.05.013

627. Bessa JM, Ferreira D, Melo I, et al. The mood-improving actions of antidepressants do not depend on neurogenesis but are associated with neuronal remodeling. *Molecular Psychiatry*. 2009;14(8):764-773. doi:10.1038/mp.2008.119

628. Travis S, Coupland NJ, Silversone PH, et al. Dentate gyrus volume and memory performance in major depressive disorder. *Journal of Affective Disorders*. 2015;172:159-164. doi:10.1016/j.jad.2014.09.048

629. Huang Y, Coupland NJ, Lebel RM, et al. Structural changes in hippocampal subfields in major depressive disorder: A high-field magnetic resonance imaging study. *Biological Psychiatry*. 2013;74(1):62-68. doi:10.1016/j.biopsych.2013.01.005

630. Cao B, Passos IC, Mwangi B, et al. Hippocampal subfield volumes in mood disorders. *Molecular Psychiatry*. 2017;22(9):1352-1358. doi:10.1038/mp.2016.262

631. Watanabe Y, Gould E, McEwen BS. Stress induces atrophy of apical dendrites of hippocampal CA3 pyramidal neurons. *Brain Research*. 1992;588(2):341-345. doi:10.1016/0006-8993(92)91597-8

632. Gass N, Becker R, Schwarz AJ, et al. Brain network reorganization differs in response to stress in rats genetically predisposed to depression and stress-resilient rats. *Translational Psychiatry*. 2016;6(12):e970. doi:10.1038/tp.2016.233

633. Gass P, Reichardt HM, Strekalova T, Henn F, Tronche F. Mice with targeted mutations of glucocorticoid and mineralocorticoid receptors: Models for depression and anxiety? *Physiology & Behavior*. 2001;73(5):811-825. doi:10.1016/S0031-9384(01)00518-2

634. Qin DD, Rizak J, Feng XL, et al. Prolonged secretion of cortisol as a possible mechanism underlying stress and depressive behaviour. *Scientific Reports 2016 6:1*. 2016;6(1):1-9. doi:10.1038/srep30187

635. Łojko D, Rybakowski JK. Atypical depression: Current perspectives. *Neuropsychiatric Disease and Treatment*. 2017;13:2447-2456. doi:10.2147/NDT.S147317

636. Thase ME. Atypical Depression: Useful Concept, but it's Time to Revise the DSM-IV Criteria. *Neuropsychopharmacology 2009 34:13*. 2009;34(13):2633-2641. doi:10.1038/npp.2009.100

637. Juruena MF, Bocharova M, Agustini B, Young AH. Atypical depression and non-atypical depression: Is HPA axis function a biomarker? A systematic review. *Journal of Affective Disorders*. 2018;233:45-67. doi:10.1016/J.JAD.2017.09.052

638. Gold PW, Chrousos GP. Organization of the stress system and its dysregulation in melancholic and atypical depression: high vs low CRH/NE states. *Molecular Psychiatry 2002 7:3*. 2002;7(3):254-275. doi:10.1038/sj.mp.4001032

639. Yamamoto M, Kim M, Imai H, Itakura Y, Ohtsuki G. Microglia-Triggered Plasticity of Intrinsic Excitability Modulates Psychomotor Behaviors in Acute Cerebellar Inflammation. *Cell Report*. 2019;28(11):2923-2938.e8. doi:10.2139/ssrn.3280241

640. Salomova M, Tichanek F, Jelinkova D, Cendelin J. Abnormalities in the cerebellar levels of trophic factors BDNF and GDNF in pcd and Lurcher cerebellar mutant mice. *Neuroscience Letters*. Published online February 25, 2020:134870. doi:10.1016/j.neulet.2020.134870

641. Locke TM, Fujita H, Hunker A, et al. Purkinje Cell-Specific Knockout of Tyrosine Hydroxylase Impairs Cognitive Behaviors. *Frontiers in Cellular*

Neuroscience. 2020;14:228. doi:10.3389/FNCEL.2020.00228/BIBTEX

642. Pisano TJ, Dhanerawala ZM, Kislin M, et al. Homologous organization of cerebellar pathways to sensory, motor, and associative forebrain. *Cell Reports*. 2021;36(12):109721. doi:10.1016/J.CELREP.2021.109721

643. Liu L, Zeng LL, Li Y, et al. Altered cerebellar functional connectivity with intrinsic connectivity networks in adults with major depressive disorder. *PLoS ONE*. 2012;7(6):1-8. doi:10.1371/journal.pone.0039516

644. Gan L, Cookson MR, Petrucelli L, La Spada AR. Converging pathways in neurodegeneration, from genetics to mechanisms. *Nature Neuroscience*. 2018;21(10):1300-1309. doi:10.1038/s41593-018-0237-7

645. Stucki DM, Ruegsegger C, Steiner S, et al. Mitochondrial impairments contribute to Spinocerebellar ataxia type 1 progression and can be ameliorated by the mitochondria-targeted antioxidant MitoQ. *Free Radical Biology and Medicine*. 2016;97:427-440. doi:10.1016/j.freeradbiomed.2016.07.005

646. Mattson MP, Gleichmann M, Cheng A. Review Mitochondria in Neuroplasticity and Neurological Disorders. *Neuron*. 2008;60(5):748-766. doi:10.1016/j.neuron.2008.10.010

647. Khacho M, Clark A, Svoboda DS, et al. Mitochondrial dysfunction underlies cognitive defects as a result of neural stem cell depletion and impaired neurogenesis. 2017;26(17):3327-3341. doi:10.1093/hmg/ddx217

648. Devine MJ, Kittler JT. Mitochondria at the neuronal presynapse in health and disease. *Nature Reviews Neuroscience*. 2018;19(2):63-80. doi:10.1038/nrn.2017.170

649. Fernandez A, Meechan DW, Karpinski BA, et al. Mitochondrial Dysfunction Leads to Cortical Under-Connectivity and Cognitive Impairment. *Neuron*. Published online 2019:1-16. doi:10.1016/j.neuron.2019.04.013

650. Arrázola MS, Andraini T, Szelechowski M, et al. Mitochondria in Developmental and Adult Neurogenesis. *Neurotoxicity Research*. Published online 2018:257-267. doi:10.1007/s12640-018-9942-y

651. Oettinghaus B, Schulz JM, Restelli LM, et al. Synaptic dysfunction, memory deficits and hippocampal atrophy due to ablation of mitochondrial fission in adult forebrain neurons. *Cell Death and Differentiation*. 2016;23(1):18-28. doi:10.1038/cdd.2015.39

652. Bachmann RF, Wang Y, Yuan P, et al. Common effects of lithium and valproate on mitochondrial functions: Protection against methamphetamine-induced mitochondrial damage. *International Journal of Neuropsychopharmacology*. 2009;12(6):805-822. doi:10.1017/S1461145708009802

653. Peng M, Ostrovsky J, Kwon YJ, et al. Inhibiting cytosolic translation and autophagy improves health in mitochondrial disease. *Human Molecular Genetics*. 2015;24(17):4829-4847. doi:10.1093/hmg/ddv207

654. Tam ZY, Gruber J, Ng LF, Halliwell B, Gunawan R. Effects of lithium on age-related decline in mitochondrial turnover and function in caenorhabditis elegans.

Journals of Gerontology - Series A Biological Sciences and Medical Sciences. 2014;69(7):810-820. doi:10.1093/gerona/glt210

655. Maurer IC, Schippel P, Volz HP. Lithium-induced enhancement of mitochondrial oxidative phosphorylation in human brain tissue. *Bipolar Disorders*. 2009;11(5):515-522. doi:10.1111/j.1399-5618.2009.00729.x

656. Bernardo TC, Marques-Aleixo I, Beleza J, Oliveira PJ, Ascensão A, Magalhães J. Physical Exercise and Brain Mitochondrial Fitness: The Possible Role Against Alzheimer's Disease. *Brain Pathology*. 2016;26(5):648-663. doi:10.1111/bpa.12403

657. Sarkar A, Mei A, Paquola ACM, et al. Efficient Generation of CA3 Neurons from Human Pluripotent Stem Cells Enables Modeling of Hippocampal Connectivity In Vitro. *Cell Stem Cell*. 2018;22(5):684-697.e9. doi:10.1016/j.stem.2018.04.009

658. Hiragi T, Andoh M, Araki T, et al. Differentiation of human induced pluripotent stem cell (hiPSC)-derived neurons in mouse hippocampal slice cultures. *Frontiers in Cellular Neuroscience*. 2017;11(May):1-10. doi:10.3389/fncel.2017.00143

659. Monnier C, Lalonde R. Elevated +-maze and hole-board exploration in lurcher mutant mice. *Brain Research*. 1995;702(1-2):169-172. doi:10.1016/0006-8993(95)01036-5

10 SUPPLEMENTARY INFORMATION

10.1 Supplementary Tables

Table S1. List of parameters from behavioural characterization. N = Number of animals per group. δ = Cliff´s non-parametric effect size. ß = standardized effect of SCA1 genotype. L,U = limits of 95% confidence interval. EPM = elevated plus maze test. OF = open field test. PPI = prepulse inhibition. MWM = Morris water maze. FST = Forced swimming test. P-values are based on permutation t-test. Gait parameters were evaluated separately for hind (H) and fore (F) legs and using 2 belt speeds (12 or 18 cm/s). Rotarod latency is average over 5 days of the experiment. MWM-hidden latency is average from days 2-7 of the experiment. MWM-visible latency is average from days 8 and 9. MWM non-moving is average from days 1-7. T-maze errors= average from all testing sessions (S3-S7 and S10-S11). T-maze learning e. is the average error rate from all *testing* sessions of the learning phase (S3-S7), whereas inflexibility reflects errors during *testing* sessions in the reversal phase (S10-S11). FST initial immobility is relative time in immobility state during the first 3 minutes of FST.

a) 6-9 weeks of age											
Behavioural parameter	**N**		**Mean**			**Cliff δ and *95% CI***			**ß and *95% CI***		
	WT	**SCA1**	**WT**	**SCA1**	**P**	**δ**	***L***	***U***	**ß**	***L***	***U***
EPM open (%)	13	16	6.6	4.6	0.3282	-0.17	-0.58	0.34	-0.19	-0.58	0.18
OF distance (m)	13	16	54.4	38.9	**0.0104**	**-0.57**	-0.83	-0.12	**-0.47**	-0.86	-0.17
OF thigmotaxis (%)	13	16	71.5	80.4	**0.0012**	**0.66**	0.23	0.90	**0.58**	0.27	0.90
OF adj. thigmotaxis	13	16	-0.11	-0.02	**<0.001**	**0.71**	0.28	0.92	**0.61**	0.32	0.93
OF corners (%)	13	16	54.2	60.9	**0.0463**	0.40	-0.05	0.75	**0.36**	0.04	0.71
PPI (%)	12	14	47.0	55.8	**0.0304**	**0.48**	0.00	0.80	**0.40**	0.09	0.80
Startle amplitude	12	14	19.6	16.7	0.1484	0.16	-0.2	0.70	0.28	-0.07	0.65
Startle latency (ms)	12	14	76.7	81.5	0.3744	0.38	-0.23	0.70	0.19	-0.24	0.55
Stance/Stride (%) [H12]	12	16	77.4	76.6	0.3692	-0.29	-0.66	0.21	-0.17	-0.51	0.21
Stride length (cm) [H12]	12	16	4.2	4.0	0.1265	-0.28	-0.65	0.21	-0.32	-0.75	0.02
Paw angle (abs°) [H12]	12	16	20.1	21.1	0.3246	0.19	-0.30	0.60	0.19	-0.18	0.56
Stance width (cm) [H12]	12	16	2.2	2.2	0.8556	-0.02	-0.47	0.47	0.04	-0.33	0.50
Stride length CV [H12]	12	16	19.2	13.3	**0.0081**	**-0.57**	-0.85	-0.01	**-0.49**	-0.90	-0.19
Stance width CV [H12]	12	16	18.6	14.1	0.3406	-0.24	-0.65	0.26	-0.20	-0.70	0.13
Stance/Stride (%) [F12]	12	16	69.2	70.9	0.1354	0.35	-0.12	0.71	0.29	-0.08	0.65
Stride length (cm) [F12]	12	16	4.1	3.8	0.1955	-0.25	-0.62	0.26	-0.26	-0.66	0.11
Stride length CV [F12]	12	16	29.4	24.8	0.1794	-0.30	-0.66	0.22	-0.27	-0.66	0.13
Stance/Stride (%) [H18]	13	16	74.0	73.1	0.5767	-0.08	-0.52	0.38	-0.11	-0.50	0.27
Stride length (mm) [H18]	13	16	5.1	4.9	0.0902	-0.41	-0.72	0.09	-0.32	-0.66	0.04
Paw angle (abs°) [H12]	13	16	19.2	18.8	0.6717	-0.12	-0.53	0.34	-0.08	-0.41	0.37
Stance width (cm) [H18]	13	16	2.1	2.1	0.9718	-0.03	-0.47	0.45	0.01	-0.38	0.40
Stride length CV [H18]	13	16	11.4	11.4	0.9995	0.19	-0.25	0.60	0.00	-0.56	0.29
Stance width CV [H18]	13	16	16.0	18.9	0.4994	0.13	-0.33	0.54	0.13	-0.25	0.48
Stance/Stride (%) [F18]	13	16	65.3	66.3	0.3608	0.18	-0.31	0.59	0.18	-0.20	0.55
Stride length (cm) [F18]	13	16	5.1	4.7	**0.0177**	**-0.51**	-0.78	-0.02	**-0.45**	-0.79	-0.12
Stride length CV [F18]	13	16	19.8	23.4	0.0829	0.30	-0.17	0.67	0.33	-0.01	0.68
Rotarod latency (s)	13	16	178	158	0.1043	-0.41	-0.76	0.07	-0.31	-0.62	0.09
MWM-hidden latency (s)	13	16	44.8	53.9	**0.0029**	**0.60**	0.08	0.90	**0.56**	0.21	0.86
MWM-visible latency (s)	13	16	26.7	45.5	**0.0015**	**0.63**	0.13	0.92	**0.60**	0.22	0.87
MWM non-moving (%)	13	16	31.3	60.3	**<0.001**	**0.65**	0.15	0.91	**0.63**	0.28	0.88
T-maze errors (%)	13	16	10.4	30.8	**<0.001**	**0.84**	0.46	1.00	**0.74**	0.50	0.97
T-maze learning e. (%)	13	16	4.8	18.4	**0.0024**	**0.59**	0.16	0.85	**0.45**	0.20	0.84
T-maze inflexibility (%)	13	16	24.6	61.9	**0.0047**	**0.49**	0.00	0.82	**0.51**	0.18	0.79
FST immobility (%)	13	16	26.4	52.5	**0.0028**	**0.61**	0.16	0.87	**0.54**	0.21	0.85
FST initial immobility (%)	13	16	13.9	29.0	**0.0078**	**0.58**	0.14	0.84	**0.50**	0.15	0.79

b) 10-14 weeks of age											
Behavioural	**N**		**Mean**			**Cliff δ and *95% CI***			**ß and *95% CI***		
parameter	**WT**	**SCA1**	**WT**	**SCA1**	**P**	**δ**	***L***	***U***	**ß**	***L***	***U***
EPM open (%)	12	14	9.8	2.9	**0.0154**	-0.45	-0.81	0.07	**-0.48**	-0.87	-0.14
OF distance (m)	12	14	51.3	32.4	**0.0074**	**-0.58**	-0.87	-0.10	**-0.53**	-0.85	-0.17
OF thigmotaxis (%)	12	14	72.6	81.4	**0.0095**	**0.57**	0.06	0.88	**0.51**	0.15	0.84
OF adj. thigmotaxis	12	14	-0.11	-0.02	**0.0097**	**0.58**	0.11	0.88	**0.51**	0.16	0.84
OF corners (%)	12	14	60.6	63.5	0.4945	0.19	-0.32	0.62	0.14	-0.28	0.52
PPI (%)	12	14	52.6	64.8	**0.0060**	**0.58**	0.08	0.87	**0.52**	0.18	0.85
Startle amplitude	12	14	19.9	18.3	0.5792	0.17	-0.32	0.60	0.11	-0.25	0.52
Startle latency (ms)	12	14	85.0	87.1	0.6877	0.01	-0.47	0.48	0.08	-0.27	0.51
Stance/Stride (%) [H12]	11	10	79.4	79.0	0.8401	0.07	-0.57	0.48	-0.05	-0.47	0.43
Stride length (cm) [H12]	11	10	4.6	4.2	**0.0106**	**-0.65**	-0.89	-0.19	**-0.48**	-0.99	-0.19
Paw angle (abs°) [H12]	11	10	17.8	17.2	0.7277	-0.2	-0.69	0.37	-0.08	-0.45	0.42
Stance width (cm) [H12]	11	10	2.2	2.1	0.1003	-0.35	-0.76	0.22	-0.38	-0.80	0.02
Stride length CV [H12]	11	10	14.5	17.4	0.3204	0.29	-0.27	0.73	0.23	-0.20	0.66
Stance width CV [H12]	11	10	23.5	25.1	0.8213	-0.01	-0.54	0.50	0.06	-0.34	0.57
Stance/Stride (%) [F12]	11	10	70.2	67.3	0.0541	-0.4	-0.78	0.18	**-0.43**	-0.85	-0.03
Stride length (cm) [F12]	11	10	4.4	3.8	**0.0019**	**-0.73**	-0.92	-0.32	**-0.60**	-1.04	-0.31
Stride length CV [F12]	11	10	25.0	27.3	0.6043	0.05	-0.49	0.58	0.12	-0.27	0.61
Stance/Stride (%) [H18]	12	10	74.7	74.4	0.8800	-0.05	-0.56	0.49	-0.04	-0.47	0.42
Stride length (mm) [H18]	12	10	5.6	5.3	0.0596	-0.51	-0.83	0.05	**-0.41**	-0.82	-0.01
Paw angle (abs°) [H12]	12	10	17.4	16.5	0.3631	-0.15	-0.65	0.45	-0.21	-0.67	0.22
Stance width (cm) [H18]	12	10	2.0	2.1	0.4963	0.08	-0.45	0.58	0.15	-0.22	0.62
Stride length CV [H18]	12	10	10.1	14.5	**0.0449**	0.38	-0.29	0.82	**0.47**	0.04	0.85
Stance width CV [H18]	12	10	18.3	15.7	0.6063	-0.1	-0.61	0.43	-0.12	-0.50	0.38
Stance/Stride (%) [F18]	12	10	65.0	68.1	**0.0464**	0.47	-0.08	0.82	**0.45**	0.07	0.88
Stride length (cm) [F18]	12	10	5.5	5.3	0.2559	-0.24	-0.67	0.30	-0.26	-0.73	0.13
Stride length CV [F18]	12	10	22.2	24.6	0.6228	0.03	-0.50	0.58	0.12	-0.28	0.63
Rotarod latency (s)	12	14	152	124	0.1456	-0.26	-0.66	0.26	-0.31	-0.73	0.04
MWM-hidden latency (s)	12	14	39.2	53.3	**<0.001**	**0.83**	0.47	0.97	**0.75**	0.47	0.99
MWM-visible latency (s)	12	14	23.2	41.5	**0.0068**	**0.65**	0.14	0.92	**0.53**	0.16	0.84
MWM non-moving (%)	12	14	25.5	58.8	**<0.001**	**0.76**	0.36	0.95	**0.67**	0.36	0.95
T-maze errors (%)	12	14	7.7	29.9	**<0.001**	**0.88**	0.51	0.99	**0.70**	0.45	0.99
T-maze learning e. (%)	12	14	4.7	20.4	**0.0174**	**0.45**	-0.02	0.78	**0.40**	0.15	0.86
T-maze inflexibility (%)	12	14	15.4	53.6	**0.0030**	**0.50**	0.01	0.84	**0.55**	0.22	0.84
FST immobility (%)	12	14	24.2	49.5	**0.0053**	**0.61**	0.15	0.88	**0.53**	0.18	0.83
FST initial immobility (%)	12	14	8.2	21.0	**0.0042**	**0.64**	0.18	0.89	**0.55**	0.20	0.85

c) 17-21 weeks of age											
Behavioural	**N**		**Mean**			**Cliff δ and *95% CI***			**ß and *95% CI***		
parameter	**WT**	**SCA1**	**WT**	**SCA1**	**P**	**δ**	***L***	***U***	**ß**	***L***	***U***
EPM open (%)	14	14	12.2	5.6	0.0525	**-0.66**	-0.89	-0.16	-0.36	-0.60	0.23
OF distance (m)	14	14	61.2	27.3	**<0.001**	**-0.93**	-0.98	-0.87	**-0.80**	-1.01	-0.55
OF thigmotaxis (%)	14	14	73.2	85.8	**<0.001**	**0.84**	0.29	1.00	**0.67**	0.35	0.92
OF adj. thigmotaxis	14	14	-0.10	0.01	**<0.001**	**0.74**	0.22	0.96	**0.61**	0.24	0.85
OF corners (%)	14	14	54.7	63.5	**0.0453**	**0.62**	0.14	0.89	0.38	-0.09	0.65
PPI (%)	14	14	47.9	59.0	0.0742	0.44	-0.07	0.79	0.34	-0.04	0.68
Startle amplitude	14	14	18.7	12.8	**0.0125**	**0.54**	0.09	0.82	**0.47**	0.15	0.81
Startle latency (ms)	14	14	92.6	100	0.4441	0.02	-0.43	0.47	0.16	-0.15	0.62
Stance/Stride (%) [H12]	14	13	77.8	80.3	0.0649	0.36	-0.14	0.72	**0.37**	0.05	0.80
Stride length (mm) [H12]	14	13	4.2	4.4	0.1591	0.3	-0.18	0.69	0.28	-0.10	0.64
Paw angle (abs°) [H12]	14	13	17.7	16.8	0.4340	-0.20	-0.61	0.29	-0.16	-0.53	0.24
Stance width (cm) [H12]	14	13	2.5	2.2	**0.0066**	**-0.61**	-0.86	-0.19	**-0.52**	-0.84	-0.20
Stride length CV [H12]	14	13	20.4	14.2	**0.0021**	**-0.60**	-0.86	-0.19	**-0.57**	-0.88	-0.26
Stance width CV [H12]	14	13	11.4	16.5	**0.0432**	**0.40**	-0.09	0.75	**0.40**	0.07	0.78
Stance/Stride (%) [F12]	14	13	66.3	66.0	0.7526	-0.12	-0.56	0.35	-0.06	-0.41	0.38
Stride length (cm) [F12]	14	13	4.1	4.2	0.3149	0.34	-0.15	0.72	0.20	-0.24	0.52
Stride length CV [F12]	14	13	28.5	29.2	0.8210	0.07	-0.43	0.54	0.05	-0.36	0.43
Stance/Stride (%) [H18]	14	12	73.6	75.5	0.4034	0.30	-0.32	0.76	0.18	-0.24	0.58
Stride length (mm) [H18]	14	12	5.4	5.6	0.4296	0.16	-0.37	0.60	0.16	-0.25	0.53
Paw angle (abs°) [H12]	14	12	16.8	15.3	0.2784	-0.27	-0.68	0.23	-0.22	-0.59	0.19
Stance width (cm) [H18]	14	12	2.5	2.2	**<0.001**	**-0.76**	-0.93	-0.39	**-0.64**	-0.93	-0.35
Stride length CV [H18]	14	12	13.0	13.0	0.9748	0.01	-0.46	0.46	0.01	-0.38	0.41
Stance width CV [H18]	14	12	10.4	12.2	0.7046	-0.04	-0.49	0.44	0.10	-0.20	0.70
Stance/Stride (%) [F18]	14	12	62.8	64.4	0.0676	0.32	-0.18	0.70	**0.34**	0.04	0.74
Stride length (cm) [F18]	14	12	5.4	5.5	0.5148	0.12	-0.37	0.57	0.13	-0.28	0.51
Stride length CV [F18]	14	12	26.8	21.9	**0.0304**	**-0.54**	-0.82	-0.05	**-0.43**	-0.76	-0.04
Rotarod latency (s)	14	14	203	92	**<0.001**	**-0.93**	-0.94	-0.88	**-0.87**	-1.06	-0.69
MWM-hidden latency (s)	14	14	41.3	55.2	**<0.001**	**0.81**	0.47	0.96	**0.70**	0.41	0.96
MWM-visible latency (s)	14	14	23.6	53.5	**<0.001**	**0.97**	0.78	1.00	**0.84**	0.62	1.03
MWM non-moving (%)	14	14	18.9	64.4	**<0.001**	**0.90**	0.60	0.99	**0.80**	0.55	1.01
T-maze errors (%)	14	14	13.6	39.8	**<0.001**	**0.90**	0.54	1.00	**0.76**	0.52	1.01
T-maze learning e. (%)	14	14	8.6	33.6	**0.0026**	**0.57**	0.05	0.87	**0.54**	0.24	0.88
T-maze inflexibility (%)	14	14	26.1	55.4	**0.0266**	0.47	-0.03	0.79	**0.43**	0.06	0.74
FST immobility (%)	14	14	31.2	51.4	0.0819	0.35	-0.13	0.71	0.34	-0.04	0.67
FST initial immobility (%)	14	14	11.8	23.6	**0.0282**	**0.48**	0.04	0.80	**0.42**	0.07	0.75

d) 26-31 weeks of age											
Behavioural	**N**		**Mean**			**Cliff δ and *95% CI***			**ß and *95% CI***		
parameter	**WT**	**SCA1**	**WT**	**SCA1**	**P**	**δ**	***L***	***U***	**ß**	***L***	***U***
EPM open (%)	18	12	11.2	6.3	0.2348	-0.33	-0.69	0.16	-0.23	-0.55	0.18
OF distance (m)	18	12	57.5	24.7	**<0.001**	**-0.89**	-0.98	-0.72	**-0.80**	-0.99	-0.53
OF thigmotaxis (%)	18	12	70.5	89.3	**<0.001**	**0.89**	0.59	0.99	**0.75**	0.52	0.99
OF adj. thigmotaxis	18	12	-0.12	0.04	**<0.001**	**0.84**	0.54	0.97	**0.71**	0.44	0.94
OF corners (%)	18	12	53.3	71.0	**<0.001**	**0.71**	0.20	0.94	**0.64**	0.32	0.95
PPI (%)	18	12	42.7	76.4	**<0.001**	**0.79**	0.38	0.95	**0.67**	0.39	0.92
Startle amplitude	18	12	19.2	10.5	**0.0027**	**0.73**	0.26	0.92	**0.51**	0.23	0.8
Startle latency (ms)	18	12	92.4	123	**0.0042**	**0.68**	0.25	0.90	**0.56**	0.23	0.92
Stance/Stride (%) [H12]	18	12	79.5	83.1	0.0507	0.42	-0.09	0.78	0.38	0.00	0.71
Stride length (mm) [H12]	18	12	4.6	4.3	**0.0302**	-0.45	-0.76	0.04	**-0.40**	-0.73	-0.06
Paw angle (abs°) [H12]	18	12	20.5	13.7	**<0.001**	**-0.88**	-0.97	-0.64	**-0.69**	-0.94	-0.46
Stance width (cm) [H12]	18	12	2.6	2.4	0.1139	-0.31	-0.67	0.11	-0.27	-0.60	0.03
Stride length CV [H12]	18	12	14.1	13.3	0.7007	-0.10	-0.52	0.35	-0.07	-0.43	0.29
Stance width CV [H12]	18	12	10.7	11.3	0.8320	-0.14	-0.59	0.36	0.04	-0.30	0.51
Stance/Stride (%) [F12]	18	12	65.2	65.7	0.7880	0.13	-0.38	0.58	0.06	-0.40	0.42
Stride length (cm) [F12]	18	12	4.5	4.2	0.1535	-0.31	-0.68	0.17	-0.27	-0.61	0.10
Stride length CV [F12]	18	12	31.1	27.0	0.2722	-0.27	-0.69	0.24	-0.23	-0.64	0.15
Stance/Stride (%) [H18]	18	10	75.7	80.4	**0.0051**	**0.59**	0.14	0.85	**0.51**	0.17	0.81
Stride length (mm) [H18]	18	10	5.9	5.4	**<0.001**	**-0.73**	-0.93	-0.43	**-0.61**	-0.97	-0.32
Paw angle (abs°) [H12]	18	10	19.3	15.1	**0.0031**	**-0.61**	-0.86	-0.20	**-0.51**	-0.78	-0.22
Stance width (cm) [H18]	18	10	2.5	2.3	**0.0475**	**-0.44**	-0.77	-0.01	**-0.36**	-0.67	-0.02
Stride length CV [H18]	18	10	10.7	12.3	0.4419	0.23	-0.27	0.64	0.19	-0.13	0.82
Stance width CV [H18]	18	10	8.9	9.9	0.6329	0.23	-0.25	0.63	0.10	-0.30	0.42
Stance/Stride (%) [F18]	18	10	64.0	64.9	0.4668	0.23	-0.36	0.71	0.17	-0.33	0.58
Stride length (cm) [F18]	18	10	5.9	5.4	**0.0314**	-0.44	-0.79	0.03	**-0.47**	-0.88	-0.09
Stride length CV [F18]	18	10	25.2	29.4	0.1510	0.36	-0.16	0.74	0.28	-0.13	0.60
Rotarod latency (s)	18	12	205	92.6	**<0.001**	**-0.90**	-0.95	-0.79	**-0.81**	-1.00	-0.62
MWM-hidden latency (s)	18	12	40.0	53.0	**<0.001**	**0.86**	0.46	0.98	**0.65**	0.43	0.91
MWM-visible latency (s)	18	12	23.1	54.4	**<0.001**	**0.90**	0.48	1.00	**0.82**	0.59	0.97
MWM non-moving (%)	18	12	27.9	46.3	**0.0161**	**0.53**	0.08	0.81	**0.44**	0.10	0.75
T-maze errors (%)	18	12	11.2	34.8	**<0.001**	**0.89**	0.60	0.98	**0.76**	0.53	1.04
T-maze learning e. (%)	18	12	8.8	31.0	**<0.001**	**0.72**	0.30	0.93	**0.63**	0.33	0.97
T-maze inflexibility (%)	18	12	17.2	44.2	**0.0054**	**0.51**	-0.03	0.86	**0.55**	0.17	0.85
FST immobility (%)	18	12	23.0	38.0	0.0897	0.36	-0.14	0.74	0.34	-0.03	0.71
FST initial immobility (%)	18	12	7.0	16.5	**0.0189**	**0.54**	0.07	0.83	**0.46**	0.10	0.80

Table S2. Permutational linear mixed-effect models with autoregressive 1 variance-covariance structure modelling latency to reach the platform during the Morris water maze test. Individual subjects represent a random factor. W.A.= weeks of age. *d.f.*= degrees of freedom. *d.d.f.*= denominator degrees of freedom. P= significance derived from LME. Perm. P= significance from permutation test of LME model.

(a) 8 W.A.	Variable	*d.f.*	*d.d.f.*	F	P	Perm. P
	intercept	1	216	1375.9521		
	Day	8	216	10.2172	<0.001	<0.001
	Genotype	1	27	12.201	0.0017	0.002
	*Day*Genotype*	8	216	3.183	0.002	0.0044
(b) 12 W.A.	Variable	*d.f.*	*d.d.f.*	F	P	Perm. P
	intercept	1	192	787.7302		
	Day	8	192	10.0637	<0.001	<0.001
	Genotype	1	24	20.2114	<0.001	<0.001
	*Day*Genotype*	8	192	1.4877	0.1639	0.1608
(c) 19 W.A.	Variable	*d.f.*	*d.d.f.*	F	P	Perm. P
	intercept	1	208	1274.7291		
	Day	8	208	7.4903	<0.001	<0.001
	Genotype	1	26	46.3835	<0.001	<0.001
	*Day*Genotype*	8	208	6.527	<0.001	<0.001
(d) 28 W.A.	Variable	*d.f.*	*d.d.f.*	F	P	Perm. P
	intercept	1	224	1201.2753		
	Day	8	224	5.703	<0.001	<0.001
	Genotype	1	28	45.4089	<0.001	<0.001
	*Day*Genotype*	8	224	4.9505	<0.001	<0.001

Table S3. Table of contrasts in latency to reach the platform during Morris water maze test between genotypes (WT vs. SCA1; first 9 rows) and within-subject comparisons between given days of the experiment. The statistical significance is based on permutation t-test or paired permutation t-test (within-subject comparison). Tests were followed by *false discovery rate* correction for multiple comparisons (Adj. P). W.A.= weeks of age.

	8 W.A.		12 W.A.		19 W.A.		28 W.A.	
Contrast	Raw P	Adj. P	Raw P	Adj. P	Raw P	Adj. P	Raw P	Adj. P
D1	0.0136	0.0268	0.0707	0.0836	0.0481	0.0695	0.0022	0.0048
D2	0.6897	0.6897	0.0138	0.0180	0.2648	0.2648	0.0039	0.0063
D3	0.0065	0.0210	0.0025	0.0047	0.0092	0.0160	0.0047	0.0067
D4	0.0145	0.0268	<0.001	0.0010	0.0099	0.0160	0.0039	0.0063
D5	0.0165	0.0268	0.0010	0.0026	<0.001	<0.001	0.0390	0.0506
D6	<0.001	0.0039	<0.001	<0.001	<0.001	<0.001	<0.001	<0.001
D7	0.0242	0.0349	0.0001	0.0009	<0.001	<0.001	<0.001	<0.001
D8	0.0120	0.0268	0.0074	0.0107	<0.001	<0.001	<0.001	<0.001
D9	<0.001	0.0039	0.0020	0.0043	<0.001	<0.001	<0.001	<0.001
D1:D7 SCA1	0.0274	0.0356	0.4767	0.4767	0.1725	0.2039	0.2889	0.3130
D1:D7 WT	0.0470	0.0509	0.0813	0.0881	0.2027	0.2196	0.0634	0.0750
D7:D9 SCA1	0.0392	0.0464	<0.001	0.0026	0.1298	0.1687	0.8157	0.8157
D7:D9 WT	<0.001	0.0012	0.0052	0.0084	0.0000	0.0002	<0.001	<0.001

Table S4. Permutational linear mixed-effect models with autoregressive 1 variance-covariance structure modelling relative non-moving time during Morris water maze test. Individual subjects represent a random factor. W.A.= weeks of age. *d.f.*= degrees of freedom. *d.d.f.*= denominator degrees of freedom. P= significance derived from LME. Perm. P= significance from permutation test of LME model.

(a) 8 W.A.	Variable	*d.f.*	*d.d.f.*	F	P	Perm. P
	intercept	1	216	1375.9521		
	Day	8	216	10.2172	<0.001	<0.001
	Genotype	1	27	12.201	0.0017	0.002
	*Day*Genotype*	8	216	3.183	0.002	0.0044
(b) 12 W.A.	Variable	*d.f.*	*d.d.f.*	F	P	Perm. P
	intercept	1	192	787.7302		
	Day	8	192	10.0637	<0.001	<0.001
	Genotype	1	24	20.2114	<0.001	<0.001
	*Day*Genotype*	8	192	1.4877	0.1639	0.1608
(c) 19 W.A.	Variable	*d.f.*	*d.d.f.*	F	P	Perm. P
	intercept	1	208	1274.7291		
	Day	8	208	7.4903	<0.001	<0.001
	Genotype	1	26	46.3835	<0.001	<0.001
	*Day*Genotype*	8	208	6.527	<0.001	<0.001
(d) 28 W.A.	Variable	*d.f.*	*d.d.f.*	F	P	Perm. P
	intercept	1	224	1201.2753		
	Day	8	224	5.703	<0.001	<0.001
	Genotype	1	28	45.4089	<0.001	<0.001
	*Day*Genotype*	8	224	4.9505	<0.001	<0.001

Table S5. Table of contrasts in relative non-moving time during Morris water maze test between genotypes (WT vs. SCA1; first 9 rows) and within-subject comparisons between given days (D) of the experiment. The statistical significance is based on permutation t-test or paired permutation t-test (within-subject comparison). Tests were followed by *false discovery rate* correction for multiple comparisons (Adj. P). W.A.= weeks of age.

	8 W.A.		**12 W.A.**		**19 W.A.**		**28 W.A.**	
Contrast	Raw P	Adj. P	Raw P	Adj. P	Raw P	Adj. P	Raw P	Adj. P
D1	<0.001	0.0018	0.0011	0.0015	0.0014	0.0023	0.0036	0.0093
D2	<0.001	0.0018	<0.001	<0.001	0.0317	0.0457	0.0026	0.0084
D3	<0.001	0.0018	<0.001	<0.001	0.0420	0.0546	0.0011	0.0047
D4	<0.001	0.0028	<0.001	<0.001	0.0012	0.0023	0.0122	0.0177
D5	<0.001	0.0018	<0.001	<0.001	<0.001	<0.001	0.0053	0.0115
D6	0.0046	0.0066	<0.001	<0.001	<0.001	<0.001	0.0364	0.0430
D7	0.0145	0.0172	<0.001	<0.001	<0.001	<0.001	0.0078	0.0144
D8	<0.001	0.0018	<0.001	<0.001	<0.001	<0.001	0.0108	0.0175
D9	0.0013	0.0024	<0.001	<0.001	<0.001	<0.001	0.0348	0.0430
D1:D7 SCA1	0.0676	0.0733	<0.001	<0.001	<0.001	<0.001	<0.001	<0.001
D1:D7 WT	0.0098	0.0127	0.3516	0.3516	0.7192	0.7192	<0.001	<0.001
D7:D9 SCA1	<0.001	0.0018	0.0261	0.0309	0.4687	0.5077	0.4992	0.4992
D7:D9 WT	0.7775	0.7775	0.0498	0.0539	0.4393	0.5077	0.0931	0.1008

Table S6. Permutational linear mixed-effect models with autoregressive 1 variance-covariance structure modelling error rate during the water T-maze test. W.A.= weeks of age. *d.f.*= degrees of freedom. *d.d.f.*= denominator degrees of freedom. P= significance derived from LME. Perm. P= significance from permutation test of LME model.

(a) 9 W.A.	Variable	*d.f.*	*d.d.f.*	F	P	Perm. P
	intercept	1	270	425.4		
	Session	10	270	41.6	<0.001	<0.001
	Genotype	1	27	11.4	0.0022	<0.001
	*Session*Genotype*	10	270	2.7	0.0034	0.0016
(b) 13 W.A.	Variable	*d.f.*	*d.d.f.*	F	P	Perm. P
	intercept	1	240	249.3222		
	Session	10	240	35.5306	<0.001	0.005
	Genotype	1	24	9.269	0.0056	0.01
	*Session*Genotype*	10	240	2.4731	0.0078	0.005
(c) 20 W.A.	Variable	*d.f.*	*d.d.f.*	F	P	Perm. P
	intercept	1	260	326.6989		
	Session	10	260	16.9003	<0.001	<0.001
	Genotype	1	26	11.1879	0.0025	0.001
	*Session*Genotype*	10	260	3.3454	<0.001	<0.001
(d) 29 W.A.	Variable	*d.f.*	*d.d.f.*	F	P	Perm. P
	intercept	1	280	447.5031		
	Session	10	280	21.8456	<0.001	<0.001
	Genotype	1	28	21.3227	<0.001	<0.001
	*Session*Genotype*	10	280	7.0813	<0.001	<0.001

Table S7. Table of contrasts in error rate during the water T-maze test between WT and SCA1 mice, specifically for each session (S) of the experiment. The statistical significances are based on permutation t-test. Tests were followed by *false discovery rate* correction for multiple comparisons (Adj. P). W.A.= weeks of age.

	9 W.A.		**13 W.A.**		**20 W.A.**		**29 W.A.**	
Contrast	Raw P	Adj. P	Raw P	Adj. P	Raw P	Adj. P	Raw P	Adj. P
S1	0.3582	0.3940	0.7957	0.7957	0.5319	0.5851	0.6599	0.6738
S2	0.0027	0.0293	0.0637	0.1709	0.1193	0.1641	0.0079	0.0173
S3	0.0223	0.0529	0.0131	0.0723	0.0066	0.0243	<0.001	0.0021
S4	0.0087	0.0431	0.1243	0.1919	0.0060	0.0243	0.0186	0.0341
S5	0.2278	0.2784	0.0514	0.1709	0.0417	0.0765	0.0849	0.1167
S6	0.0627	0.1150	0.1324	0.1919	0.0291	0.0641	<0.001	0.0010
S7	0.0240	0.0529	0.1396	0.1919	0.0033	0.0243	0.0016	0.0058
S8	0.1126	0.1548	0.4902	0.5991	0.2138	0.2614	0.1055	0.1290
S9	0.7592	0.7592	0.6950	0.7645	0.7759	0.7759	0.6738	0.6738
S10	0.1057	0.1548	0.0777	0.1709	0.0948	0.1489	0.0789	0.1167
S11	0.0118	0.0431	0.0018	0.0199	0.0195	0.0536	0.0030	0.0081

Table S8. Permutational linear mixed-effect models with autoregressive 1 variance-covariance structure modelling latency on accelerating rotarod. W.A.= weeks of age. *d.f.*= degrees of freedom. *d.d.f.*= denominator degrees of freedom. P= significance derived from LME. Perm. P= significance from permutation test of LME model.

(a) 7 W.A.	Variable	*d.f.*	*d.d.f.*	F	P	Perm. P
	intercept	1	108	613.0018		
	Day	4	108	8.9994	<0.001	<0.001
	Genotype	1	27	1.2183	0.2794	0.2486
	*Day*Genotype*	4	108	2.9436	0.0236	0.0158
(b) 11 W.A.	Variable	*d.f.*	*d.d.f.*	F	P	Perm. P
	intercept	1	96	903.682		
	Day	4	96	15.7475	<0.001	<0.001
	Genotype	1	24	1.947	0.1757	0.1536
	*Day*Genotype*	4	96	0.064	0.9923	0.9908
(c) 18 W.A.	Variable	*d.f.*	*d.d.f.*	F	P	Perm. P
	intercept	1	104	2363.8692		
	Day	4	104	18.2746	<0.001	<0.001
	Genotype	1	26	88.5653	<0.001	<0.001
	*Day*Genotype*	4	104	4.7874	0.0014	<0.001
(d) 27 W.A.	Variable	*d.f.*	*d.d.f.*	F	P	Perm. P
	intercept	1	112	1844.6508		
	Day	4	112	20.838	<0.001	<0.001
	Genotype	1	28	59.3181	<0.001	<0.001
	*Day*Genotype*	4	112	3.9682	0.0048	0.0016

Table S9. Table of contrasts in rotarod latency between genotypes (WT vs. SCA1; first 5 rows) and within-subject comparisons between the first and the last day (D) of the experiment. Contrasts were computed by permutation t-test or paired permutation t-test (within-subject comparison). Tests were followed by *false discovery rate* correction for multiple comparisons (Adj. P). W.A.= weeks of age.

	7 W.A.		**11 W.A.**		**18 W.A.**		**27 W.A.**	
Contrast	Raw P	Adj. P	Raw P	Adj. P	Raw P	Adj. P	Raw P	Adj. P
D1	0.8492	0.8512	0.2398	0.2822	<0.001	<0.001	<0.001	<0.001
D2	0.0287	0.1042	0.1500	0.2822	<0.001	<0.001	<0.001	<0.001
D3	0.0627	0.1265	0.1524	0.2822	<0.001	<0.001	<0.001	<0.001
D4	0.0819	0.1265	0.1818	0.2822	<0.001	<0.001	<0.001	<0.001
D5	0.5664	0.6578	0.2337	0.2998	<0.001	<0.001	<0.001	<0.001
D1:D5 WT	0.0281	0.1042	0.0042	0.0147	<0.001	<0.001	<0.001	<0.001
D1:D5 SCA1	0.0869	0.1265	0.0013	0.0093	0.0013	0.0013	0.0026	0.0026

Table S10. Results of permutational multivariate analysis of variance (PERMANOVA) describing similarity in general gait pattern (WT vs. SCA1 mice) based on gait parameters measured using DigiGait device. W.A.= weeks of age. *d.f.*= degrees of freedom. *s.s.*= sum of squares. *m.s.*= mean squares.

(a) 6 W.A.	Variable	*d.f.*	*s.s.*	*m.s.*	F	R^2	P
	Genotype	1	0.01	0.01	1.56	0.06	0.1068
	Residuals	26	0.17	0.0064		0.94	
(b) 10 W.A.	Variable		*s.s.*	*m.s.*	F		P
	Genotype	1	0.01	0.01	1.74	0.08	0.0726
	Residuals	19	0.12	0.0064		0.92	
(c) 17 W.A.	Variable		*s.s.*	*m.s.*	F		P
	Genotype	1	0.02	0.02	3.88	0.14	<0.001
	Residuals	24	0.14	0.0059		0.86	
(d) 26 W.A.	Variable		*s.s.*	*m.s.*	F		P
	Genotype	1	0.03	0.03	5.04	0.16	<0.001
	Residuals	26	0.15	0.0059		0.84	

Table S11. Results of permutational multivariate analysis of variance (PERMANOVA) comparing the pattern of functional impairments in SCA1 mice of different age cohorts. (**a**) All age cohorts together. (**b**) *Pre-ataxic* mice only (age ≤ 14 weeks of age). (**c**) *Ataxic* mice only (age≥ 17 weeks of age). W.A.= weeks of age. *d.f.*= degrees of freedom. *s.s.*= sum of squares. *m.s.*= mean squares.

(a) all SCA1	Variable	*d.f.*	*s.s.*	*m.s.*	F	R^2	P
	Age	3	0.068	0.023	3.6	0.17	<0.001
	Residuals	52	0.329	0.006		0.83	
(b) ≤ 14W.A.	Variable		*s.s.*	*m.s.*	F		P
	Age	1	0.005	0.005	0.7	0.02	0.65
	Residuals	28	0.209	0.008		0.98	
(c) ≥ 17 W.A.	Variable		*s.s.*	*m.s.*	F		P
	Age	1	0.010	0.010	1.5	0.06	0.21
	Residuals	24	0.162	0.007		0.94≤	

Table S12. Brain regions which were evaluated in terms of their volume or thickness in WT and SCA1 mice (32 weeks of age; N = 8 animals/group). WT, SCA1= genotype-specific means (mm^3 or mm). ß= standardized regression coefficient for SCA1 genotype. CI= limits for 95% confidence intervals (CI-L: lower limit, CI-U: upper limit) based on BCa bootstrap. perm.P= significance based on permutation t-test. CA= *Cornu ammonis* hippocampal region. DG= dentate gyrus.

Brain area	WT	SCA1	*ß*	CI-L	CI-U	perm. P
Cerebellar granular layer	2.5	2.4	-0.24	-0.81	0.20	0.3691
Cerebellar molecular layer	2.9	2.1	-0.77	-1.14	-0.50	<0.001
Molecular/granular cb. layers	1.16	0.87	-0.92	-1.10	-0.74	<0.001
Hypoglossal nucleus	0.0144	0.0150	0.18	-0.27	0.75	0.4913
Parietal cortex thickness	0.534	0.524	-0.11	-0.61	0.40	0.6691
CA strata pyramidalis + oriens	4.32	4.04	-0.27	-0.79	0.18	0.3027
CA strata radiatum + lac. mol.	5.1	4.4	-0.85	-1.09	-0.58	<0.001
DG granular layer	0.61	0.57	-0.28	-0.85	0.27	0.7433
DG polymorph layer	0.56	0.55	-0.12	-0.62	0.42	0.4710
DG molecular layer	3.0	2.6	-0.69	-1.08	-0.34	0.0043

Table S13. Results of general linear models describing the effect of total brain weight and SCA1 genotype on the volume of *stratum radiatum* and *lacunosum-moleculare* of *Cornu ammonis* (CA-SRLM). (**a-d**) Age cohort-specific models (N= 8 WT and 10 SCA1 mice). (**e-f**) Models are based on merged data from two age cohorts (N = 16 WT and 20 SCA1 mice). *ß*= standardized regression coefficient. CI= limits for 95% confidence intervals based on BCa bootstrap. P= significance based on parametric approach. boot. P= significance based on percentile bootstrap.

(a) 10 W.A.	*ß*	CI-L	CI-U	P	boot. P
Brain weight	0.34	-0.1	0.76	0.12	0.13
Genotype	-0.5	-0.93	0.01	0.036	0.028
(b) 15 W.A.	*ß*	CI-L	CI-U	P	boot. P
Brain weight	0.55	0.12	0.91	0.022	0.01
Genotype	-0.33	-0.84	-0.04	0.12	0.041
(c) 22 W.A.	*ß*	CI-L	CI-U	P	boot. P
Brain weight	0.44	0.05	0.09	0.073	0.055
Genotype	-0.44	-0.83	0.09	0.075	0.068
(d) 32 W.A.	*ß*	CI-L	CI-U	P	boot. P
Brain weight	0.3	-0.09	0.5	0.052	0.076
Genotype	-0.72	-1.08	-0.48	<0.001	<0.001
(e) ≤ 15 W.A.	*ß*	CI-L	CI-U	P	boot. P
Brain weight	0.48	0.26	0.7	0.002	<0.001
Genotype	-0.38	-0.69	-0.15	0.009	0.002
(f) ≥ 22 W.A.	*ß*	CI-L	CI-U	P	boot. P
Brain weight	0.35	0.11	0.57	0.007	0.011
Genotype	-0.57	-0.82	-0.34	<0.001	<0.001

Table S14. Results of general linear models describing the effects of total brain weight and SCA1 genotype on the volume of the molecular layer of the dentate gyrus (DG-ML) of the hippocampus. (**a-d**) Age cohort-specific models (N= 8 WT and 10 SCA1 mice). (**e-f**) Models based on merged data (N = 16 WT and 20 SCA1 mice). W.A. = weeks of age. See Suppl. Table S13 for abbreviations.

(a) 10 W.A.	*ß*	CI-L	CI-U	P	boot. P
Brain weight	0.56	0.24	0.97	0.001	0.007
Genotype	-0.4	-0.80	-0.02	0.018	0.025
(b) 15 W.A.	*ß*	CI-L	CI-U	P	boot. P
Brain weight	0.45	0.04	0.85	0.025	0.024
Genotype	-0.53	-0.86	-0.22	0.006	<0.001
(c) 22 W.A.	*ß*	CI-L	CI-U	P	boot. P
Brain weight	0.47	0.22	0.75	0.003	0.01
Genotype	-0.53	-0.8	-0.25	<0.001	<0.001
(d) 32 W.A.	*ß*	CI-L	CI-U	P	boot. P
Brain weight	0.4	-0.06	0.68	0.062	0.078
Genotype	-0.49	-0.9	-0.16	0.019	0.007
(e) ≤ 15 W.A.	*ß*	CI-L	CI-U	P	boot. P
Brain weight	0.46	0.24	0.65	<0.001	<0.001
Genotype	-0.51	-0.75	-0.28	<0.001	<0.001
(f) ≥ 22 W.A.	*ß*	CI-L	CI-U	P	boot. P
Brain weight	0.46	0.2	0.65	<0.001	0.001
Genotype	-0.49	-0.74	-0.26	<0.001	<0.001

Table S15. Results of models describing an association between DG-ML volume and given sensitive indicator adjusted for the effect of SCA1 genotype, specifically for young mice (age ≤15 weeks) of both genotypes (N = 16 WT and 20 SCA1 mice). See Suppl. Table S13 for abbreviations.

(a) OF thigmotaxis	*ß*	CI-L	CI-U	P	boot. P
Genotype	0.27			0.21	
DG-ML volume	-0.49	-0.89	-0.05	0.025	0.032
(b) OF distance moved	*ß*	CI-L	CI-U	P	boot. P
Genotype	-0.58			0.02	
DG-ML volume	0.02	-0.35	0.47	0.93	0.94
(c) Rotarod latency	*ß*	CI-L	CI-U	P	boot. P
Genotype	-0.22			0.42	
DG-ML volume	0.15	-0.42	0.7	0.60	0.58
(d) MWM non-moving	*ß*	CI-L	CI-U	P	boot. P
Genotype	0.52			0.003	
DG-ML volume	-0.39	-0.78	-0.13	0.02	0.005
(e) T-maze errors	*ß*	CI-L	CI-U	P	boot. P
Genotype	0.83			<0.001	
DG-ML volume	0.14	-0.11	0.42	0.43	0.28
(f) T-maze inflexibility	*ß*	CI-L	CI-U	P	boot. P
Genotype	0.19			0.41	
DG-ML volume	-0.34	-0.76	0.09	0.16	0.10
(e) FST immobility	*ß*	CI-L	CI-U	P	boot. P
Genotype	0.21			0.26	
DG-ML volume	-0.66	-1.04	-0.19	0.001	0.001

Table S16. Results of models describing an association between Cb-ML volume and given sensitive indicator adjusted for the effect of SCA1 genotype, specifically for young mice (age ≤15 weeks) of both genotypes (N= 16 WT and 20 SCA1 mice). See Suppl. Table S13 for abbreviations.

(a) OF thigmotaxis	*ß*	CI-L	CI-U	P	boot. P
Genotype	0.46			0.009	
Cb-ML volume	-0.24	-0.53	0.05	0.17	0.09
(b) OF distance moved	*ß*	CI-L	CI-U	P	boot. P
Genotype	-0.41			0.008	
Cb-ML volume	0.00	-0.35	0.29	0.99	0.98
(c) Rotarod latency	*ß*	CI-L	CI-U	P	boot. P
Genotype	-0.33			0.11	
Cb-ML volume	0.06	-0.40	0.45	0.78	0.84
(d) MWM non-moving	*ß*	CI-L	CI-U	P	boot. P
Genotype	0.67			<0.001	
Cb-ML volume	-0.12	-0.35	0.12	0.45	0.31
(e) T-maze errors	*ß*	CI-L	CI-U	P	boot. P
Genotype	0.84			<0.001	
Cb-ML volume	0.14	-0.05	0.42	0.29	0.18
(f) T-maze inflexibility	*ß*	CI-L	CI-U	P	boot. P
Genotype	0.35			0.049	
Cb-ML volume	-0.25	-0.51	0.12	0.17	0.13
(e) FST immobility	*ß*	CI-L	CI-U	P	boot. P
Genotype	0.47			0.004	
Cb-ML volume	-0.27	-0.63	0.02	0.09	0.07

Table S17. Results of models describing an association between CA-SRLM volume and given sensitive indicator adjusted for the effect of SCA1 genotype, specifically for young mice (age ≤15 weeks) of both genotypes (N= 16 WT and 20 SCA1 mice). See Suppl. Table S13 for abbreviations.

(a) OF thigmotaxis	*ß*	CI-L	CI-U	P	boot. P
Genotype	0.50			0.012	
CA-SRLM volume	-0.21	-0.61	0.22	0.27	0.29
(b) OF distance moved	*ß*	CI-L	CI-U	P	boot. P
Genotype	-0.45			0.023	
CA-SRLM volume	0.22	-0.11	0.65	0.26	0.25
(c) Rotarod latency	*ß*	CI-L	CI-U	P	boot. P
Genotype	-0.31			0.2	
CA-SRLM volume	0.04	-0.45	0.52	0.85	0.87
(d) MWM non-moving	*ß*	CI-L	CI-U	P	boot. P
Genotype	0.73			<0.001	
CA-SRLM volume	-0.14	-0.36	0.13	0.36	0.24
(e) T-maze errors	*ß*	CI-L	CI-U	P	boot. P
Genotype	0.78			<0.001	
CA-SRLM volume	0.08	-0.20	0.31	0.59	0.48
(f) T-maze inflexibility	*ß*	CI-L	CI-U	P	boot. P
Genotype	0.36			0.083	
CA-SRLM volume	-0.13	-0.53	0.26	0.52	0.50
(e) FST immobility	*ß*	CI-L	CI-U	P	boot. P
Genotype	0.58			0.003	
CA-SRLM volume	-0.20	-0.53	0.18	0.28	0.23

Table S18. Results of models describing an association between brain weight and given sensitive indicator adjusted for the effect of SCA1 genotype, specifically for young mice (age ≤15 weeks) of both genotypes (N= 25 WT and 30 SCA1 mice). See Suppl. Table S13 for abbreviations.

(a) OF thigmotaxis	*ß*	CI-L	CI-U	P	boot. P
Genotype	0.54			<0.001	
Brain weight	0.05	-0.31	0.27	0.87	0.87
(b) OF distance moved	*ß*	CI-L	CI-U	P	boot. P
Genotype	-0.50			<0.001	
Brain weight	-0.01	-0.31	0.34	0.91	0.92
(c) Rotarod latency	*ß*	CI-L	CI-U	P	boot. P
Genotype	-0.24			0.11	
Brain weight	0.09	-0.24	0.38	0.58	0.56
(d) MWM non-moving	*ß*	CI-L	CI-U	P	boot. P
Genotype	0.64			<0.001	
Brain weight	-0.02	-0.31	0.24	0.84	0.88
(e) T-maze errors	*ß*	CI-L	CI-U	P	boot. P
Genotype	0.72			<0.001	
Brain weight	-0.002	-0.19	0.19	0.99	0.97
(f) T-maze inflexibility	*ß*	CI-L	CI-U	P	boot. P
Genotype	0.48				
Brain weight	-0.09	-0.34	0.14	0.51	0.45
(e) FST immobility	*ß*	CI-L	CI-U	P	boot. P
Genotype	0.42			0.002	
Brain weight	-0.24	-0.47	0.05	0.073	0.080

Table S19. Results of linear mixed-effect models describing partial effects of SCA1 genotype and specific citrate synthase activity (mIU/mg) on mitochondrial respiration (pmolO_2/s/mg) in cerebellar (**a-e**) and hippocampal (**f-i)** tissue. The following states of mitochondrial respiration were evaluated: 1) complex I OXPHOS capacity in the ADP-activated state of oxidative phosphorylation (*P I*). 2) Complex I + II OXPHOS capacity (*P I+II*). 3) Maximum capacity for electron transport (*E I+II*). 4) Complex II uncoupled capacity (*E II*). 5) *Complex IV* capacity. N = 5 WT and 6 SCA1 animals (in quadruplicates). *ß*= standardized regression coefficient. CI= limits for 95% confidence intervals based on BCa bootstrap. P= significance based on parametric approach. boot. boot. P= significance based on percentile bootstrap. perm. P= statistical significances from a permutational variant of the model.

(a) Cb – P I	*ß*	CI-L	CI-U	P	boot. P	perm. P
Citrate synthase activity	0.64			<0.001		
Genotype	-0.14	-0.74	0.44	0.65	0.66	0.66
(b) Cb – P I + II	*ß*	CI-L	CI-U	P	boot. P	perm. P
Citrate synthase activity	0.67			<0.001		
Genotype	-0.11	-0.50	0.29	0.60	0.59	0.60
(c) Cb – E I + II	*ß*	CI-L	CI-U	P	boot. P	perm. P
Citrate synthase activity	0.72			<0.001		
Genotype	-0.17	-0.53	0.20	0.39	0.38	0.38
(d) Cb – E II	*ß*	CI-L	CI-U	P	boot. P	perm. P
Citrate synthase activity	0.72			<0.001		
Genotype	-0.07	-0.32	0.17	0.57	0.57	0.59
(e) Cb – complex IV	*ß*	CI-L	CI-U	P	boot. P	perm. P
Citrate synthase activity	0.70			<0.001		
Genotype	0.01	-0.28	0.30	0.93	0.93	0.93
(f) Hp – P I	*ß*	CI-L	CI-U	P	boot. P	perm. P
Citrate synthase activity	0.60			<0.001		
Genotype	-0.31	-0.69	0.06	0.14	0.10	0.12
(g) Hp – P I + II	*ß*	CI-L	CI-U	P	boot. P	perm. P
Citrate synthase activity	0.68			<0.001		
Genotype	-0.29	-0.56	-0.01	0.07	0.039	0.048
(h) Hp – E I + II	*ß*	CI-L	CI-U	P	boot. P	perm. P
Citrate synthase activity	0.73			<0.001		
Genotype	-0.29	-0.48	-0.10	0.015	0.004	0.006
(i) Hp – E II	*ß*	CI-L	CI-U	P	boot. P	perm. P
Citrate synthase activity	0.60			<0.001		
Genotype	-0.36	-0.63	-0.08	0.031	0.010	0.022
(j) Hp – complex IV	*ß*	CI-L	CI-U	P	boot. P	perm. P
Citrate synthase activity	0.60			<0.001		
Genotype	-0.36	-0.62	-0.09	0.025	0.011	0.012

10.2 Supplementary Figures

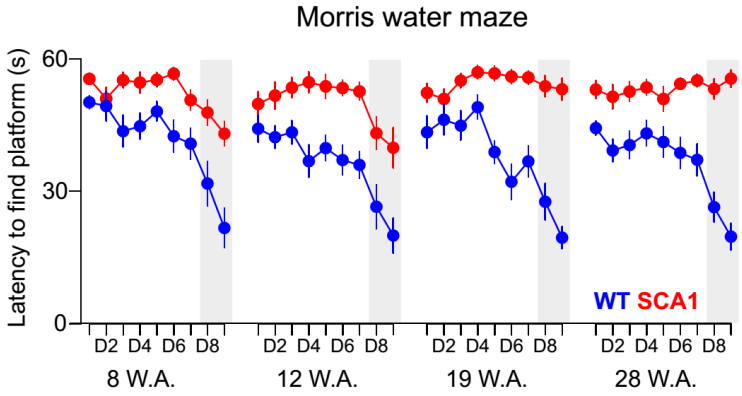

Figure S1. Mean latencies to find a platform during the Morris water maze test. The Gray area indicates the phase of the test with a visually marked platform. Mean ± SEM is visualized.